GEORG-AUGUST-UNIVERSITÄT
GÖTTINGEN

Dissertation

Ageing-associated myelin dysfunction as a driver of amyloid deposition in Alzheimer's disease

For the award of the degree "Doctor rerum naturalium"
of the Georg-August-Universität Göttingen

within the doctoral programme "Cellular and Molecular Physiology of the Brain"
of the Göttingen Graduate Center for Neurosciences, Biophysics, and Molecular Biosciences

Submitted by
Constanze Martha Depp
from Offenbach am Main, Germany

October 2021, Göttingen

Thesis Advisory Committee

Prof. Klaus-Armin Nave (1st Reviewer)
Department of Neurogenetic, Max Planck Institute for Experimental Medicine, Göttingen

Prof. Thomas Bayer (2nd Reviewer)
Division of Molecular Psychiatry, University Medical Center Göttingen

Prof. Nils Brose
Department of Neurobiology, Max Planck Institute for Experimental Medicine, Göttingen

Extended Examination Board

Prof. Hannelore Ehrenreich
Clinical Neuroscience, Max Planck Institute for Experimental Medicine, Göttingen

Prof. Susann Boretius
Functional Imaging, German Primate Center, Göttingen

Prof. Thomas Dresbach
Department of Anatomy and Embryology, University Medical Center Göttingen

Date of Oral Examination

01.12.2021

Declaration

I hereby declare that I wrote this PhD thesis independently by myself with no other contributory sources and aids than quoted.

This thesis forms the basis of the manuscript “Depp, C. et al. Ageing-associated myelin dysfunction drives amyloid deposition in mouse models of Alzheimer's disease. bioRxiv (2021)” that was recently uploaded to the preprint server BioRxiv and is currently under review. The manuscript figures that I assembled were adapted and expanded for presentation in this thesis.

Göttingen, October 2021

Constanze Depp

"Unfortunately, nature seems unaware of our intellectual need for convenience and unity, and very often takes delight in complication and diversity."

— Ramón y Cajal (1906).

Contents

Abstract

Alzheimer's disease (AD) is the most common neurodegenerative disease with increasing prevalence due to longer lifespans in the human population. AD manifests as various age-associated cognitive impairments summarised under the syndrome of dementia. Why ageing constitutes the greatest risk factor for the development of AD, however, remains poorly understood. Ageing markedly affects the integrity of myelin at the ultrastructural level, with myelin splitting, outfoldings and secondary low-grade inflammation. In addition to the well-established role of oligodendroglia in producing insulating myelin, these glia cells also provide throphic support to ensheathed axons. Structural breakdown of myelin during ageing likely effects both insulation and metabolic support function of oligodendrocytes. This puts ensheathed axons and their neurons at risk for starvation and malfunction which could contribute to the development of neurodegenerative diseases upon ageing. Intriguingly, age-related myelin breakdown coincides with the beginning of amyloid build-up in the brain, the primary neuropathological hallmark of AD. I propose a mechanistic link between ageing-associated myelin dysfunction and the deposition of amyloid-β (Aβ) and hypothesised that breakdown of myelin - especially in cortical regions – is an upstream driver of amyloid deposition in AD. In my doctorate, I examined this possible link in proof of principle experiments *in vivo* by combining mouse models of myelin dysfunction with AD mouse models. I here show that in mouse models of AD (5xFAD, APP^{NLGF}) genetically induced myelin defects (knockout of CNP or PLP1) as well as direct demyelinating injuries (experimental autoimmune encephalomyelitis, Cuprizone feeding) are potent drivers of amyloid deposition as shown by quantitative 3D light sheet microscopy. Conversely, lack of compact myelin in forebrain specific MBP knockout animals ("shiverer") ameliorates plaque deposition. Behavioural analysis revealed synergistic effects of myelin defects and amyloid pathology on the manifestation of impairments. Mechanistically, I show that myelin dysfunction leads to the accumulation of the Aβ producing machinery (APP, β- and ɣ-secretase) in axonal spheroids and enhanced cortical APP cleavage. Additionally, I observed a profound loss of plaque-corralling microglia in AD mice with defective myelin. Transcriptomic analysis of isolated microglia revealed, however, that the disease-associated microglia (DAM) signature found in plaque-corralling microglia in 5xFADs is preserved in microglia additionally challenged with myelin. Indeed, myelin dysfunction alone is sufficient to induce a DAM-like state as shown by single nuclei RNA sequencing. I conclude that upon myelin damage in the brain microglia become primarily engaged in myelin clearance which renders them unresponsive to amyloid and prevents the protective reactions of microglia to Aβ plaques. The work presented in this thesis identifies myelin ageing as a previously overlooked risk factor for AD and makes the case for myelin health-directed therapies to combat AD.

1 Introduction

More than glue: glia cells in the nervous system

Neurons are the primary excitable cells in the nervous system which are highly specialised in conveying electrochemical impulses. They connect to one another by building physical connections in the form of synapses at the end and alongside long and thin cellular processes. Axons are the primary output elements that transmit action potentials by regulating ion movement across the axolemma. The seminal work of Hodgkin and Huxley on the squid giant axon revealed the nature of the action potential (Hodgkin and Huxley 1952): with the arrival of a depolarising signal voltage-gated sodium channels open and sodium ions enter the axon along an electrochemical gradient changing the resting membrane potential of neurons at around -70mV to about +30mV. With depolarisation, voltage-gated potassium channels open allowing for potassium ions to leave the axon eventually repolarising it to its resting potential after a short period of hyperpolarisation. The exact shape, pattern and duration of the action potential (in the order of a couple of milliseconds) depends on the neuronal subtype (Bean 2007). "Information" seems to be encoded both in the spike frequency of action potentials, in the spike time arrival, and on a populational level, in the joint activation profiles of single neurons (Averbeck, Latham, and Pouget 2006; Kumar, Rotter, and Aertsen 2010). While the mechanistic underpinnings remain enigmatic, this electrical activity of neurons is the basis for brain function and higher mental experiences.

Neurons, however, do not work in isolation and they certainly gained their specialisation at the expense of high energetic demands and an almost unbearable cytoarchitecture. In fact, for mouse cortical pyramidal neurons brain-wide morphological construction showed that axonal trees on average reach a total length of about 6 cm, several times the length of the typical mouse brain. In the case of the longest nerve of the human body, the sciatic nerve, axons can exceed lengths of 1m. To support neurons and axons, evolution has equipped the centralised nervous system of Bilateria with supporting cells. Rudolf Virchow dismissed these cells as rather meaningless connective tissue of the nervous system, hence their name glia (Greek *glia* for "glue"). Nowadays, it is well established that glia cells fulfil a multitude of vital functions from metabolic support, and structural guidance, to modulation of neurotransmission, synapse formation and waste removal – to name a few (Barres 2008). While glia cells in invertebrates such as *C.elegans* remained rather primitive, mammalian central nervous system (CNS) glia, themselves, developed into highly specialised subtypes. Astrocytes - most alike to the primordial glia found in invertebrates (Freeman and Rowitch 2013) - are star shaped cells that metabolically support neurons, help in the clearance of neurotransmitters from the synaptic cleft, contribute to forming the blood-brain-barrier (BBB) and react to injury (Haim and Rowitch 2017). Microglia are the brain resident innate immune cells and actively shape neuronal circuitry during development and homeostasis (Butovsky and Weiner 2018). In disease, microglia acquire an activated phenotype and phagocytose cellular debris and waste products. Finally, as a third major class of glia cells, Schwann cells in the periphery and oligodendrocytes in the CNS produce myelin, an insulating sheath around axons that consists of wrappings of a flattened membrane protrusion. Oligodendrocytes and myelin evolved in gnathostomes (jawed vertebrates) approximately 420 million years ago from ensheathing glia cells as they are found in invertebrates and agnathostoma such as lampreys (Zalc, Goujet, and Colman 2008; Weil et al. 2018). In this chapter, I will in more detail describe the development, architecture and functions of this fascinating cellular specialisation that is myelin.

1.1 Oligodendrocytes and myelin

The discovery of myelin and oligodendrocytes

Myelin is the reason the CNS can be macroscopically divided in areas that appear grey and white. Renaissance anatomist Vesalius was the first to describe and illustrate this division in detail in his famous work "De humani corporis fabrica libri septem"(Catani and Sandrone 2015). Grey and white matter represent distinct organisational domains in the CNS and more specifically of neurons: while grey matter contains both neuronal somata, neurites and glia cells, white matter is devoid of neuronal cell bodies and exclusively contains axonal fibres that are heavily myelinated and glial cells. White matter derives its colour from the high fat content and the accompanying strong reflective properties of myelin as a layered mixture of lipids and proteins. Of note, though grey matter appears grey, there is still considerable amount of myelin in grey matter areas such as the cortex.

Von Leeuwenhoek with the power of his newly designed lenses was arguably the first one to observe myelin microscopically (reviewed in (Boullerne 2016)). Later, Ehrenberg and Remak in more detail examined nerve fibres and described the presence of cylindric, primitive tubes (axons) covered by a peculiar opaque substance (Rosenbluth 1999). Under the impression that this substance is within the nerve fibre, Virchow coined the term "myelin" (Greek for "marrow") in analogy to the marrow of bones. Though early on Ranvier hypothesised that myelin is an intracellular secretion product of an adipocyte, for a long time it was advocated that myelin is of axonal origin (Boullerne 2016). Pio Del Rio-Hortega, using novel metal impregnation techniques, discovered a type of glia he termed oligodendrocytes referring to the couple of cellular processes these cells extended (Del Rio-Hortega 1921). It was also noticed that these cells were particularly abundant in myelin-rich regions in the brain and that their cellular processes associated with myelin similar to Schwann cells in the periphery (Wilder Penfield and Oxon 1924). However, it took until the 1950s and the advent of electron microscopy (EM) to overhaul the opinion that myelin is axonally generated. In the classic work of Betty Ben Geren on peripheral nerves in the developing chick embryo, she came to the conclusion that myelin is a spiralling membrane extension of Schwann cells (Geren 1954).

The primary function of myelin: insulation

It is textbook knowledge that myelination speeds up propagation of the action potential along axons by the mechanism of saltatory conduction (Fig1.1a). But how does myelin achieve this exactly? Myelin decreases axonal membrane capacitance by increasing the distance between the electrostatic forces of axonal ions and extracellular ions. At the same time, myelin as a lipid/protein mixture shows much lower permittivity than the extracellular fluid. As a result, transverse electrostatic forces and leak currents through the axolemma are weakened and longitudinal forces can act further distal in the axon. With this, the depolarisation is strong enough to activate voltage gated sodium channels (Na_V) that are positioned further away from the site of primary ion influx. In myelinated axons, no Na_V channels are found underneath the myelin sheath, but they are clustered inbetween myelin sheaths at nodes of Ranvier. As shown in Tasaki's seminal work (Tasaki 1939) action potentials, therefore, appear to saltate from one node to the next. In myelin-covered internodal areas, action potentials are conveyed by fast electrostatic forces rather than slow ion movement (Fig1.1a). Myelination and ion channel clustering synergistically speed up conduction velocity from 0.5-2m/s in unmyelinated up to 120m/s in myelinated nerves. Intriguingly, irrespective of the insulating properties of myelin, clustering of Na_V channels in pre-nodes is sufficient to significantly enhance conduction velocity (Freeman et al. 2015). Only very recently, the Kole Lab has revealed a submyelin electrical nanocircuit refining the double cable model for saltatory conduction (Cohen et al. 2020). Myelin is, without exception, present wherever axons become tightly bundled such as in peripheral nerves or "central nerves" like the optic nerve or the corpus callosum. Just like the insulation around electrical wires which protects the surroundings from conducting electricity or which separates different wire entities, myelin also insulates axons against one another preventing ephaptic coupling and the lateral spread of activation to other axons (Reutskiy, Rossoni, and Tirozzi 2003).

Without myelin, increases in conduction velocity can be achieved by increasing axonal diameter as this lowers axonal axial resistance to current flow (Xu and Terakawa 2013). This has led to the formation of abnormally huge axons – a phenomenon known as axonal gigantism- in time-sensitive circuitry e.g. the innervation of the squid contractile mantle (Hartline and Colman 2007). Axonal gigantism, however, is not only space consuming but also energy demanding due to the maintenance of increased amounts of axonal cytoplasm and membrane. Myelin, hence, is an evolutionary achievement that enables fast signal conduction in confined spaces (like the skull) at an economical energy expense.

1.1.1 Molecular anatomy and cellular architecture of myelin

General features of myelin

Myelin is a flat cellular protrusion, consisting of plasma membrane, that is spirally wrapped around the axon. Oligodendrocytes can generate 20 - 60 internodes of variable thickness (6-160 wraps (Hildebrand et al. 1993)) and length (20-200µm). Intriguingly, the amount of total myelin membrane that can by generated by an oligodendrocyte as measured by the surface of the "unrolled" sheath (Fig1.1a) appears constant estimated at $20 \times 10^5\,\mu m^2$. To better illustrate this: with the assumption of a squared sheet this number for example equals 30 sheaths with 50µm in length and width (unrolled). Myelination follows strict rules: Axonal size-cut off for myelination by oligodendrocytes is 0.2µm in the mouse CNS (Goebbels et al. 2017) and myelin thickness scales almost linearly with the axon diameter as expressed in the g-ratio value (diameter axon/diameter complete myelinated fibre). In the PNS the typically observed g-ratio is 0.6, while in the CNS greater g-ratio values are observed indicative of thinner myelin (mouse optic nerve, 0.75; mouse corpus callosum 0.8).

As every biological membrane, myelin is composed of proteins and lipids. Myelin, however, is special in regards to its unique lipid and protein composition profile that enables tight membrane wrapping. Myelin shows an unusual high 70-85% lipid content and a correspondingly low protein fraction (15-30%). Cholesterol is particularly abundant representing 40% of myelin lipids, while phospholipids represent another 40% and glycolipids constitute 20% in comparison to 25%:65%:10% for classical cell membranes (Poitelon, Kopec, and Belin 2020). Likewise, myelin is unique in its protein composition: myelin-specific proteins such as myelin basic protein (MBP), 2',3'-cyclic nucleotide phosphodiesterase (CNP) and proteolipid protein (PLP) (in more detail reviewed later in this chapter) dominate the proteome profile together constituting over 70% of all proteins (Jahn et al. 2020) (Fig1.1a).

Molecular make-up of myelin

From its early beginnings, electron microscopy has been instrumental in elucidating the detailed architecture of myelin. In EM cross sections of internodes, concentric staggered layers of membranes around axons are visible (Fig1.1a,b). The outer leaflets of the two adjacent wraps are tightly joint to the exclusion of extracellular space. Likewise, the cytoplasmic leaflets of the opposing plasma membranes are tightly zipped together to the exclusion of cellular cytoplasm. With this, using electron microscopy, a 3nm electron-dense amorphous protein phase between the two cytoplasmic lipid layers can be visualised that is known as the myelin major dense line (MDL) (Fig1.1a,b). The intraperiod line (IPL) represents the zipped two outer membranes leaflet. Membrane zipping of myelin is, however, not complete and cytoplasm filled canals remain at the rim of the myelin sheet. The structure and location of this canal system (also referred to as myelinic channels, cytoplasmic channels, non-compact myelin areas (Stassart et al. 2018)) can be best viewed in a hypothetically unrolled myelin sheath (Fig1.1a,b): the designated outer tongue presents the rim of the myelin sheath proximal to the oligodendrocyte cell body which is connected to the soma via a cellular process. The cytoplasm at both lateral rims of the sheet in its wrapped state will form the paranodal loops. The distal rim of the myelin sheet also called the inner tongue spans alongside the axon in the innermost wrap of myelin. From this architecture, it becomes clear that both paranodal loops and inner tongue are in very close physical

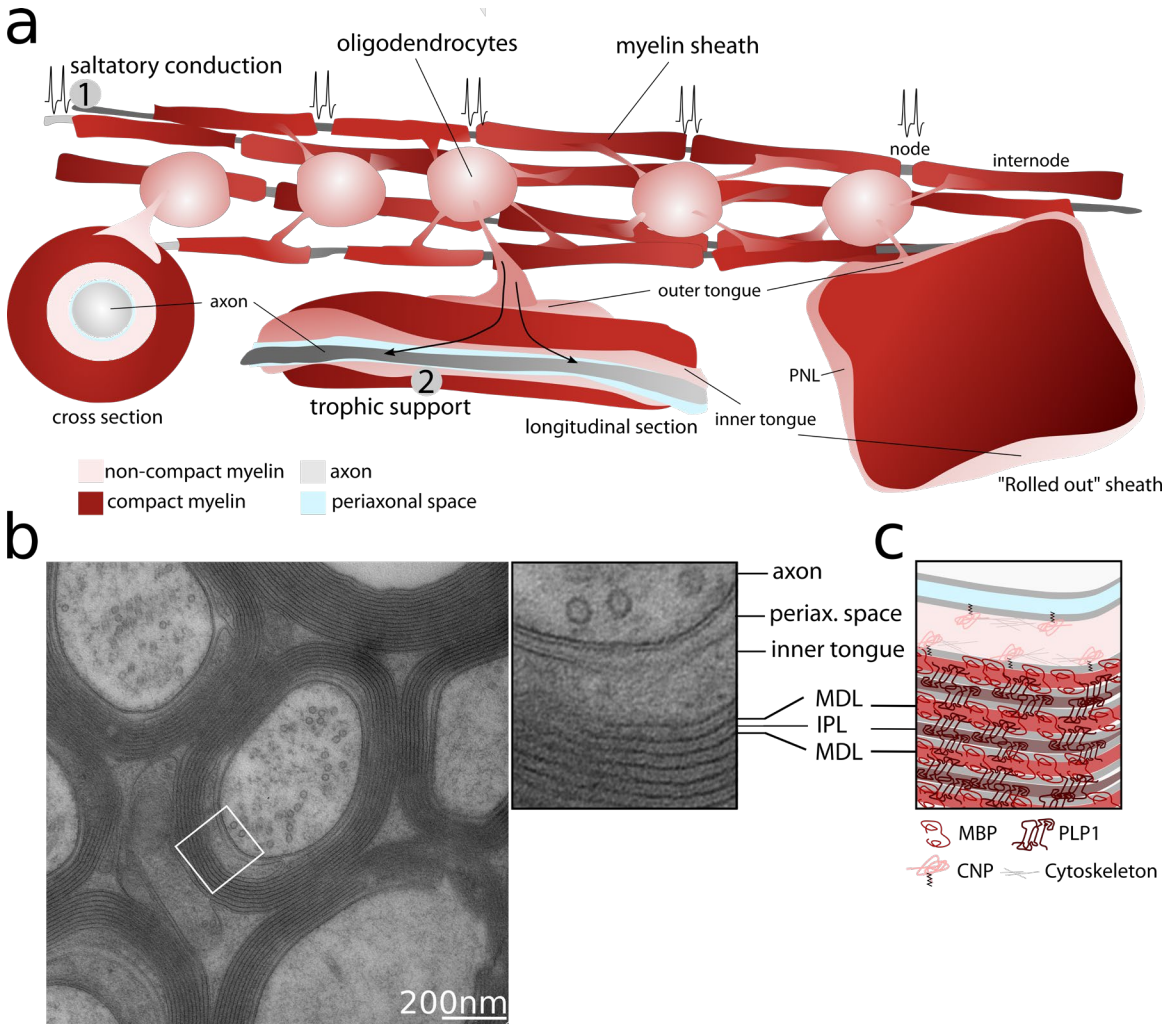

Figure 1.1 From structure to function: oligodendrocytes and myelin. (a) Scheme illustrating a stretch of white matter in which multiple oligodendrocyte myelinate axonal segments. Lower part shows schemes of cross and longitudinal sections of a myelinated axon and a hypothetically "unrolled" myelin sheath. Note the continuity of the myelinic channel system composed of inner and outer tongue and paranodal loops with the oligodendrocyte cytoplasm. The two main functions of myelin that are linked to the two different myelin domains (compact and non-compact) are illustrated: (1) Compact myelin enables saltatory impulse propagation. (2) Non-compact myelin (inner tongue, outer tongue, paranodal loops (PNL)) enables trophic support of axons that become largely isolated from the extracellular environment. **(b)** High pressure freezing electron microscopy superbly preserves myelin ultrastructure (mouse optic nerve; image by Wiebke Möbius). In the blow-up in the middle ultrastructural details of the myelin structure become visible. **(c)** Schematic representation of the myelin sheath as seen in the blow-up. The major dense line (MDL) represents the cytoplasmic leaflets of two opposing myelin membranes tightly zipped by the myelin basic protein (MBP). The intraperiod line (IPL) represents the two opposing extracellular leaflets of two neighbouring myelin membranes joint by the myelin proteolipid protein 1 (PLP1). 2′-3′ Cyclic nucleotide phosphodiesterase (CNP) interacts with the membrane (via isoprenylation) and the cytoskeleton to maintain non-compacted myelin regions such as the inner tongue. Schematic representations of MBP, PLP1 and CNP are inspired/based on structural studies.

proximity to the axon. The paranodal loops are tethered to the axon by the *trans* interaction of the adhesion molecule Neurofascin in its oligodendrocyte-specific 155kDa isoform with Contactin and Contacting associated protein (CASPR) in the axonal membrane (Charles et al. 2002). These protein complexes form septate-like junctions that restrict lateral diffusion of membrane proteins e.g. Nav1.6 sodium channels that are tightly clustered at nodes of Ranvier (Rasband and Peles 2016). To a certain degree, these septal junctions also electrically seal the nodal areas due to hindrance of ion fluxes between the periaxonal space and the extracellular space (Cohen et al. 2020).

Myelin membrane zipping is mediated by the functions of the most abundant CNS myelin proteins, myelin basic protein (MBP) and proteolipid protein 1 (PLP1) – reviewed in more detail in the next paragraphs (Fig1.1b). In the PNS, the P0 protein additionally joins this group. Based on their large abundancy in white matter areas, molecular biologists were able to clone the cDNA for the structural myelin proteins relatively early on (Lemke 1988). Likewise, spontaneously occurring mouse mutants with neurological diseases that could be traced back to defects in white matter were instrumental in the identification and functional studies of myelin proteins. The most studied of these are *shiverer* and *jimpy* mice that were shown to harbour mutations in the two most abundant structural proteins of CNS myelin, MBP (*shiv*) (March, Biddle, and Miller 1973) and PLP (*jp*) (Sidman, Dickie, and Appel 1964).

1.1.2 Functions of the major myelin proteins MBP, PLP and CNP

Myelin basic protein (MBP)

MBP was first isolated, and its amino acid (AA) sequence determined from extracts of bovine spinal cord (Eylar et al. 1971). According to latest proteomic approaches, MBP constitutes 30% of the total CNS protein in the c57Bl/6N mouse (Jahn et al. 2020). MBP exists in several isoforms (14 – 21.5kDa) as a result of multiple splicing and the major isoform of MBP is of 18.5kDa in humans. MBP is of exceptional positive charge with a high - name-giving - basic isoelectric point at pH10 (Boggs 2006). MBP belongs to the class of intrinsically disordered proteins, but upon membrane interaction and charge neutralisation experiences a great conformational shift and forms c-like structures (Han et al. 2013) (Fig1.1b). In myelin, MBP interacts with negatively charged head groups of phospholipids in the cytoplasmic leaflet and forms a tight protein meshwork where single MBP molecules likely interact with both opposing leaflets. A detailed molecular mechanism of membrane zipping has been recently proposed by the Kursula Lab (Raasakka et al. 2017).

As shown by the analysis of the recessive, spontaneously occurring *shiverer* mutant that lacks MBP expression (March, Biddle, and Miller 1973), MBP is essential for the formation of compacted myelin membranes in the CNS, but surprisingly not in the PNS (Kirschner and Ganser 1980). If myelin membranes are present in *shiverer* mice, these are not appropriately compacted forming so-called myelin whorls. *Shiverers* were found to completely lack MBP expression due to a large deletion in the *mbp* locus on chromosome 18 (Roach et al. 1983). *Shiverer* mice present with the name-giving generalised action tremors and seizures starting at 2 weeks of age that eventually lead to premature death at around 3 months.

Proteolipid protein 1 (PLP1)

PLP is a 30kDa, very hydrophobic protein that belongs to the class of tetraspan membrane proteins with both N and C-termini located in the cytoplasm. With 38% of total protein, PLP presents the most abundant myelin protein (Jahn et al. 2020) while it is only present in trace amounts in the PNS (0.2% of total protein) (Siems et al. 2020). PLP was shown to be the affected gene product in *jimpy* (Nave et al. 1986; Willard 1985; Milner et al. 1985) and *rumpshaker (rsh)* mice (Griffiths et al. 1990; Schneider et al. 1992) as well as the in the rat mutant *myelin-deficient (md)* (Duncan, Hammang, and Trapp 1987). For all mutants, it became clear relatively early on that the disease-causing mutation is X-chromosome linked and indeed the PLP sequence was mapped to the long arm of the X-chromosome (Milner and Sutcliffe 1983). The corresponding AA sequence was determined shortly thereafter (Jollès, Nussbaum, and Jollès 1983; Stoffel et al. 1983). By alternative splicing, the PLP gene also gives rise to a shorter protein variant that lacks an intracellular loop, designated DM-20 (Nave et al. 1987a). Similar to *shiverer* mice, *jp* mice and *md* rats exhibit severe hypomyelination, resulting in tremors, seizures and eventually premature death at 4 weeks of age. *Rsh* mice generally exhibit a less severe phenotype of hypomyelination and show a normal life span. However, in contrast to *shiverer* mice, *jp/md/rsh* myelin (if formed) shows correct zipping of the cytoplasmic leaflets, but abnormalities in the IPL (Griffiths et al. 1990). This is in accordance with a role of PLP in mediating compaction of the extracellular leaflets. In *jimpy* mice, a point mutation leads to inactivation of a splice site

that alters the reading frame to encounter a premature stop codon (Nave et al. 1987b). In *md* rats, a point mutation in PLP (T75P) hinders PLP integration into the plasma membrane (Boison and Stoffel 1989).

Interestingly, the severe hypomyelination phenotype in PLP mutant animals is not a result from loss of normal protein function but stems from toxic gain of function effects: PLP mutations are linked to excessive ER stress due to misfolding and accumulation of PLP in the ER that is cytotoxic to oligodendrocytes and leads to apoptosis (Dhaunchak and Nave 2007). In fact, targeted null mutations of PLP do not induce oligodendrocyte cell death and myelin appears grossly normal and appropriately compacted (Griffiths et al. 1998; Klugmann et al. 1997). The IPL, however, is also here less distinct and of reduced physical stability (Klugmann et al. 1997). Additionally, both *jp/md* and *rsh* associated PLP forms are impaired in cholesterol-binding and show reduced association with lipid rafts leading to enhanced PLP turnover (Krämer-Albers et al. 2006). Along this line, cholesterol-PLP interactions seem to regulate cholesterol levels in myelin (Werner et al. 2013).

Intriguingly, though myelin can be assembled properly, axonal swellings accumulating multivesicular bodies and mitochondria are frequently observed in PLP null mice (Griffiths et al. 1998; Trevisiol et al. 2020). These accumulations are particularly abundant in the distal paranodal/juxtaparanodal axonal stretches and are associated with decreased axonal transport rates as revealed by FITC-conjugated cholera toxin tracing of retinal ganglion axons (Edgar, McLaughlin, Barrie, et al. 2004). Elegant experiments using PLP heterozygote females in which PLP deficient and PLP wildtype myelin co-exist due to random X-chromosome inactivation as well as transplantation approaches of PLP null oligodendrocytes into *shiverer* mice demonstrated that PLP related axonal pathology is confined to overlaying PLP deficient myelin (Edgar, McLaughlin, Yool, et al. 2004; Griffiths et al. 1998).

Jimpy, *myelin deficient* and PLP overexpressors (Karim et al. 2007) are commonly used as animal models for Pelizaeus-Merzbacher-Disease (PMD), a rare and very severe genetic leukodystrophy with hypomyelination (Inoue 2017). Typically, PMD manifests in early infancy with nystagmus, developmental delay, severe motor disabilities and affected children usually do not survive until adolescence. Akin to *jp/rsh*, affected children suffer from either duplication (Ellis and Malcolm 1994) or point mutations in the PLP gene. PMD phenotypes in mice are ameliorated by feeding a cholesterol-enriched diet which partly restores PLP trafficking to the myelin membrane (Saher et al. 2012). Reflecting the milder phenotype of PLP null mice, PLP pure loss of function mutations typically give rise to a milder form of the disease also referred to as spastic paraplegia type 2.

2',3'-Cyclic nucleotide phosphodiesterase (CNP)

After MBP and PLP, CNP is the most abundant myelin protein making up 5% of total myelin protein (Jahn et al. 2020). CNP, however, is a cytoplasmic protein, that is, in contrast to MBP and PLP, not located to compacted myelin membranes but confined to non-compacted myelin areas (oligodendroglial cytoplasm and the myelinic cannels as its extensions). CNP cDNA clones were isolated and sequenced in 1992 (Douglas et al. 1992; Monoh et al. 1993). Two isoforms of CNP exist, termed CNP1 (46kDa) and CNP2 (48kDa) as a result of alternative translation start sites (O'Neill et al. 1997). The longer isoform CNP2 harbours additional 20 AA at the N-terminus with a mitochondrial targeting motif. As the name suggests, CNP's C-terminal half displays 3'-phosphoesterase activity against cyclic 2'-3' nucleotide monophosphate (2'-3'-cNMPs) i.e. it can hydrolyse cyclic nucleotides in which phosphate is covalently bound to both the 2' and 3' ribose site in nucleotides (Drummond, Iyer, and Keith 1962). Potential substrates for this rather peculiar enzyme activity include certain intermediates in tRNA splicing as well as 2'-3'-cAMP molecules that have been recently identified in the brain. 2'-3'-cAMP are positional isomers of 5'-3'-cAMP that likely originate from mRNA degradation upon injury and exhibit mitochondrial toxicity (Jackson 2011; Verrier et al. 2012). Oligodendrocyte derived CNP helps detoxifying this waste product into neuroprotective adenosine (Verrier et al. 2013). CNPs N-terminal domain though structurally less well described appears to function as RNA binding moiety and is also capable of mediating self-dimerisation of CNP as well as binding to calmodulin (Myllykoski et al. 2012; Raasakka and Kursula 2014). CNP's N-terminus also exhibits microtubule-associated

protein (MAP) like activity and associates both with tubulin and the actin cytoskeleton (De Angelis and Braun 1996). Since CNP is additionally tethered to the intracellular leaflet of the plasma membrane via isoprenylation/palmitoylation of its C-terminus (Braun et al. 1991; De Angelis and Braun 1996), CNP acts as a membrane anchor for the cytoskeleton. Actin binding activity was recently shown for the C-terminus of CNP as well (Snaidero et al. 2017). Based on its cytoskeletal association, RNA binding capability and potential RNA metabolism enzymatic activity, it is hypothesised that CNP is involved in trafficking RNAs in the myelin sheath. Such a role seems plausible as RNA transport and local translation of myelin genes such as MBP in the myelin sheath has been observed (Ainger et al. 1993; Li, Zhang, et al. 2000; Yergert et al. 2021; Torvund-Jensen et al. 2014).

While the role of CNP in RNA trafficking and metabolism as well as its enzymatic activity is severely understudied, the structural role of CNP is better understood. Using high-pressure freezing (HPF)-EM of mouse spinal cord, it was shown that CNP works to maintain the cytoplasmic nanochannel system in an "open" configuration counteracting the membrane zipping functions of MBP (Snaidero et al. 2017). The generation of CNP deficient animals by insertion of a Cre-cassette into the endogenous *cnp* locus has been instrumental in elucidating this described *in vivo* function of CNP (Lappe-Siefke et al. 2003). Accordingly, CNP deficient animals showed reduced amounts of cytoplasmic channels in myelin which could be alleviated by reducing MBP amounts in MBP heterozygote/CNP null crossbreedings. Interestingly, this also reduced pathology associated with the CNP null phenotype such as severe gliosis and formation of axonal swellings. Only very recently, a human leukodystrophy has been identified that is also caused by CNP loss of function in a consanguineous family from Oman (Al-Abdi et al. 2020).

1.1.3 Beyond insulation: novel functions of oligodendrocytes

Axonal pathology is a well-known accompanying phenomenon of myelin injury e.g. in Multiple Sclerosis (MS). But why exactly myelin defects entail axonal distress remains incompletely understood. Besides harmful exposure to immune cell mediators secreted by activated macrophages/microglia (Nikić et al. 2011; Sorbara et al. 2014), another plausible mechanism for this is a direct disturbance of axon-supportive functions of oligodendrocytes - independent of breakdown of myelin as insulator. The analysis of PLP and CNP null mice which assemble normal appearing myelin but show progressive axonal pathology provided first evidence for an uncoupling of myelin-forming function and axonal support functions of oligodendroglia (Lappe-Siefke et al. 2003; Griffiths et al. 1998). Likewise, in experimental autoimmune encephalomyelitis (EAE), axonal distress arises independent of full demyelination of the overlaying internode (Nikić et al. 2011) and the full loss of compact myelin does not necessitate axonal pathology as *shiverer* mice remain shielded from axonal pathology. These complementary observations, early on, illustrated that oligodendrocytes are likely to fulfil functions that are important for axonal health (disturbed in CNP and PLP deficient myelin) (Fig1.1a), but are independent of enabling saltatory conduction by insulating properties of compact myelin (disturbed in *shiverer* mice).

Transfer of metabolites from oligodendrocytes to axons

Axonal spheroids/swellings, the primary phenotype assessed to study axonal pathology, are commonly viewed as being the result of axonal transport deficits. In addition to direct disturbance of axonal transport tracks i.e., microtubules, energy shortage can slow down axonal transport rates (Sorbara et al. 2014). A prerequisite for an energetic support function of oligodendrocytes to ensheated axons are direct contact sites of oligodendrocytes to axons beyond inert myelin. Indeed, as outlined above, the cytoplasm-filled myelinic channel system with direct contact to the axon represents a direct communication pathway between axons and oligodendrocytes, in which a plethora of metabolites, proteins or ions could be transferred (Fig1.1). The existence of direct metabolic support mechanisms to myelinated axons seems plausible considering that in well myelinated axons large amounts of the axon become physically separated from the extracellular milieu and with that lose rapid access to metabolites (Nave 2010). Likewise, energetic demands of axons likely cannot be met by diffusion of metabolites from the distant neuronal somata. In seminal work by the Rothstein

and Nave lab, it was shown that akin to the astrocyte-neuron-lactate-shuttle glycolytic oligodendrocytes metabolically support axons by providing glycolysis endproducts such as pyruvate/lactate to axons (Lee et al. 2012). More specifically, Fünfschilling et al. showed that oligodendrocytes survive *in vivo* in the absence of functional mitochondrial respiration in conditional COX10 mutant mice (Fünfschilling et al. 2012) suggesting that post-myelination oligodendrocytes do not rely very much on respiration but are rather intrinsically glycolytic cells. They proposed a model in which glycolytic oligodendrocytes secrete lactate/pyruvate through monocarboxylate transporters (MCTs) to the axonal compartment where it is rapidly metabolised by active neurons. Befittingly, Lee et al. studied MCT1 localisation in oligodendrocytes and could show that indeed MCT1 is majorly expressed in oligodendrocytes and that its downregulation by *Mct1* $^{+/-}$ genotype causes axonopathy. Importantly, they verified their results by reducing MCT1 expression specifically in oligodendrocytes using a lentivirus-mediated *mbp* ::shRNA against MCT1 that was able to replicate the axonal phenotypes (Lee et al. 2012). Later, it was shown that the rate of oligodendroglial support is adjusted to meet the metabolic needs of axons dependent on their electrical activity (Saab et al. 2016). Here, adaxonally located NMDA receptors in the inner tongue of oligodendrocytes respond to trace amounts of glutamate released from the axon upon neuronal activity. In a calcium dependent fashion, this regulates the surface levels of the glucose transporter 1 (Glut1) in oligodendrocytes eventually controlling lactate/pyruvate production that can be shuttled to axons (Saab et al. 2016). The preferred metabolite that is transferred to the axonal compartment seems to vary in different white matter tracts. Using direct filling of oligodendrocytes via patch-pipettes, it was shown that in the corpus callosum - different to previous optic nerve bath application setups - compound action potentials (CAPs) during glucose deprivation were rescued more efficiently by filling the oligodendrocyte glial networks with glucose rather than lactate or pyruvate (Meyer et al. 2018). Paradoxically, MCTs were however still required for the prevention of CAP decline (Meyer et al. 2018).

Direct evidence for a role of oligodendrocytes in axonal ATP metabolism - beyond measuring CAPs as surrogate marker for sufficient energetic status - was made possible by genetically introducing a FRET-based ATP sensor into neurons/axons (Trevisiol et al. 2017). Indeed, ATP metabolic imaging in the optic nerve proved more sensitive than CAP measurements in reporting axonal energy shortage in response to inhibited lactate metabolism (Trevisiol et al. 2017). Using this technique to study axonal ATP metabolism in PLP$^{-/y}$ mice, it was found that baseline ATP levels are reduced and vary greatly along axons in PLP-deficient animals (Trevisiol et al. 2020). This study very clearly showed that compromising oligodendrocyte functions other than forming compact myelin (which is present in PLP deficient mice) directly impacts axonal energetic status. Independent support of a role of PLP in axonal energy support is derived from studies in which PLP is replaced by the PNS myelin protein P0. These mice designated P0-CNS show similar, but more progressive phenotypes compared to PLP null mice and P0 apparently cannot substitute for PLP function in the CNS (Yin et al. 2006). Also here, ATP levels in optic nerve lysates were reduced (though a cell type specificity is lacking using this method) (Yin et al. 2016).

Exosomes as a route for trophic support

Another route by which oligodendrocyte-to-neuron transfer can occur is likely the release of exosomes, 50-100nm vesicular particles derived from fusion of multivesicular bodies with the plasmamembrane (Krämer-Albers et al. 2007). Oligodendroglial exosomes are frequently found in the inner tongue and are thereby ideally localised to be transferred to ensheathed axons (Frühbeis et al. 2013). Intriguingly, exosome release is akin to lactate/pyruvate transport via MCT1, regulated in an activity-dependent manner via calcium entry through ionotropic glutamate receptors (Frühbeis et al. 2013). Oligodendroglial exosomes seem to carry both proteins and mRNA that are still functional after uptake by neurons as revealed by elegant use of the Cre-recombinase reporter system (Fröhlich et al. 2014; Frühbeis et al. 2013). Among these are classical myelin proteins such as PLP, CNP, MBP and Sirtuin-2 (SIRT-2) but also chaperons (HSP70, HSP90) and interestingly oxidative stress related proteins such as Glutathione S-transferase P (GSTP1), Peroxiredoxin1/2, catalase and superoxide dismutase. In fact, it was shown that oligodendrocytes boost axonal antioxidant defence by secreting ferritin heavy chain in exosomes (Mukherjee et al. 2020). In myelin-dysfunction models that manifest with axonal degeneration such as CNP and PLP null mice, exosome release is significantly

hampered, and vesicle content is qualitatively and quantitatively reduced. Accordingly, axonal transport deficits evoked by energy deprivation of neuronal cultures are less efficiently rescued by CNP and PLP deficient oligodendrocyte derived exosomes as compared to wildtype exosomes (Frühbeis et al. 2020).

1.1.4 The developing myelin sheath

Myelination is a relatively late event in neurodevelopment that follows a precise spatiotemporal pattern. In rodents, myelination starts very shortly before birth and commences in the following early postnatal days in the spinal cord and nearly completes at 2 months of age with the myelination of neocortical regions. This follows an overall peripheral-central, inferior-superior and posterior-anterior gradient. Myelination rate peaks at three weeks of age with a preceding cell state change to oligodendrocytes (Semple et al. 2013). In humans, these processes are extended, and myelination continues well into adolescence and adult stages. Likewise, myelination in human development starts already *in utero* at around gestation week 30 reaching its peak at 2-3 years of age (Semple et al. 2013).

Oligodendrocyte progenitor cells

Oligodendrocytes are derived from a glial progenitor cell termed oligodendrocyte precursor cells (OPCs) or NG2 glia due to the abundant expression of NG2/CSPG4 proteoglycan on their surface. OPCs first start to appear in the ventral ventricular zone at embryonic day 12.5 (E12.5) in mice after which they migrate into their destined regions all over the neural parenchyma. The "first wave" of differentiated OPCs is then partly replaced by a "second wave" of dorsally-derived, newly differentiated OPCs that will displace ventral OPCs primarily in dorsal areas (Bergles and Richardson 2016). While these processes proceed in an analogous fashion in the telencephalon and the developing spinal cord, in the forebrain a "third" wave of OPCs is generated postnatally in the dorsal cortical ventricular zone that will eventually eliminate the second wave OPCs in the pallium i.e., cortex, hippocampus and subcortical white matter (Kessaris et al. 2006). This population of OPCs (as well as other cells in the dorsal telencephalon) is characterised by expression of the homeobox protein EMX1 and constitutes around 80% of all cortical OPCs as revealed by a dual Cre-reporter-system fate mapping (Tripathi et al. 2011).

In contrast to other progenitor cells, OPCs remain as an abundant cell population in the adult brain and represent around 5% of cells (Fernandez-Castaneda and Gaultier 2016). They rapidly respond to injuries by proliferation and differentiation into oligodendrocytes for example in demyelinating scenarios such as EAE or Cuprizone treatment. However, their large abundancy in adulthood that by far exceeds the necessity of oligodendrocyte replenishment points towards OPC functions beyond oligodendrocyte/myelin generation. These functions are only about to be unravelled and OPCs by now have been shown to fulfil functions such as antigen representation, modulation of neuroinflammation (Kirby et al. 2019), OPC-neuron crosstalk at synapses (Bergles et al. 2000) and the regulation of the BBB (Akay, Effenberger, and Tsai 2021). Differentiation of OPCs into oligodendrocytes is regulated by extrinsic factors (such as LINGO-1, GPR17 signalling, neuronal activity) and intrinsic factors such as epigenetic regulation (Emery 2010). OPCs are early on identifiable by the expression of the transcription factor OLIG2, OLIG1 and SOX10 that also remain expressed in mature oligodendrocytes (Lu et al. 2002). Induction of terminal differentiation to oligodendrocyte requires exit from the cell cycle and derepression/induction of oligodendrocyte gene products (Emery and Lu 2015). First, OPCs differentiate into pre-myelinating oligodendrocyte that start to generate numerous cell processes which is accompanied by downregulation of repressive transcription factors ID2/3, SOX5/6 and HES5, the upregulation of CNP and the transcription factor myelin regulatory factor (MYRF). MYRF controls the transcription of a variety of structural myelin proteins such as MBP and PLP as well as lipid metabolism genes and it is critical for normal myelin development (Emery et al. 2009).

How to wrap a sheath

For the process of myelin wrapping itself several models have been proposed: the "carpet crawler" model proposed that the myelinating process contacts the soon-to-be ensteathed axon, extends to the full size of the future internode and then the tip process crawls underneath the membranes which creates the wraps (Bunge, Bunge, and Ris 1961). Conversely, the "liquid croissant" model based on live-cell imaging in myelinating cerebellar slices proposed that a smaller tip of the inner tongue wraps around the axons with subsequent lateral growth giving rise to a croissant-like appearance of the developing sheath (Sobottka et al. 2011). Snaidero and colleagues confirmed and refined this model by performing focused ion beam- serial electron microscopy (FIB-SEM) on high pressure frozen samples that allows for superior ultrastructural preservation (Snaidero et al. 2014). They showed that membrane growth occurs at the inner tongue in a PIP_3-dependent manner and highlighted the importance of cytoplasmic channels as means for cargo delivery to the sheath growth zone (Snaidero et al. 2014). These cytoplasmic channels are abundantly found in the developmental myelin sheath where multiple cytoplasmic cannels cross the prospective internode. Gradually, these channels close until the paranodal loops and inner and outer tongue remain as uncompacted regions at the rim of the myelin sheath. Overall, compaction of the myelin layers here follows an outward to inward gradient with "older" membrane being compacted first (Snaidero et al. 2014).

1.1.5 The degenerating myelin sheath

The long lifetime of myelin and oligodendrocytes

Once fully developed and compacted, myelin seems to be a rather inert cellular specialisation. Indeed, metabolic pulse-chase experiments using ^{15}N isotope labelling in the rat brain revealed that the myelin structural proteins MBP, PLP, MOG, CNP, ENPP6 (Xiao et al. 2016) and SIRT2 together with nuclear proteins such as histones belong to a class of very long-lived proteins (Toyama et al. 2013). For example, 6 months after chase around 20% of MBP and PLP peptides are still ^{15}N labelled indicative of slow turnover of compact myelin. While this finding is comprehensible for MBP and PLP due to difficult turnover logistics of compacted membrane stacks, it was at least surprising for CNP, SIRT2 and ENPP6 which are not part of compact myelin, but cytosolic proteins that reside in the cytoplasmic channels. Despite long lifetimes, myelin proteins are, however, continuously transcribed, and synthesised. The generation of conditional *shiverer* mice, in which the MBP locus is floxed, and MBP expression can be silenced upon tamoxifen-inducible Cre-recombination using the oligodendrocyte specific PLP-CreERT2 driver line, revealed that continuous expression of MBP and its incorporation into myelin is required for myelin maintenance (Meschkat et al. 2020). In this model, MBP protein levels drop to around 25% 6 months after tamoxifen induction and internodes shortened to 50% 5 months after induction (Meschkat et al. 2020). In a very similar experimental setup using mice with a floxed PLP allele, Lüders et al. showed that PLP protein levels dropped to 50% 6 months after tamoxifen-mediated recombination (Lüders et al. 2019). These findings confirm the longevity of myelin proteins, yet highlight that myelin is still continuously turned over.

Similar to myelin proteins, myelin lipids exhibit an exceptional long lifetime: using isotope labelling of water (deuterium) and mass-spectrometry, the half-life of myelin cholesterol in adult mice was reported to be almost a year (Ando et al. 2003). Phosphatidylcholine/ethanolamine showed higher turnover rates of approximately 3 weeks and cerebrosides of 3 months (Ando et al. 2003). A long lifetime makes both proteins and lipids vulnerable to oxidative damage that alters them structurally and potentially interferes with proper functioning (Hamilton et al. 2016). In the case of proteins, age-related posttranslational modifications can lead to structural changes and misfolding (Truscott and Friedrich 2018). Indeed, lipid peroxidation products are found in striking higher amount in the aged brain and myelin is rendered more instable (Chia, Thompson, and Moscarello 1983). Likewise, there are degradative changes to myelin protein such as CNP and MBP as

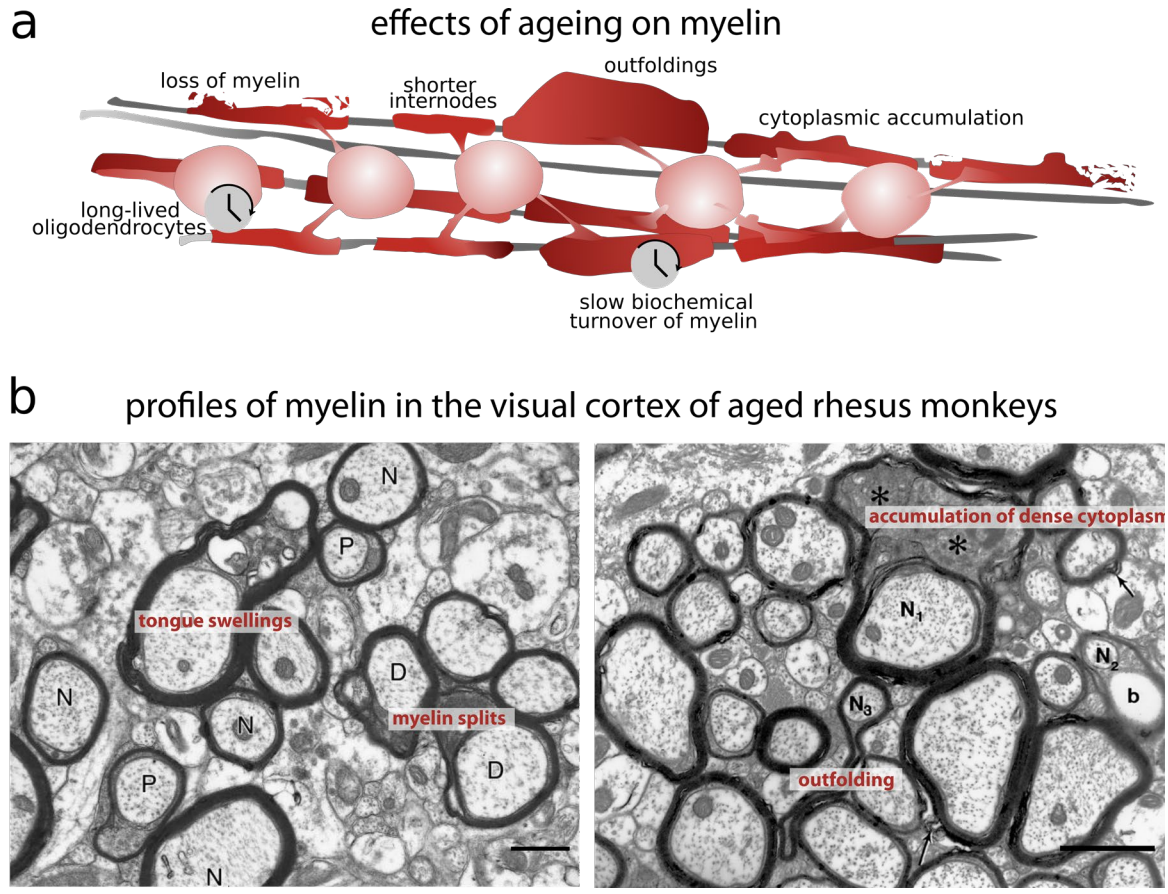

Figure 1.2 The wear and tear of time on myelin and oligodendrocytes (a) Scheme illustrating a stretch of ageing white matter with multiple age-related structural alterations. The long lifetime of oligodendrocytes and slow biochemical turnover of myelin (time icons) make myelin vulnerable to deterioration during ageing. Structural defects include loss of myelin, shorter internodes, myelin outfoldings and accumulation of dense cytoplasm. **(b)** Electron micrographs of myelinated fibres in the visual cortex of aged rhesus monkey. Multiple pathological features of aged myelin are visible: Swellings of the inner tongue, myelin splits with the following accumulation of dense cytoplasm and the formation of redundant myelin (outfoldings). Left: Adapted from (Peters 2002). Right: Adapted from (Peters 2009). Scalebar corresponds to 1µm.

evidenced by the accumulation of degradation products (Hinman et al. 2008). The measurement of protein amounts of classic myelin proteins with age has yielded conflicting results and does not allow for a conclusive statement at this point (Hinman and Abraham 2007). For example, downregulation of CNP with age has been reported in mouse (Hagemeyer et al. 2012), while in rhesus monkey an upregulation occurred (Hinman et al. 2008). However, considering the long lifetime of proteins changes in myelin composition are highly likely.

Not only the myelin components but also oligodendrocytes are astonishingly long-lived (Fig1.2a): elegant experiments using carbon-dating of ^{14}C content in nuclei and myelin derived from nuclear bomb testing in the 1960s revealed that only 0.3% of all oligodendrocytes in the corpus callosum are annually turned over at adult ages (after 5 years of age) (Yeung et al. 2014). This means that at age 90, still approximately 75% of the corpus callosum oligodendrocyte population is as old as their human carrier. In regards to their lifetime, the majority of oligodendrocytes are, therefore, very similar to postmitotic neurons. In the pertaining study, biochemical myelin isolation revealed that myelin membranes do not contain significant amounts of ^{14}C indicating that myelin is completely turned over in a lifetime (Toyama et al. 2013) – paralleling the findings of continuous myelin synthesis by Meschkat and colleagues.

Old oligodendroglial cell bodies are likely to experience age-related changes to their genome and transcriptome. Single-cell transcriptomic analysis of aged mice revealed that similar to other cell types aged oligodendrocytes upregulate ribosomal transcripts during ageing hinting towards heightened protein biosynthesis in aged oligodendrocytes presumably as a stress response (Ximerakis et al. 2019). An interesting study reported, furthermore, the loss of epigenetic marks (decline in histone methylation and increases in acetylation) in aged oligodendrocytes leading to the re-expression of OPC markers (Shen et al. 2008). However, this study worked with 8-month-old mice for the aged timepoint which is at most mature/middle-aged. If this applies to appropriately aged mice (> 2 years) remains to be investigated. Ageing is also well known to reduce remyelination efficiency hinting towards age-dependent changes to oligodendrocytes and OPCs (Doucette, Jiao, and Nazarali 2010).

Decline in brain myelin content with age

Not surprisingly, pathological phenotypes of myelin are accumulating in the aged brain (Fig.1.2). In fact, white matter seems to be primarily affected by ageing – much more so than grey matter. Accordingly, magnetic resonance imaging (MRI) studies have shown that there is a starker reduction in white matter volume than grey matter volume in both humans and monkeys (Guttmann et al. 1998; Wisco et al. 2008; Salat, Kaye, and Janowsky 1999; Gunning-Dixon et al. 2009). Over the lifetime, myelination/myelin content follows an inverted U-shape trajectory starting to decline approximately in the 5th decade of life assessed by MRI (Bartzokis et al. 2004; Yeatman, Wandell, and Mezer 2014; Westlye et al. 2010). Diffusion tensor imaging (DTI) is superior to T1-weighted MRI to detect early changes in white matter (Giorgio et al. 2010). DTI is based on the phenomenon that water molecules in axonal and myelinated tracts experience anisotropic diffusion i.e. water molecules diffuse faster along the axis with low lateral diffusion (O'Donnell and Westin 2011). Though formally myelin changes cannot be distinguished from axonal changes in this imaging modality, reduced fractional anisotropy is a hallmark of demyelinating diseases, is severely reduced in *shiverer* mice (Tyszka et al. 2006) and is in general considered a "biomarker" of white matter dysfunction. DTI studies very consistently report reduced fractional anisotropy and concurrent increases in radial diffusivity indicative of myelin damage that are even earlier detectable than volume changes in white matter (Sullivan and Pfefferbaum 2011; Cox et al. 2016; Xie et al. 2016; Westlye et al. 2010). White matter hyperintensities are also regularly seen in the aged human brain which are considered consequences of cerebral small vessel disease and white matter hypoperfusion (Prins and Scheltens 2015).

There certainly is regional variability when it comes to age-related effects on myelin given the high organisational degree and regional specialisation of the brain. Anterior fibre tracts in the subcortical white matter seem to be especially vulnerable to age-related changes as revealed by DTI (Engelhardt, Moreira, and Laks 2009; Xie et al. 2016; Bartzokis et al. 2004; O'Sullivan et al. 2001). These include subcortical association, projection and commissural fibres (forceps minor, genu corpus callosum) of the frontal and parietal lobe. Especially association fibres connecting brain regions intrahemispherically seem to be highly vulnerable to ageing (Cox et al. 2016). These fibres belong to a class of fibres that are myelinated relatively late in development while less affected fibre tracts have become myelinated earlier and more robustly. These findings gave rise to the idea that the retrogenesis/last-in-first-out model, which postulates that age-related decline mirrors developmental processes, also applies to brain ageing (Reisberg et al. 1999; Brickman et al. 2012). The decline in association fibres would then lead to cortical disconnection explaining overall cognitive decline in ageing (Bartzokis et al. 2004; O'Sullivan et al. 2001).

Volumetric shrinkage in white matter volume is likely to originate from loss of myelin or loss of myelinated axons. Indeed, using stereology on ultra-thin sections of human brain white matter Marner et al. estimated a striking 45% decrease in myelinated fibres total length between 80- and 20-year-olds (Marner et al. 2003). Again, thinly myelinated fibres seem to be most vulnerable here. Of note, macroscopic brain imaging studies such as DTI/MRI classically segment larger myelinated tracts such as different subcortical white matter tracts but fail to include intracortical myelin changes in the classical grey matter. Most of these studies are, therefore,

inherently limited to describing "proper" white matter. However, recent refinements in analysis allows for mapping of intracortical myelin content (Glasser and Van Essen 2011). Using this technique, it could be shown that also intracortical myelin content shows an inverted U-shape aged-dependent trajectory with association areas being the most affected by structural deterioration (Grydeland et al. 2013). Unfortunately, convincing microscopic studies that are able to validate these findings do not exist to my knowledge (despite (Lintl and Braak 1983)).

Ultrastructural alterations of myelin with ageing

Loss of myelin is likely to be preceded by structural deterioration of myelin. Seminal work by Allen Peters and his team described pronounced changes to myelin ultrastructure in the aged rhesus monkey brain as assessed by electron microscopy (Peters 2009, 2002) (Fig.1.2b): these include splits along the major dense line filled with accumulation of dark cytoplasm/vesicles and splits of the intraperiod line into so-called myelin ballons (that can reach >10µm in size!). Redundant myelin or myelin outfoldings are likewise frequently observed. Since these structures are also partially detectable in development, at a time when myelin is heavily generated, this could possibly hint towards ongoing remyelination attempts in the ageing brain. Similarly, paranodal profiles are increased in the aged brain, yet another hallmark of remyelination (Peters and Sethares 2002, 2003). Oligodendrocytes themselves also experience age-related accumulation of dense cytoplasmic inclusions (Peters 2009). More than rodents, rhesus monkeys are expected to reflect human brain ageing much more accurately, yet in comparison to humans offer the possibility for perfusion fixation and with that preferable ultrastructural preservation.

There is conflicted data on changes to the number of oligodendrocytes in the aged brain: while it was reported for humans that oligodendrocyte numbers decrease in the cortex (Soreq et al. 2017), there seems to be an increase in aged rhesus monkeys (Peters and Sethares 2004). In mice, the number of oligodendrocytes was reported to be unaltered (whole brain, RNA-seq, cell count, 20-month-old mice (Ximerakis et al. 2019)). Elegant *in vivo* imaging experiments by Jaime Grutzendler's group have shown that even in mice intracortical myelination in upper cortical layers also follows a U-shape trajectory with increases in myelin density until 20 month and striking decline afterwards. This was also paralleled by a decline in oligodendrocyte numbers in the analysed regions (Hill, Li, and Grutzendler 2018). These experiments also revealed the increased formation of myelin spheroids, focal enlargement of the myelin sheath as well the accumulation of myelin debris in the aged brain.

Consequences of myelin decay: neuroinflammation

These abundant age-related deteriorations to myelin are not going "unnoticed" in the brain. Age-dependent myelin damage has been convincingly shown to elicit astroglial and microglial responses with age. Electron microscopy as well as fluorescence microscopy analysis show the phagocytosis of myelin with age by both microglia (Hill, Li, and Grutzendler 2018; Safaiyan et al. 2016) and maybe surprisingly astrocytes (Nag and Wadhwa 2012; Peters and Sethares 2003). Microglial responses are indeed much more pronounced in the aged white matter than in grey matter in both mice and humans (Raj et al. 2017; Gefen et al. 2019; Safaiyan et al. 2021; Safaiyan et al. 2016). Complete phagocytosis of myelin membranes is comprehensibly challenging due to the high lipid amount and tight membrane stacking of myelin. In fact, myelin does not seem to be completely dismantled or broken down by microglia but elicits the accumulation of lipofuscin – intralysosomal, autofluorescent non-degradable lipid-protein-metal particles (Safaiyan et al. 2016). The authors hypothesised that this burdens the clearance function of microglia with age. This seems highly likely considering their unusual longevity and slow turnover for myeloid cells: carbon-dating experiments in humans have shown that microglia are on average 4 years old (in comparison to days - few weeks of other immune cells) with single cells being able to live decades (Réu et al. 2017). Likewise, genetic labelling approaches and longitudinal *in vivo* imaging experiments in aged mice demonstrated that in mice microglia frequently become 15 months and older and half of the microglia pool survives the entire lifespan of the mouse (Füger et al. 2017). Recently, Safaiyan and colleagues have expanded their findings on myelin-loaded

aged microglia using single cell transcriptomics by which they characterised the generation of aged white matter associated microglia (WAM). This microglia pool is highly activated and expresses genes involved in phagocytosis and lipid handling and arises - in concordance with an earlier study ((Poliani et al. 2015) in a Triggering Receptor Expressed On Myeloid Cells 2 (Trem2)-dependent manner (Safaiyan et al. 2021).

1.2 Alzheimer's disease

1.2.1. Overview and epidemiology

Alzheimer's disease (AD) is the most common neurodegenerative disease affecting around 50 million people worldwide at present (Prince et al. 2015). Its greatest risk factor is age and disease incidence increases sharply after the age of 65 with an exponential kinetic (doubling time ca. 5 years after age of 65) (Qiu, Kivipelto, and von Strauss 2009). Clinically, AD manifests as dementia (derived from latin *de* = "without" and *mens* = "mind") which describes a complex symptomatology characterised by the decline in overall cognitive abilities, memory retrieval/formation and language skills. Accompaniments of the neuropsychiatric spectrum include mood and sleep disturbances, depression, agitation, disinhibition and psychotic syndromes (Lanctôt et al. 2017). The impairments gradually worsen during the disease course, eventually leading to problems in everyday life and the sacrifice of independence.

AD patients typically require intense caregiving by family members and/or health care professionals in the form of permanent assistance or the move into a care institution. Family members experience, therefore, not only the psychological distress of witnessing a close relative fade away but must potentially put up with the high financial burden associated with intense care needs. The World Alzheimer Report 2015 calculated the global financial burden of dementia to 818 billion US$ and estimated its rise to 2 trillion US$ by 2030 (Prince et al. 2015). In the United Kingdom, societal dementia costs exceed the costs associated with cancer or heart disease which is unfortunately not reflected in the amount of research funding dementia research receives (Luengo-Fernandez, Leal, and Gray). Disease cases and associated costs are expected to rise in the future due to demographic changes in the world's population. With an ever-increasing number of older people throughout high- and low-income countries, estimated case numbers are projected to increase to approximately 75 million by 2030 and 130 million by 2050 (Prince et al. 2015). Interestingly, disease incidence appears to have fallen in high income countries in the past decades presumably due to higher educational training which conveys some sort of cognitive resilience towards the disease (Satizabal et al. 2016).

Medical diagnosis of AD is made by combined assessment of the patient's medical history, neurological evaluation, cognitive testing (e.g. mini mental state examination (MMSE) (Tombaugh and McIntyre 1992)), Mini-Cog) and possibly brain imaging. Computer tomography (CT) or magnetic resonance imaging (MRI) are specifically used to rule out other possible reasons for dementia such as cerebrovascular disease, tumours, or head traumas. Occasionally, positron emission tomography (PET) with tracer compounds is performed to specifically look at the protein aggregates accumulating in the AD brain. Likewise, cerebrospinal fluid (CSF) biomarkers can be assessed for signs of protein build-up in the brain. *Bona fide* diagnosis of AD, however, can only be achieved by *post-mortem* analysis of the patient's brain. Here, neuropathologists assess the presence of the two histopathological hallmarks of the disease: the overt accumulation of two proteins, amyloid beta (Aβ) and the microtubule associated protein tau. While amyloid-β aggregates are found in large parenchymal deposits known as amyloid plaques, tau protein piles up mainly intracellularly and primarily in neurons in so-called neurofibrillary tangles. Seminal work by Heiko and Eva Braak characterised the spatiotemporal pattern of amyloid and tau deposition during the disease course (Braak and Braak 1991) defining the Braak stages still used to assess neurofibrillary tangle pathology in the Amyloid-Braak-CERAD (ABC) scoring system today (Hyman et al. 2012). Tau tangles start to build up in in the transentorhinal and entorhinal cortex (stage I-II). Previous to this, pre-tangle stages are visible throughout the neocortex and tangles are formed in the locus coereleus (a-c, 1a-b pre-tangle stages). Tau tangles spread from there to the entire hippocampal formation/limbic system (Braak stage III-IV) and entire neocortex (Braak stage V-VI)

while they become more frequent in already affected regions. Dietmar Thal in more detail described the evolution of amyloid deposition (Thal et al. 2002). Amyloid deposition starts in the basal areas of the frontal and temporal lobe (phase 1) followed by expansion throughout the entire neocortex (phase 2), involvement of the striatum (phase 3) and finally all midbrain structures (phase 4), the brainstem and cerebellum (phase 5).

AD is no exception in the series of classical neurodegenerative diseases that are all characterised by abnormal protein aggregates that spread throughout the brain: Huntingtin aggregates in Huntington's, Lewy bodies composed of α-synuclein in Parkinson's, super-oxide dismutase aggregates in amyotrophic lateral sclerosis and prion proteins in Creutzfeldt-Jakob disease. Although there is still considerable debate on how exactly Aβ and tau cause the AD (specific) symptomatology and how these two pathological hallmarks are interrelated, massive protein aggregates will inevitably interfere with proper neuronal functioning and synaptic signalling and, in the late disease stage, lead to axonal and neuronal decay.

1.2.2 A short history of Alzheimer's disease

German physician Alois Alzheimer first described a case of a "peculiar disease of the cerebral cortex"/"Über eine eigenartige Erkrankung der Hirnrinde" in a short, not particularly well received lecture at a psychiatrist meeting in Germany in 1906 (Maurer, Volk, and Gerbaldo 1997). Later, he published his findings as a case report that should become the first description of a patient suffering from a particular form of presenile dementia (Alzheimer 1907). Later, Alzheimer's mentor Emil Kraepelin would name the disease after his mentee coining the eponym Alzheimer's disease (AD). In his report from 1907, he presented the case of Auguste Deter, an only 50-year-old woman presenting with gradually worsening signs of paranoia, forgetfulness, disorientation, and overall cognitive decline (Fig1.3a,b). After her death Alois Alzheimer was able to examine her brain and described brain atrophy, neuronal degeneration, and strange changes to the neurofibrils as investigated by silverstaining ("sehr merkwürdige Veränderungen der Neurofibrillen"). He also described the deposition of a peculiar substance forming miliary ("in the size of a millet grain") foci throughout the upper cortical layers (Fig1.3c,d).

Such aggregates had been previously reported in a study of aged epileptic patients by Blocq and Marinescu (Blocq and Marinescu 1892) and in reports of senile dementia by Emil Redlich in 1898 (Redlich 1898) and Oscar Fischer in 1907 (Fischer 1907) who already referred to them as "sclerotic miliar foci" and "plaques". Alzheimer's disciple Perusini described more cases of presenile dementia cases in the following years complementing Alzheimer's original description of Auguste Deter. Due to the young age of the patients, Alzheimer was originally convinced that the underlying disease etiology is different from that of senile dementia which seems to present with the same histopathological and clinical features (Alzheimer 1907). However, he acknowledged that earlier work from Redlich and Fischer described the same histopathological hallmarks (changes to neurofibrils and plaques) in senile dementia cases and discussed the implication of this (Alzheimer 1911). Already at the beginning of the 20th century these scientists revealed two different manifestations of the disease - a classification that outlasts until today: the first known as familial, early onset manifestation of AD and the other much more common sporadic type with senile onset. The neuropathological drawings and description of what will be later known as amyloid plaques and tau tangles are of mesmerising detail revealing important microscopic disease characteristics. Exemplarily, this early work documented a profound reaction of glia cells to plaques – so much so that Redlich hypothesised that the plaque is of glial origin (Redlich 1898). It describes the net-like nature of plaque reminiscent of bacterial films and the variety of plaque morphologies found in the brain. Using Bielschowsky's silverstaining technique

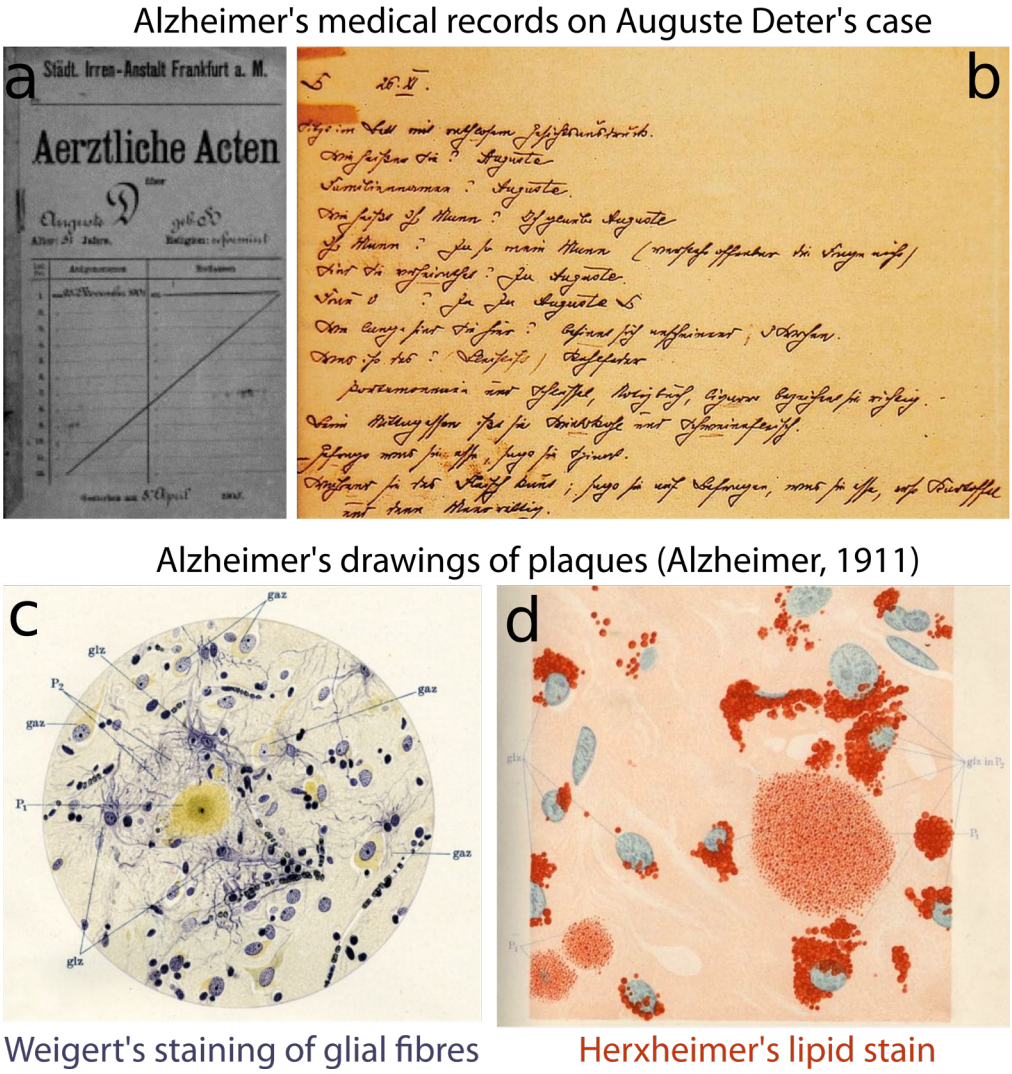

Figure 1.3 Original work by Alois Alzheimer (a) The rediscovered case file of Auguste Deter, Alzheimer's first patient. Taken from Maurer et al. 1997. **(b)** Handwritten report on an examination of patient Auguste Deter. The beginning reads: "What's your name? – Auguste. Family name – Auguste. What's your husband's name – I think, Auguste." Image is courtesy of Eli Lilly and Company. **(c,d)** Drawings of histopathological observations in different staining techniques of brain tissue of Alzheimer's patients. gaz: Ganglienzelle, glz: Gliazelle, P1: plaque core, P2: plaque rim. Association of glia cells (presumably astrocytes) with the amyloid plaque can be seen. Herxheimer's lipid staining reveals lipid accumulation in the plaque as well as in the surrounding glia presumably corresponding to lipofuscin

club-like neuronal processes were revealed to extend towards or surround the plaque. Astonishingly, based on these early microscopic observations, Alzheimer, Fischer, and others developed ideas and raised questions many of which would become central to the AD research field today: Where are plaques derived from and how do they form? Are plaques detrimental to the surrounding tissue or are they protective agents? What is the involvement of glia cells in the formation plaques? With their work these pioneers laid the foundations for the ensuing era of molecular research on AD that would unravel the molecular identity of the plaque-forming agent, decipher the genetics behind the familial form of the disease and eventually identify potential drug targets for the prevention or treatment of AD.

1.2.3 Amyloid beta and its precursor protein

Amyloid beta (Aβ) protein and its precursor protein amyloid precursor protein (APP) have been identified based on biochemical analysis of plaque content in the early 1980s. First, Glenner and Wong purified the content of cerebrovascular amyloid deposits from human autopsies and sequenced the first 24 amino acids of a highly enriched 4 kDa (A4) protein that they called amyloid beta protein (Glenner and Wong 1984). Later on, the same protein could be isolated from AD amyloid plaque cores (Masters et al. 1985). The identified protein sequence was subsequently used to construct cDNAs and identify a mRNA coding for a larger polypeptide - termed amyloid precursor protein - spanning the amyloid beta peptide sequence (Tanzi et al. 1987; Goldgaber et al. 1987; Kang et al. 1987). In addition to the originally described 695 AA long protein, two other APP isoforms were identified in the following years: a 751 AA (Ponte et al. 1988) and a 770 AA long protein isoform resulting from alternative splicing of Exon 7 and 8. In the nervous system, the 695 AA long protein is the predominant isoform.

Relatively early it became clear that AD-related neuropathology can be found in patients with trisomy 21 (Down Syndrome) at relatively early ages hinting towards a critical role of a faulty gene product from chromosome 21 in AD. Indeed, the amyloid beta protein gene was mapped to chromosome 21 (Tanzi et al. 1987; Goldgaber et al. 1987; Kang et al. 1987) pointing towards increased gene dosage as a potential mechanism driving amyloid accumulation in the Down Syndrome brain. Likewise, an autosomal dominant mutation linked to familial AD (FAD) was mapped to chromosome 21 (St George-Hyslop et al. 1987). Finally, a mutation in A4 could be identified in Dutch patients with an autosomal dominant form of cerebral amyloid angiopathy with cerebral haemorrhage (Levy et al. 1990; Van Broeckhoven et al. 1990) and a number of studies detected mutations in the APP gene in families affected by FAD (Murrell et al. 1991; Goate et al. 1991; Chartier-Harlin et al. 1991; Mullan et al. 1992; Hendriks et al. 1992). These studies affirmed a causal link between pathological amyloid deposition and changes to the A4 protein. Over the years many more of such mutations have been identified (for an overview see https://www.alzforum.org/mutations/app) and a few became known under eponyms derived from the origin of the families studied: London mutation V717I (Goate et al. 1991), Dutch mutation E693Q (Levy et al. 1990), Arctic mutation E693G (Nilsberth et al. 2001), Iberian mutation I716F (Guerreiro et al. 2010), Florida mutation I716V (Eckman et al. 1997) and most famously the Swedish double mutation KM670/671NL (Mullan et al. 1992) (Fig1.4a,b).

1.2.4 Amyloid precursor protein cleavage

The identification of the mRNA coding for a larger polypeptide from which the Aβ peptide originated from suggested that Aβ represents a cleavage product of a larger protein. Based on its protein sequence, APP was hypothesised to be a glycosylated integral membrane protein (Kang et al. 1987) with a single transmembrane domain and a short C-terminal tail. Indeed, it was shown that membrane-bound APP undergoes proteolytic cleavage resulting in the release of a large N-terminal fragment into the environment (medium or CSF) and the stable accumulation of a membrane bound C-terminal fragment (Weidemann et al. 1989; Oltersdorf et al. 1990) (Fig1.4). Surprisingly, further studies showed that an abundantly detected N-terminal APP fragment is the result of cleavage inside the Aβ sequence and with that precludes generation of Aβ (Sisodia 1992; Sisodia et al. 1990; Esch et al. 1990). Due to the fact that the observed APP fragment was secreted into the extracellular environment, the processing enzymes were designated “secretases” (Esch et al. 1990; Maruyama et al. 1991). Using human cell culture and CSF, Seubert et al. showed that there is an additional APP processing site at the exact N-terminus of Aβ and proposed the distinction between the first described “α-secretase” site and the newly identified “β-secretase” cleavage site (Seubert et al. 1993) (Fig1.4a,b). The third secretase site that generates the C-terminus of Aβ or after prior α-cleavage the C-terminus of a small peptide fragment of 3kDa (p3) was dubbed γ-secretase.

In the following years, the characteristics of activities of the three secretases (then of yet unknown molecular identity) have been elucidated. It became clear that α-secretory cleavage, the non-amyloidogenic pathway, represents the major shunt during normal metabolism. This occurs on the cell surface or intracellularly in the

trans-golgi-network (TGN) or post-Golgi compartment (Haass and Selkoe 1993) (Fig4c). However, amyloid-beta is generated during normal cell metabolism *in vitro* and *in vivo* in nanomolar quantities as quantified by immunoprecipitation and enzyme linked immunosorbent assay (ELISA) (Haass et al. 1992; Seubert et al. 1992). The amyloidogenic pathway involving β-site cleavage was shown to be sensitive to pH-shifts and with that occurs in an acidic compartment such as late Golgi secretory vesicles, endosomes, or lysosomes (Haass and Selkoe 1993). APP could reach these destinations after potential reinternalisation from the cell surface or by direct targeting from the TGN to this compartment (Haass and Selkoe 1993). The cellular location of γ-secretase activity was less well defined, but studies showed that γ-cleavage can occur at multiple sites in the transmembrane domain of APP resulting in short (40AA) or longer (42AA) peptides the latter of which harbour greater aggregation potential (Suzuki et al. 1994). In processing of wildtype APP, $A\beta_{40}$ is the major form representing 90% of total Aβ, but $A\beta_{42}$ is the major constituent of amyloid plaques. The next years have seen the hunt for the molecular identification of the APP processing enzymes with α-, β, γ-secretase activity that I will review in more detail below.

α-secretase

As discussed above, α-secretase activity cleaves most of APP inside the Aβ region (AA 687/688 of APP, AA 16/17 of Aβ) (Fig1.4) resulting in the shedding of sAPPα and the accumulation of the C-terminal fragment of 83 AA (CTF83). α-secretase activity falls into two categories: the first one is referred to by a constitutive activity, the second one by "regulated" activity. α -cleavage was shown to be rather insensitive to sequence alterations of APP. Early studies revealed that tumour necrosis factor α (TNFα) undergoes ectodomain shedding similar to APP and that this was mediated by *a disintegrin and metalloproteases* (ADAM), namely ADAM-17, originally named TACE for TNF-α converting enzyme. In the following, it was demonstrated that ADAM-17 shows properties of the regulated α– secretase activity but not the constitutive one (Buxbaum et al. 1998). Lammich et al. investigated if in an analogous manner another member of the ADAM family, ADAM10, could represent α-secretase (Lammich et al. 1999). They showed that ADAM10 levels dictate sAPPα in cell culture and that the properties of ADAM10 matched those described for both the constitutive and regulated α-secretase activity (plasma membrane/Golgi location, inhibitor profile). Also, yet another protein of the ADAM10 family, ADAM9, was shown to harbour α–secretase activity (Koike et al. 1999). Indeed, overexpression of any of these ADAM family members increases α-shedding. ADAM family members are zinc-dependent proteases with a single transmembrane domain that resemble a snake venom metalloprotease. Definitive proof for the identity of ADAM10 as the primary α-secretase under physiological conditions (i.e., no overexpression) came from studies involving knockdown approaches in multiple cell lines and importantly primary neurons (Kuhn et al. 2010; Jorissen et al. 2010). ADAM9 and ADAM17, however, could still play a role in stimulated α-secretase activity. Stimulation of α-secretase activity has been discussed as therapeutic intervention in AD as this would lower the amount of full-length APP presented to β-secretase activity and with that amyloid generation (Endres and Deller 2017).

β-secretase

In 1999, multiple labs reported the molecular identification of the protein with β-secretase activity termed β-site APP cleavage enzyme 1 (BACE1) (Vassar et al. 1999; Sinha et al. 1999; Yan et al. 1999; Hussain et al. 1999). BACE1 is a transmembrane aspartic protease with one transmembrane domain near its C-terminus and its active site on the luminal surface. BACE1/ β – secretase was shown to have an acidic pH optimum at around pH4.5 and to cleave membrane-bound substrates in a sequence specific manner (Cole and Vassar 2008). BACE1 is abundantly expressed in the brain but is also found in other tissues (Esler and Wolfe 2001). BACE1 was shown to harbour all characteristics described for β-secretase among them cleavage of APP at AA 671/672 resulting in the release of soluble APP β (sAPPβ) and the accumulation of a 99 AA C-terminal fragment C99 (Fig1.4a,b). Unequivocally, BACE1 was shown to be the primary β-secretase in *vivo* by the creation of BACE1 knockout animals which silenced Aβ production *in vivo* (Luo et al. 2001; Cai et al. 2001). Surprisingly, constitutive BACE1 KOs were healthy and long-lived with no obvious neurological phenotype

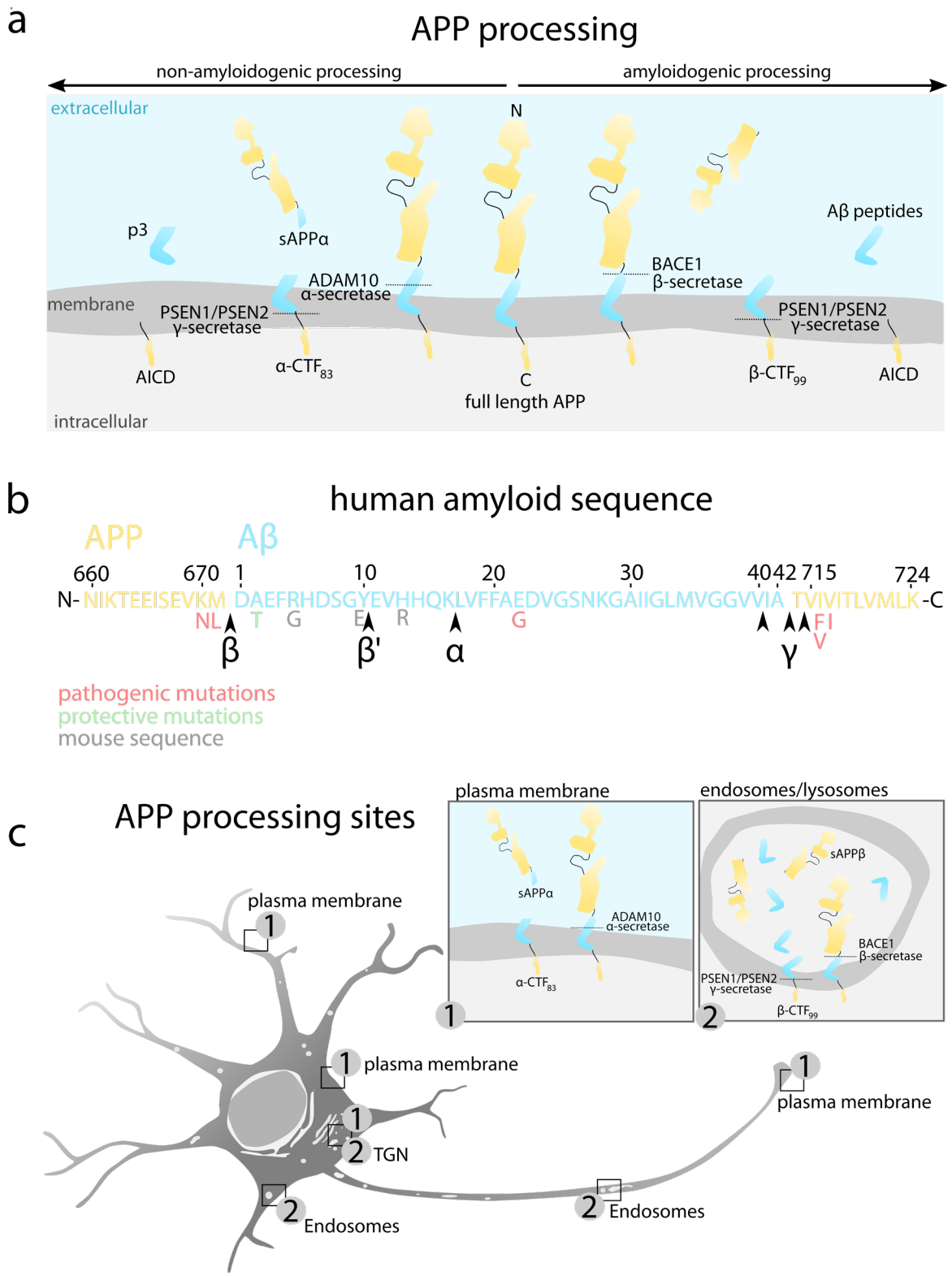

Figure 1.4 The generation of amyloid-β (a) Schematic overview of cellular APP processing pathways. Full-length APP (yellow) can undergo α-secretase/γ-secretase mediated non-amyloidogenic cleavage that releases the p3 fragment and prevents production of Aβ (blue). In the amyloidogenic pathway, APP is cleaved by β-secretase and subsequently γ-secretase producing the Aβ peptide. Both pathways release the APP intracellular domain. **(b)** Graphical representation of the human APP sequence (yellow) giving rise to Aβ peptides (blue) in the one letter amino acid code. α/β/γ secretase cleavage sites are indicated. Familial AD linked mutations (used for the generation of 5xFAD and APP^{NLGF} mice) are indicated in red: KM670/671NL (Swedish), E693G (Arctic), I716F (Iberian), I716V (Florida), V717I (London). The protective Icelandic mutation A673T is depicted in green. Amino acid differences to the mouse sequence are indicated in grey. **(c)** Subcellular locations of amyloid generation. α-cleavage is thought to occur mainly at the plasma membrane and the trans-Golgi network (1). β-cleavage occurs in an acidic environment such as the trans-Golgi network and along the endocytic pathway (endosomes/lysosomes) (2).

though later studies showed that BACE1 cleaves Neuregulin-1 type III as an additional substrate and controls peripheral nerve myelination (Willem et al. 2006). This is, however, not the case in the CNS where normal myelination is observed (Treiber et al. 2012). While no mutations in BACE1 directly have been shown to cause familial AD, the Swedish double mutation sits at the β-cleavage site and increases BACE1-dependent cleavage massively (10 to 50-fold). Conversely, the Icelandic mutation (A673T) confers protection against AD by decreasing β-cleavage (Jonsson et al. 2012). BACE1 can cleave APP at yet another site between AA 681/682 termed β'-site giving rise to CTF_{89} and the $A\beta_{11\text{-}x}$ fragment preventing generation full-length $A\beta_{1\text{-}x}$ (Kimura, Hata, and Suzuki 2016; Zhang et al. 2017). β-secretase cleavage is considered the rate-limiting step in Aβ production and BACE1 levels are regulated on multiple levels including transcriptional, translational and posttranslational mechanisms (Vassar and Cole 2007). Particularly interesting studies have shown BACE1 levels are heightened under conditions of energy deprivation (O'Connor et al. 2008). Further, BACE1 protein levels and activity are increased in AD patients (Fukumoto et al. 2002; Li et al. 2004; O'Connor et al. 2008).

γ-secretase

Molecular identity of the γ-secretase was the most difficult one to determine – in hindsight, this was likely linked to the fact that γ-secretase activity is carried out by a multiprotein complex that harbours an unusual transmembrane activity. This multiprotein complex is composed of one presenilin, APH1, PEN2 and Nicastrin (De Strooper 2003). Studies on loci on chromosome 1 and 14 linked to the majority of familial AD cases let to the identification of the gene family of "presenilins" (Rogaev et al. 1995): presenilin-1 (PSEN1) (Sherrington et al. 1995) and presenilin-2 (PSEN2) (Levy et al. 1990; Rogaev et al. 1995). Dominant gain-of-function mutations in presenilins detected in multiple kindreds of familial AD increase the production of $A\beta_{42}$ over $A\beta_{40}$ (Citron et al. 1997). While PSEN1 deficiency was early on shown to inhibit γ-secretase cleavage (to roughly 20%), PSEN1/2 double knockout completely abolishes γ-secretase activity. Due to their structure, presenilins were first not considered the putative secretase themselves but rather regulatory proteins (De Strooper et al. 1998). However, it was recognised that two aligning transmembrane aspartate residues in the presenilin transmembrane domains could possibly render it an unusual intramembrane aspartyl protease (Wolfe, Xia, Moore, et al. 1999; Wolfe, Xia, Ostaszewski, et al. 1999). An elegant photoaffinity labelling approach by γ-secretase inhibitors revealed selective binding to PSEN1 suggesting that it harbours the active protease activity (Li, Xu, et al. 2000).

However, PSENs do not work in isolation: it was shown that PSEN1 co-immunoprecipates with a large macromolecular complex (Li, Lai, et al. 2000). The identities of the co-assembling proteins were revealed in the following years, mainly by work on *C. elegans* Notch signalling (another substrate to γ-secretase activity): Nicastrin (Yu et al. 2000), APH1 (Goutte et al. 2002; Francis et al. 2002) and PEN2 (Francis et al. 2002). These four proteins mutually regulate their stability and intracellular trafficking (De Strooper 2003) and constitute γ-secretase activity in a hetero-tetrameric complex of likely 1:1:1:1 stoichiometry. Due to the fact of two presenilin genes and different spliced isoforms of human APH1, there is heterogeneity in terms of γ-secretase composition whose functional consequences are still incompletely understood. Presenilins, especially PSEN1, show abundant localisation to the ER but γ-secretase activity/Aβ generation takes place in endosomal/ lysosomal structures or the plasma membrane and not in the ER – this apparent discrepancy became known as the "spatial paradox" in presenilin biology (Annaert and De Strooper 1999). It was, however, partially resolved by studies showing minute amount of Psen1 at the plasma membrane and in lysosomes (Dries and Yu 2008). An intriguing study showed, further, that PSEN2-containing γ-secretase preferentially localises to late endosomes/lysosomes and generates an intracellular/luminal pool of Aβ, especially of aggregation prone $A\beta_{42}$ (Sannerud et al. 2016). This study shed light on γ-secretase activity regulation by subunit heterogeneity as well as spatial location.

To date, in addition to APP and Notch, 149 potential γ-secretase substrates have been identified that all possess a single transmembrane domain (Güner and Lichtenthaler 2020). γ-secretase activity in many cases requires ectodomain shedding before efficient cleavage (in the case of APP by α- or β secretase). Nicastrin is

involved in sterically hindering the cleavage of proteins with unshed or larger ectodomains (Bolduc et al. 2016). During their maturation, presenilins additionally undergo endoproteolytic cleavage resulting in a 20 and 30kDa fragment which seems to be important for their activation (Thinakaran et al. 1996; Lessard, Wagner, and Koo 2010). Mutations that lead to the exclusion of the endoproteolytic site harbouring exon 9 (commonly referred to as ΔE9) are found in familial AD and the mechanism - though not fully understood - apparently involves overall reduced γ-secretase activity that shifts the Aβ40/42 ratio towards more $A\beta_{42}$ (Woodruff et al. 2013). With the identification of the γ-secretase complex components, γ-cleavage become an interesting drug target that proved problematic due to other physiologically important γ-secretase substrates such as Notch (De Strooper, Iwatsubo, and Wolfe 2012). Rather than fully abolishing all γ-secretase activity, work is now focussing on "Notch-sparing" inhibitors or inhibitors that specifically abolish $A\beta_{42}$ generation.

1.2.5 Mouse models of Alzheimer's disease

The identification of the underlying genetic mutations of familial forms paved the way for the creation of animal models of AD. In 1995, Games et al. created the first mouse model overexpressing a mutated APP version (V717F, Indiana mutation) known as the PD-APP mouse using a PDGFβ-promotor driven human APP minigene. These mice exhibited AD-related neuropathology such as deposition of Aβ in amyloid plaques, reactive gliosis and localised synaptic defects (Games et al. 1995). In a similar approach, Hsiao and colleagues created mice overexpressing the human APP_{695} isoform with the Swedish double mutation (KM670/671NL) under the hamster prion protein promoter, now known under the synonym Tg2576 (Hsiao et al. 1996). These mice also exhibit parenchymal plaque deposition at around 1 year of each. In order to further accelerate amyloid deposition (for the convenience of researchers), transgenic mice were created that harboured both mutations in APP and PSEN1 such as APP/PS1 (APPswe/PS1ΔE9) that express Swedish mutated APP under the prion protein promotor and a human PSEN1 variant lacking exon 9 (that mimic splice deficit mutations in FAD leading to exclusion of Exon9) (Jankowsky et al. 2004). Other mouse models like this include the widely used APP/PS1-21 generated in the Jucker Lab (Radde et al. 2006) harbouring the Swedish mutated APP and PSEN1 L166P under the control of the Thy1 promoter. This approach of accelerating amyloid deposition perhaps culminated in the creation of the 5xFAD mouse that expresses two transgenes under the Thy1 promoter with a total of 5 FAD linked mutations: in APP, the KM670/671NL (Swedish), I716V (Florida) and V717I (London) mutation and in PSEN1 the M146L (A>C) and L286V mutation (Oakley et al. 2006) (Fig1.4b). This mouse model is yet the earliest and most aggressive in terms of plaque deposition (starting at around 6 weeks of age in the hippocampal formation).

Better mouse models?

AD mouse models - as every mouse model of a human disease - must be considered incomplete models for the human condition. The most obvious limitations of AD mouse models include: mimicry of familial AD and not sporadic AD, the lack of induction of tau-tangle pathology, limited cognitive deficits (depending on mouse model and specific behavioural paradigm used) and an artificial temporospatial induction of plaque deposition due to the use of transgenes with onset of plaque deposition in a young brain environment. Attempts were made to partially correct these imperfections. To additionally induce the formation of tau tangles as the other prominent feature of AD pathology, tau mutations that are linked to Frontotemporal Dementia have been introduced on top of a APP/PSEN1 transgenic background (3xTg Thy1.2::APP KM670/671NL; Thy1.2:: MAPT P301L; PSEN1 M146V Knock-in (Oddo et al. 2003)). To overcome the artificial spatial pattern of transgene expression as well as artefacts from overexpression and faulty cell type specificity, Saito and colleagues created a "second generation" AD mouse model that is based on a knock-in approach of FAD-linked APP variants into the endogenous mouse locus (Saito et al. 2014). The triple mutated APP^{NLGF} model harbouring the APP mutations KM670/671NL (Swedish), APP E693G (Arctic) and APP I716F (Iberian) (Fig1.4b) develops plaque deposition as early as 2 month in homozygous animals.

1.2.6 Amyloid-β generation: where and how?

The question where amyloid is generated can be addressed on multiple hierarchical levels: first, would be the question in which cell type in the brain amyloid beta is generated (neurons or glial cells?). Second, in which cellular domain within these cells this is happening (cell processes like the axon versus the cell body?) and finally which organelle is involved in this (plasma membrane, Golgi, endosomes, lysosomes?). Though these questions are still escaping a definite answer, I will try to shortly summarise current beliefs in the following paragraphs (Fig1.4c).

The cell type

Amyloid plaques are found in the extracellular space of the brain parenchyma and with that the source of amyloid is not obvious. The prevailing view is that the majority of Aβ is produced in neurons, especially excitatory neurons. *In vitro* , these cells were shown to produce ample amounts of Aβ. This is and was the basis for the generation of a multitude of AD mouse models with restricted transgene expression to neuronal populations such as the 5xFAD model under the Thy1 promotor (Oakley et al. 2006). However, APP, BACE1 and γ-secretase are widely expressed in all neuronal subtypes as well as glia cells as shown in cell-type specific bulk sequencing (Zhang et al. 2014) as well as in virtually all recent single cell transcriptomics studies e.g. (Zeisel et al. 2018). An intriguing study investigated the effects of conditional inactivation of an ubiquitously expressed mutant PSEN1 construct in excitatory neurons (CaMKIICre PrP:: deltaE9-Psen1$^{fl/fl}$) in the presence of an ubiquitously expressed mutant APP (PrP::APPswe) (Veeraraghavalu et al. 2014). It was shown that later in the disease plaque load is indifferent between animals with silenced overexpression of Psen1 in excitatory neurons and control mice highlighting potential other sources of Aβ (inhibitory neurons, glia cells). Indeed, *in vitro* glia cells are capable of producing Aβ which is exacerbated by neuroinflammatory responses (Blasko et al. 2000; Zhao, O'Connor, and Vassar 2011; Skaper et al. 2009). Interpretation of studies aimed at elucidating contributions of different cell types to amyloid load by using transgenic overexpressors of APP and/or PSEN1 is difficult because the use of transgenes intrinsically manipulates expression patterns. In a major step forward, the Bart de Strooper lab recently used an elegant approach of silencing endogenous BACE1 in the APP^{NLGF} knock-in model of AD (Rice et al. 2020). Silencing amyloid production in inhibitory neurons reduced amyloid burden identifying inhibitory neurons as site of Aβ generation – however only the hippocampus was analysed in this study (Rice et al. 2020).

The subcellular location

In principle, APP could meet its secretases in the biosynthetic pathway in the ER, Golgi, trans-Golgi network and secretory vesicles as well as in the endosomal/lysosomal pathway upon reinternalisation of the proteins. Indeed, APP as well as all secretases have been mapped to virtually all of these compartments - though in different abundancies (Sun and Roy 2018). While it is generally believed that APP encounters proteins with α-secretase activity such as ADAM10 mainly at the cell surface, the extracellular environment shows an unfavourable pH for β-secretase activity. β-secretase and γ-secretase activity are presumably restricted to endosomal/lysosomal compartments due to the low pH optimum of BACE1 (pH4.5). Indeed, BACE1 shows a punctate staining pattern and colocalises with endosomal and lysosomal markers (Huse et al. 2000). More specifically, early endosomes are likely to be the primary compartment for β-cleavage (Rajendran et al. 2006; Udayar et al. 2013). This postulates that APP needs to undergo at least one round of endocytosis to become targeted to the same intracellular location as BACE1 and the γ-secretase complex (Koo and Squazzo 1994). Alternatively, APP sorted in secretory vesicles from the TGN could meet BACE1 in the endocytic compartment after fusion without previous recycling (Toh et al. 2017). In accordance with the first scenario, it has been shown that APP traffics through the Golgi network to the plasma membrane where it is indeed rapidly internalised into recycling endosomes and partially lysosomes for degradation. Supporting the latter scenario, a study showed that APP can traffic directly from the TGN to early endosomes without recycling through the plasma membrane (Toh et al. 2017). No matter the exact scenario, membrane trafficking, undoubtedly, controls APP cleavage and amyloid production by regulating the encounter time of full-length

APP with the site-specific secretases. For example, reductions in RAB11 levels as a component of a slow recycling pathway in recycling endosome decreased β-site cleavage of APP and Aβ production (Udayar et al. 2013). Lipid rafts, cholesterol rich membrane microdomains found on the plasma membrane and the endolysosomal system (Lingwood and Simons 2010), have been suggested as the membrane microregions APP encounters BACE1 and Aβ is generated in (Cordy et al. 2003). Accordingly, cholesterol depletion reduces amyloidogenic processing of Aβ (Simons et al. 1998).

APP trafficking in neurons

The subcellular trafficking was initially described in cultures of non-neuronal cells with no or slight polarization. Here, APP shows abundant Golgi and TGN localisation. Trafficking of APP, however, might markedly differ in nerve cells as highly polarised cells with distinct subcellular domains such as dendrites, the neuronal soma and axon. APP definitely shows dendritic and axonal targeting and undergoes fast axonal transport mediated by kinesins (Koo et al. 1990). Fluorescent tracking of tagged-APP in primary neurons together with cycloheximide blocking of translation, suggested that APP undergoes axon-to-dendrite transcytosis in cultured neurons (Simons et al. 1995). The identity and characteristics of the APP transport vesicle in axons has been debated: APP is generally transported in vesicular structures with a tubular appearance (Haass et al. 2012; Goldsbury et al. 2006). First, it was shown that APP, BACE1 and PSEN1 are co-transported (Kamal et al. 2001), which could not be replicated in subsequent studies (Goldsbury et al. 2006; Szodorai et al. 2009; Lazarov et al. 2005). Later studies showed that under physiological conditions, the majority of BACE1 and APP appear to be sorted into distinct vesicles limiting their convergence and the production of Aβ (Das et al. 2013). However, a small fraction of presynaptic APP was identified in synaptic vesicles (10%) where it also colocalises with presenilin and BACE1 which helps explain how synaptic activity increases Aβ secretion (Groemer et al. 2011; Kamenetz et al. 2003; Cirrito et al. 2005). Supporting this view, another study identified APP in RAB3-positive transport vesicles – a small GTPase implicated in synaptic vesicle exocytosis (Szodorai et al. 2009). In contrast to these studies, bifluorescent complementation assays and dual-colour live imaging of fluorescently tagged BACE1 and APP in primary neuronal cell culture, revealed that while in dendrites most BACE1 and APP interacted in acidic recycling endosomes (Rab11, Transferrin Receptor positive organelles), in axons they are surprisingly co-transported in Golgi-derived vesicles and to a lesser extent in endosomal structures (Das et al. 2016).

A general note: extrapolation of the findings from *in vitro* experiments investigating APP/BACE1 intracellular trafficking to the *in vivo* situation is difficult. Neuronal cells *in vitro* represent an early state of neuronal differentiation (axonal outgrowth, presence of growth cones) and of course show markedly reduced complexity when compared to the *in vivo* situation (number of synapses, reduced axonal length, lack of myelination). Nevertheless, BACE1 and APP *in vivo* are axonally enriched proteins and encounter of BACE1 and APP in axonally transported vesicles is therefore likely. There is a need for more studies investigating APP and BACE1 trafficking and its implications for Aβ generation in the adult brain *in vivo* .

Axonally generated Aß

How important is axonal transport for the generation of Aβ? BACE1 and APP *in vitro* and *in vivo* are axonally enriched proteins. Using microfluidic devices which allow for soma/axon separation of cultured neurons, it was estimated that about 40% of cellular Aβ is derived from axons (Niederst, Reyna, and Goldstein 2015). In this system, axonal Aβ production was dependent on somatic endocytosis (Niederst, Reyna, and Goldstein 2015). Intriguingly, induction of axonal transport deficits that lead to axonal swellings consistently elevate Aβ levels: slowdown of general axonal transport rates by genetic disruption of kinesin (kinesin light chain, KLC1) (Stokin et al. 2005) or the kinesin-1 adaptor Calsyntenin-1 (Vagnoni et al. 2012) leads to axonal swellings and enhanced Aβ generation. Similarly, impairments of organelle specific transport e.g. JIP3-dependent axonal lysosome transport (Gowrishankar, Wu, and Ferguson 2017) or snapin-dependent retrograde transport of late endosomes (Ye and Cai 2014) elevate Aβ levels. Importantly, JIP3 and KLC1 heterozygosity exacerbates amyloid plaques load *in vivo* in AD mouse models (Gowrishankar, Wu, and Ferguson 2017; Stokin et al. 2005).

Intriguingly, impairments in membrane trafficking impact amyloid production, also via altering axonal targeting of BACE1. Loss of BACE1 s-palmitoylation (important for its lipid raft targeting) for example (Andrew et al. 2017) or its interaction with endocytic recycling proteins of the EHD family (EHD1, EHD3) (Buggia-Prévot et al. 2013) reduce its axonal targeting and subsequently reduce Aβ levels. AP2 likewise controls lysosomal targeting of BACE1 and knockout of AP2 results in increased axonal Aβ levels due to insufficient BAC1 degradation (Bera et al. 2020). BIN1 and CD2AP also regulate endosomal convergence of APP and BACE where BIN1 specifically regulates BACE1 recycling in axons (Ubelmann et al. 2017). Dysfunction of retromer, an essential protein complex for endosome-to-TGN retrieval, results in enhanced β-cleavage of APP by trapping APP in an endosomal compartment in neurites (Bhalla et al. 2012). Unexpectedly, massive BACE1 elevation by transgenic overexpression actually decreases amyloid deposition *in vivo* (Lee et al. 2005). This seems to be a consequence of shifting the subcellular site of β-cleavage from the axonal compartment to neuronal somata highlighting the importance of the axonal origin of Aβ peptides for plaque formation (Lee et al. 2005).

Dystrophic neurites: sites of Aβ production?

The corona of dystrophic neurites found around amyloid plaques as observed in both AD patients and mouse models has also been hypothesised to be a local site of Aβ production. Ultrastructurally, these are filled with autophagic vesicles, multivesicular bodies and vesicle structures reminiscent of endosomes/lysosomes (Sanchez-Varo et al. 2012). They enrich autophagic markers such as LC3 (Sanchez-Varo et al. 2012) and lysosomal markers LAMP1/2 and endosomal markers RAB5/7. These swellings stain overwhelmingly positive for axonally transported pre-synaptic vesicle proteins such as VGLUT1 (vesicular glutamate transporter 1; glutamatergic presynapse marker) and VGAT (vesicular GABA transporter; gabaergic presynapse marker) (Sanchez-Varo et al. 2012) and negative for dendritic markers such as MAP2 (Microtubule-associated Protein 2) and are, therefore, of axonal origin. Furthermore, some axonal swellings appear to be still myelinated (Sanchez-Varo et al. 2012). Axonal dystrophies around amyloid plaques have been shown to accumulate the Aβ producing machinery (APP, BACE1, γ-secretase complex) (Sadleir et al. 2016; Gowrishankar et al. 2015) and subsequently enrich Aβ. It was speculated that axonal dystrophies serve as the primary production sites of Aβ which precipitates plaque formation. However, longitudinal *in vivo* 2-photon imaging revealed that at least in AD mouse models axonal swellings in a corona-like structures occur secondary to plaque formation (Meyer-Luehmann et al. 2008). Nevertheless, these structures could still exacerbate amyloid production in a vicious cycle scenario.

1.2.7 Amyloid-β aggregation

A fibril in the making

What is the fate of the Aβ peptide chain after its release from APP? First it is noteworthy, that Aβ peptides can vary in length with both shorter or longer versions at the N- or C-terminus: in addition to so-called full-length Aβ starting with an aspartate at $Aβ_{1-x}$ (see Fig1.4c) N-terminally truncated Aβ peptides exist with starts at every AA from $Aβ_2$ to $Aβ_{11}$. Pyroglutamylated $Aβ_3$ ($Aβ_{pE3-x}$) and $Aβ_{4-x}$ are particularly abundant (Wirths et al. 2017; Portelius et al. 2010). Importantly, N-terminally truncated peptides can be detected in similar abundancy to full length peptides in human AD plaques (Portelius et al. 2010). Aβ peptides can also end at various AA at the C-terminus (AA37- AA49). While referred to as "amyloid β" in their entirety, Aβ peptides are, therefore, actually a heterogenous array of differently-sized peptides – with direct consequences for their biophysical properties.

Aβ monomer peptide structural studies have reported various degrees of secondary structures in the monomer dependent on solution and exact peptide examined (Chen et al. 2017). In general, full-length Aβ monomers are rather believed to be intrinsically unstructured. During fibrillogenesis, a conversion from this unstructured protein as a random coil formation to a β-sheet structure with potential α-helical intermediates occurs (Klimov and Thirumalai 2003). The structure Aβ adopts in fibrils is better understood: here the peptide

folds into two name-giving β-sheets and a disordered N-terminal tail. In a model reported by Petkova and colleagues for Aβ40, residues 1-8 are disordered and AA 12-24 constitute the first β-sheet (β1) and residues 30-40 the second β-sheet (β2) (Petkova et al. 2002). In a model reported by Lührs et al. (Lührs et al. 2005) for $A\beta_{42}$, residues 1-17 remain disorders, but residues 18-42 (in the case of $A\beta_{42}$) form a U-shaped β-strand-turn-β-strand (also called β-arch motif) with residues 18–26 forming β1 and 31–42 forming β2. In a protofibril, β1 forms intermolecular interactions with β2 of the next Aβ peptide which gives rise to "staggering" – a shift of the two intramolecular β-strands against each other. This staggering creates different ends of the stack and explains unidirectional growth of amyloid fibres. Despite shown to be disordered in structural studies, the N-terminal residues play important roles in the aggregation behaviour of Aβ (Söldner, Sticht, and Horn 2017). The β-sheets usually run in-parallel and in-register to one another (though other conformations have also been observed (Qiang et al. 2012; Gao et al. 2020)) and perpendicular to the fibril axis ("cross-β"). In the supramolecular architecture of a fibril, multiple protofibrils i.e. staggered β-sheet are associated with another along their longitudinal axis. Typically, three stacks are associated with threefold symmetry and a periodically twisted morphology (Paravastu et al. 2008; Petkova, Yau, and Tycko 2006). The so-called striated ribbon morphology of two-fold symmetry consisting of two protofibrils is also observed. A more recent study has, in principle, validated this structure in *in vivo* derived $A\beta_{40}$ fibrils (as opposed to *in vitro* derived fibrils) (Lu et al. 2013).

Fibril growth follows a sigmoidal kinetic of a slower nucleation phase followed by a steady growth phase and plateaus in a maturation phase where mature fibres are present as revealed by classical ThioflavinT assays. Folding of $A\beta_{42}$ into fibrils involves a stable pentameric, disc-shaped assembly of monomers that do not yet show a β-sheet structure (Ahmed et al. 2010) but in which the hydrophobic stretches fold into a strand-turn-strand formation. Of note, the two hydrophobic extra residues in $A\beta_{42}$ seem to stabilise this toxic and pentameric oligomer which could explain the heightened aggregation behaviour of $A\beta_{42}$. *In vivo*, $A\beta_{42}$ is the form predominantly found in amyloid plaques and only overexpression of $A\beta_{42}$ but not $A\beta_{40}$ leads to the accumulation of amyloid plaques (McGowan et al. 2005). Another explanation for $A\beta_{42}$ specific properties was recently given by Xiao et al. and Wälti et al. that showed that $A\beta_{42}$ can fold in more than two β sheets in a double horseshoe like fashion that $A\beta_{40}$ cannot adopt (Xiao et al. 2015; Wälti et al. 2016).

Amyloid plaques

The conversion from fibrils to amyloid plaques as observed *in vivo* is not well understood. However, plaque formation does typically not occur in a cell-free environment (*in vitro* incubation of amyloid in buffers). A few (but not well recognised) studies have shown that in primary cell culture repetitive incubation with synthetic Aβ leads to the formation of plaque-like structures (Friedrich et al. 2010; Gellermann et al. 2006). This very likely has to do with the fact that amyloid plaques are not exclusively made up of Aβ but various proteins and lipids are co-accumulating in plaques. Recent proteomic approaches using laser capturing of amyloid plaques revealed over 40 proteins that were significantly enriched in amyloid plaques (Xiong, Ge, and Ma 2019; Drummond et al. 2017). Among them is APOE which can be readily found in amyloid plaques using conventional immunostaining approaches. Other proteins found in plaques are members of the complement family (C4), APOJ (clusterin), ubiquitin and multiple heatshock proteins. Under the top50 enriched proteins, multiple myelin proteins (MBP, CNP, TUBB4A) are also found.

AD plaques are categorised based on their different morphological characteristics and they show tremendous heterogeneity. The most common types include diffuse plaques, fibrillar, dense-cored and burned-out plaques - though many more types have been described with partly confusing nomenclature (Dickson and Vickers 2001). Diffuse plaques are typically very well stained with anti-amyloid-β antibodies and to a weaker extent with β-sheet interacting dyes such as Thioflavin, Congo red, Methoxy-04 (Wu, Scott, and Shea 2012) and they do not show distinct boarders. Fibrillar plaques are much better stained with dyes and show a fibrous morphology. Dense-cored plaques show a core that is intensely stained with dyes with a void around it and a "second layer" of fibrillar amyloid deposit. Burned-out plaques typically only present with a dense core without an additional layer of any fibrillar Aβ around them. Condensed plaques that present with dystrophic

neurites around them have been termed neuritic plaques. Patients typically present with a multitude of these morphologies. Elegant *in vivo* imaging of amyloid plaques in AD mouse models have revealed a gradual, sigmoidal growth curve of plaques where small plaques grow fastest (Burgold et al. 2014; Burgold et al. 2011).

Oligomers versus plaques: what is toxic (the most)?

It is a long-standing debate which amyloid entity represents the neurotoxic species in AD: monomers, oligomers or mature fibrils in plaques? Closely related to this, is the idea that the build-up of amyloid plaques in the brain is a protective reaction to sequester toxic Aβ oligomers. However, everyone who histopathologically examined amyloid plaques in the brain of mouse models and patients must agree that amyloid plaques cause local tissue damage with the surrounding parenchyma disintegrating and the formation of neuritic beads. In theory, such changes alone could well explain AD related functional declines. However, the fact that the severity of AD cognitive symptoms and the number of amyloid plaques is not well correlated with AD progression (indeed cognitively healthy elderlies can show abundant amyloid deposition) and that amyloid plaque targeting therapeutic interventions did not significantly better clinical outcome (yet), has fuelled the idea that an amyloid species other than plaques is to blame for neurotoxicity. The mature fibrils and oligomeric species are likely to be present in an equilibrium state in the brain. Indeed, it is thought that amyloid plaques form a halo of oligomeric Aβ around them. Various types, but not well-defined amyloid oligomers that form during the nucleation process cause cell death *in vitro* and can disturb synaptic transmission (Benilova, Karran, and De Strooper 2012). In a broader description, these oligomeric species are termed Aβ derived diffusible ligands (ADDLs) (Lambert et al. 1998). Importantly, these oligomeric species also show *in vivo* neurotoxicity and inhibit hippocampal long-term potentiation (Walsh et al. 2002). In general, it is thought that the oligomers elicit toxicity by interacting either directly with biological membranes or proteins such as glutamate receptors or the cellular prion protein (Laurén et al. 2009).

1.2.8 Microglial responses in Alzheimer's Disease

As outlined above, glial responses to amyloid deposition have been one of the first features of AD observed by Alois Alzheimer. Inflammatory reaction in the brain (neuroinflammation) is, indeed, a prominent feature in AD. In the last decade, the AD field has shifted its attention from neurons to additionally studying glial cells, especially microglia cells. This has been certainly fuelled by a number of genome wide association studies (GWAS) and other genetic studies that showed correlations of genetic variants in/near genes mainly expressed in glia cells (see continuously updated database alzgene.org (Bertram et al. 2007)). Among these genetic risk factors, is the long-known risk allele *ApoE4* that is majorly expressed in astrocytes and microglia, another Apolipoprotein Clusterin (APOJ) expressed in astrocytes and OPCs and many genes that seem involved in microglial biology such as CR1, SPI1, the MS4A family, TREM2, ABCA7 and CD33 and many more (Efthymiou and Goate 2017).

Microglia reaction to amyloid plaques

Microglia cells clearly react to amyloid plaques by clustering or "corralling" around them as revealed by microscopy – a phenomenon of human AD well replicated in mouse models (Fig1.5). This is associated with the typical morphological changes seen in microglia or macrophages that react to tissue damage from highly branched to an amoeboid shape. Microglia sense amyloid via a couple of receptors that are classically involved in the detection of danger associated molecular patterns (DAMP) such as toll like receptors and scavenger receptors (Heneka et al. 2015). For example, CD36 was shown to mediate inflammatory cytokine release (TNFα, Interleukin-1, Interleukin-6) upon fibrillar amyloid exposure and have been long known to be upregulated in AD patients (El Khoury et al. 2003; Koenigsknecht and Landreth 2004). Importantly, the

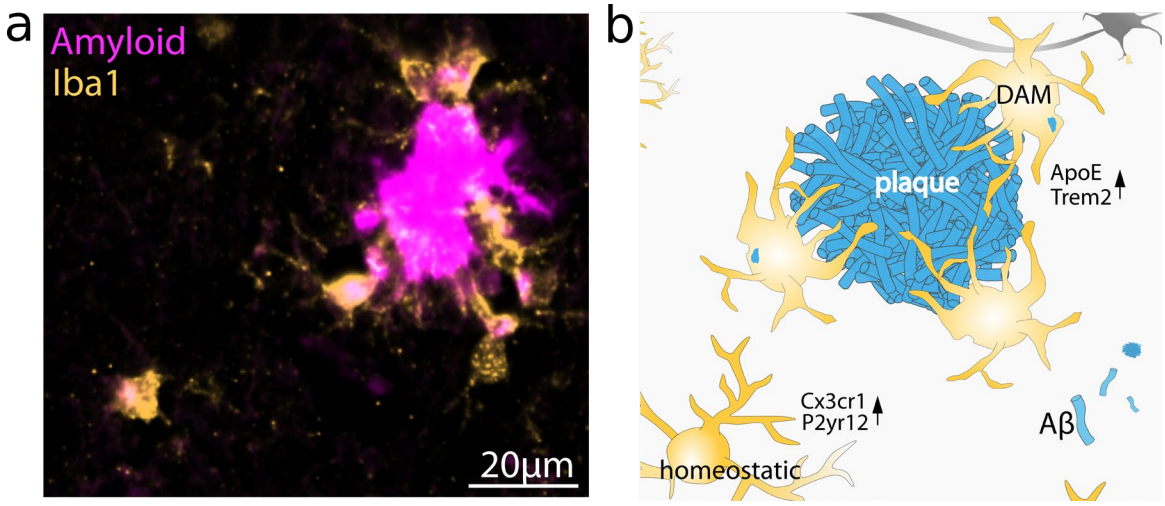

Figure 1.5 Reaction of microglial cells to amyloid plaques. **(a)** Fluorescence microscopy of microglial reactions to plaques in a paraffin-brain section of a 6-month-old 5xFAD mouse. Microglia (stained by Iba1 in yellow) are found in close physical association with amyloid plaques. Partially, amyloid material (stained with Methoxy-04) can be seen in the microglial cell body indicative of phagocytosis. **(b)** Schematic representation of the reaction of microglial to plaques. Microglia around plaques show a disease-associated microglia (DAM) signature characterized by high levels of ApoE and Trem2. Homeostatic microglia further away from plaques exert a highly branched morphology and express the microglial homeostasis markers Cx3cr1 and P2ry12.

inflammatory reactions seem highly localised to the vicinity of amyloid plaques. Elegant *in vivo* co-imaging studies of fluorescently labelled microglia and plaques probed the reaction of microglia to plaques in AD mouse models (Meyer-Luehmann et al. 2008; Bolmont et al. 2008). These studies revealed that microglial activation is secondary to plaque formation and that microglia associate stably with plaques. In certain cases, microglia show internalised amyloid indicative of phagocytosis attempts. Earlier *in vitro* studies, indeed, showed that microglia cells are able to internalise amyloid (Paresce, Ghosh, and Maxfield 1996) but this phagocytosis occurs by a non-classical phagocytotic mechanism (Koenigsknecht and Landreth 2004) and amyloid fibrils are only inefficiently degraded (Paresce, Chung, and Maxfield 1997; Stalder et al. 2001). In fact, microglia seem much more effective in degradation of oligomeric/protofibrillary amyloid than fibrillar amyloid (Liu et al. 2010). Microglia become increasingly dysfunctional with the time they are exposed to amyloid in aged AD mouse models which reduces their phagocytic activity and ramps up inflammatory cytokine production (Hickman, Allison, and El Khoury 2008; Krabbe et al. 2013). Accordingly, it is still a matter of intense debate to what extent microglia actually remove Aβ from plaques and if they restrict plaque growth. However, Aβ immunotherapy studies have shown that plaque-association of microglia and phagocytosis can be boosted by administration of anti-amyloid antibodies which subsequently reduces plaque load (Koenigsknecht-Talboo et al. 2008; Krabbe et al. 2013).

Plaque-associated microglia: Safe-guards for neurites and plaque machines?

Given the apparently limited phagocytosis of amyloid by microglia, what might be other potential roles of microglia around amyloid plaques? Using exogenously injection of fluorescently labelled Aβ peptides and *in vivo* imaging, Condello et al. showed that microglia constitute a barrier that prevents further Aβ binding/ plaque expansion which protects the surrounding tissue from developing neuritic dystrophies (Condello et al. 2015). Accordingly, microglia decorated amyloid plaques are more compact and show less abundant dystrophic neurites. Genetic and pharmacological microglia depletion experiments have shown no or limited effects on plaque burden in terms of plaque number in AD mouse models (Grathwohl et al. 2009; Spangenberg et al. 2016) but revealed morphological remodelling of plaques (Zhao et al. 2017; Casali et al. 2020). The exception to this are two interesting studies employing colony stimulate factor 1 receptor (CSF1R) antagonists to deplete microglia (Elmore et al. 2014). These studies reported early long-term administration (as early as 1.5 months for up to 6 month) to massively diminish, almost prevent, plaque

burden in 5xFAD mice (Spangenberg et al. 2019; Sosna et al. 2018). In these mice, however, cerebral amyloid angiopathy emerged and behavioural symptoms worsened after microglia depletion (Spangenberg et al. 2019). The authors speculated that very early in disease progression, microglia actually help seed amyloid plaques by different mechanisms. This could involve secretion of factors facilitating amyloid formation in the extracellular environment or the uptake of Aβ into acidic organelles and its subsequent release to the extracellular environment. Indeed, it was shown that ASC specks following inflammasome activation cross-seed amyloid (Venegas et al. 2017). Likewise, deletion of TAM-receptors reduces plaque seeding by inhibiting microglial amyloid uptake (Huang et al. 2021).

Trem2 and ApoE: Partners in crime

Genetic analyses in AD have particularly sparked interest in TREM2, a lipid receptor that is primarily expressed in microglia. These studies showed that heterozygous TREM2 variants such as the R47H mutation are associated with increased AD risk (Guerreiro et al. 2013; Jonsson et al. 2013). Early work in Christian Haass' group showed that TREM2 deficiency impairs chemotaxis and migration and microglia are apparently transcriptionally locked in a homeostatic state (Kleinberger et al. 2014). Further they showed that TREM2 undergoes ADAM10 mediated shedding which is reduced together with maturation and phagocytosis in TREM2 variants implicated in AD and frontotemporal dementia (Kleinberger et al. 2014). The microglial barrier function is also critically dependent on the expression of Trem2. Work by Marco Colonna's lab established that in Trem2 heterozygous or homozygous knockout mice microglia fail to cluster around amyloid plaques and plaques are subsequently more diffuse and neuritic damage increased (Wang et al. 2016; Wang et al. 2015; Ulrich et al. 2014). While different studies reported variable effects of TREM2 loss of function on plaque load (from diminished plaque load to increase plaque burden - dependent on mouse model and time points analysed (Jay et al. 2015; Wang et al. 2016; Wang et al. 2015; Yuan et al. 2016; Jay et al. 2017; Krasemann et al. 2017)), the loss of the microglial plaque-corralling phenotype is consistently reported in mice and human Trem2 mutation carriers (Yuan et al. 2016; Parhizkar et al. 2019). An elegant study involving amyloid seeding experiments and longitudinal *in vivo* amyloid PET imaging showed that especially early plaque formation is markedly affected by Trem2 loss of function: plaque seeding is enhanced, and amyloid accumulation rate is very high early in disease progression in APP/PS1 mice, but rapidly declines afterwards partly reconciling contradicting reports on plaque burden changes in Trem2 knockout animals (Parhizkar et al. 2019).

Surprisingly, plaques in Trem2 knockout/AD mice contained significantly less APOE (Parhizkar et al. 2019). APOE plaque content is also diminished by microglia depletion highlighting microglia as the source of APOE that is found in amyloid plaques (Parhizkar et al. 2019). APOE is usually found in tight association with Aβ in amyloid plaques. What is the role of APOE in plaques and AD? ApoE is the most well studied genetic risk factor for late onset AD, especially in regards to its roles in glia cells. Approximately, 15% of the world's population carry the *APOE4* allele which increases the likelihood of developing AD in comparison to the more frequent *APOE3* isoform [odds ratio (E3/E4 to E3/E3)= 3.2; odds ratio (E4/E4 to E3/E3=14.93) in a Caucasian population (Farrer et al. 1997)]. The three human APOE isoforms differ in the AA positions 112 and 158 which change receptor, lipid and amyloid binding (Kanekiyo, Xu, and Bu 2014). APOE is involved in the transport of lipids, especially cholesterol, between cell types in the brain and is majorily expressed by astrocytes under homeostatic conditions (Liu et al. 2013). However, APOE becomes elevated in activated microglia. *In vitro* experiments have shown that APOE and especially the APOE4 isoforms massively enhanced amyloid fibrillisation (Ma et al. 1994). In the meanwhile, these findings have been replicated *in vivo* in AD mouse models using different (over)expression approaches of human APOE isoforms (Liu et al. 2017; Castellano et al. 2011; Bales et al. 2009). These studies consistently show that amyloid load is enhanced in *APOE4* expressing mouse models. Conversely, decreasing APOE levels ameliorates fibrillar plaque deposition (DeMattos et al. 2004; Bales et al. 1997) – independent of the specific APOE isoform (Kim et al. 2011). The *APOE4* allele seems to exert its negative effect on plaque burden by a dual mechanism involving both enhanced plaque seeding and reduced drainage (Castellano et al. 2011; LaDu et al. 1994; Deane et al. 2008). Lipidated APOE in lipoprotein particles can bind soluble Aβ which can be taken up by cells via lipoprotein

receptors such as LRP1 and LDLR (Kanekiyo et al. 2011) and then degraded or drained via the blood brain barrier. Indeed, LDLR overexpression massively decreases amyloid burden by stimulated cellular amyloid drainage (Kim et al. 2009). The APOE4 isoform seems to be both less efficient in binding soluble amyloid and is more poorly lipidated both of which reduces drainage (Fernandez et al. 2019). Intriguingly, immunotherapy directed against APOE reduces plaque burden and CAA pathology in mice (Xiong et al. 2021).

Plaques damn microglia

The microglial response in AD has been recently characterised in unprecedented detail in a number of transcriptomic studies that have further underscored the importance of both APOE and TREM2 function in guiding microglial reaction in AD (Krasemann et al. 2017; Keren-Shaul et al. 2017). Using scRNA-seq, Keren-Shaul et al. identified a small population of microglial cells that was overrepresented in 5xFAD mice and showed reduced expression of homeostatic microglia (such as *P2ry12, CxCr1* or *Tmem119*) and increased expression of *ApoE, Trem2, Tyrobp, Lpl, Spp1, Clec7a* and *Itgax*. This signature was baptised "disease-associated microglia" (DAM) signature and was shown to be restricted to microglia that were in contact with amyloid plaques and of a phagocytic phenotype (Fig1.5). This study further showed that Trem2 loss of function blocks full conversion to a DAM phenotype and microglial became arrested in a precursor DAM state. At the same time, Krasemann and colleagues described the same signature in AD mice using bulk sequencing and nanostring analysis of sorted microglia (microglial neurodegeneration phenotype, MGnD) (Krasemann et al. 2017). In concordance with the Keren-Shaul findings, the proper induction of this MGnD pool was dependent on *Trem2* as well as additionally *ApoE* expression. Intriguingly, however, despite describing the same pool of microglia the two studies differ in the interpretation of the function of this microglia subset: While Keren-Shaul et al. attribute protective functions, Krasemann and colleagues assign a detrimental role to DAM. This well reflects the two current schools of thoughts and the conflict in the field. It might, however, be resolved by acknowledging a dichotomous role of microglia in AD with a temporal trajectory from early-protective to late-dysfunctional and harmful – which awaits further experimental proof.

1.2.9 The amyloid cascade hypothesis and beyond

The early and undeniable observation of Aβ as the main constituent of plaques as the unique neuropathological feature of AD, together with the genetic support from familial Alzheimer's disease and Down Syndrome patients has led to the formulation of the amyloid-cascade hypothesis by Hardy and Higgins in 1992 (Hardy and Higgins 1992). The amyloid hypothesis states, that it is the build-up of Aβ in the brain that starts a cascade of events that ultimately leads to neuronal dysfunction and neuronal cell death. In this cascade, the second neuropathological hallmark of AD, namely tau-tangles, as well as the overt neuroinflammation is placed downstream of Aβ. Given the limited evidence of direct toxicity of Aβ (in plaques), tau-tangles are likely to lead to the overt cell death present in the very late pathological stages of AD. Multiple other theories trying to explain AD pathology exists, but the amyloid-cascade is the prevailing hypothesis in the field.

However, it faced substantial criticism mainly based on the failure of amyloid-lowering therapeutics in clinical trials (Karran, Mercken, and De Strooper 2011; Makin 2018). These included both β- and γ-secretase inhibitors and Aβ immunotherapy (both passive and active). A number of clinical trials were discontinued due to side-effects (e.g., encephalomyelitis in the case of active Aβ immunotherapy), others did not proof effective in changing clinical outcome (though this could be likely explained by the treatment paradigm in late disease phases). Very recently, in June 2021, the US Food and Drug administration has granted accelerated approval to Aducanumab (Aduhelm, Biogen) as the first approved anti-amyloid antibody for the therapeutic treatment of AD. The approval, however, was met with substantial criticism from the AD research field (Karlawish and Grill 2021) as the clinical trials showed lowering of Aβ burden in Aβ-PET scans but failed to provide evidence for ameliorating cognitive decline. Given apparent shortcomings of the amyloid cascade hypothesis, it has been refined (or replaced) to accommodate other features of the disease progression. This

includes theories focussing on regulating the neuroinflammatory response in AD, targeting primarily tau, oxidative stress, and the role of microbe/viral infections in AD pathogenesis (present theories are reviewed in (Liu et al. 2019)). No matter the underlying theoretical construct, it is clear that therapeutic interventions aimed at prevention rather than treatment of AD are more desirable. In this regard, understanding the initial steps of the disease at or even prior to the first signs of amyloid deposition is crucial. Inherently linked to this is the question what exactly causes the accumulation of amyloid in the aged brain in sporadic AD. It is interesting that for the majority of the adult life span no plaque accumulation is observed despite abundant expression of APP and the secretases. Hypotheses trying to explain emergence of amyloid plaques upon ageing include - among others - a loss of overall proteostasis and the fatigue of other cellular recycling/degradation mechanism which would ramp up amyloid production or reduce amyloid degradation (Hipp, Kasturi, and Hartl 2019; Hou et al. 2019). This makes clear that in order to understand the age-dependency of amyloid build-up it is crucial to understand the effects "normal" ageing has on the brain and its different cell types.

1.3 Aims of this study

Is myelin ageing a risk factor for amyloid deposition in Alzheimer's disease?

As reviewed above, brain ageing fundamentally affects the integrity of myelin, especially intracortical myelin in the frontal lobe. The late George Bartzokis was the first one to hypothesise that this age-related myelin breakdown could be a risk factor for the development of AD (Bartzokis et al. 2004). Neuropathological studies by the Braaks revealed an inverse relationship of AD pathology and myelination (Braak and Braak 1991): thinly and in development lately myelinated areas that are affected most by age-dependent myelin decline are also the most susceptible to AD pathology. Conversely, heavily and in development early myelinated tracts remain unaffected until the very late disease stages. Indeed, white matter damage was shown to occur in the preclinical phases of AD in a number of macroscopic brain imaging studies (Dean et al. 2017; Bendlin et al. 2012; Bendlin et al. 2010). Intriguingly, the decline in myelin integrity starting already in the 5th decade of life coincides with the first signs of amyloid build-up in the brain as seen by amyloid PET imaging or changes in amyloid biomarkers (Fig1.6) (Jansen et al. 2015; Bartzokis et al. 2010). While Bartzokis put together a well thought hypothetical model of AD aetiology, it awaits experimental proof. Importantly, while he meticulously

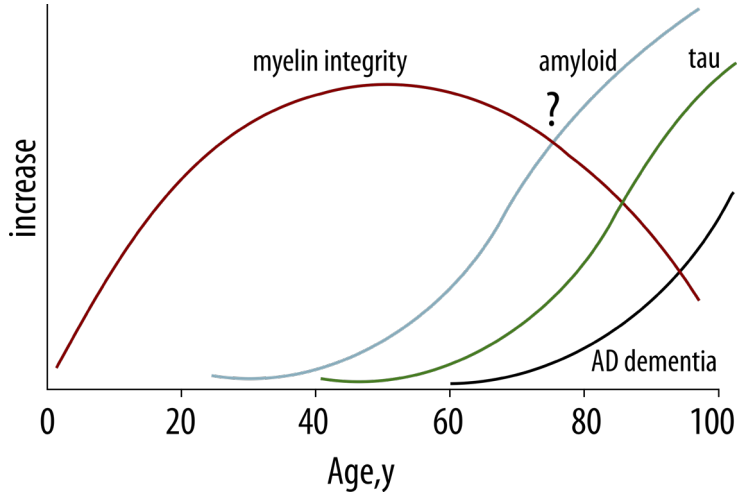

Figure 1.6 Schematic illustration of the relationship of myelin integrity break-down and AD-related neuropathologies across the human lifespan. X-axis represents age in years (y). Y-axis depicts relative increases. Y-values are not represented in scale. Age-trajectory of these parameters is schematically depicted based on Bartzokis et al. 2010 and Jansen et al. 2015.

collected evidence linking myelin degeneration to AD the metabolic support function of oligodendrocytes was not unravelled yet. I interpret Bartzokis' hypothesis of 'myelin damage drives brain Alzheimerisation' mainly in the light of the lately described metabolic support function of oligodendroglia and hypothesised that in humans age-dependent structural changes in oligodendrocytes compromise the trophic support rather than insulating function of myelin. I envision a mechanism in which axonal starvation downstream of myelin defects, leads to reduced axonal transport and lysosomal degradation promoting the accumulation of APP, β and γ-secretase in axonal swellings which would propel amyloid accumulation. In my doctoral thesis, I set out to provide a proof of principle for the link of myelin dysfunction and AD pathology *in vivo* (Fig1.7). For this, I performed an in-depth analysis of mouse models of myelin dysfunction combined with AD mouse models and investigated effects on amyloid plaque burden using 3D light sheet microscopy (Fig1.7). Using immunohistochemistry as well as biochemical and transcriptional analysis of double mutant mice, I aimed at elucidating the underlying mechanism of action.

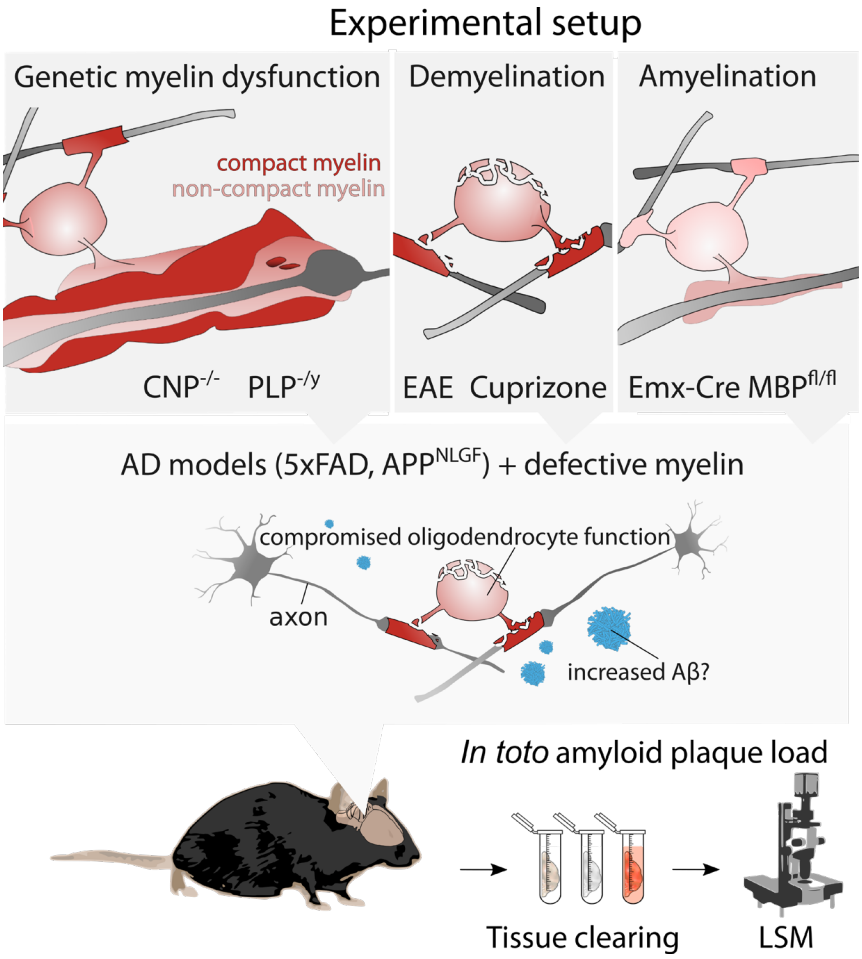

Figure 1.7 Experimental setup to study the impact of myelin dysfunction on amyloid deposition *in vivo*. Upper panel: Genetic models of chronic myelin dysfunction ($CNP^{-/-}$, $PLP^{-/-}$), acute demyelination (Experimental autoimmune encephalomyelitis (EAE) and Cuprizone-mediated demyelination) and amyelination (lack of compact myelin in Emx-Cre $MBP^{fl/fl}$) were combined with AD mouse models (5xFAD, APP^{NLGF}). Lower panel: The impact of defective myelin on plaque burden was assessed by tissue clearing and light sheet microscopy (LSM) of amyloid plaques stained by Congo red. Figure adapted from Depp et al. 2021.

2 Material and Methods

2.1 Materials

2.1.1 Chemicals

All chemicals described in the methods section of this thesis were purchased from Merck/Sigma Aldrich albeit stated otherwise.

2.1.2 Solution and buffers

Solutions and buffers were prepared at room temperature by weighing required amounts of chemicals using a (precision) laboratory balance and solving them in the respective solvent. Unless stated otherwise, deionised water was used as the default solvent. The solution's pH was adjusted using a pH-meter when required. Application is given in the last column (WB= Western Blot; IHC=Immunohistochemistry; LSM= Light sheet microscopy).

Table 2.1 List of solutions and buffers

Name	Composition	Application
Citrate buffer	1.8 mM Citric acid 8.2 mM Sodium citrate pH 6	IHC
Diethylamine-buffer (DEA)	0.25% Diethylamine 50mM NaCl pH 10	WB
FastGreen-Wash (FG-W)	30% MeOH 7% Acetic acid 63% H_2O	WB
Laemmli sample buffer	2%SDS, 10% glycerol 0.0025% bromophenol blue 0.125M Tris-HCl pH 6.8 0.05M DTT	WB
PBS-T with Heparin (PTwH)	PBS/0.2% Tween-20 10 mg/ml heparin 5mM sodium azide	LSM
PFA/PB	4% PFA 0.04M NaH2PO4 0.16M Na2HPO4 pH 7.4	IHC
Phosphate buffer	0.04M NaH2PO4 0.16M Na2HPO4 pH 7.4	IHC

Phosphate-buffered saline (PBS)	137mM NaCl 2.7mM KCl 10mM Na_2HPO_4 1.8mM $KH_2PO_{4;}$ pH 7.2	LSM, IHC, WB
Radioimmunoprecipitation assay buffer (RIPA)	20mM Tris-HCl pH7.5 150mM NaCl 1%NP-40, 1%SDS 2.5mM sodium pyrophosphate 1mM Na2EDTA	WB
SDS running buffer	25 mM Tris base 190 mM Glycine 0.1% SDS pH 8.3	WB
Separating gel	8-10% Acrylamid/Bisacrylamid 29:1 0.4 M Tris/HCl pH 8.8 0.1% SDS 0.03% APS 0.08% TEMED	WB
Stacking gel	4% Acrylamid/Bisacrylamid 29:1 125 mM Tris/HCl pH 6.8 0.1% SDS 0.05% APS 0.1% TEMED	WB
Tris-Tricine-running buffer	100 mM Tris 100 mM Tricine 0.1% SDS pH 8.3	WB
Transfer buffer	25 mM Tris base 190 mM Glycine 20% Methanol pH 8.3	WB
Basic antigen retrieval buffer	10mM Tris 1mM EDTA pH 10	IHC
Tris-buffered saline with Tween (TBS-T)	20mM Tris-base, pH7.5 150mM NaCl 0.1% Tween-20	WB

2.1.3 Antibodies and staining reagents

Primary and secondary antibody solutions were prepared in PBS/10%GS or PBS/5%BSA for immunohistochemistry (IHC), in PTwH with 0.2% Triton X-100, 5% DMSO and 3% GS for light sheet microscopy (LSM) and in TBS-T with 5% BSA for western blotting (WB).

Table 2.2 List of primary antibodies

Target	Species	Company	Dilution	Application
ApoE(D719N)	rabbit	Abcam	1:200	IHC
APP	rabbit	Thermo Fisher	1:1000	WB
APP	rabbit	SySy	1:1000	IHC, WB
APP(22c11)	mouse	Merck	1:1000	IHC, WB
Aβ (6E10)	mouse	Biolegend	1:1000	IHC
Aβ1-x (6C3)	mouse	Abcam	1:200	IHC
Aβ4-x	Guinea pig	Custom (Wirths)	1:200	IHC
Aβx-42 (D3E10)	rabbit	CST	1:1000	IHC
BACE1	rabbit	Abcam	1:100	IHC
BACE1	rabbit	CST	1:1000	WB
CNP	mouse	Atlas	1:1000	IHC
GFAP	mouse	Leica	1:200	IHC
Iba1	rabbit	Wako	1:500	IHC, LSM
MBP	rabbit	Custom (Nave)	1:1000	IHC
PLP(aa3)	rat	Custom (Nave)	1:200	IHC

Table 2.3 List of secondary antibodies

Target	Fluorophor	Species	Company	Dilution	Application
Mouse IgG	Alexa 555	Donkey or goat	Thermo	1:1000	IHC
Rabbit IgG	Alexa 555	Donkey or goat	Thermo	1:1000	IHC
Mouse IgG	Dylight 633	Donkey or goat	Thermo	1:1000	IHC
Rabbit IgG	Dylight 633	Donkey or goat	Thermo	1:1000	IHC, LSM
Rat IgG	Dylight 633	Donkey	Thermo	1:1000	IHC, LSM
Rabbit IgG	IRDye 800CW	Goat	Licor	1:5000	WB
Mouse IgG	IRDye 680CW	Goat	Licor	1:5000	WB
LSAB2 Kit (mouse, rabbit)	Chromogenetic labelling	-	Dako	IHC	IHC

Table. 2.4 Other staining reagents

Target	Name	Company	Dilution	Application
DNA	DAPI	Thermo Fisher Scientific	300nM PBS	IHC
DNA	ToPro3	Thermo Fisher Scientific	1:1000 in PBS	IHC
DNA	GelRed	BioTrend	1:2500	Genotyping
β-sheets	Congo red	Tocris	0.01% in PTwH	IHC, LSM
β-sheets	Methoxy-X04	Tocris	4µg/mL in 50% EtOH	IHC
Protein	Fastgreen (FG)	Serva	0.0005% in FG-Wash	WB
HRP-activity	DAB	Zytomed	According to manual	IHC

2.1.4 Mouse strains

Table 2.5 Mouse lines

Name	Genetic modifications	Original reference
5xFAD	APP KM670/671NL; I716V; V717I, PSEN1 M146L; L286V	Oakley et al. 2006
CNP null	Cre-cassette insertion into CNP locus; gene deletion	Lappe-Siefke et al. 2004
PLP null	Neomycin-cassette insertion PLP1 locus; gene deletion	Klugmann et al. 1997
Emx-Cre	Emx1::IRES-cre; cre-insertion downstream of Emx-Cre coding sequence	Gorski et al. 2002
$MBP^{fl/fl}$	Floxed Exon1 of the MBP gene	Meschkat et al. 2020

2.1.5 Genotyping

Table 2.6 Genotyping primer sequences

Name	Genotyping
5xFAD	Protocol 31769; JAX
	36758: 5'- CAT GTC CTA CAG CCC CTC TC -3'
	36759: 5'- ACC ATT TGC AAG GAA AGC AC -3'
	oIMR2093: 5'- AAG CTA GCT GCA GTA ACG CCA TTT -3'
CNP null	Internal protocol;
	2016: 5'- GCCTTCAAACTGTCCATCTC -3'
	7315: 5'- CCCAGCCCTTTTATTACCAC -3'
	4193: 5'- CCTGGAAAATGCTTCTGTCCG -3'
	4192: 5'- CAGGGTGTTATAAGCAATCCC -3'
PLP null	Internal protocol;
	1864: 5'- TTGGCGGCGAATGGGCTGAC -3'
	2729: 5'- GGAGAGGAGGAGGGAAACGAG -3'
	2731: 5'- TCTGTTTTGCGGCTGACTTTG -3'
Emx-Cre	Internal protocol;
	26532: 5'-CATCGCCACGAAGCAGGCCAACGG -3'
	26533: 5'-AGCCAGCCCATTCTCTTGTCCCTC -3'
	25250: 5'-ATTTTCCACCATATTGCCGTCT -3'
	25251 5'-AGCCATTTGACTCTTTCCACAAC -3'
$MBP^{fl/fl}$	Internal protocol;
	23500: 5'-GGGTGATAGACTGGAAGGGTTG -3'
	23501: 5'-GCTAACCTGGATTGAGCTTGC -3'
	15048: 5'-CAACGGGTTCTTCTGTTAGTCC -3'

Table 2.7 Genotyping master mix per reaction

Reagent	Amount	Company
Go-Taq 5x buffer	4µL	Promega
dNTP (2mM)	2µL	Promega
Primermix	Typically 0.5µL per primer	Custom; AGCT Lab MPI-EM
GoTaq	0.1µL	Promega
DNA	1µL	-
dH_2O	To 19µL	-

Table 2.8 Standard PCR programme

Step	Time, Temperature	
Initial denaturation	95°C, 3min	
Denaturation	95°C, 30sec	35 cycles
Annealing	55-60°C (depending on primer), 30sec	
Elongation	72°C, 30sec	
Final extension	72°C, 5min	

2.1.6 Software

Table 2.9 Software

Name	Company	Version
FIJI	Schindelin et al. 2012	v1.53c
Inkscape	Inkscape.org	1.1
Prism	Graphpad	8.0
Vision4D	Arivis	v3.2
ZEN	Zeiss	3.2 Lite, 2012

2.1.7 Devices

Table 2.10 Devices

Name	Company	Application
AxioImager Z1	Zeiss	IHC, Brightfield
AxioObserverZ1	Zeiss	IHC, Fluorescence
Eon High Performance Microplate Spectrophotometer	BioTek	WB
Microm HMP110 tissue processor	Microm	IHC
Odyssey infrared imager	Licor	WB
T3/Gradient Thermocycler	Biometra	Genotyping
UltramicroscopeII	LaVision Biotech	LSM
STP 120	Leica Microsystems	Paraffin embedding
HistoStar	Epredia	Paraffin embedding

2.1.8 Other materials

Table 2.11 Miscellaneous materials

Name	Company	Application
Aqua-Polymount	Polysciences	IHC, fluorescence
DC protein assay	BioRad	WB
GeneRuler 100bp DNA ladder	Thermo	Genotyping
Low fluorescence Immobilon PVDF 0.45µm	Merck	WB
Mounting medium Eukitt	Kindler	IHC, chromogenetic

PageRuler (10-250kDa)	Fermentas	WB
Paraffin (Paraplast)	Leica	IHC
Precellys soft tissue lysis kit	Bertin Instruments	WB
Protease Inhibitor Mix (500x)	Sigma	WB
RNeasy Miniprep Kit	Qiagen	Bulk sequencing
Tris-Tricine Novex 10-20% Gel	Thermo Fischer	WB

2.2 Methods

2.2.1 Human tissue analysis

Human tissue was kindly provided by Dr. Ruth Stassart (Leipzig University Hospital). Material was selected from a pool of patients that underwent routine autopsy and neuropathological assessment in the years 2018-2019 at the Leipzig University Hospital. The very small patient cohort was not stratified regarding specific age, gender or genotype. The only inclusion criteria were a medical history of dementia and a NIA-AA score of A2B3C2 or A3B2C2 (for AD patients) without presence of any other severe neurological disease. Accordingly, control patients did not fulfil the aforementioned criteria despite also not suffering from other severe neurological diseases. Selected patients were of mixed age (60-90 years) and gender. Upon admission, patients provided written consent for the scientific use of autopsy tissue. Biopsies from the medial temporal lobe containing the hippocampal formation from 3 AD patients and 3 control patients were analysed by immunohistochemistry for amyloid plaques, microglia and intracortical myelin content. See section on Immunohistochemistry (IHC) for details regarding the IHC protocol.

2.2.2 Mouse strains, husbandry and genotyping

Animal experiments were performed according to German animal welfare practices and approved by the local authorities. Mice were housed at the animal facility of the Max Planck Institute for Experimental Medicine under the care of qualified animal caregivers, veterinarians and scientists. Housing was typically performed in groups with a 12-h dark/12-h light cycle, with *ad-libitum* access to food and water and regular cage changes. The original mouse strains used to perform crossbreeding to generate experimental double mutant animals are given in Table 2.5. All strains used were maintained on C57BL/6 background prior to the start of this project. For most of the analysis presented here littermate controls of the same sex were used. Partially, a corresponding control line was established from the initial F1 generation of crossbreedings. Various ages were analysed throughout this study (3-6 months) and the exact age of the experimental cohort is given in the experimental setup or in the respective figure legend. Initial genotyping was performed on ear punches generated during earmarking for identification of the animals. DNA was isolated from frozen biopsies by alkaline lysis by incubation in 300µL of 50mM NaOH for >1h at 95°C and subsequent neutralisation by adding 30µL 1M Tris/HCl pH8.0 and centrifugation at 13,000rpm. Genotyping was then performed using polymerase chain reaction (PCR) and gel electrophoresis with GelRed (BioTrend) of amplified DNA fragments on 1.5% Ultra-pure agarose (Thermo Fischer) gel. Mastermix composition for the respective genotyping PCR is given in Table 2.7 and the standard PCR programme used is given in Table 2.8. Primers for the respective mouse lines are given in Table 2.6 and were synthesised in the local AGCT lab facility. For the genotyping of 5xFAD mice, the publicly available JAX protocol 31769 was followed which could differentiate between heterozygous and homozygous mice. Typically, 1µL of crudely isolated DNA was used as PCR input. Genotypes of animals were reconfirmed on tail tips taken at the end of the respective experiment. Genotyping was performed with the help of Katharina Overhoff (student assistant) and Carolin Böhler (technician).

2.2.3 Demyelination models

Cuprizone-intoxication was conducted as described previously (Berghoff et al. 2021). In brief, 14 weeks old 5xFAD mice were put on a powder diet containing 0.2% (w/w) Cuprizone (Sigma-Aldrich) for 28 days. This was followed by a 28-days recovery period on normal pelleted food. Animals were monitored carefully for weight changes and other signs of sickness. At the end of the experiment, brain tissue was harvested following perfusions. Experimental autoimmune encephalomyelitis (EAE) was performed as described in (Berghoff et al. 2021). In brief, 2.5 months old 5xFAD mice were immunised against myelin oligodendrocyte glycoprotein (MOG) by subcutaneous injection of 200mg MOG_{35-55} peptide in complete Freund's adjuvant (Mycobacterium tuberculosis at 3.75 mg/ml; BD). Animals were additionally injected with 500ng of pertussis toxin at day 1 and 3 post EAE induction (dpi 1 and 3). Neurological scoring was performed daily according to the following parameters as listed in (Berghoff et al. 2021): "0 - normal; 0.5 - loss of tail tip tone; 1 - loss of tail tone; 1.5 - ataxia and mild walking deficits (slip off the grid); 2 - mild hind limb weakness, severe gait ataxia and twist of the tail causing rotation of the whole body; 2.5 - moderate hind limb weakness and inability to grip the grid with the hind paw but ability to stay on an upright tilted grid; 3 - mild paraparesis and falls from an upright tilted grid; 3.5 - paraparesis of the hind limbs (legs strongly affected but move clearly); 4 - paralysis of the hind limbs and weakness in the forelimbs; 4.5 - forelimbs paralyzed; 5 - moribund or dead. Animals were perfused at 28 dpi at 14 weeks of age". At day 28 dpi animals were perfused and brain and spinal cord tissue harvested. Experiments were performed together with Lena Spieth and Dr. Stefan Berghoff.

2.2.4 Mouse behavioural testing

Clasping motoric deficits were assessed by evaluating the position of limbs during a very short suspension during cage changes. Clasping was scored according to : "0 – no impairments, hindlimbs normally spread and moved; 1 - one hindlimb shows slightly less mobility; 2 - both hindlimb show less mobility, 3- both hindlimbs show reduced mobility and reduced spread; 4- both hindlimbs show severely reduced movement and severely reduced spread" as described in (Depp et al. 2021). For unbiased analysis and representation, short videos were recorded. Animals were tested in two different maze-types: the elevated plus (EPM) for assessment of anxiety-related behaviours and Y-maze (YM) for assessment of working memory. Mazes were crafted from grey plastic in standardised sizes by the local workshop at the Max Planck Institute for Experimental Medicine (Y-maze: 40cm per arm; EPM: 50cm per arm). Mazes were thoroughly cleaned with ethanol and water inbetween assessment of different mice. In the EPM, mice freely explore a plus-shaped platform that is 60cm elevated from the ground for 5 minutes. Two opposing arms (closed arms) are covered by 30cm plastic shields and two opposing arms remain uncovered. Mice prefer the closed arms over open arms which is seen as expression of intact natural anxiety towards open, unprotected spaces. In the YM, animals explore a Y-shaped maze with fully enclosed arms for 8min. Out of natural curiosity, mice tend to visit arms in a sequential manner, preferring a new arm over a recently visited arm. Alternating visits are interpreted as a sign of intact working memory as this indicated that the animal remembers which arm was recently visit. Animals were tested in a closed room without experimenter interference. A camera was mounted above the respective experimental setup to record videos. Videos were analysed in a Bio-Observe Viewer computer setup. Animals were automatically detected and tracked in the software by virtue of contrast from their black fur. Analysis zones were defined in the software (arms and centre) to track the time and track length in each zone. Images of tracks and time-resolved positional data and were exported as spreadsheet and further analysed. As parameters for EPM performance, I analysed the time spent in both open arms and total track length. For evaluation, arms were assigned to letters (ABC) and the number and sequence of arm entries was manually recorded. A correct triad is defined as the sequential visit of the three arms (e.g. ABC and its permutations). An arm visit was counted when mice entered the arm with their full body (excluding tail). The alternation index was calculated by the number of observed divided arm entries by the total number of arm entries minus 2 which is the maximal amount of triads. For statistical analysis, several different type III

analyses of variance tests (ANOVAs) that probed the main effects for the 5xFAD and myelin mutant genotype as well as their interaction.

2.2.5 Tissue preparations for microscopy

For microscopic analyses, animals were transcardially perfused following deep anaesthesia or euthanisation via CO asphyxiation. Animals were first flushed with ice-cold Hank's buffered salt solution (HBSS) until full decolourisation of the liver was observed. This was followed by flushing with ice-cold 4% paraformaldehyde (PFA) in 0.1M phosphate buffer. Desired tissue (brain, spinal cords, optic nerves) were extracted and further postfixated. Tissue was then thoroughly washed in PBS and stored at 4°C sitting in PBS.

2.2.6 Tissue preparations for biochemical analysis

For western blot analysis of brain tissue, animals were sacrifised, and brain and spinal cord quickly extracted. Tissue was immediately fresh-frozen on dry-ice and stored at -80°C until further processing. Partially, the brain was further microdissected upon extraction. First, the brain was washed in ice-cold HBSS and meninges removed. Then the brain was transferred into a custom-made coronal brain matrix (workshop, Max Planck Institute for Experimental Medicine) with approximately 1mm spacing. Brain slices were carefully transferred to a pre-chilled glass plate sitting on an ice bucket. Cortex, white matter and hippocampus were excised out from brain slices. White matter primarily contained corpus callosum and parts of the fornix system as these white matter tracts are easily dissectible. Harvested tissue was then frozen on dry-ice and stored at -80°C until further use.

2.2.7 Whole tissue staining and clearing for LSM

In toto staining was performed on PFA fixed tissue according to a modified iDisco protocol given in Table 2.12 (Liebmann et al. 2016; Renier et al. 2014). All steps were carried out under gentle agitation in 2mL Eppendorf tubes.

Table 2.12 LSM staining

Step	Solution	time	temperature
Dehydration	50% MeOH/ 50% PBS	1h	RT
	80% MeOH/20% PBS	1h	RT
	100% MeOH	1h	RT
	100% MeOH	1h	RT
Bleaching	1:1:4 H_2O_2:DMSO:MeOH	O/N	4°C
Delipidation	100% MeOH	0.5h	4°C
	100% MeOH	3h	-20°C
	100% MeOH	O/N	4°C
	80% MeOH/20% MeOH	2h	RT
Rehydration	80% MeOH/20% PBS	2h	RT
	50% MeOH/ 50% PBS	1h	RT
	100% PBS	1h	RT
	0.2% Triton X-100/PBS	1h	RT
	0.2% Triton X-100/PBS	1h	RT
Permeabilisation	PBS/0.2% Triton X-100/ 20% DMSO/0.3 M glycine	O/N	37°C

	PBS/0.2% Tween-20/10 mg/ml heparin/5mM sodium azide (PTwH)	1h	RT
	PTwH	1h	RT
Labelling	PTwH 0.01% Congo red	3d	37°C
Or blocking	0.2% Triton X-100, 10% DMSO and 6% goat serum	3d	37°C
Antibody labelling	PTwH/0.2% Triton X-100, 5% DMSO and 3% GS + 1st antibody	14d	37°C
	6x PTwH	1d	RT
	PTwH	O/N	37°C
	PTwH/3% GS + 2nd antibody	7d	37°C
Washing	6x PTwH	1d	RT
Embedding	Phytagel 1.5% w/v in PBS for spinal cords	-	-
Dehydration	20% MeOH/ 80% PBS	1h	RT
	40% MeOH/ 60% PBS	1h	RT
	60% MeOH/ 40% PBS	1h	RT
	100%	1h	RT
Delipidation	1:2 MeOH:dichloromethane	O/N	RT
	DCM	40min	RT
Clearing	Ethylcinnamate (Eci)	1h	RT
Storage	Ethylcinnamate (Eci)	-	-

2.2.8 *In toto* light sheet microscopy

Light sheet microscopy of cleared samples was performed at an commercial light sheet setup (UltraMicroscope II, LaVision Biotec) equipped with a 2x objective lens, zoom body, and a corrected dipping cap. Samples were imaged being submerged in a sample cuvette containing Eci. Cleared hemispheres were mounted into the sample holder to acquire sagittal images (medial surface down). Images were acquired in the mosaic acquisition mode using the following settings: 5 µm light sheet thickness, 20% sheet width, 0.154 sheet numerical aperture, 4 µm z-step size, 1000x1600 pixel field of view, 4x4 tiling, dual light sheet illumination, and 100 ms camera exposure time. Laser settings were as followed: 80% power 561 nm and 585/40 emission filter (Congo red); 30% power 640 nm excitation at 30% and a 680/30 emission filter (antibody labelling); 50% power 488nm laser and 525/20nm emission filter (autofluorescence). Raw data were imported into Vision4D v3.2/v3.1 (Arivis) and stitched using the tile sorter setup. Partly, images were imported and stitched using the Imaris Importer and Stitcher v9.1 (Bitplane). Regions of interest (ROI) were manually annotated according to the sagittal Allen mouse brain atlas with automated interpolation between planes. ROIs were cropped in a similar manner between brains with a medial cut-off of approximately ~0.4 mm and a lateral cut-off of ~4.4 mm. Plaques were detected automatically with different algorithms dependent on the sample: For 3-month-old 5xFAD brain data, a simple intensity thresholding was sufficient. 6-month-old 5xFAD data were segmented using the blob finder algorithm in Vision4D. For quantification of amyloid plaques in the APP^{NLGF} brains, segmentation was performed using the machine learning segmenter in Vision4D. Subsequently, datasets were inspected and noise was removed by deleting objects with voxel sizes <10. Objects were then critically reviewed and any additional noise (especially blood vessels) were removed. For quantification, the object number, object total volume and mean volume were extracted.Visualisation was performed in Vision4D. Maximal intensity projections of cropped ROIs were created. Additionally, hippocampal, isocortical and alveus plaques are represented as centroids and colour-coded according to location.

2.2.9 Paraffin sections and immunohistological stainings

Fixed tissues were embedded in paraffin following the protocol given in Table 2.13. using the STP 120 tissue processing machine (Leica microsystems) and the HistoStar embedding workstation (Epredia). Paraffin-embedded blocks were sectioned coronally in 5 µm thick slices and mounted onto glass slides and dried overnight. Paraffin sections were stored at RT until further use. Staining of paraffin slices was carried out according to the protocol given in Table 2.14 for fluorescent stainings using coverplates. Asteriks mark steps specific for labelling of amyloid beta by different means. For chromogenetic labelling, a few changes were implemented. All incubation and washing steps were carried out in Tris/2% Milk. An additional step of inactivation of endogenous peroxidases was implemented prior to blocking by incubation in 3% H2O2. The LSAB2 Kit (Dako) for rabbit/mouse and the DAB-Kit from Zytomed was used according to the manufacturers' protocols and slides were dehydrated and mounted using Eukitt. Stainings were partially performed by Annette Fahrenholz (technician) and Andrew Sasmita (Master's thesis student). Antibodies used are given in Table2.2.

Table 2.13 Paraffin embedding

Step	Solution	time
Dehydration	50% EtOH	2h
	80% EtOH	2h
	100% EtOH	2h
	100% Isoproponal	2h
	50%Isoproponal/50% Xylol	2h
	100% Xylol	2h
	100% Xylol	2h
Embedding	Melted paraffin	>2h
	Cool down + storage	RT

Table 2.14 Immunofluorescence stainings

Step	Solution	Time/temp
Deparaffinisation	60°C oven	5min
	100% Xylol	10min
	100% Xylol	10min
	50% Xylol/50%Isopropanol	10min
Rehydration	100% EtOH	5min
	90% EtOH	5min
	70% EtOH	5min
	50% EtOH	5min
	H2O	5min
Antigen retrieval	Citrate buffer pH6 or Tris/EDTA buffer pH10	5min
	boiling	10min
	Cool-down	20min
*Amyloid retrieval	88% formic acid	3min
Permeabilisation	0.1% Triton X-100/PBS	5min
Washing	PBS	2x5min
Blocking	10% Goat serum/PBS	1h
1st antibody(AB)	10% Goat serum/PBS or 5%BSA/PBS + 1st AB	O/N 4°C
Wash	PBS or Tris/2% milk	3x5min
2nd antibody	10% goat serum/PBS + 2nd AB	2h at RT

Dye labelling	DAPI or ToPro in PBS	5min
*Amyloid dye labelling	Methoxy-X04 in 50% EtOH	30min
*Contrasting	50% EtOH	5min
Washing	PBS	3x5min
Mounting	Aqua Polymount	-
Storage	covered	4°C

2.2.10 Epifluorescence and brightfield microscopy

Epifluorescence microscopy was performed on a Zeiss Observer Z1 microscope with the following specifications. Objectives: Plan-Apochromat 20x/08 and Fluar 2.5x/0.12 objectives. Excitation: Colibri 5 LED light source (630nm, 555nm, 475nm 385nm excitation). Zeiss Filter sets: 96 HE BFP, 90 HE DAPI/GFP/Cy3/Cy5, 38 GFP, 43 DsRed, 50 Cy5. Camera: Axiocam MrM. Stage: SMC900 motorised stage. To acquire images of the entire brain slice, a preview scan at 2.5x magnification was carried out in the ZEN2012 imaging software. Support points for focus adjustment were distributed and each support point was manually adjusted for imaging at 20x magnification. The focus surface was automatically extrapolated for the entire slice surface in ZEN. Stitching was performed post acquisition in ZEN. For display of images, different channels were assigned pseudocolours. I chose a colour-blind friendly colour scheme with good contrast: cyan, magenta and yellow. Intensity display was adjusted for optimised display in the same manner throughout a specific staining cohort and images were exported from ZEN. Alternatively, images were directly opened in FIJI (Schindelin et al. 2012). Brightfield microscopy was performed on a Zeiss Axiophot Imager.Z1 with the following specifications. Objectives: Achroplan 4x/0.1, PlanFluar 20x/0.75 and Plan Neofluar 40x/0.75. Camera: AxioCamMrc. Whole brain slice microscopy was performed in an analogous manner to epifluorescence microscopy using preview scan mode and focus support points. RGB images were adjusted in terms of brightness and contrast in the same fashion throughout a respective staining cohort and images exported from ZEN.

2.2.11 2D microscopy quantification

Quantification of 2D immunofluorescence stainings was performed in FIJI (v1.53c) (Schindelin et al. 2012). For determining a positive area, the ROI was first traced manually using the polygon tool and its area calculated. Then automated thresholding was performed (using different presets in FIJI) to segment bright pixels. Thresholding converted the images into binary images in which white pixels were segmented using the "create selection" tool and the area covered by white pixels was measured. Plaque corralling in 5xFAD mice was assessed in an automated fashion in hundreds of plaques using a FIJI macro-script. This macro in Iba1/plaque-co-stainings detects individual plaques using thresholding and creates masks from them. Masks are applied to the Iba1 channel and the percentage of plaque covered by Iba1 is determined after thresholding and segmentation of the Iba1 channel. Plaque-microglia coverage can then be expressed as percentage. APOE levels in plaques were quantified by segmenting APOE positive plaques and determine mean fluorescence per plaque.

2.2.12 High pressure freezing electron microscopy

HPF-EM was performed by Dr. Wiebke Möbius and is in detail described in the primary manuscript originating from this thesis (Depp et al. 2021). Methods are copied here for the sake of completeness. "Sample preparation by high pressure-freezing (HPF) and freeze substitution was performed as described (Weil et al. 2019; Steyer et al. 2020). In brief, optic nerves of 6-months-old $CNP^{-/-}$ and control wildtype mice were freshly dissected, immersed in 20% PVP in PBS and placed into HPF sample carriers (Wohlwend, Sennwald, Switzerland). After freezing using a HPM100 high pressure freezer (Leica Microsystems, Vienna, Austria), samples were embedded in EPON after freeze substitution using 0.1 % tannic acid in acetone followed by 2%

OsO4 and 0.1 % uranyl acetate in acetone. After polymerization, samples were sectioned with a UC7 ultramicrotome (Leica Microsystems, Vienna, Austria) and imaged with a LEO912 transmission electron microscope (Carl Zeiss Microscopy GmbH, Oberkochen, Germany) using an on-axis 2k CCD camera (TRS, Moorenweis, Germany)." (Depp et al. 2021)

2.2.13 Cell fractioning

Prior to western blot analysis of 5xFAD tissue, cell fractioning was performed to separate soluble from membrane-bound proteins and solubilise fibrillar amyloid in formic acid. Protocols were kindly provided by Dr. Michael Willem/Prof. Christian Haass and was performed as described in (Parhizkar et al. 2019). Steps are given in Table 2.15. All buffers and solutions were supplemented with protease inhibitor cocktail (P8340, Merck). For tissue homogenisation, the Precellys lysing Kit "soft tissue homogenising, 1mL REF P000933-LYSKO-4" was used. For ultracentrifugation a TLA-100.3 rotor with conical tube adaptors was used at an Optima-Max Beckmann Coulter tabletop ultracentrifuge. For fractioning of corpus callosum and cortex 200µL per homogenisation step was used. For fractioning of entire brains 1mL of homogenisation buffer was used.

Table 2.15 Cell fractioning

Fraction-step	Solution	Specifications
Soluble	Homogenisation in DEA-buffer	Precellys; 6500rpm, 30sec, 4°C
	Centrifugation	5000g, 10min, 4°C
	→ Soluble: Ultracentrifugation	130 000g, 1h, 4°C
	→ Soluble: DEA-fraction	pH adjustment 10% 0.5M Tris pH6.8
		Store -80°C
Membrane-bound	→ Pellet: RIPA	
	Homogenisation in RIPA-buffer	Precellys: 5000rpm, 12sec, 4°C
	Centrifugation	5000g, 10min, 4°C
	→ Soluble: Ultracentrifugation	130 000g, 1h, 4°C
	→ Soluble: RIPA-fraction	Store -80°C
Amyloid/formic acid	→ Pellet: Formic acid (70%)	
	Homogenisation in Formic acid	Sonication, 7min
	Ultracentrifugation	130 000g, 1h, 4°C
	→ Soluble: Formic acid fraction	Store -80°C
	Neutralisation	1M Tris pH9.5 (1:20)

2.2.14 SDS PAGE and western blotting

Protein concentrations in DEA and RIPA-fractions were determined by running detergent compatible protein assays (Biorad). Samples were run in duplicates and plotted against a BSA standard. Concentrations in SDS-PAGE samples were adjusted to contain 1µg/µL in order to load 20µg-30µg per lane onto the gel and mixed with Laemmli loading buffer. For BACE1 western blotting, standard self-casted Tris-Glycine SDS-PAGE gels (8%) were used using the standard separating and collecting gel compositions (Biorad systems). For better resolution in the lower molecular weight spectrum (APP and Trem2 fragments), Tris-Tricine SDS PAGE gels (10-20%, Novex, Thermo Fisher) were used.

Both gel types were run at 100-120V for approximately 1h in the respective tanks in SDS-PAGE running buffer or Tris-Tricine running buffer. Run was stopped dependent on the range of proteins of interest (typically after 1h). Proteins were transferred onto low fluorescent Immobilon-FL membrane (0.45µm por size, Merck) using the Biorad wet-blot system (1.15h, 500mA) and blot transfer buffer. Blots were subsequently washed in water and transferred into Fastgreen-staining solution for 5min. Fastgreen is a fluorescent protein stain that can be used for quality check of the transfer as well as for normalisation to total protein load which was conducted in this thesis. Blots were washed 5min in Fastgreen washing and imaged at a ChemoStar fluorescent imager (Intas) equipped with a 670 nm/20 nm excitation filter and near infrared emission collection. After this, membranes were thoroughly rinsed in water until no acidic smell could be detected. Membranes were then further washed in TBS-T. Blocking was conducted in 5% BSA in TBS-T for 1h at room temperature at constant rolling with the membrane sitting in a falcon tube with 5mL blocking solution. Primary antibodies were also applied in 5%BSA TBS-T overnight at 4°C in a rolling falcon tube. Primary antibodies used are given in Table 2.2. The next day, membranes were thoroughly rinsed in PBS-T and fluorescent secondary antibodies (see Table 2.2) were applied for 2h at room temperature in falcons protected from light. After additional washing in TBS-T, TBS and finally water the membranes were imaged at an Odyssey scanner platform (Licor). Quantification of western blots was performed using FIJI. Background was subtracted form raw images (rolling ball radius 50), an equally sized ROI was placed over individual bands and the integrated density was measured. Band densities were normalised either against the full length version of the protein of interest or against the lane intensity of the fastgreen whole protein staining.

2.2.15 Magnetic activated cell sorting of microglia and bulk RNA-sequencing

Magnetic activated cell sorting (MACS) of microglial cells was performed together with Lena Spieth. Animals of the following genotypes (WT, $Cnp^{-/-}$, 5xFAD, $Cnp^{-/-}$ 5xFAD) at 6-month of age were sacrificed via cervical dislocation and brains were extracted. Four replicates were used for each genotype. Hemibrains were further dissected, and forebrain cleaned from cerebellum and olfactory bulb. Brain tissue was then cut in small pieces and further mechanically and enzymatically dissociated using the Miltenyi Biotec adult brain dissociation kit. Steps were carried out according to manufacturer's protocol. For superior purity of the microglial fraction, the cell suspension was first cleaned from myelin using ultracentrifugation, and additionally from oligodendrocytes and astrocytes via MACS. For oligodendrocyte and astrocyte removal, the respective beads recommended from Miltenyi Biotec were used: O4 beads for positive-selection of oligodendrocytes and ACSA-2 microbeads for astrocytes. Sorting was performed according to the manufacturer's protocols. Finally, positive selection of microglia was performed using CD11b microbeads. For all isolation steps, LS columns were used (Miltenyi Biotec). Cell fractions were directly eluted in RLT buffer (RNeasy Micro Kit, Qiagen) and frozen at -20°C. RNA was extracted using the RNeasy Micro Kit (Qiagen) according to the manufacturer's protocol. RNA was eluted in 30 µl nuclease-free water and subjected to 50 bp single-end mRNA sequencing using HiSeq 4000 (Illumina). Sequencing was performed by the NGS Integrative Genomics Core Unit, University Hospital Göttingen. Raw data analysis was performed by Ting Sun. Raw sequencing data were quality-checked using FASTQC v0.72, and subsequently aligned to the reference mouse genome GRCm38 using STAR v2.5.2b-2 (Dobin et al. 2013) with default parameters. Gene raw counts were extracted using featureCounts v1.6.3 (Liao, Smyth, and Shi 2014) for differential gene expression (DGE) analysis using DESeq2 v.1.26.0 (Love, Huber, and Anders 2014). Gene raw counts were converted to TPM value. For DGE analysis, each genotype was compared with all other genotypes separately. Gene targets with adjusted P-value < 0.05 were considered as significantly regulated between genotypes. Normalised TPM profiles were embedded using principal component analysis (PCA) to assess overall similarity between samples.

2.2.16 Single-nuclei transcriptome sequencing

Single-nuclei transcriptome sequencing is in detail described in the primary manuscript originating from this thesis (Depp et al. 2021). Methods are copied here for the sake of completeness. Analysis was performed together with Ting Sun. Raw data analysis was performed by Ting Sun. Sequencing was performed in collaboration with Daniel Geschwind and Riki Kawaguchi (Department of Neurology, David Geffen School of Medicine, University of California Los Angeles, Los Angeles, USA).

"Cortex and corpus callosum from 3-month-old $Cnp^{-/-}$ and WT controls were micro-dissected and subjected to single-nuclei transcriptome sequencing. For each genotype and replicate, the tissue of two animals were pooled. Two replicates per genotype were sequenced. Nuclei were isolated according to previously published methods(Corces et al. 2017). Briefly, frozen tissue was transferred into 2ml of pre-chilled homogenisation buffer (320mM sucrose, 0.1% NP40, 0.1mM EDTA, 5mM $CaCl_2$, 3mM $Mg(Ac)_2$, 10mM pH 7.8 Tris, 167uM β-mercaptoethanol and 1x protease inhibitor (Roche)). Tissue was carefully homogenised and filtered through a 80µm strainer, and further centrifuged for 1min under 100 rcf. For each sample, 400 ul supernatant was collected into a pre-chilled 2ml low-binding Eppendorf tube, followed by adding 400ul 50% iodixanol solution (in 1x homogenisation buffer containing 480mM sucrose) to reach a 25% iodixanol concentration. By layering 600ul of 29% iodixanol underneath the 25% iodixanol mixture, then 600ul of 35% iodixanol underneath the 29% iodixanol, two clear interfaces between different concentrations of buffers were created, and the tube was centrifuged for 20 min under 3000 rcf. After centrifugation, nuclei were collected from the band between the 29% and the 35% iodixanol layers and transferred to a fresh pre-chilled tube. Isolated nuclei were washed and resuspended in cold resuspension buffer (1xPBA, 1% BSA, 0.1U/ul RNase inhibitor) and further subjected to single-nuclei transcriptome libraries using the chromium single cell 3' reagent kit according to the manufacturer's instruction (10x Genomics). The constructed libraries were sequenced using Novaseq 6000 (Illumina). Raw snRNA-seq data were collected in Fastq format and first aligned to the reference profile pre-mRNA (ENSEMBL GRCh38) using CellRanger toolkit v3.0.2 (10x Genomics). Matrices containing UMI count of each gene in each nuclei were extracted for all samples, by filtering out nuclei with <200 detected genes and <500 total transcripts, as well as nuclei with outlier level transcripts quantity or gene detection rate identified according to individual sample sequencing depth. Genes expressed in less than 3 cells were excluded for further analysis. Filtered expression matrices were combined, and UMI of each nucleus were normalised towards its total UMI counts with a scale factor of 10,000 and then log transformed.

Dimensionality reduction, clustering analysis and cell type annotation

The normalised UMI matrix of all samples was mainly analysed using the R package Seurat v3.2.3(Stuart et al. 2019). High variable genes were calculated and scaled to support linear dimensionality reduction using PCA. For all cells, the first 50 PCs were used for further neighbouring embedding using uniform manifold approximation and projection (UMAP) (McInnes, Healy, and Melville 2018), as well as for performing the clustering analysis (resolution=0.5) using K nearest neighbour (KNN) algorithm. Cluster marker genes were calculated using the MAST algorithm (Finak et al. 2015) to determine cluster cell type annotations. Clusters with undefined cell identities were removed from further analysis. To perform cell type specific analysis for microglia the corresponding cell population was firstly subset and reduced for its dimensionality using PCA. Similarly, selected top PCs were used for UMAP embedding and clustering analysis, with cluster marker genes calculated by MAST.

External data integrative analysis

Integrative analysis was carried out between $CNP^{-/-}$ and GSE140511(Zhou et al. 2020). More specifically, microglia from $Cnp^{-/-}$ and corresponding controls were integrated with microglia profiles from 7-month-old WT, 5xFAD from GSE140511, to unravel the disease associated microglia (DAM) subpopulation. Integrative analysis was conducted using the SCTransform pipeline implemented in the Seurat toolkit. The batch effect corrected data underwent PCA dimensionality reduction, neighbouring embedding and unbiased clustering." (Depp et al. 2021)

2.2.17 Data visualisation

Graphs were created in Prism 8.0 (Graphpad) and final figure composites were assembled in Inkscape (v1.1, www.inkscape.org). Schemes shown in this thesis were also created in Inkscape.

3 Results

3.1 Identification of mouse models to study the impact of ageing myelin defects on amyloid pathology

Analysis of human subjects/material (brain imaging, CSF biomarkers, neuropathological assessments of autopsy samples) is limited to describing putative correlations of myelin abnormalities and amyloid deposition. Often these methods are not sensitive enough to temporally resolve which pathology precedes the other. Mouse models offer the possibility for experimental intervention and specifically study the outcome of experimentally disrupting myelin on amyloid pathology.

I first identified suitable mouse models that would offer the possibility to study the effect of premature myelin ageing on AD. Previous work in our lab has established that the non-compact myelin protein CNP declines in abundancy in myelin preparation of the aged mouse brain (2 years) (Hagemeyer et al. 2012). CNP heterozygote mice show a premature ageing phenotype that manifests approximately 7 months earlier than in wildtype controls (Hagemeyer et al. 2012). This "premature" ageing phenotype is characterised by more pronounced gliosis as identified by GFAP, IBA1 and MAC3 labelling as well as axonal pathology (Hagemeyer et al. 2012). Full deficiency of CNP can - to a certain extent - be interpreted as a hyper-ageing phenotype: early work by Lappe-Siefke et al. showed that CNP null mice exhibit strong micro- and astrogliosis at younger age (here analysed at 14 months of age). Later studies showed that significant gliosis occurs much earlier (3 months) (Snaidero et al. 2017) and axonal pathology is virtually present with onset of myelination (Edgar et al. 2009). With outfoldings and cytoplasmic accumulations, myelin structural changes in CNP null mice also well mimic age-associated deterioration of myelin (Snaidero et al. 2017). Similarly, PLP deficient mice present with gliosis, myelin lamella splits and other structural defects that resemble ageing-associated changes (Rosenbluth et al. 2006; Gould et al. 2018; Lüders et al. 2017). To further establish CNP and PLP null mice as models of advanced brain/myelin ageing, I first examined histopathological similarities between myelin mutant brains at 6 months of age and wildtype (C57BL/6) aged brains at 24 months. As ageing was specifically shown to impact intracortical myelin, I first investigated changes to myelinated fibres in the cortex using MBP immunolabelling. Changes to myelinated fibres were visible in the upper cortical layers where myelination becomes sparser and individual fibres can be distinguished (Fig3.1a). Young wildtype animals showed long internodes with myelinated fibre bundles running perpendicular to the brain surface mapping to cortical layer 2/3. Additionally, multiple myelinated profiles could be identified in layer 1 just under the pial surface that run horizontally to the brain surface. Both myelin profiles showed age related deterioration noticeable as an overall decline and apparent shorting. This phenotype was mimicked with further exacerbation in $CNP^{-/-}$ and $PLP^{-/y}$ mice that virtually lost subpial myelin profiles. Further, $CNP^{-/-}$ and $PLP^{-/y}$ myelin profiles were less bundled and organised.

Myelin structure in white matter tracts can be easily inspected using autofluorescence. Healthy myelin shows a smooth appearance in which the fibre direction can be determined. In aged and more pronounced in $CNP^{-/-}$ and $PLP^{-/y}$ myelin, I recognised multiple speckles in the white matter together with a seemingly disorganised overall structure (Fig3.1b). Similar but much larger myelin bodies have been previously characterised in aged myelin (Hill, Li, and Grutzendler 2018). I further performed immunolabeling and microscopic analysis of astrogliosis (GFAP) and microgliosis (IBA1) (Fig3.1c,d). As previously reported, age-induced gliosis was more prominent in white matter than grey matter. This was again well replicated in myelin mutants that showed enhanced gliosis in both white and grey matter albeit stronger than in aged wildtype brains. This histological analysis reveals profound similarities between natural brain ageing and phenotypes driven by CNP and PLPL null myelin. It identifies CNP and PLP null mice as adequate models to study the effects of premature myelin ageing on amyloidosis.

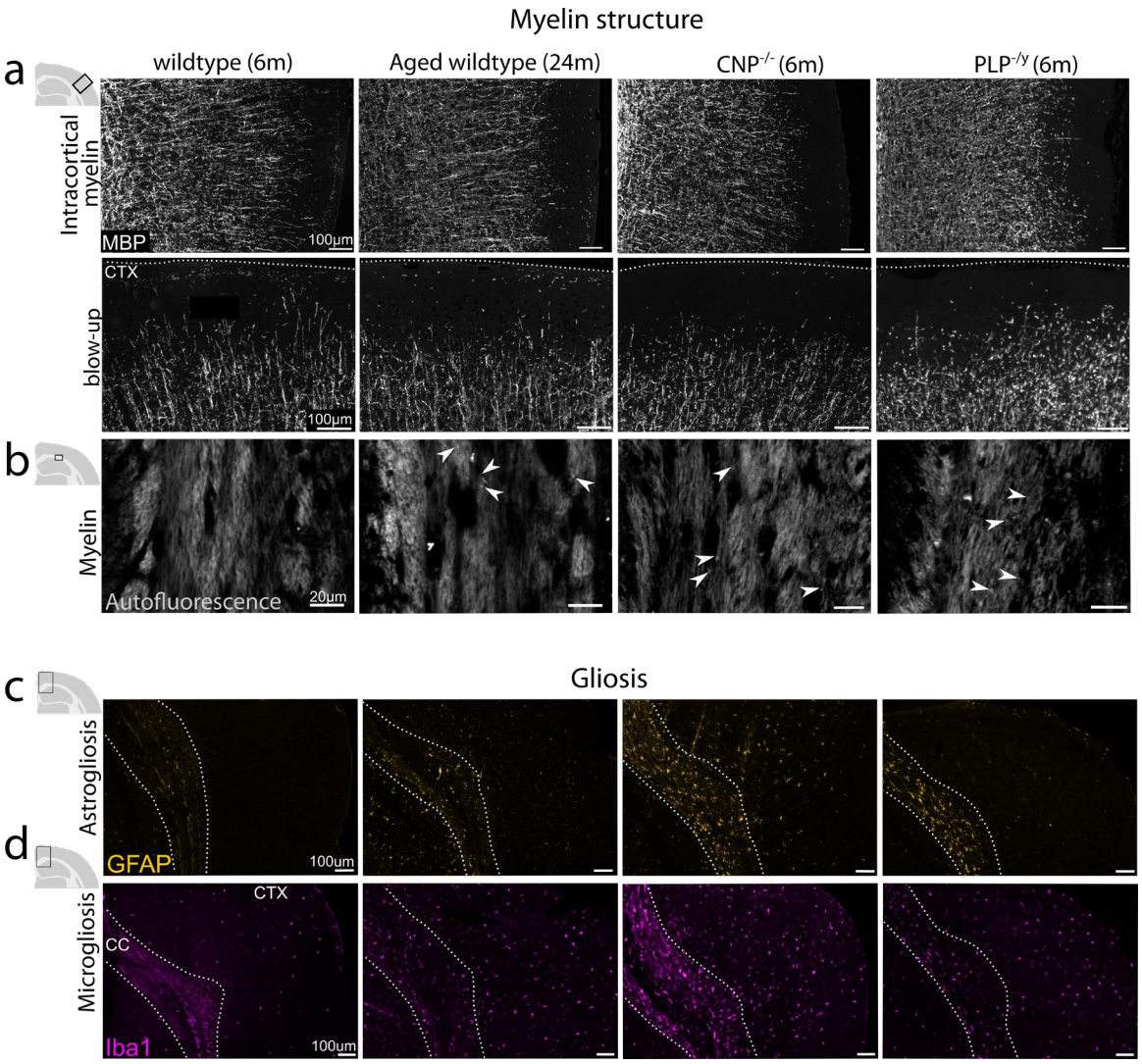

Figure 3.1 CNP and PLP deficiency induce a premature ageing phenotype in the mouse brain. (a) Fluorescence microscopy of myelinated fibres in the cortex stained against (MBP) in 6-month-old wildtype, $CNP^{-/-}$, $PLP^{-/y}$ and 24-months-old wildtype mouse brain. Lower panel shows blow-up of upper cortical layers and cortical surface. **(b)** Analysis of autofluorescent profiles of myelin in the corpus callosum in the respective genotype. **(c,d)** Analysis of gliosis in 6-month-old wildtype, $CNP^{-/-}$, $PLP^{-/y}$ and 24-months-old wildtype mouse brain. GFAP immunostaining indicates astrogliosis and IBA1 immunostaining indicates microgliosis. Figure adapted from Depp et al. 2021.

3.2 Establishment of *in toto* plaque quantification in AD mouse models

Central to my PhD project was the assessment of differences in the distribution and amount of plaque pathology in AD mouse models. 5xFAD mice show considerable interindividual variability in plaque burden and a specific spatiotemporal pattern of amyloid pathology mainly determined by the Thy1-transgene promotor. Plaques start to appear in the subiculum of the hippocampus at around 8 weeks of age and further spread through the hippocampal formation. In the cortex, plaques appear at around 12 weeks with a strong medial-lateral and frontal-occipital gradient. Classical histological analysis of single brain slices introduces yet another level of variability as this reflects only a (not necessarily representative) sample of the total plaque burden. Likewise, in comparative studies, it is difficult to process and analyse the exact same plane/position in the brain which biases quantifications of plaque burden.

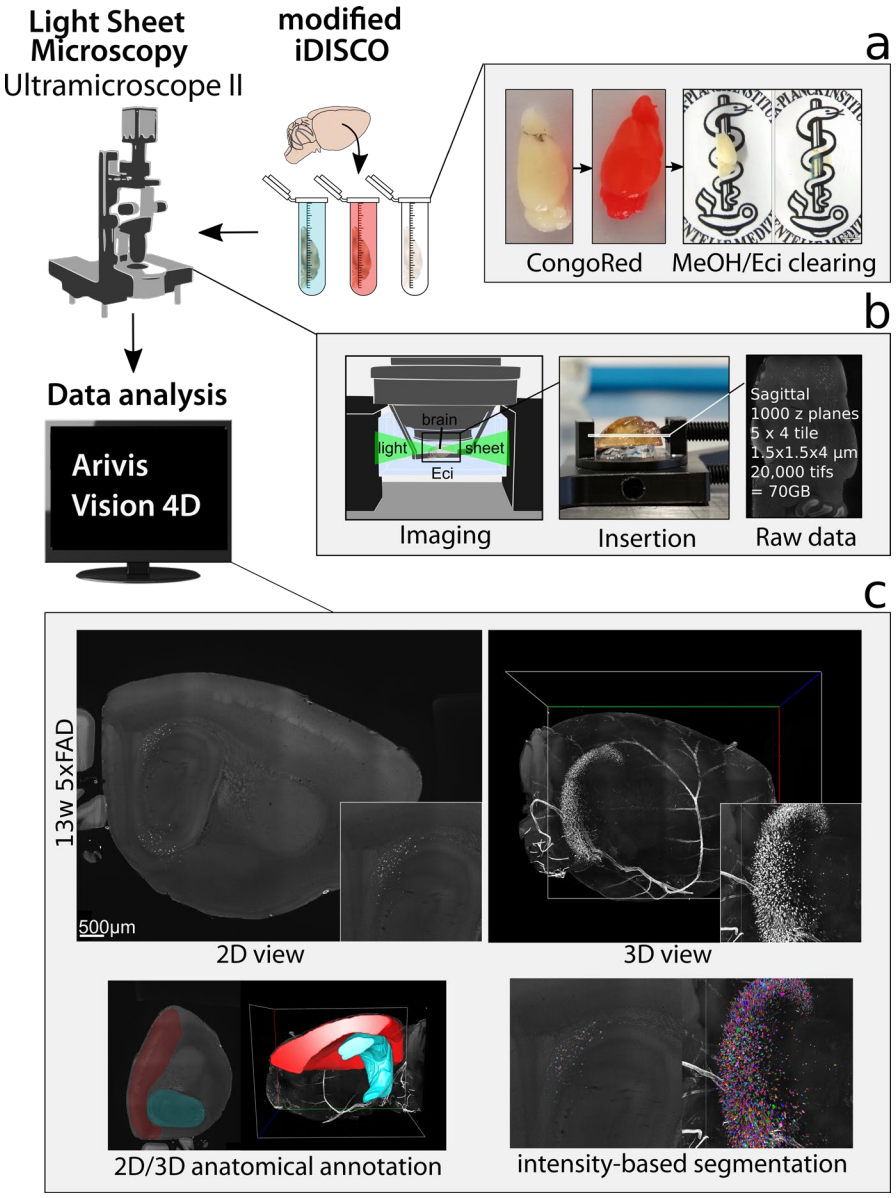

Figure 3.2 Establishment of *in toto* analysis of amyloid burden by light sheet microscopy. (a) Brains were subjected to *in toto* staining with the β-sheet dye Congo red according to a modified iDisco protocol (see Material and Methods) followed by clearing in Ethylcinnamate (Eci). **(b)** Cleared brains were imaged on an Ultramicroscope II (LaVision Biotech) light sheet setup to obtain sagittal optical slices. **(c)** Raw data were visualised and analysed in Arivis Vision 4D using manual region of interest annotation for hippocampus and cortex and automated plaque segmentation. Figure adapted from Depp et al. 2021.

With the advent of light sheet microscopy (LSM) and clearing techniques, it became possible to perform 3D histological assessment of samples (Dodt et al. 2015; Ertürk and Bradke 2013). Here, a laser light sheet optically "slices" through the intact sample making physical slicing obsolete. A prerequisite for optimal light sheet penetration is clarity of the sample which allows the light sheet to pass through it unobstructedly. Tissue shows high variability in its chemical composition consisting of a mixture of lipids, water and proteins and these compounds deflect light to different degrees. Tissue, therefore, profoundly scatters light causing it to appear opaque. Clearing methods are aimed at matching these refractive indices inside tissues typically by harsh delipidation and dehydration. The submerging of the eroded tissue in a solution with the same refractive renders it transparent and easily penetrable for the light sheet. The brain turned out to be notoriously difficult to clear due to its high lipid content and numerous clearing protocols have been established (for an overview see (Ueda et al. 2020; Molbay et al. 2021)). In a major step forward, antibody and dye labelling approaches were established that were compatible with clearing (immunolabeling-enabled 3-dimensional imaging of solvent-cleared organs, iDisco) (Renier et al. 2014).

In a proof of principle study, Liebmann and colleagues showed that the β-sheet dye Congo red as well as a few anti-amyloid antibodies can be used to stain amyloid plaques in AD mouse models and patients (Liebmann et al. 2016). Despite obvious advantages of using this technique to quantify amyloid burden, this technique has rarely been used in the field to interrogate differences in plaque burden between experimental cohorts.

I aimed at establishing an iDisco-based Congo red staining protocol and analysis pipeline for whole brain quantification of amyloid plaques (Fig3.2). Here, it was crucial to diverge from the published protocol that reported usage of 2µM Congo red to 0.01% (corresponding to 140µM) to achieve sufficient staining of amyloid plaques. Though brains incubated in 0.01% Congo red solution acquired a deep red colour (Fig3.2a), washes in an ascending methanol series removed unspecific binding. Further, delipidation steps in methanol were extended for superior clearness of the sample and the toxic clearing agent was replaced by the non-toxic and less erosive ethylcinnamate (Eci) (Klingberg et al. 2017). Microscopy was performed at a commercial light sheet microscopy setup (Ultramicroscope II, LaVision Biotech) to acquire sagittal optical slices in tiling mode (Fig3.2b). Raw data were imported, stitched and analysed using Vision4D (Arivis). Different algorithms were employed to segment Congo red labelled amyloid plaques in the 5xFAD model. In younger animals, simple intensity thresholding ways performed that reliably segmented single plaques (Fig3.2c) without including considerable amount of noise. For animals >6 months the blob finder algorithm detection (implemented in Arivis) was used to exclude bright lipofuscin accumulation observable with age. Created objects were manually curated and a size exclusion was implemented to exclude large objects such as blood vessels. For quantification of objects in different brain regions, isocortex and hippocampus – as the most affected regions in the 5xFAD model - were manually traced on a few slices according to the Allen mouse brain atlas with anatomically defined medial and lateral cut-offs and the 3D object were automatically extrapolated (Fig1c left). Later, I established a pipeline to automatically annotate cleared brains to the new 3D Allen brain atlas (Wang, Ding, et al. 2020) using Elastix for non-rigid image registration (not shown in this thesis) (Klein et al. 2009). I validated the quality and sensitivity of this *in toto* plaque burden approach by analysis of known parameters influencing plaque burden such as sex and age. Typical parameters assessed were: The raw number of plaques as the plaque count per region, the total plaque volume as total sum of single plaque volumes, the average plaque size as the average plaque volume through all single plaques, the plaque density as the number of plaques per mm^3 in a region of interest (ROI) and the percentage volume as the plaque positive volume per ROI volume. For better clarity, values are expressed as normalised values to the respective control.

3.3 Premature myelin ageing drives amyloid plaque deposition in the 5xFAD model

Next, I used this technique to study the effect of dysfunctional myelin on plaque burden in 5xFAD mice. To induce myelin dysfunction in the 5xFAD model, I crossbred $CNP^{-/-}$ and $PLP^{-/y}$ mice to 5xFADs and analysed plaque burden in $CNP^{-/-}$ 5xFAD and $PLP^{-/y}$ 5xFAD double mutants in comparison to their respective 5xFAD controls ($CNP^{+/+}$ 5xFAD; $PLP^{+/y}$ 5xFAD). As sex-and age-matched controls either littermates or controls from a control line derived from the same original crossbreeding were used. Using LSM to study 6 months old animals, plaque load differences became apparent in $CNP^{-/-}$5xFAD mice (Fig3.3): In both cortex and hippocampus, I detected increased plaque burden in double mutant mice. A striking difference was observed in the alveus, the white matter tract that collects efferent and afferent axons in the hippocampus as it progresses posteriomedial and then anterior to bundle into the fimbria. Together with the body and the anterior columns they build the fornix system as the major output pathway of the hippocampus. Intriguingly, reductions in fornix functions have been correlated with memory loss, also in AD (Senova et al. 2020). In the alveus, I observed the very striking presence of numerous, very small amyloid aggregates in $CNP^{-/-}$ 5xFAD mice. Effects were also readily visible in 3D representations (Fig3.3b,c). Normalised 3D quantification revealed a region-dependent increase in plaque load with the alveus as a classical white matter tract being affected the most showing an approximately 2-fold increase, the cortex showing a 50% increase and the

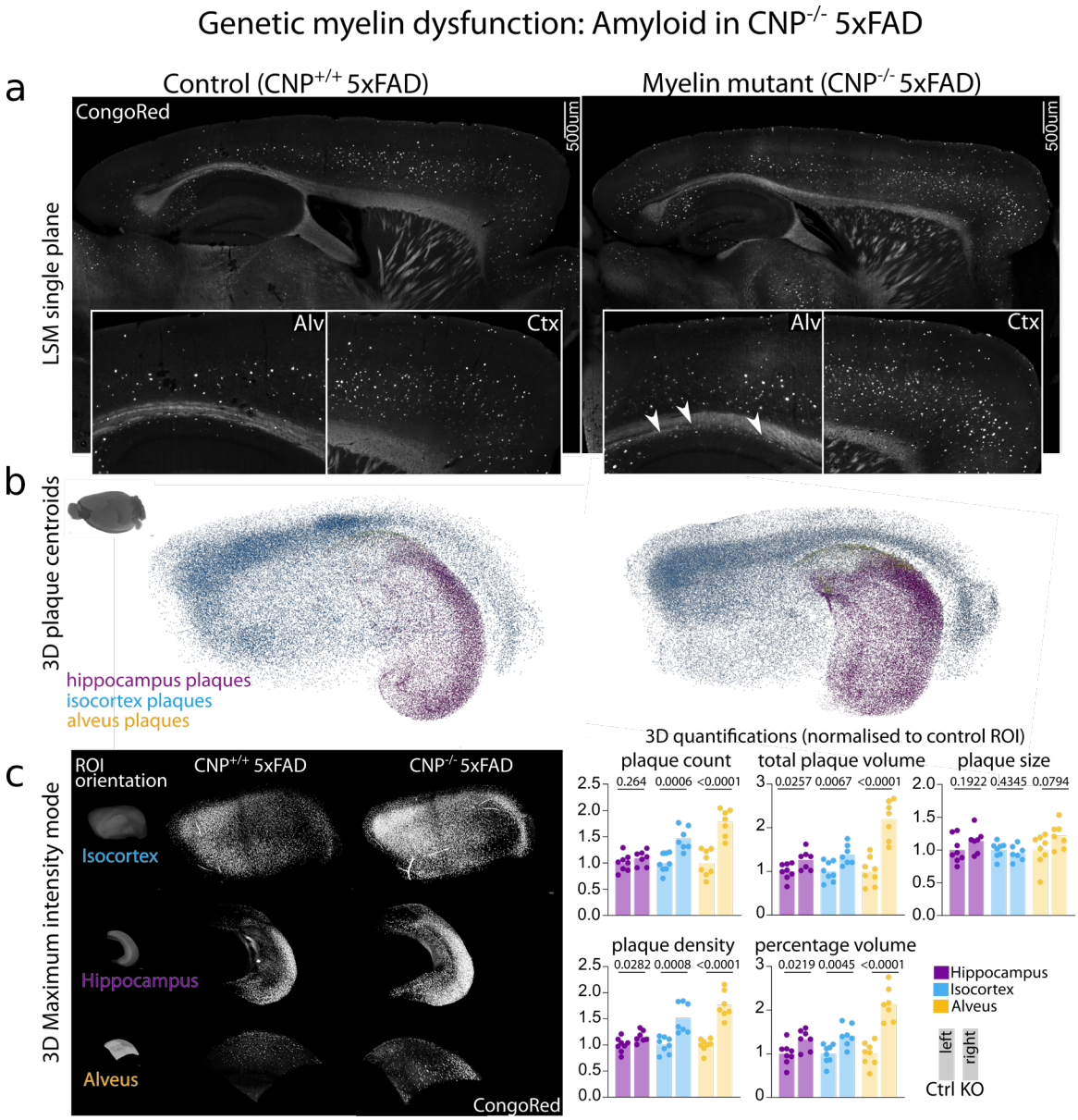

Figure 3.3 Light sheet microscopic analysis of plaque load in 6-month-old CNP$^{-/-}$ 5xFAD brains. (a) 2D light sheet single planes of controls (CNP$^{+/+}$ 5xFAD) and CNP deficient myelin mutant (CNP$^{-/-}$ 5xFAD) brains stained *in toto* with Congo red shown in grey scale. Close-ups show higher magnification image of the alveus (Alv) and the frontal cortex (Ctx). Note the small deposits of fibrillar amyloid along the alveus (indicated by white arrows). **(b)** 3D visualisation of plaque load in different brain regions of two representative brains. Plaques are visualised as spheroids coloured according to their location. **(c)** Left panel shows 3D representation of plaque load in different virtually cut out regions of interest as maximum intensity projections. Right panel shows normalised 3D quantifications of plaque load. Left bar graphs represent control values, right bars show knockout. Dots represent single animals. For statistical analysis of LSM data, two-sided unpaired Student's t-test was performed. P-values are indicated above bar graphs. Dots represent single animals and bars represent mean. n=8 for control, n=7 for mutant. Females were analysed. Figure adapted from Depp et al. 2021.

hippocampal formation showing an ~25% in all parameters (despite no changes in average plaque size). Expectedly, effect sizes were positively correlated with the myelination status (alveus > cortex > hippocampus). These findings were replicated in PLP$^{-/y}$ 5xFAD mice at 6 months of age (Fig3.4). Here, the presence of PLP deficient myelin increased plaque burden in a remarkably similar fashion to CNP deficiency in terms of effect size and region dependency. Various small deposits were very prominently present in the alveus. Verification of the findings of enhanced plaque load in PLP deficient animals gives confidence that the plaque promoting effect in CNP knockout animals does not stem from other direct consequences of CNP deficiency (e.g. effects of hypothetically secreted CNP on plaque load or CNP deficiency in neurons) but is

derived from an underlying phenomenon shared in CNP and PLP deficient mice i.e. myelin defects. These effects were observed at 6 months of age in the two models of myelin dysfunction. I next analysed if plaque load is enhanced to an extent that it shifts onset of amyloid deposition/amount of amyloid at earlier time points. For this, 3-months-old CNP$^{-/-}$5xFAD and PLP$^{-/-}$5xFAD crossbreedings were analysed. The 3 months timepoint represents a timepoint when animals are adult, but plaque load in the isocortex is at its initial stage and subiculum plaque load is far from satisfied. The alveus is not yet affected by plaque load which is why it

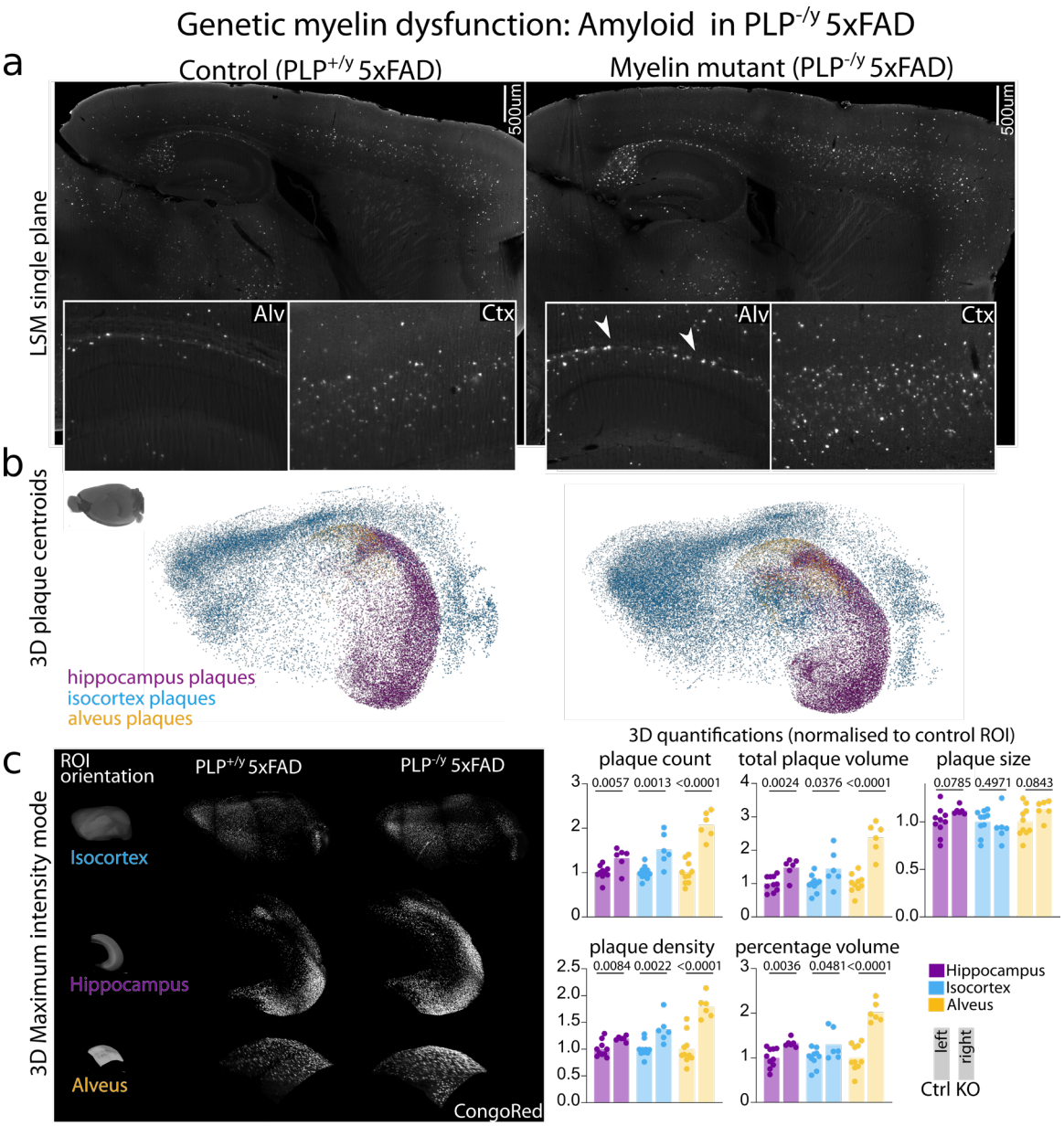

Figure 3.4 Light sheet microscopic analysis of plaque load in 6-month-old PLP$^{-/y}$ 5xFAD brains. (a) 2D light sheet single planes of controls (PLP$^{+/y}$ 5xFAD) and PLP deficient myelin mutant (PLP$^{-/y}$ 5xFAD) brains stained *in toto* with Congo red shown in grey scale. Close-ups show higher magnification image of the alveus (Alv) and the frontal cortex (Ctx). Note the small deposits of fibrillar amyloid along the alveus (indicated by white arrows). **(b)** 3D visualisation of plaque load in different brain regions of two representative brains. Plaques are visualised as spheroids coloured according to their location. **(c)** Left panel shows 3D representation of plaque load in different virtually cut out regions of interest as maximum intensity projections. Right panel shows normalised 3D quantifications of plaque load. Left bar graphs represent control values, right bars show knock out. Dots represent single animals. For statistical analysis of LSM data, two-sided unpaired Student's t-test was performed. P-values are indicated above bar graphs. Dots represent single animals and bars represent mean. n=10 for control, n=6 for mutant. Males were analysed. Figure adapted from Depp et al. 2021.

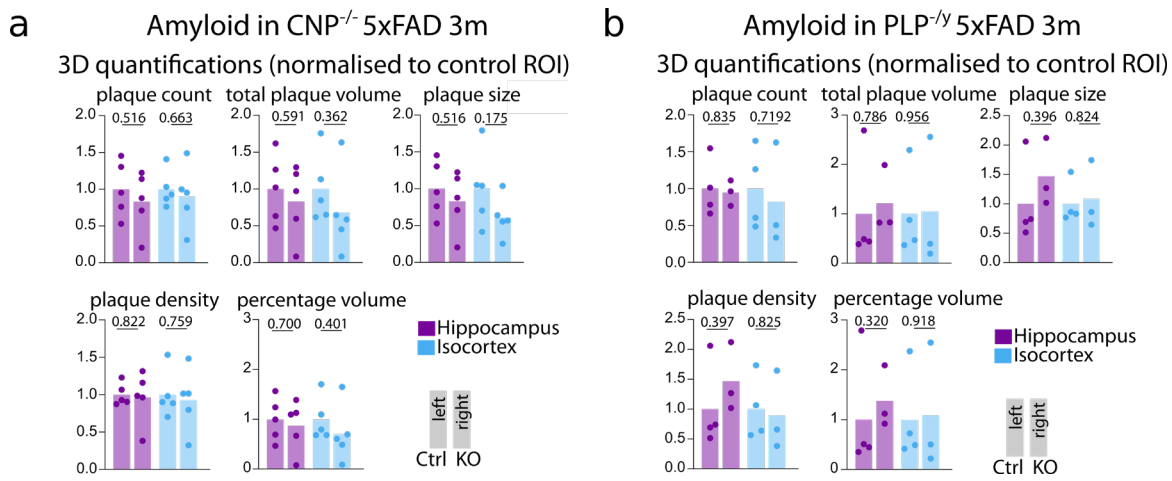

Figure 3.5 Light sheet microscopic analysis of plaque load in young 3-month-old PLP$^{-/y}$ 5xFAD and CNP$^{-/-}$ 5xFAD brains. (a) Normalised 3D quantifications of plaque load in 3-months-old CNP$^{-/-}$5xFAD mice as quantified by Congo Red LSM. Left bar graphs represent control values, right bars show knock out. Dots represent single animals. For statistical analysis of LSM data, two-sided unpaired Student's t-test was performed. P-values are indicated above bar graphs. Dots represent single animals and bars represent mean. n=5 for control, n=5 for KO. **(b)** Normalised 3D quantifications of plaque load in 3-month-old PLP$^{-/y}$ 5xFAD mice as quantified by Congo red LSM. n=4 for control, n=3 for KO. Figure adapted from Depp et al. 2021.

is not quantified. There was no significant difference in all analysed parameters of plaque load between controls and respective myelin mutant 5xFAD crossbreedings. Intriguingly, variability seemed to be much higher at the 3-month timepoint as compared to 6-month-old 5xFADs (in both control and mutants) indicating a larger variability at the beginning of amyloidosis than at progressive stages. 3 months of age also represents an early time point in regard to myelin pathology and secondary gliosis in the brains of CNP and PLP null mice. Therefore, it is perfectly reasonable to not observe differences in plaque load at this age. Collectively, this data hint towards myelin defects as being the primary cause of increased plaque load in these myelin mutants.

3.4 Myelin defects drive amyloid deposition in the APP^{NLGF} knock-in model

The 5xFAD model, though a widely used model to study amyloidosis in AD, suffers from artefacts such as overexpression of APP and non-native expression pattern in Thy1-positive neurons. APP^{NLGF} mice were developed to overcome such limitations offering a new model system for plaque deposition with the endogenous expression pattern and level (Saito et al. 2014). Replication of findings in other AD models is important to rule out that effects are only inherent to a specific model potentially resulting from direct regulation of transgene expression. I, therefore, crossed CNP knockout mice with APP^{NLGF} mice to obtain double mutant mice and compared plaque load in CNP$^{-/-}$APP^{NLGF} to CNP$^{+/-}$APP^{NLGF} littermate controls at 6 month of age. Of note, CNP heterozygosity at the young timepoints analysed has no effect on myelin structure or secondary gliosis and heterozygotes are comparable to wildtype animals (data not shown). Since amyloid plaques in the APP^{NLGF} model are less compact when compared to the 5xFAD mouse and typically do not show a dense-core morphology, the LSM protocol was adapted to further increase Congo red concentration (0.02%). At age 6-month 0.02% Congo red led to sufficient labelling of fibrous plaques throughout the cortex in APP^{NLGF} mice. While readily visible by eye, segmentation of plaques with the established pipeline was challenging due to a different intensity distribution and in general less intense staining. A machine learning based segmentation pipeline was successfully implemented in Arivis Vision4D (fast fluorescence modus) that was trained with manually segmented plaques from all datasets to analyse. This pipeline reliably detected APP^{NLGF} plaques. Analysis of a small cohort revealed a stark increase in amyloid deposition in the cortex of CNP$^{-/-}$APP^{NLGF} when compared to CNP$^{+/-}$APP^{NLGF} reproducing findings in the 5xFAD model (Fig3.6).

Importantly, this result established that myelin dysfunction drives amyloid deposition irrespective of the specific mouse model used and independent of APP overexpression.

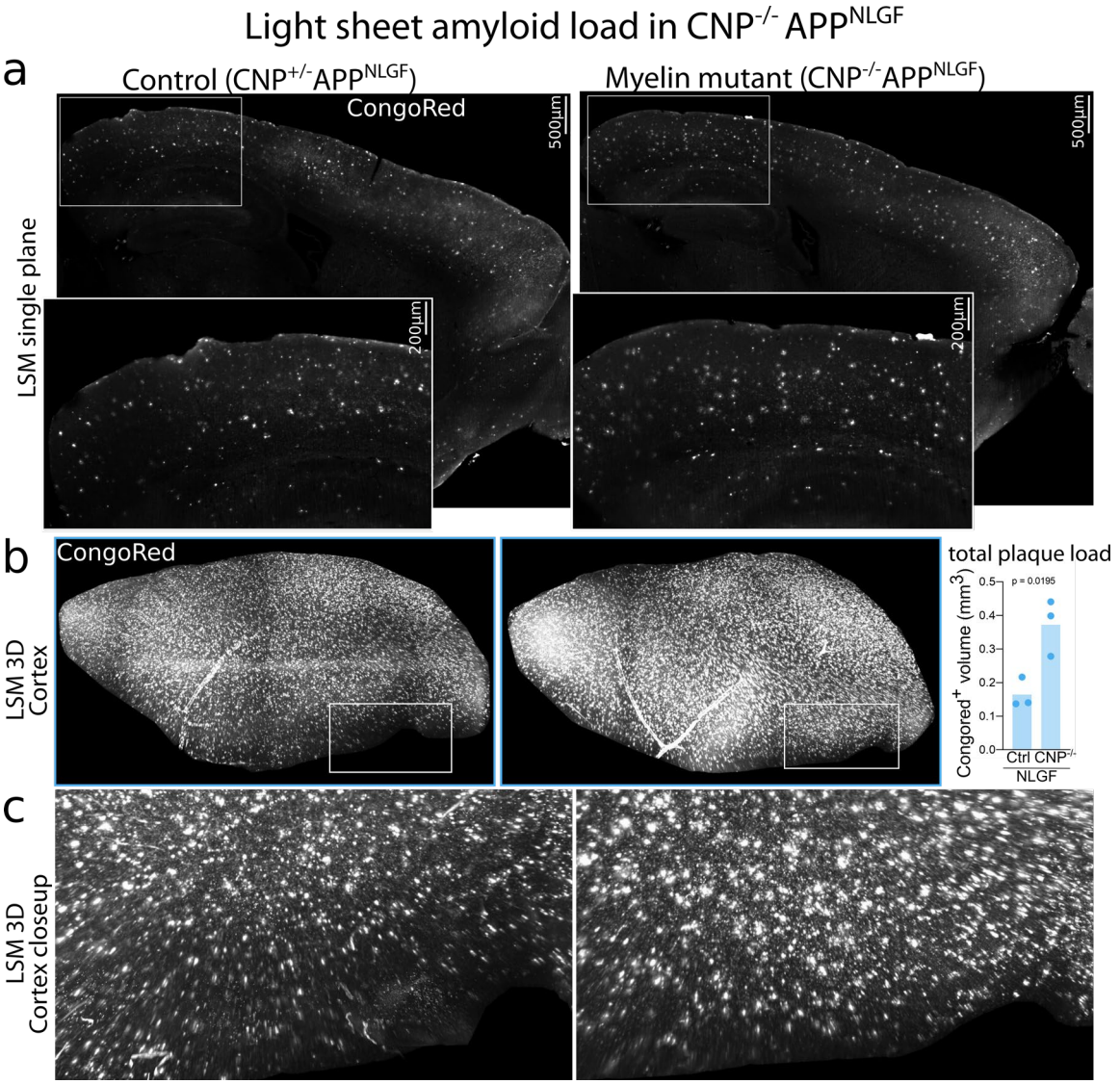

Figure 3.6 Light sheet microscopic analysis of plaque load CNP$^{-/-}$ APP^{NLGF} mice. (a) Upper panel shows LSM single plane and a closeup of a cortical region. **(b)** 3D maximum intensity projection of the cropped isocortical region of interest. Plaque burden was quantified using machine-learning based segmentation of amyloid plaques. **(c)** Closeup of region indicated in (b). Dots represent single animals and bars depict mean. Unpaired, two-tailed Student's t-test was performed for statistical analysis. n=3 for control; n=3 for CNP$^{-/-}$. Figure adapted from Depp et al. 2021.

3.5 Myelin defects and amyloid pathology synergistically lead to profound behavioural deficits in mice

AD patients show abundant cognitive deficits not limited to memory problems but including an array of psychological symptoms including anxiety, depression, and agitation. To a variable degree, these behavioural deficits are present in AD mice (Kosel, Pelley, and Franklin 2020). Given the exacerbation of plaque load by myelin defects in 6-month-old CNP$^{-/-}$ and PLP$^{-/y}$ 5xFAD mice, I tested if myelin defects impact 5xFAD behavioural phenotypes. Reports on behavioural deficits in the 5xFAD model, however, are not fully consistent between laboratories and studies, and seem to depend on the specific behavioural paradigm, timepoints, sex and genetic background used. I chose to perform elevated plus maze (EPM) to test anxiety related phenotypes and Y-maze (YM) to probe working memory as these tests present very established

behavioural paradigms and have been previously reported to expose deficits in 5xFAD mice (Jawhar et al. 2012; Oakley et al. 2006). In the EPM, animals explore a cross-formed platform that is elevated from the floor with two arms closed and two open arms. Mice naturally prefer the closed arms as safe spots and avoid the open arms. In the YM, animals explore a Y-shape maze with three closed arms and show a curiosity-driven preference of alternating visits between the arms. Additionally, motor deficits were probed by scoring clasping behaviour.

Intriguingly, in both maze types, 5xFAD, CNP$^{-/-}$ and CNP$^{-/-}$ 5xFAD double mutants presented with hyperactivity indicated by increased track length in the EPM and increased number of arm entries in the YM (Fig3.7a,b). Hyperactivity was more pronounced in CNP$^{-/-}$ and especially in CNP$^{-/-}$ 5xFAD mice. Statistical analysis using a two-way-ANOVA to probe for interaction between genotypes revealed a supra-additive effect of CNP$^{-/-}$ and 5xFAD in mediating hyperactivity. Such a supra-additive effect was also observed in the open arm time parameter in the EPM. Both 5xFAD and CNP$^{-/-}$ mice expressed reduced level of anxiety spending more time in the open arms when compared to wildtype CNP$^{+/+}$ animals. This finding is in good agreement with other published studies reporting reduced anxiety in 5xFAD mice (Jawhar et al. 2012). CNP$^{-/-}$ 5xFAD double mutants, however, presented with tremendously reduced anxiety, preferring open arms over closed arms in the 300sec trial. Indeed, in a few instances mice had apparently lost their natural fear of height and voluntarily jumped off the maze (not shown). Though the number of arm entries was massively increased in

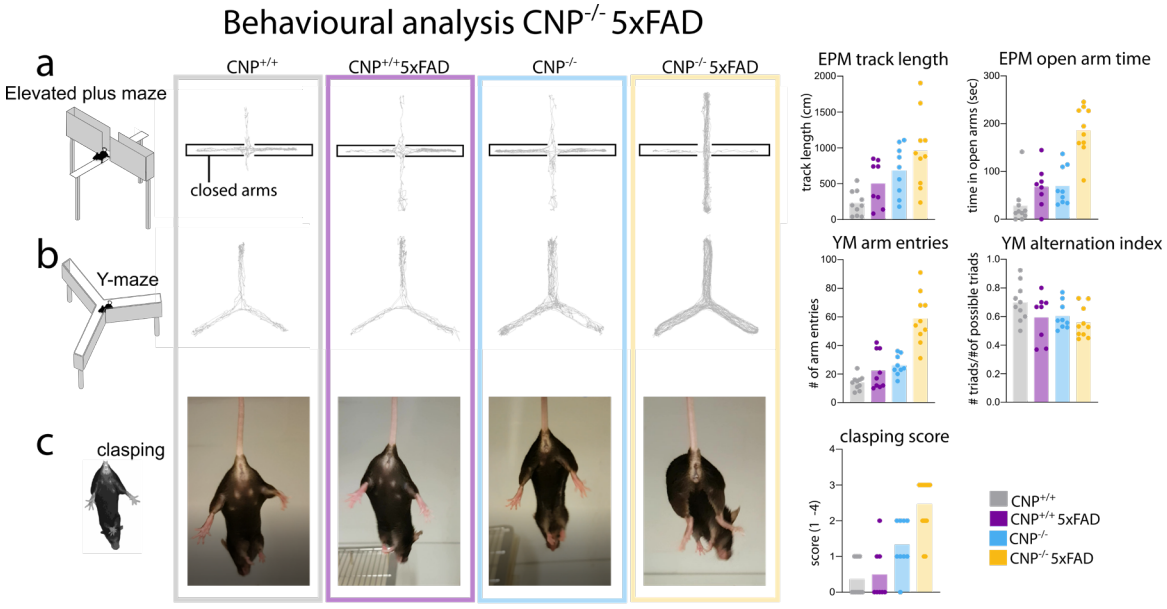

d

Two-way-ANOVA Behavioural Testing CNP$^{-/-}$ 5xFAD

	Parameter	*F* (1,33)	*p*	partial η2	η2 90% CI
EPM Track Length	5xFAD	35.02	< .001	0.51	[0.31, 0.65]
	CNP$^{-/-}$	24.57	< .001	0.43	[0.21, 0.59]
	CNP$^{-/-}$ 5xFAD	8.94	0.005	0.21	[0.04, 0.40]
EPM Open Arm Time	5xFAD	34.25	< .001	0.51	[0.30, 0.65]
	CNP$^{-/-}$	29.67	< .001	0.47	[0.26, 0.62]
	CNP$^{-/-}$ 5xFAD	6.89	0.013	0.17	[0.02, 0.36]
YM Alternation Index	5xFAD	0.82	0.372	0.02	[0.00, 0.16]
	CNP$^{-/-}$	0.02	0.876	7.54E-04	[0.00, 0.05]
	CNP$^{-/-}$ 5xFAD	0.64	0.429	0.02	[0.00, 0.15]
YM Arm Entries	5xFAD	36.15	< .001	0.52	[0.32, 0.66]
	CNP$^{-/-}$	43.91	< .001	0.57	[0.38, 0.70]
	CNP$^{-/-}$ 5xFAD	15.62	< .001	0.32	[0.12, 0.50]
Clasping Score	5xFAD	12.11	0.001	0.27	[0.08, 0.45]
	CNP$^{-/-}$	42.73	< .001	0.56	[0.37, 0.69]
	CNP$^{-/-}$ 5xFAD	5.78	0.022	0.15	[0.01, 0.34]

Figure 3.7 Behavioural analysis of CNP$^{-/-}$ 5xFAD mice. (a,b) Behavioural analysis of mice in the elevated plus maze (EPM) and Y-maze (YM). Middle panels show representative tracks for each genotype analysed. Right panels show quantification. **(c)** Clasping test. Middle panel shows representative images of mice during clasping test. Right panel shows quantification according to scoring system. **(d)** For statistical analysis, several different type III ANOVAs were performed for each behavioural test that probed the main effects for the 5xFAD genotype and the myelin-mutant genotype as well as their interaction. Dots represent single animals, bars depict mean. Females were analysed. n=9 for CNP$^{+/+}$, n=8 CNP$^{+/+}$ 5xFAD, n=9 for CNP$^{-/-}$, n=9 CNP$^{-/-}$. Figure adapted from Depp et al. 2021.

CNP$^{-/-}$ 5xFAD mice, there was no significant change to the alternation index as measure of working memory throughout the groups as assessed in a two-way ANOVA. However, a trend towards decreased alternation percentage was visible when comparing CNP$^{-/-}$ 5xFAD to wildtype control mice. Motor deficits as assessed in the clasping test were exclusively present in myelin mutant animals (both CNP$^{-/-}$ and CNP$^{-/-}$ 5xFAD) and the 5xFAD genotype, again, exacerbated deficits when present together with the CNP$^{-/-}$ genotype.

Similar, but less pronounced effects were obtained by behavioural analysis of PLP$^{-/y}$ 5xFAD and respective controls (Fig3.8). Hyperactivity was present in animals with PLP null background (with and without 5xFAD transgene) in both maze types but no supra-additive effects were observed for the interaction between 5xFAD and PLP$^{-/y}$. 5xFAD, PLP$^{-/y}$ and PLP$^{-/y}$ 5xFAD had reduced anxiety levels and spend significantly more time on open arms to a very similar extent. Similar to the YM results in CNP$^{-/-}$ 5xFAD, no significant changes in working memory performance were observed albeit a trend towards reduced alternation index was again observed in double mutant mice. The clasping test showed significant impairments in PLP deficient animals and indicated significant interactions between the PLP and 5xFAD genotype. Differences in behavioural analysis results between PLP$^{-/y}$ and CNP$^{-/-}$ 5xFAD are likely a result from the different sexes analysed with female 5xFAD being more effected by plaque load. Likewise, CNP deficiency linked phenotypes such as

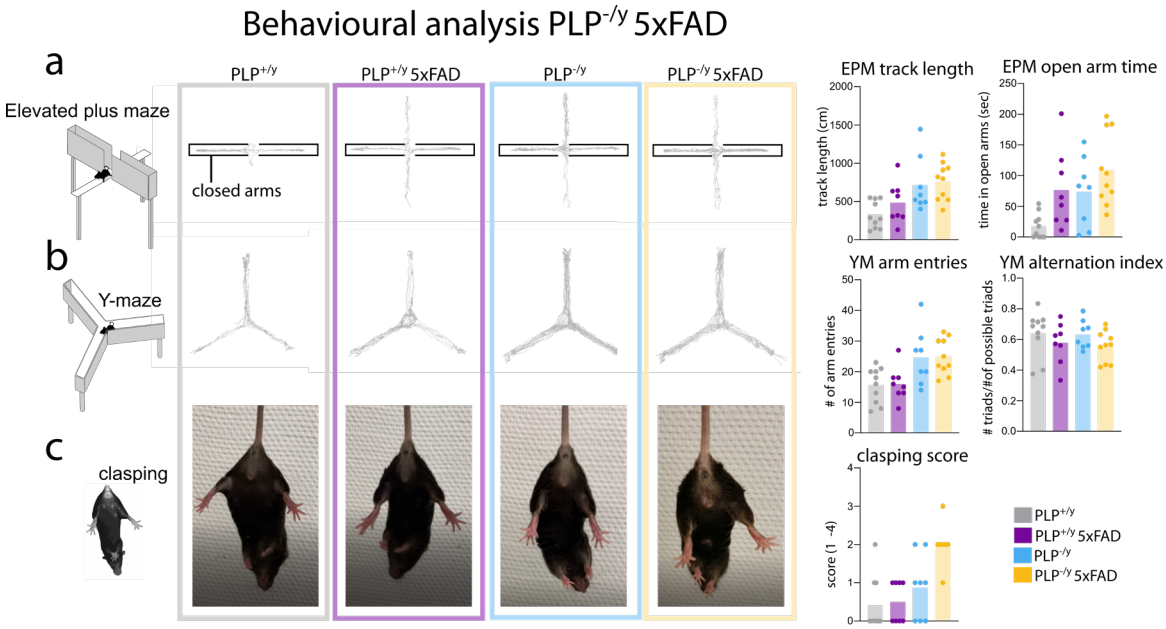

d

Two-way-ANOVA Behavioural Testing PLP$^{-/y}$ 5xFAD

	Parameter	*F* (1,32)	*p*	partial η2	η2 90% CI
EPM Track Length	5xFAD	2.45	0.127	0.07	[0.00, 0.25]
	PLP$^{-/y}$	13.74	< .001	0.3	[0.10, 0.49]
	PLP$^{-/y}$ 5xFAD	0.36	0.554	0.01	[0.00, 0.13]
EPM Open Arm Time	5xFAD	9.19	0.005	0.22	[0.05, 0.42]
	PLP$^{-/y}$	6.5	0.016	0.17	[0.02, 0.36]
	PLP$^{-/y}$ 5xFAD	0.45	0.506	0.01	[0.00, 0.14]
YM Alternation Index	5xFAD	3.09	0.089	0.09	[0.00, 0.27]
	PLP$^{-/y}$	0.12	0.733	3.68E-03	[0.00, 0.10]
	PLP$^{-/y}$ 5xFAD	0.03	0.86	9.94E-04	[0.00, 0.06]
YM Arm Entries	5xFAD	0.4	0.534	0.01	[0.00, 0.14]
	PLP$^{-/y}$	16.45	< .001	0.34	[0.13, 0.52]
	PLP$^{-/y}$ 5xFAD	3.16E-05	0.996	9.89E-07	[0.00, 0.00]
Clasping Score	5xFAD	11.32	0.002	0.26	[0.07, 0.45]
	PLP$^{-/y}$	20.89	< .001	0.4	[0.18, 0.56]
	PLP$^{-/y}$ 5xFAD	5.63	0.024	0.15	[0.01, 0.34]

Figure 3.8 Behavioural analysis of PLP$^{-/y}$ 5xFAD mice. (a,b) Behavioural analysis of mice in the elevated plus maze (EPM) and Y-maze (YM). Middle panels show representative tracks for each genotype analysed. Right panels show quantification. **(c)** Clasping test. Middle panel shows representative images of mice during clasping test. Right panel shows quantification according to scoring system. **(d)** For statistical analysis, several different type III ANOVAs were performed for each behavioural test that probed the main effects for the 5xFAD genotype and the myelin-mutant genotype as well as their interaction. Dots represent single animals, bars depict mean. Males were analysed. n=10 for PLP$^{+/y}$, n=8 PLP$^{+/+}$ 5xFAD, n=8 for PLP^{-y-}, n=10 PLP$^{-/y}$. Figure adapted from Depp et al. 2021.

secondary gliosis or reduced lifespan are more pronounced than PLP deficiency linked phenotypes. Though working memory assessed in the YM remained intact, it cannot me excluded that more sensitive and sophisticated tests (such as Barnes maze, Plus maze, Morris water maze) would have revealed differences. Intriguingly, phenotypes that were induced or exacerbated in myelin mutant/5xFAD mice fall into the category of disinhibition (reduced anxiety, hyperactivity) that is a neuropsychiatric symptom also present in AD patients (Keszycki, Fisher, and Dong 2019; Chung and Cummings 2000). Taken together, this behavioural analysis revealed that myelin defects and amyloid pathology appear to synergistically worsen behavioural deficits.

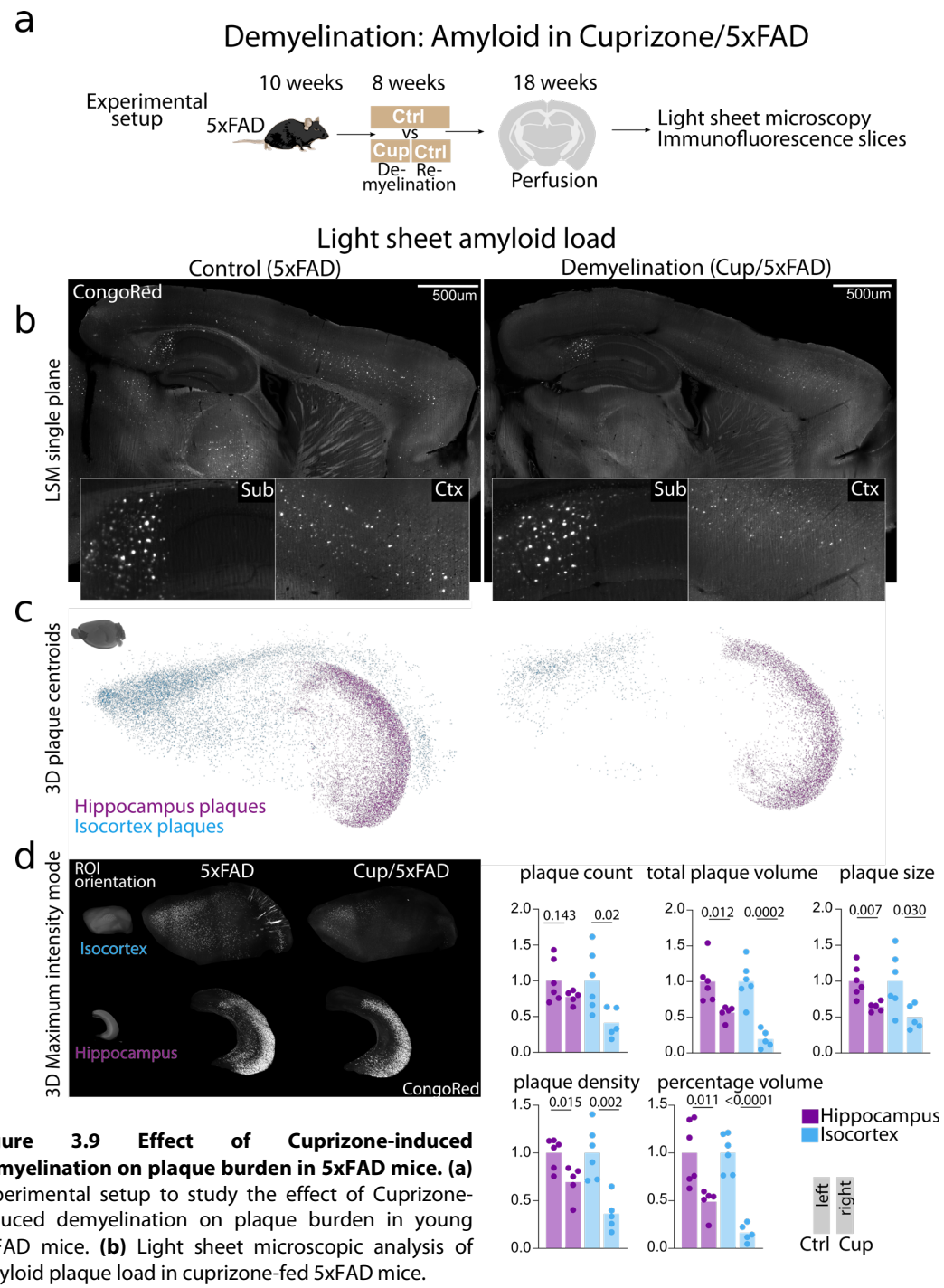

Figure 3.9 Effect of Cuprizone-induced demyelination on plaque burden in 5xFAD mice. (a) Experimental setup to study the effect of Cuprizone-induced demyelination on plaque burden in young 5xFAD mice. **(b)** Light sheet microscopic analysis of amyloid plaque load in cuprizone-fed 5xFAD mice. Images show LSM single planes and closeups of the indicated regions (Sub: Subiculum; Ctx: Cortex). **(c)** 3D distribution of isocortical and hippocampal plaques represented as centroids. **(d)** Left panel shows 2D maximum intensity projection of cropped regions of interested. Right panel shows 3D quantifications of plaque burden parameters. n=6 for control, n=5 for Cup. Males were analysed. Student's t-test was performed.

3.6 Acute demyelination injuries drive local deposition of amyloid

Both CNP and PLP deficiency lead to a chronic state of subtle myelin dysfunction throughout the CNS. While this reflects certain aspects of myelin brain ageing very well, it is difficult to distinguish chronic effects that potentially involve other mechanism than only myelin dysfunction from direct consequences of dys- or demyelination. I, therefore, became interested in studying the effect of an acute demyelinating hit on plaque deposition asking the question if shorter (but more severe) defects in myelination status would also drive amyloidosis. I chose two different models classically used as mouse models in Multiple Sclerosis research: Cuprizone-intoxication and EAE.

In the Cuprizone model, animals are fed a powder diet supplemented with 0.2% Cuprizone. The copper-chelator Cuprizone leads to acute and specific cell death of oligodendrocytes with subsequent demyelination due to a not fully understood mechanism (Zhan et al. 2020; Gudi et al. 2014). There is regional variability in regard to Cuprizone-mediated demyelination with cortical areas, the medial corpus callosum and hippocampal white matter being classically affected by demyelination. Robust remyelination occurs in this model upon Cuprizone withdrawal (Berghoff et al. 2017). For Cuprizone-induced demyelination, I opted for a paradigm in which 2.5-month-old 5xFAD animals at the very beginning of amyloid pathology were put on a Cuprizone-containing diet for 4 weeks (Fig3.9a) in which consistent demyelination occurs in our hands (Berghoff et al. 2017). This was followed by a recovery period of 4 weeks in which remyelination had occurred as verified by Gallyas-staining (data not shown). Using light sheet microscopy, I observed obvious differences in the appearance of the splenium and body of the corpus callosum in Cuprizone treated animals where white matter was less well recognisable. Surprisingly and against my initial hypothesis, Cuprizone demyelination

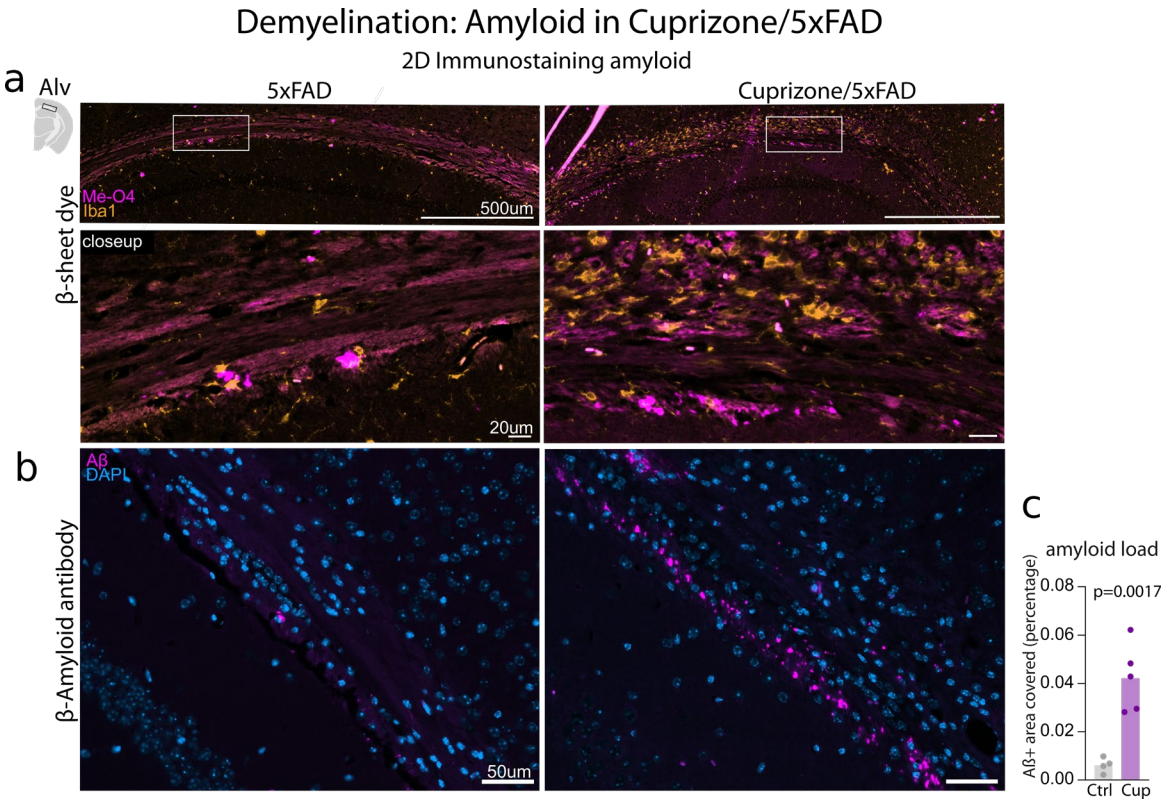

Figure 3.10 Immunostaining against amyloid in the alveus of Cuprizone/5xFAD brains. (a) Iba1 and Methoxy-X04 co-staining in the alveus of Cuprizone/5xFAD and 5xFAD controls. Note the presence of amoeboid microglia in Cuprizone-fed animals. **(b)** Anti-amyloid immunostaining reveals abundant small amyloid deposits in the alveus of Cuprizone/5xFAD mice. **(c)** Quantification of images shown in (b). n=4 for control, n=5 for Cuprizone treatment. Student's t-test was performed for statistical analysis. Figure adapted from Depp et al. 2021.

proved to seemingly alleviate plaque deposition in both cortex and hippocampus and present plaques were smaller in size (Fig3.9c). This effect is, however, rather attributable to the direct copper chelating properties of Cuprizone than to a protective action of demyelination. Copper chelation has been previously shown to solubilize fibrillar amyloid *in vitro* and inhibit plaque deposition in amyloidosis models (Cherny et al. 2001). Indeed, the plaque reducing effect was also visible in brain regions that are typically not affected by demyelination (e.g. thalamus). In retrospect, the interpretation of this experiment is, therefore, complicated.

Closely examining the LSM raw data, I, however, noticed very small Congo red positive aggregates in the ventral corpus callosum and the alveus that escaped automatic detection in the LSM pipeline because they fell under the size exclusion threshold. These smaller aggregates were seemingly confined to regions heavily affected by demyelination. To rule-out non-specific staining of myelin debris by the Congo red dye, I performed 2D immunostainings on paraffin slices using both anti-amyloid antibodies and an additional β-sheet dye that shows better signal-to-noise ratio (Methoxy-X04). For analysis, I focused on the alveus as a region that is both heavily affected by demyelination in the Cuprizone model and capable of generating plaques in the 5xFAD model. The presence of numerous, amoeboid microglia revealed that the repair processes in the dorsal corpus callosum were not fully completed 4 weeks after cuprizone withdrawal (Fig3.10a). Intriguingly, both Methoxy-X04 and anti-amyloid staining revealed a severe increase in amyloid plaque deposition in the alveus (Fig3.11a,b). These plaques were "atypical" in terms of their very small size and lesser compaction as revealed by superior staining by antibodies than by Methoxy-X04. Lack of compaction is probably a consequence of copper chelation occurring upon Cuprizone treatment. The measured effect of the acute demyelinating injury on amyloid deposition is, hence, likely to be underestimated. Indeed, it seems remarkable that in the alveus the plaque-promoting effect of demyelination can override the copper chelation driven inhibition of plaque formation. These findings confirm the previous findings using chronic dysmyelination models and clearly indicate that myelin dysfunction can drive amyloid deposition.

To support the results obtained in the Cuprizone model, I next studied 5xFAD mice challenged with EAE. Young 10-weeks-old 5xFAD mice were immunised using MOG peptide fragment and complete Freund's adjuvant (CFA) to elicit an immune attack against myelin (Fig3.11a). Neurological scoring confirmed successful induction of EAE with typical disease course in 5xFADs (Fig3.11b). MOG-induced EAE in C57BL/6 mice affects the spinal cord that shows large, demyelinated lesions at its surface whereas such lesions are typically not found in the brain (Merkler et al. 2006). However, the brain in EAE is still affected by immune cell infiltration and exposed to neuroinflammatory modulators (Kuerten et al. 2007). I detected no differences in amyloid load in both hippocampus and cortex in EAE/5xFAD mice using light sheet microscopy (Fig3.12a). This is contrast to an earlier study with aged (14-16 months) J20 and Tg2576 AD mice in which

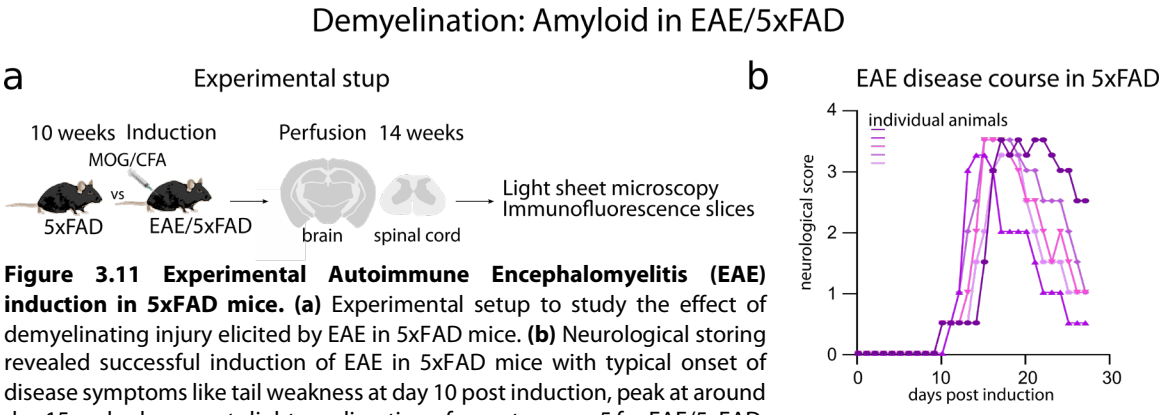

Figure 3.11 Experimental Autoimmune Encephalomyelitis (EAE) induction in 5xFAD mice. (a) Experimental setup to study the effect of demyelinating injury elicited by EAE in 5xFAD mice. **(b)** Neurological storing revealed successful induction of EAE in 5xFAD mice with typical onset of disease symptoms like tail weakness at day 10 post induction, peak at around day 15 and subsequent slight amelioration of symptoms. n=5 for EAE/5xFAD. For clarity, 5xFAD controls that did not develop any neurological symptoms are not shown. Figure adapted from Depp et al. 2021.

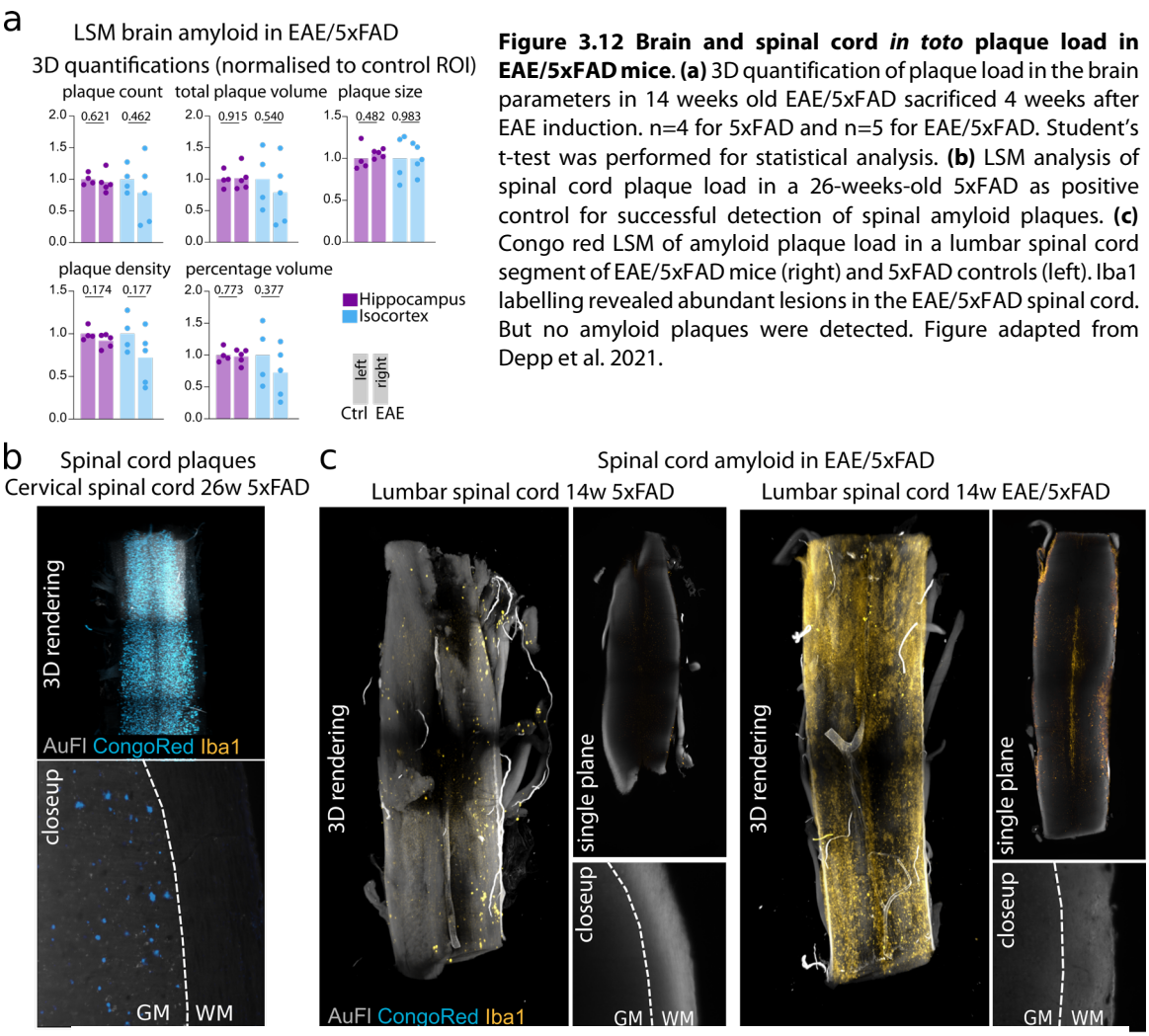

Figure 3.12 Brain and spinal cord *in toto* plaque load in EAE/5xFAD mice. (a) 3D quantification of plaque load in the brain parameters in 14 weeks old EAE/5xFAD sacrificed 4 weeks after EAE induction. n=4 for 5xFAD and n=5 for EAE/5xFAD. Student's t-test was performed for statistical analysis. **(b)** LSM analysis of spinal cord plaque load in a 26-weeks-old 5xFAD as positive control for successful detection of spinal amyloid plaques. **(c)** Congo red LSM of amyloid plaque load in a lumbar spinal cord segment of EAE/5xFAD mice (right) and 5xFAD controls (left). Iba1 labelling revealed abundant lesions in the EAE/5xFAD spinal cord. But no amyloid plaques were detected. Figure adapted from Depp et al. 2021.

EAE reportedly reduced brain plaque load extensively (Frenkel et al. 2005). The authors claimed that the plaque-clearing effect in EAE stems from massive activation of microglia cells in the brain parenchyma that would subsequently target amyloid plaques. In our hands, no such massive microglial activation could be observed (data not shown). The contradictory findings could also be linked to different mouse models used (5xFAD versus J20/Tg2576) or different disease stage analysed (initial stage in this study versus very late stage in Frenkel et al. 2005).

I, next, focused on assessing amyloid pathology in a large segment of the lumbar spinal cord as the primary region affected by demyelination in EAE. Of note, although the spinal cord is only a late affected region in AD patients, the 5xFAD model shows abundant amyloid plaques in the spinal cord grey matter and to a lesser extent in the white matter due to the activity of the Thy1 promotor. I verified the successful detection of spinal cord amyloid plaques using Congo red labelling and LSM in 26-week-old 5xFADs and observed a strong cervical-lumbar gradient with the cervical regions being affected most severely (Fig3.12b). Examining EAE/5xFAD mice, IBA1 labelling revealed large lesions in the spinal cord, however, this was not accompanied by classical amyloid plaque deposition in EAE/5xFAD mice in grey or white matter. Control mice also did not develop amyloid plaques in the lumbar spinal cord at 14-weeks. However, similarly to observations in Cuprizone/5xFAD mice, I observed small Congo red deposits in the lesion environment in the EAE/5xFAD spinal cord that were not detected in the quantification pipeline. Using classical immunofluorescence staining on paraffin slices, I in more detail evaluated if these deposits present proper amyloid aggregates. The aggregates were found to be particularly abundant in the perilesion environment and not inside lesions (Fig3.13a,b). Intriguingly, this is the location where also abundant APP swellings are found in EAE. The deposits stained positive with both anti-amyloid antibodies as well as Methoxy-X04. Importantly, I ruled-out

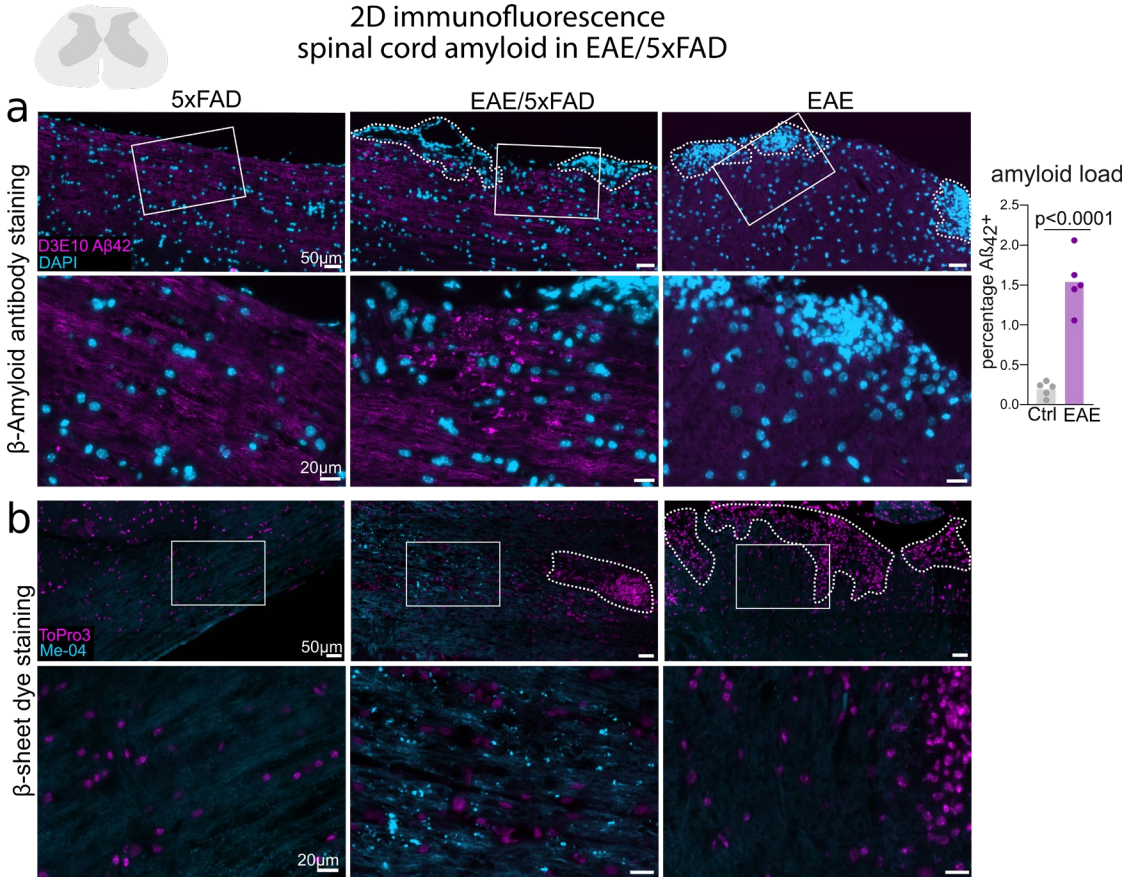

Figure 3.13 Immunostaining against amyloid in EAE/5xFAD spinal cord sections. (a) Anti-amyloid beta antibody staining in EAE/5xFAD spinal cord and 5xFAD and EAE controls. Lesions are identified by nuclei (DAPI) accumulation and indicated by dashed lines in the upper panel. Lower panel show close-ups of the regions indicated in the upper panel. Multiple small amyloid deposits are visible exclusively in EAE/5xFAD mice. Quantification of images of 5xFAD (Ctrl, grey) and EAE/5xFAD (EAE, purple) is shown on the right. n=5 for control, n=5 for EAE/FAD. Student's t-test was performed for statistical analysis. **(b)** Staining of EAE-induced amyloid deposits by Methoxy-X04 (Me-04). Lesions are identified by nuclei accumulation (ToPro3) and are indicated by dashed lines. Lower panels show closeups of the region indicated in the upper panel. No staining was observed in EAE or 5xFAD controls. Figure adapted from Depp et al. 2021.

non-specific binding of the anti-amyloid antibody and the dye to lipid/myelin accumulation in lesions by staining EAE/wildtype animals where no significant staining was observed (Fig3.13b). Taken together with the findings in Cuprizone/5xFAD mice, these observations indicate that acute myelin injuries give rise to small amyloid deposits in and around affected areas.

3.7 Lack of compact myelin ameliorates amyloid deposition

The results obtained make the strong suggestion that myelin defects - both chronic and acute – drive amyloid deposition in AD mouse models and that the presence of dysfunctional myelin is a risk factor for amyloid deposition. From an evolutionary point of view, with brain expansion primates have acquired a large amount of subcortical (and intracortical) myelin in comparison to mammals with smaller brains (Herculano-Houzel et al., 2014). In humans especially, prefrontal white matter is disproportionally enlarged even when compared to other apes (Schoenemann, Sheehan, and Glotzer 2005). Cell type specific transcriptomic studies of human, chimpanzee and macaque oligodendrocytes also hint towards an accelerated evolution of oligodendrocyte gene expression as compared to neurons in the human lineage (Berto et al. 2019; Khrameeva et al. 2020). This raises the question if the extent of cortical myelination *per se* is a risk for amyloid deposition and the development of AD in humans.

To probe this and as an orthogonal approach to induction of myelin dysfunction, I aimed at investigating the effect of absence of compact myelin on amyloidosis. Classically, *shiverer* mice have been used to study downstream effects of absence of myelin. These mice lack MBP expression, fail to assemble compact myelin sheaths in the CNS and represent with general tremor (see Introduction). However, recurrent seizures as well as premature death occurring at 2-3 month of age preclude analysis of *shiverers* and respective crossbreedings at later time points. Our lab therefore generated MBP$^{fl/fl}$ mice that allow for conditional recombination (Meschkat et al. 2020). By using telencephalic driver lines such as the Emx-Cre line (Gorski et al. 2002), recombination and subsequent absence of compacted myelin can be restricted to the forebrain which leaves mid- and hindbrain structures intact. Consequently, Emx-Cre MBP$^{fl/fl}$ lack the typical *shiverer*-associated phenotypes and are long-lived (Subramanian, Möbius, Nave, unpublished). As such, these forebrain *shiverer* mice are an ideal and novel model to probe the role of cortical myelination in amyloid deposition.

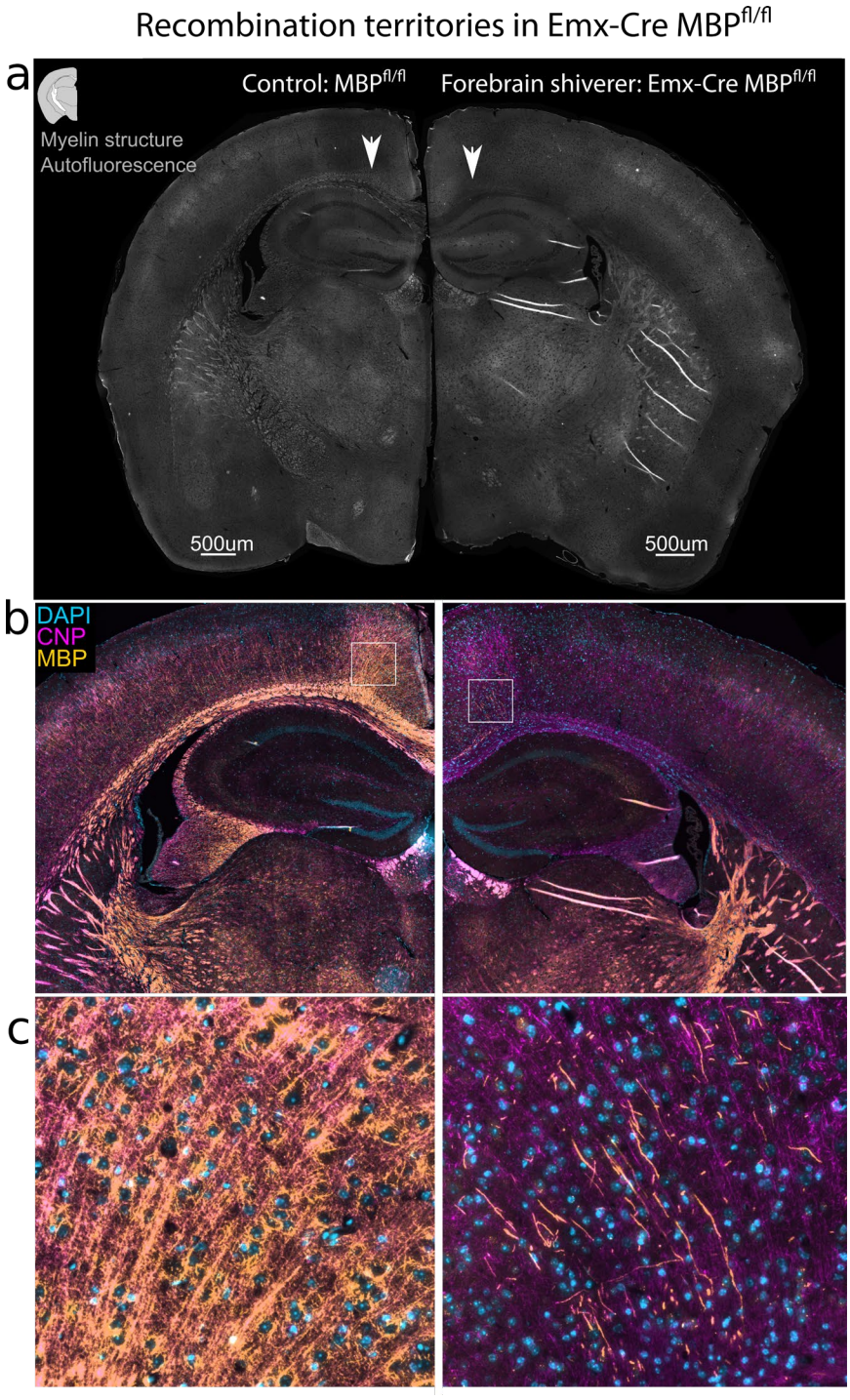

Figure 3.14 Recombination territories in forebrain-specific *shiverer* mice
(a) Basic characterisation of myelination patterns in Emx-Cre MBP$^{fl/fl}$ mice. Autofluorescence shows clear lack of myelinated profiles in corpus callosum and alveus (arrows). Thalamus and striatum are normally myelinated. **(b)** CNP/MBP-co-immunolabelling in Emx-Cre MBP$^{fl/fl}$ and control mice. **(c)** Close-up of the indicated regions in (b). Note the presence of abundant cortical myelin in control animals. In forebrain *shiverer* brains, CNP positive profiles are still visible, but most myelin is non-compacted as indicated by lack MBP staining. According to these findings recombined areas comprise the cortex, subcortical white matter (corpus callosum) and hippocampal white matter. Adapted from Depp et al. 2021.

I first verified the intended forebrain-specific recombination patterns by gross assessment of brain morphology in paraffin sections and myelin immunostaining (Fig3.14a). Typical autofluorescent myelin profiles were absent throughout the corpus callosum and hippocampal white matter in forebrain *shiverer* mice while midbrain structures such as the thalamus and the striatum as cerebral nucleus remained unaffected by recombination. Anti-MBP/CNP immunolabelling confirmed these observations and demonstrated the absence of compact myelin from cortical and hippocampal regions (Fig3.14b). Recombined regions included the grey matter regions cortex and hippocampus including the white matter tracts corpus callosum, cingulum,

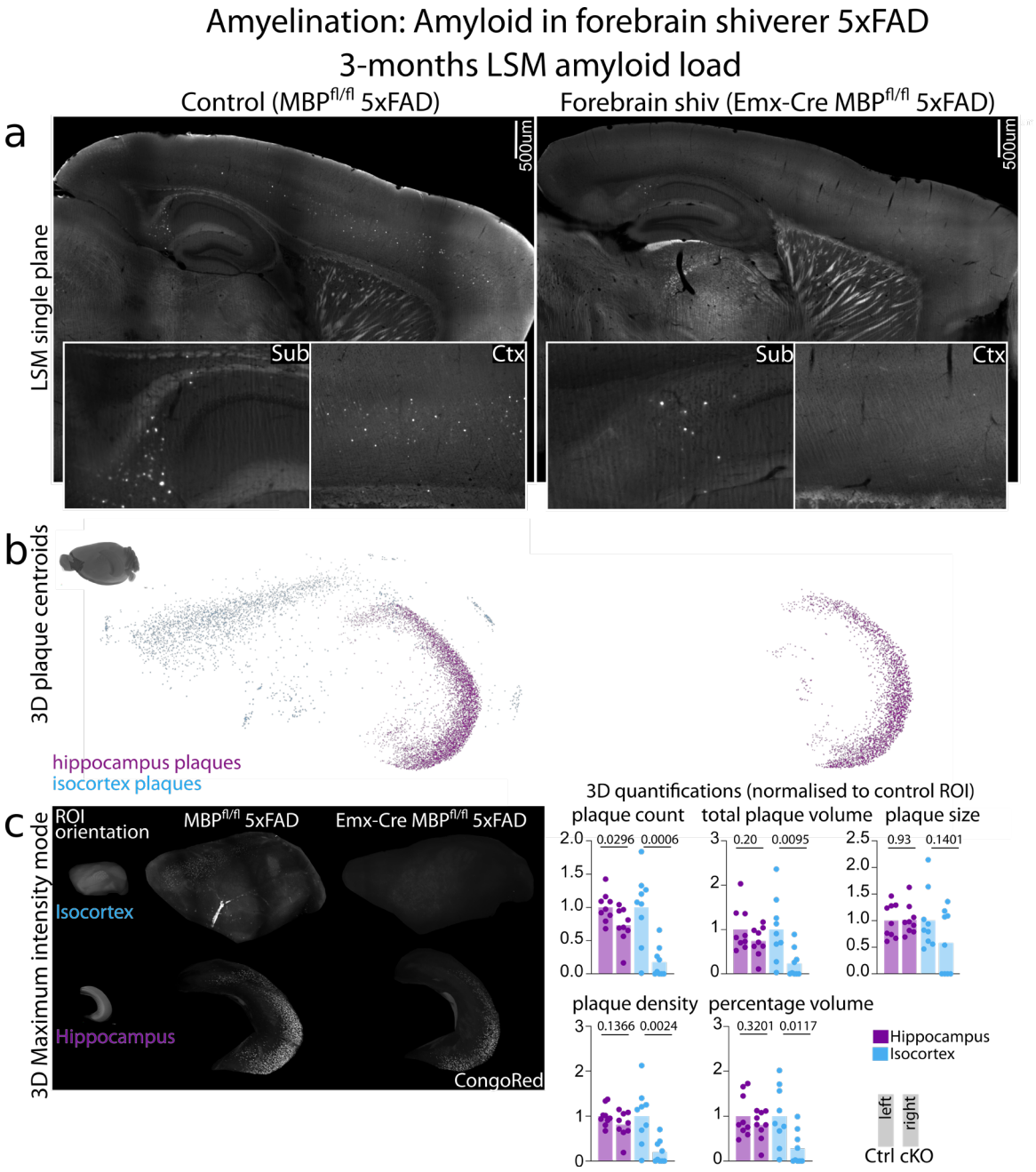

Figure 3.15 Plaque load in 3-month old forebrain *shiverer* 5xFAD mice (a) LSM single planes of Congo red labelling in Emx-Cre MBP$^{fl/fl}$ 5xFAD mice and MBP$^{fl/fl}$ 5xFAD control mice. Note the obvious lack of the corpus callosum and the alveus in forebrain *shiverer* mice. The anterior part of the corpus callosum becomes partially myelinated by oligodendrocytes from the underlying non-recombined striatum. Lower panels show closeups of the subiculum (Sub) and Cortex (Ctx). Forebrain *shiverer*/5xFADs lacked cortical plaques. **(b)** 3D visualisation of plaques as spheroids colour-coded by region in two representative examples. **(c)** Left panels show maximum intensity projection of cropped regions of interest. Right panel shows 3D quantification of plaque parameters. n=9 for control (MBP$^{fl/fl}$ 5xFAD), n=9 for conditional KO (cKO, Emx-Cre MBP$^{fl/fl}$ 5xFAD). Student's t-test was performed to statistical analysis. Adapted from Depp et al. 2021.

alveus and fimbria. Importantly, as in full *shiverer* mice, oligodendrocytes and association of oligodendrocyte processes with axons as revealed by CNP staining remained intact. Occasionally, a few MBP positive myelin sheaths were observed indicative of incomplete genetic recombination or migration of OPCs/oligodendrocytes from not genetically targeted areas. I next generated forebrain *shiverer* 5xFAD mice by crossbreeding Emx-Cre MBP$^{fl/fl}$ to 5xFADs and analysed plaque burden via LSM in the resulting offspring at 3 and 6 months of age. Littermate Cre-driver negative MBP$^{fl/fl}$ 5xFAD mice were used as controls. Early in amyloidosis at 3-months, forebrain *shiverer* mice were massively protected against cortical amyloid load (Fig3.15). Hippocampal plaque load was only minorly reduced (only in the parameter of plaque count). At 6 months of age, this effect was largely gone revealing an interesting temporal delay in amyloid deposition by the lack of compact myelin (Fig3.16). Intriguingly, lack of compact myelin in the corpus callosum and alveus at 6-month of age appeared to increase white matter plaque formation (Fig3.16).

These results reveal an ambiguous role of healthy myelin in plaque formation in 5xFAD mice: on the one hand side, compact myelin in the cortex is a prerequisite for rapid amyloid deposition even in a genetic amyloidosis model. On the other hand, healthy myelin in white matter tracts inhibits plaque formation. It seems feasible that white matter composed of tightly bundled axons and associated myelin is a difficult space to seed and expand plaques due to physical constraints. Removing compact myelin might act to loosen up white matter facilitating plaque formation. The results in young MBP$^{fl/fl}$ mice, are in agreement with an earlier study that attempted to analyse amyloid deposition in *shiverer*/5xFAD mice and also showed a reduction in insoluble Aβ levels (Ou-Yang and Van Nostrand 2013). This study, however, was limited to analyse 2-month-old mice due to the early premature death of *shiverer* mice. At this young age 5xFAD mice are barely affected by plaque load which precluded a quantitative analysis of plaque burden in these animals. Likewise, this study suffers from potential artefacts from the severe phenotype of *shiverer* mice (e.g. effects of recurrent seizures on amyloid levels).

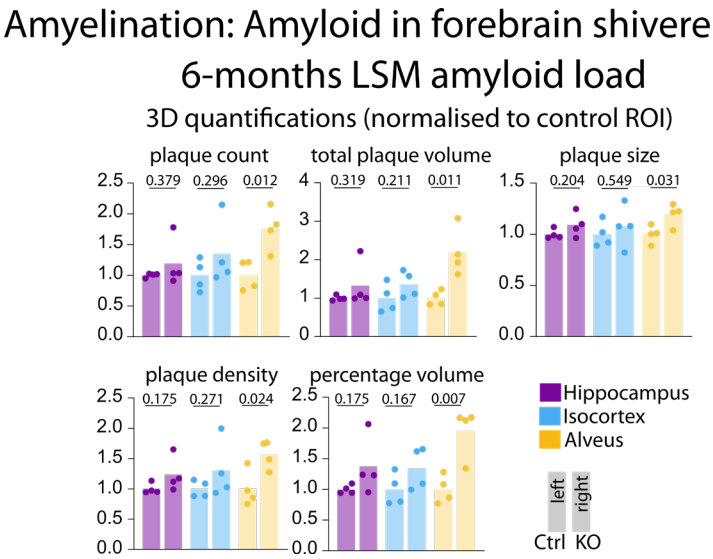

Figure 3.16 Plaque load in 6 month old forebrain *shiverer* 5xFAD mice. 3D quantification of plaque parameters in the hippocampus, isocortex and alveus. n=4 for control (MBP$^{fl/fl}$ 5xFAD), n=4 for conditional KO (cKO, Emx-Cre MBP$^{fl/fl}$ 5xFAD). Student's t-test was performed for statistical analysis comparing cKO and Ctrl in different brain regions. Adapted from Depp et al. 2021.

3.8 Effects of dysfunctional myelin on APP metabolism

LSM analysis of plaque burden in multiple *in vivo* models of myelin dysfunction, acute myelin injury and finally amyelination identified myelin *per se* and more so compromised function of myelin as an upstream risk factor for amyloid deposition. How could myelin defects mechanistically drive Aβ deposition? In theory, defects could drive amyloid deposition by either altering Aβ processing from its precursor APP or inhibiting Aβ degradation. I first investigated if dysmyelination impacted APP metabolism and Aβ production from APP. These experiments were carried out in CNP$^{-/-}$ 5xFAD mice as the model that showed robust effects in terms of plaque load as well as behavioural changes.

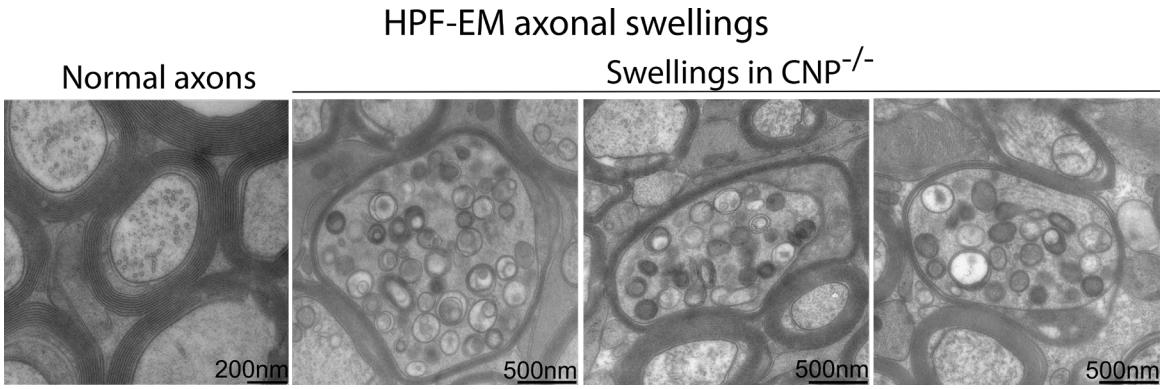

Figure 3.17 High pressure freezing electron microscopy (HPF-EM) analysis of axonal swellings in the optic nerve of CNP$^{-/-}$ mice. Images show representative images of axons without swellings (normal axon in a wildtype control mouse) and multiple examples of axonal swellings found in CNP null mice. HPF-EM performed by Wiebke Möbius. Adapted from Depp et al. 2021.

Axonal swellings are prominent features of myelin diseases and are potentially derived from breakdown of trophic support functions from distressed oligodendrocytes. They are also well-known to stain for APP, and I speculated that these swellings might be novel production sites of Aβ under defective myelin sheaths. Such swellings have been described to occur in mouse models of MS as well as in CNP and PLP null mice (Snaidero et al. 2017; Steyer et al. 2020). I queried previously acquired HPF-EM images (performed by Wiebke Möbius) of optic nerves of 6-month-old CNP null mice to closely examine the content of axonal swellings. Most of the organelles accumulating in axonal swellings were of lamellar, multivesicular morphology. These structures likely arise through fusions of late endosomes and autophagosomes in axons (Ferguson 2018). Some vesicles had only a single membrane and accumulated electron dense material indicative of lysosomes. According to these morphological characteristics, these organelles can be, thus, identified as belonging to the degradative pathway consisting of a mixture of lysosomes/endosomes/autophagosomes and numerous fusion products thereof. As discussed in the introductory part of this thesis in detail, these vesicular organelles are considered primary production sites of Aβ which in theory could render axonal swellings a source of Aβ. Intriguingly, their vesicular content is similar to the content of axonal swellings associated with amyloid plaques that also have been suggested to be sites of Aβ production (Sadleir et al. 2016).

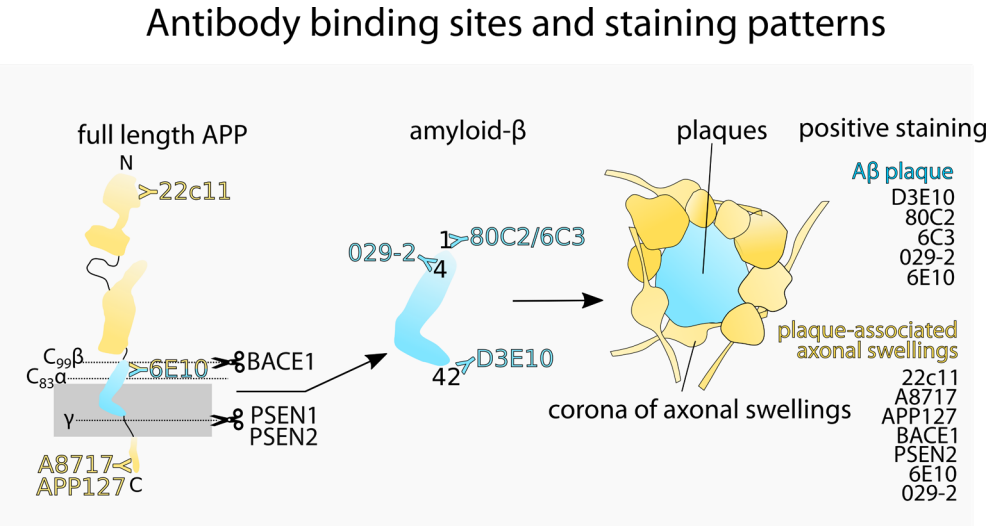

Figure 3.18 Schematic representation of epitopes and staining patterns of the antibodies used. On the left a schematic representation of full length APP with the Aβ domain in blue is shown and the different secretase cleavage sites are marked. Antibody binding sites to Aβ and APP are shown (indicated by Y). On the right side, a typical amyloid plaque (blue) is depicted with multiple axonal swellings in its vicinity (yellow). Typically, plaque cores are stained with multiple Aβ antibodies and axonal swellings are stained with antibodies directed against APP, Presenilins and BACE1. Figure adapted from Depp et al. 2021.

Next, I aimed at showing that these axonal swellings indeed accumulate the Aβ producing machinery (APP as substrate and β- and γ-secretase) and subsequently Aβ peptides using immunostainings. Interpretation of these results critically depends on the specificity of the antibodies used as well as exact knowledge of their recognised epitope. Fig3.18 gives an overview of the antibodies used in this study and their typical staining patterns. I first examined distribution of APP, BACE1 and PSEN2 as part of the γ-secretase complex. As expected, and previously shown for $CNP^{-/-}$, $CNP^{-/-}$ 5xFAD mice developed numerous APP positive swellings throughout grey and white matter. Swellings are more abundantly found in the white matter due to the concentration of myelinated axons there. Morphologically, the swellings are singular round structures that reach up to several micrometre in diameter. In contrast, axonal swellings associated with amyloid plaques (here called plaque-swellings) are found in groups in a corona-like structure with an unstained core that corresponds to the core of the plaque (Fig3.19). Plaque-associated swellings are typically bigger in size and can balloon out to the size of a nucleus. Plaque-associated swellings and "myelin-dysfunction"-associated swellings (here called myelin-swellings) can, therefore, be morphologically well distinguished. While in $CNP^{+/+}$ 5xFAD control mice, only occasionally plaque-swellings were observed in the white matter that stained positive for APP using both a C-terminal and N-terminal targeted antibodies, abundant single myelin

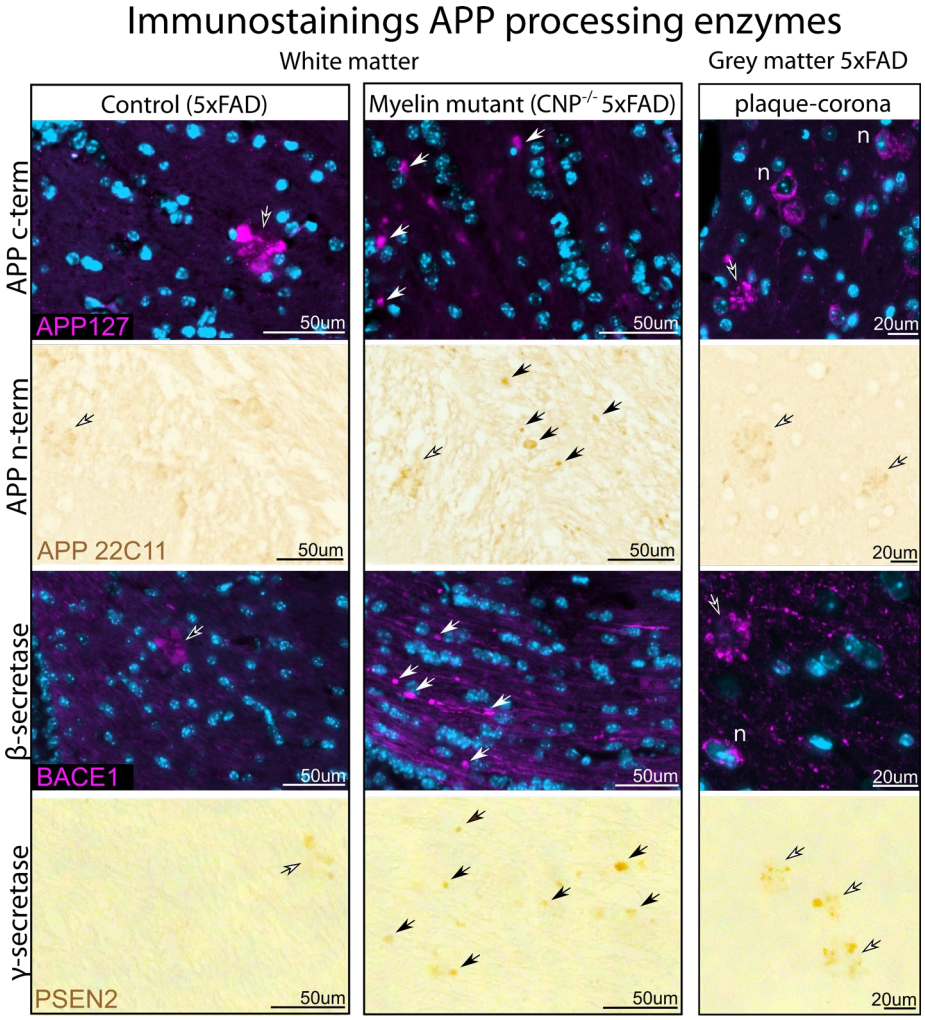

Figure 3.19 Analysis of Aβ-producing machinery in myelin dysfunction associated axonal swelling. Representative images of fluorescent and chromogen immunostaining against the N- and C-terminus of APP, BACE1 and PSEN2 in paraffin slices of 5xFAD controls and $CNP^{-/-}$ 5xFAD mice at 6 months of age. On the right, as additional control to illustrate plaque-associated swellings a snapshot of the cortex is shown where amyloid plaques are abundant. Contoured arrows mark plaque-associated axonal swellings typically forming a corona as found in the cortex of 5xFAD mice. Non-contoured arrows indicate plaque-independent axonal swellings as observed exclusively in $CNP^{-/-}$ 5xFAD mice. n indicates neurons. As white matter tract corpus callosum or fimbria are shown. Figure adapted from Depp et al. 2021.

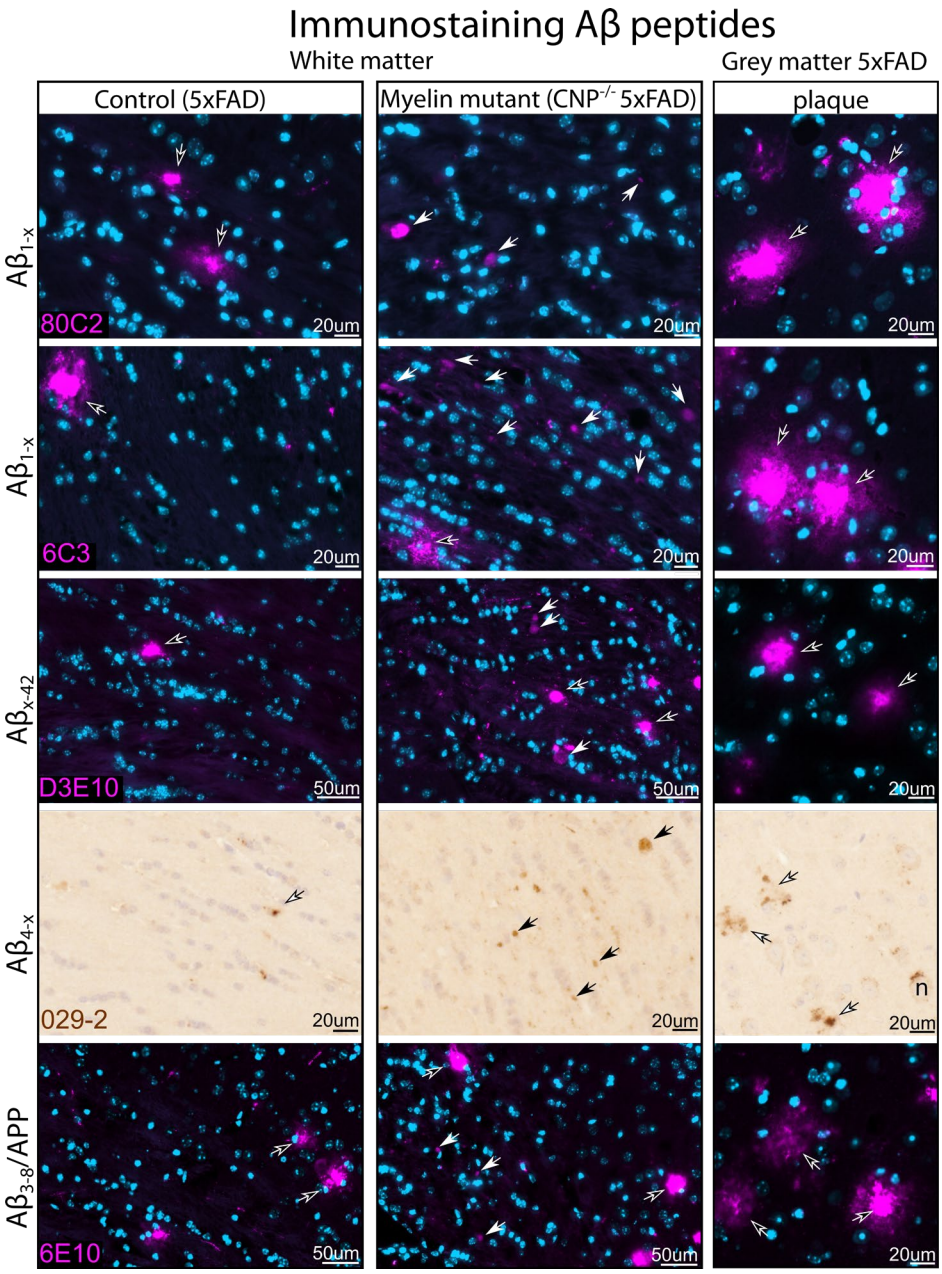

Figure 3.20 Analysis of Aβ accumulation in myelin dysfunction associated axonal swelling. Representative images of fluorescent and chromogen immunostainings against different Aβ peptides. Specificity of the antibody is indicated on the left. Different Aβ antibodies recognising N-terminal ($Aβ_{1-x}$ /$Aβ_{4-x}$) and C-terminal ($Aβ_{x-42}$) neoepitopes after APP cleavage. 6E10 recognising an epitope contained in both APP and Aβ is shown as an additional control. Antibody name is indicated in the lower left. Contoured arrows mark Aβ deposits. Non-contoured arrows indicate plaque-independent axonal swellings as observed exclusively in $CNP^{-/-}$ 5xFAD mice. n indicates neurons. As white matter tract corpus callosum or fimbria are shown. Figure adapted from Depp et al. 2021.

dysfunction associated swellings were found in in $CNP^{-/-}$ 5xFAD mice. Plaque-swellings in 5xFAD mice were morphologically very similar to plaque-associated swellings found in the cortex. Note that also neuronal cell bodies stain positive for APP. In principle soluble, N-terminal APP fragments as well as C-terminal fragments and not only full length APP can be detected by the antibodies used. Nevertheless, these findings indicate an enrichment of APP and/or its fragments in myelin-associated myelin-swellings. Likewise, the numerous swellings in $CNP^{-/-}$ 5xFAD mice accumulated BACE1 and PSEN2 that otherwise could only be detected in plaque-associated swelling in 5xFAD controls. Intriguingly, BACE1 also became elevated in thickened axon that not yet developed mature swellings. Unfortunately, no double immune-staining could be performed on the tissue because the antibodies were largely derived from the same species. However, it is highly likely that

APP, BACE1 and PSEN2 become elevated in the same compartment as it occurs in plaque-associated axonal swellings. Of note, I validated the specificity of the antibodies used by comparing the resulting staining patterns in brain slices to published studies (e.g. mossy fibre staining by anti-BACE1 antibodies, plaque-associated swelling staining).

I next studied if the myelin dysfunction associated swellings stain positive for Aβ which - together with findings of APP and secretase accumulation - would implicate that Aβ is locally produced in axonal swellings. Specifically staining Aβ peptides is challenging as antibodies targeting the Aβ sequence also recognise the sequence still contained in full length APP. For example, the widely used 6E10 antibody recognises an epitope between $Aβ_{3-8}$ and shows full cross-reactivity with full length, uncleaved APP in both histology and western blot analysis. It abundantly stains neurons, plaque-associated axonal swellings as well as Aβ plaques. I opted for a strategy mainly employing Aβ antibodies that recognise neoepitopes generated after cleavage and as such do not show cross-reactivity with full length APP (Fig3.20). These antibodies very intensely stain amyloid plaques after formic acid treatment to loosen up the β-sheet structure but do usually not stain neurons and plaque-associated swellings (that stain for APP) (Fig3.20). However, the N-terminal ($Aβ_{1-x}$) and C-terminal ($Aβ_{x-42}$) specific antibodies were able to stain swellings in the white matter of $CNP^{-/-}$ 5xFAD mice (Fig3.20). This hints towards an intriguing qualitative difference between plaque-associated swellings and swellings elicited by myelin dysfunction with the latter harbouring greater potential for amyloid generation.

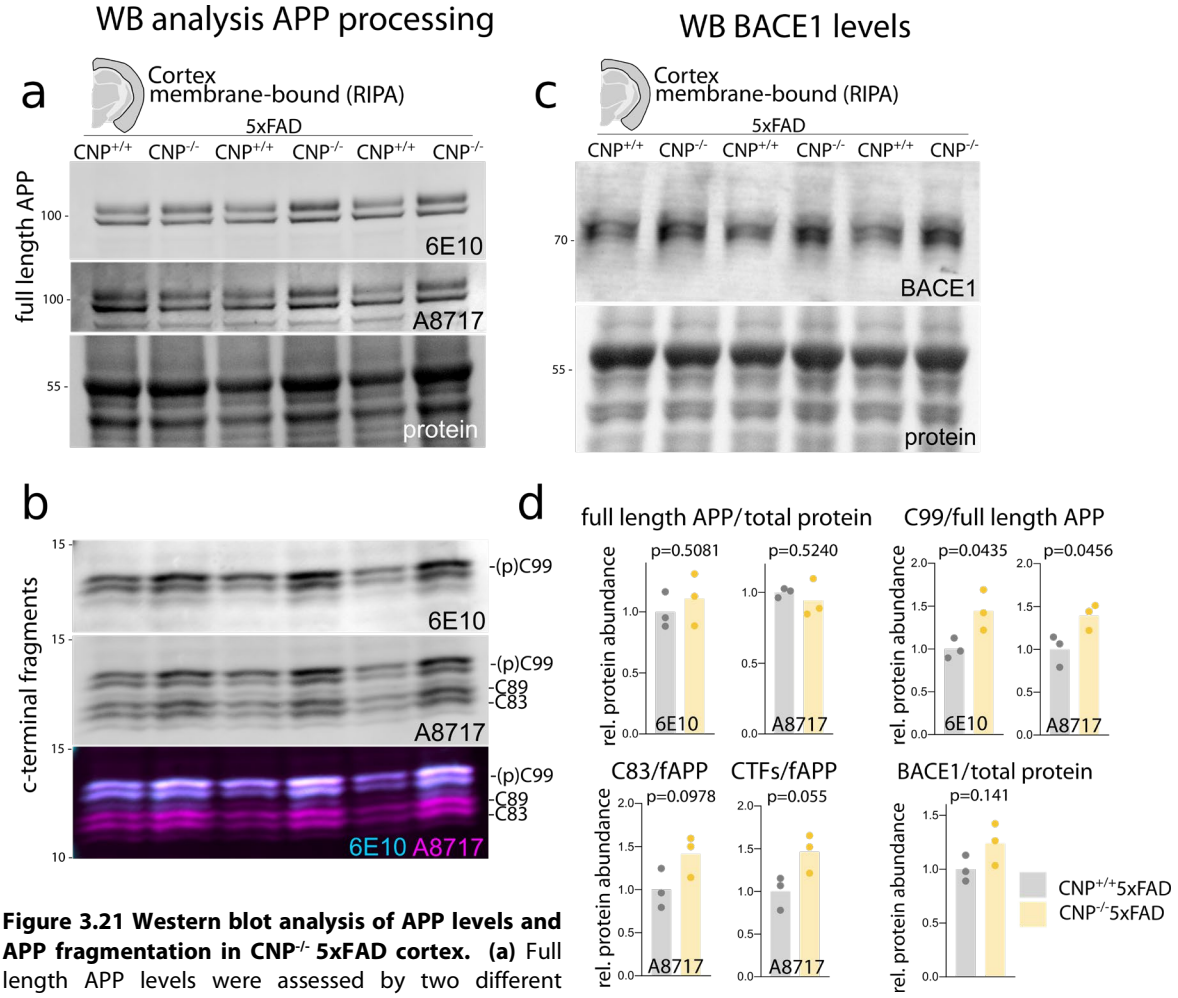

Figure 3.21 Western blot analysis of APP levels and APP fragmentation in $CNP^{-/-}$ 5xFAD cortex. (a) Full length APP levels were assessed by two different antibodies (6E10, A8717) and normalised to total protein fastgreen staining. All three images shown represent the same blot sequentially probed with fastgreen and antibodies (different secondary antibodies). Quantification of blots is shown on the right. **(b)** Immunoblot analysis of α- and β-cleaved APP c-terminal fragments (CTFs). Images show the same blot as in (a) with the corresponding loading scheme. **(c)** Western blot analysis of BACE1 levels in the cortex. **(d)** Quantification of band intensity normalised to full-length APP or total protein (fastgreen blot staining) in the same lane. Lanes/dots present different animals. n=3 for $CNP^{+/+}$5xFAD, n=3 for $CNP^{-/-}$5xFAD. Student's t-test was performed for statistical analysis. Figure adapted from Depp et al. 2021.

CNP$^{-/-}$ 5xFAD swellings could further be stained with an antibody specifically recognising an N-terminally truncated Aβ variant (Aβ$_{4-x}$) that is majorly found in plaque cores (Wirths et al. 2017). These histological results indicate that axonal swellings elicited by myelin dysfunction are accumulating the Aβ producing machinery and a variety of Aβ peptides revealing a direct link between myelin dysfunction and Aβ metabolism.

I further validated these findings on changes in APP metabolism using immunoblot analysis of brain tissue lysates. For this, I micro-dissected subcortical white matter (mainly composed of corpus callosum/alveus) and cortex from CNP$^{-/-}$ 5xFAD mice and CNP$^{+/+}$ 5xFAD controls and fractioned tissue lysates into soluble and membrane-bound fraction. In the membrane bound fraction, I assessed full length APP, APP fragments (α/β cleavage) and BACE1 levels. Overall cortical full length APP levels remained unchanged in CNP$^{-/-}$ 5xFAD mice when normalised to whole protein levels (Fig3.21a). However, fragmentation of APP was enhanced by myelin dysfunction and an approximately 50% increase in C-terminal fragments (CTFs) was observed. This was the case for both CTFs generated by β-secretase (C_{99}, phospho (p)-C_{99}, C_{89}) and α-secretase generated α -CTF (C_{83}) (Fig3.21b). Increases in both CTFs do not necessarily indicate an increase in α-secretase cleavage of full length APP as β-cleavage generated C_{99} and C_{89} are also substrates of ADAM10 generating C_{83} from $C_{89/99}$ (Kuhn et al. 2010). Therefore, it is likely that in the presence of enhanced BACE activity, C_{83} levels are raised alongside β-CTFs. Indeed, BACE1 levels were seemingly increased in the cortex as revealed by immunoblot analysis (Fig3.21c) though not reaching statistical significance in the testing performed.

Counterintuitively, in samples of white matter, more specifically the corpus callosum with adjacent fornix system white matter (alveus, fimbria), no obvious increase in full length APP or APP fragmentation was observed in CNP$^{-/-}$ 5xFAD (Fig3.22a). BACE1 levels, however, were increased by 75% in white matter samples uncoupling BACE1 levels from local CTF fragmentation. Together with the histological analysis showing enrichment of BACE1 in axonal swellings this indicates that while BACE1 steady-state levels are definitely increased in CNP$^{-/-}$ 5xFAD axonal tracts this apparently does not correlate with increased CTF levels to an extent visible by western blot analysis. Indeed, it is likely that enhanced amyloid production in white matter is very localised to axonal swellings as investigated by immunohistochemistry. On the other hand, I surprisingly found enhanced fragmentation of amyloid in the cortex where APP positive swellings are much more rarely detected than in white matter. Please note that increased plaque deposition was not only observed in the white matter alveus, but also in the grey matter e.g. the cortex. The bulk of detected APP and APP CTFs in the cortex is likely derived from neuronal cell bodies that produce ample amounts of APP in the 5xFAD model (especially layer V neurons). This points towards an additional mechanism driving enhanced amyloid production other than locally enhanced amyloid production in axonal swellings. It is tempting to speculate that the "peripheral" axonal distress neurons experience due to faulty myelin increases APP fragmentation in

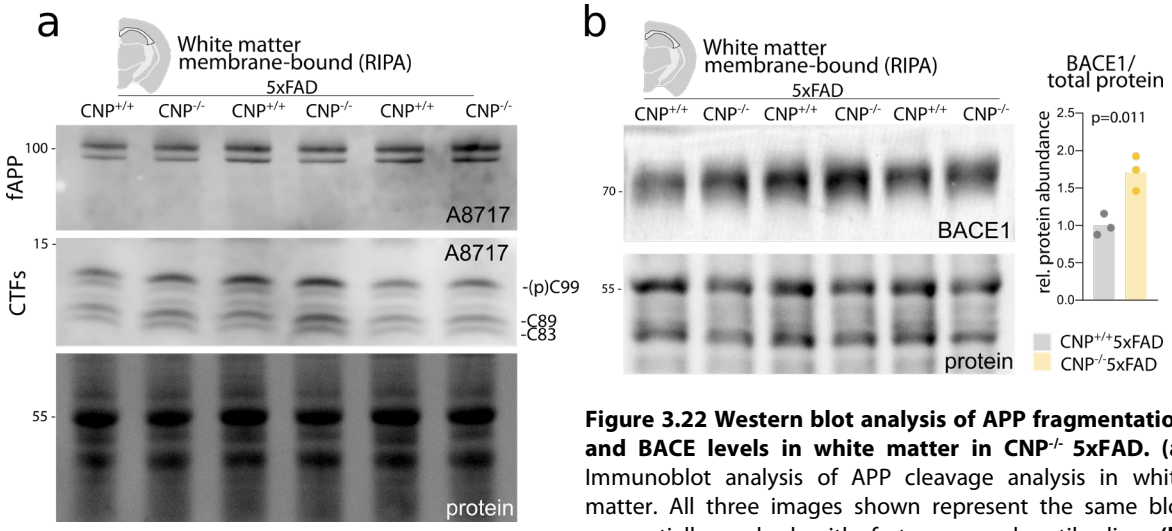

Figure 3.22 Western blot analysis of APP fragmentation and BACE levels in white matter in CNP$^{-/-}$ 5xFAD. (a) Immunoblot analysis of APP cleavage analysis in white matter. All three images shown represent the same blot sequentially probed with fastgreen and antibodies. **(b)** Western blot analysis of BACE1 levels in the white matter and corresponding quantification. Lanes/dots present different animals. n=3 for CNP$^{+/+}$5xFAD, n=3 for CNP$^{-/-}$5xFAD. Student's t-test was performed for statistical analysis. Figure adapted from Depp et al. 2021

the neuronal cell body by a mechanism involving decreased axonal transport rates and trapping APP in the somatic compartment.

3.9 Dysfunctional myelin changes glial responses to amyloid plaques

Next to enhanced amyloid production, decreased amyloid removal, especially removal of seeded amyloid plaques, could potentially drive an overall increase in plaque deposition in brains with myelin defects. As glia cells play an important role in amyloid elimination (see Introduction), I next investigated the responses of glial cells being confronted with both myelin defects and amyloid plaque deposition in $CNP^{-/-}$ 5xFAD mice. I first examined the distribution of microglial cells in $CNP^{-/-}$ 5xFAD and $CNP^{+/+}$ 5xFAD brains. Very similar to $CNP^{-/-}$ single mutants, profound proliferation and morphological changes of microglia indicative of gliosis were observed (Fig3.23). This was most striking in brain regions rich in myelin such as the corpus callosum

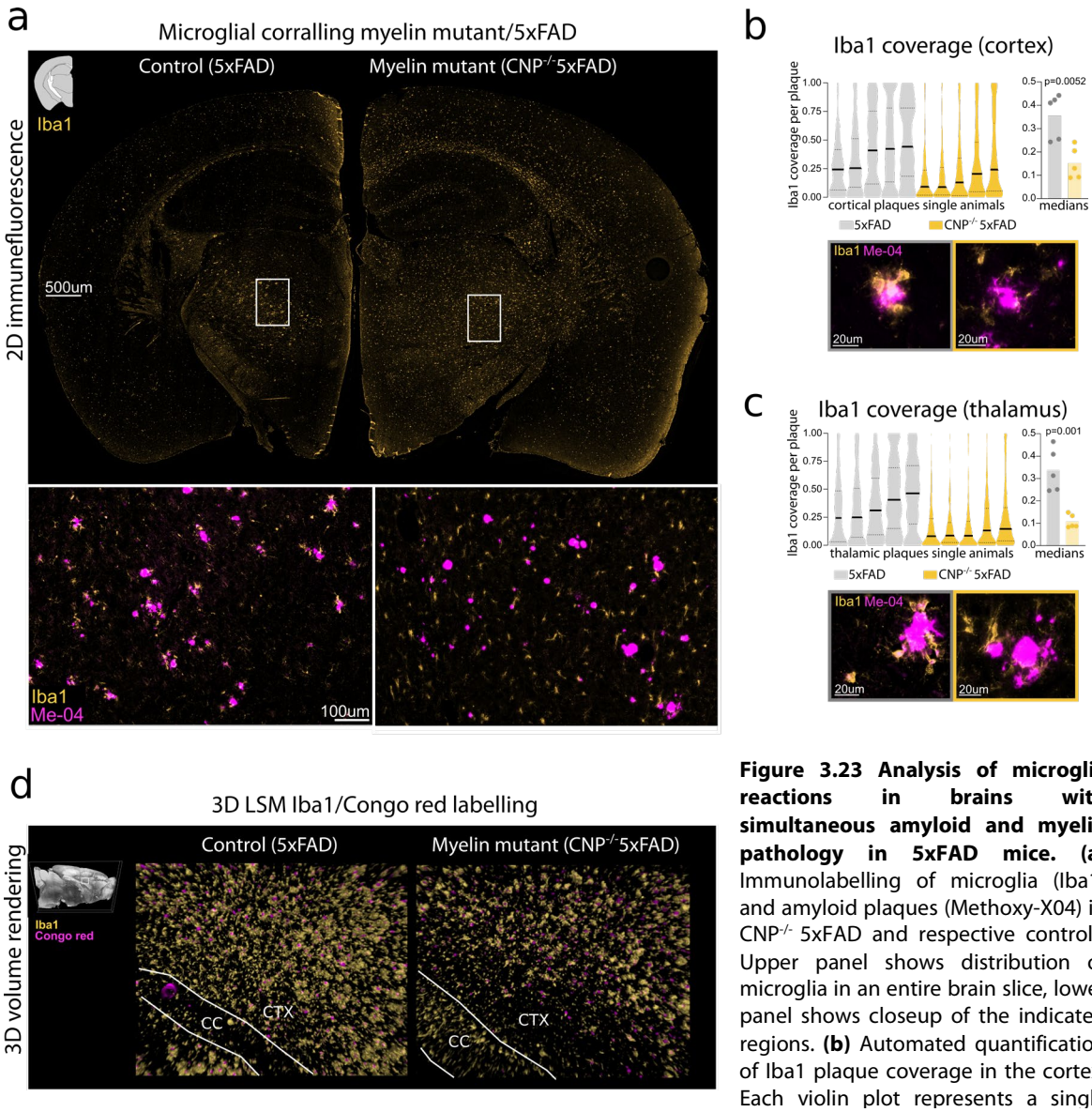

Figure 3.23 Analysis of microglia reactions in brains with simultaneous amyloid and myelin pathology in 5xFAD mice. (a) Immunolabelling of microglia (Iba1) and amyloid plaques (Methoxy-X04) in $CNP^{-/-}$ 5xFAD and respective controls. Upper panel shows distribution of microglia in an entire brain slice, lower panel shows closeup of the indicated regions. **(b)** Automated quantification of Iba1 plaque coverage in the cortex. Each violin plot represents a single animal. 3271 individual cortical plaques were analysed in 5xFAD, 1941 in $CNP^{-/-}$ 5xFAD brain slices. For both (b) and (c) bar plots represent the median of each individual animal shown in the violin plots. Unpaired, two-tailed Student's t-test p-value is given in the bar plot. n=5 per group. **(d)** 3D light sheet microscopic analysis of plaque-corralling in $CNP^{-/-}$ 5xFAD and 5xFAD mice. Brain region shown in blow up is indicated on the left. CC: Corpus callosum. CTX: Cortex. Figure adapted from Depp et al. 2021.

or thalamus. In 5xFAD control mice, only localised microglia proliferation was seen that corresponded to amyloid deposition in plaques. This obvious clustering phenotype of microglia which has been previously described as "corralling" and is associated with the disease-associated microglia signature (Keren-Shaul et al. 2017; Krasemann et al. 2017) was largely lost in CNP$^{-/-}$ 5xFAD mice. Here, microglia seemed more evenly dispersed and microglia lost their intimate contact with amyloid plaques when additionally confronted with dysfunctional myelin by the CNP$^{-/-}$ genotype. Remaining microglia were, however, still of an amoeboid morphology indicating activation. To exclude a bias in visual inspection of microglia/plaque association due to overall increased number of microglia in CNP$^{-/-}$ 5xFAD mice, I developed an ImageJ macro script to automatically quantify microglia coverage of amyloid plaques. In plaque/microglia co-stainings, this script automatically detects amyloid plaques, generates masked of single plaques as objects, and calculates the percentage of the plaque mask covered by Iba1 segmentation. Using this script, I found that typically 30-50% of the plaque is covered by microglia at its periphery with the central plaque core being uncovered (Fig3.23b,c). Importantly, plaque coverage was significantly reduced in CNP$^{-/-}$ 5xFAD mice to ca. 10% in both cortex and thalamus. Visualisation in violin plots revealed interesting distribution changes in plaque coverage with great reductions in plaques that were normally extensively covered. The loss of the corralling phenotype was also observable by light sheet microscopy of Congo red and Iba1 labelled brains (Fig3.23d). Intense microgliosis was seen in the corpus callosum in CNP$^{-/-}$ 5xFAD, but numerous plaques remained uncovered by microglia.

Importantly, the same phenotype of diminished plaque-corralling was reproduced in APP^{NLGF} with myelin damage induced by CNP$^{-/-}$ knockout. Here, the phenotype was even clearer: In APP^{NLGF} control mice multiple microglia clustered around amyloid plaques giving rise to numerous microglia nodules throughout the brain (Fig3.24a). As plaques in APP^{NLGF} are less compact microglia can infiltrate amyloid plaques with their

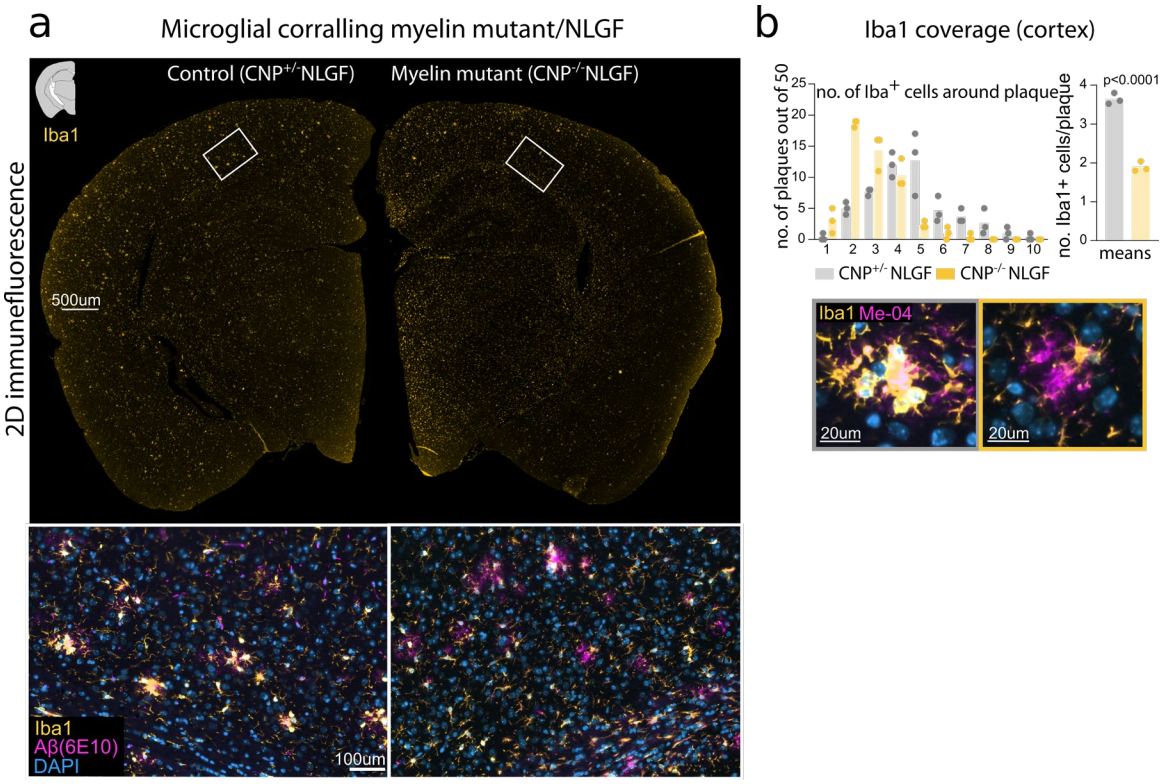

Figure 3.24 Analysis of microglia reactions in brains with simultaneous amyloid and myelin pathology in APP^{NLGF} mice. (a) Immunolabelling of microglia (Iba1) and amyloid plaques (6E10) in CNP$^{-/-}$ APP^{NLGF} and respective controls. Upper panel shows distribution of microglia in an entire brain slice, lower panel shows closeup of the indicated regions of co-stainings. **(b)** Histogram distribution of the number of microglia per amyloid plaque in 50 representative plaques in CNP$^{-/-}$APP^{NLGF} and APP^{NLGF} control mice. Dots represent single animals and bar represents mean values. Unpaired, two-tailed Student's t-test p-value is given in the bar plot. n=3 per group. Figure adapted from Depp et al. 2021.

processes often covering them to a full extent. Conversely, in CNP$^{-/-}$APP^{NLGF} many plaques remained uncovered and microglia associated only loosely with plaques. Automated quantification of the microglia plaque association employing the established script was challenging as APP^{NLGF} plaques do not show a clear border and are frequently of a fissured morphology. Therefore, 50 representative plaques per animal in the cortical region were quantified regarding the number of microglia in their immediate vicinity. Very similar to findings obtained in 5xFAD mice, the number of microglia per plaque was reduced from 4 on average in controls to only about 2 in CNP$^{-/-}$ APP^{NLGF} mice. Accordingly, histogram analysis revealed that larger clusters of microglial cells (>6 microglia per plaque) were almost never observed in CNP$^{-/-}$ APP^{NLGF} mice, however frequency of small clusters increased tremendously.

3.10 Transcriptomic analysis of amyloid and myelin challenged microglia

The described imaging data suggest that in CNP$^{-/-}$ 5xFAD plaque corralling microglia are lost/massively diminished. As this microglial population has been described as disease-associated microglia (DAM) with a unique transcriptional profile, I became interested in studying if microglia in CNP$^{-/-}$ 5xFAD transcriptionally loose the core DAM signature. A diminished corralling phenotype has been best described in scenarios of TREM2 loss – a core DAM signature gene (Yuan et al. 2016; Parhizkar et al. 2019; Wang et al. 2016). Recently a similar phenotype was observed in double knockouts of the TAM-receptors MER and AXL (Huang et al. 2021). I hypothesised that CNP$^{-/-}$ 5xFAD microglia could likewise fail to upregulate TREM2 hampering their responses to amyloid plaques. To acquire a full picture of the transcriptional response in dysmyelinated 5xFAD, microglia from hemispheres (excluding olfactory bulb and cerebellum) of wildtype (CNP$^{+/+}$), CNP$^{-/-}$, 5xFAD and CNP$^{-/-}$ 5xFAD double mutants were magnetically sorted using anti-CD11b beads (Fig3.25a). RNA was isolated and subjected to bulk RNA sequencing (performed together with Ting Sun). Differential expression analysis using the DESeq2 analysis pipeline revealed largely overlapping sets of regulated genes between the 5xFAD, CNP$^{-/-}$ and CNP$^{-/-}$ 5xFAD when compared to wildtype animals (Fig3.26b). Intriguingly, the CNP$^{-/-}$ 5xFAD microglia showed the largest number of regulated genes in total. Principal component analysis (PCA) revealed that the transcriptional signature in CNP$^{-/-}$ 5xFAD mice was dominated by the CNP$^{-/-}$ response as these samples clustered tightly together in the PCA plot. The 5xFAD signature in its principal components was more similar to wildtype cells. The CNP$^{-/-}$ associated signature especially contributed to the formation of PC1 (here displayed on the y-axis) which explained 80.1% of data variability.

For investigating differentially regulated genes between the four genotypes, we opted to extract the top100 genes contributing to PC1 (Fig3.25d). The extracted genes clearly fell in 4 major clusters with different trajectories throughout the experimental groups: To my surprise, a prominent cluster (cluster 4) mainly comprised of myelin/oligodendrocyte-enriched gene products such as *Plp1*, *Mag*, *Car2* that were detected in the microglial fraction and showed a striking downregulation in all mutant animal with the double mutant CNP$^{-/-}$ 5xFAD being most affected. *Cnp* was also included in this group which was virtually absent in CNP null single mutants and crossbreedings validating successful knockout out of *Cnp*. As microglial cells typically express only very low amounts of these genes (see brain sequencing database (Zhang et al. 2014)), it is likely that these transcripts that were picked-up in the RNA-seq analysis are a contamination from myelin. Expression of classical myelin genes, however, is not massively altered in Cnp$^{-/-}$ or 5xFAD when oligodendrocytes or myelin are assessed directly (Sun, Depp, Nave, unpublished). Though a dedicated myelin removal step is implemented in the isolation protocol, myelin is of a very sticky nature and cannot be completely removed. Why would myelin contamination amounts change in response to injury (5xFAD, CNP$^{-/-}$)? During inflammation, tissue to a certain degree swells up and disintegrates as a result of secreted immune factors (such as proteases etc.). This would potentially lead to a more efficient separation of myelin from microglia as the targeted cell type. Likewise, during inflammation the amount of microglia is increased raising chances of microglia/capture-antibody interaction during cell isolation eventually leading to a purer microglia fraction. Therefore, changes in cluster 4 genes should be interpreted with caution.

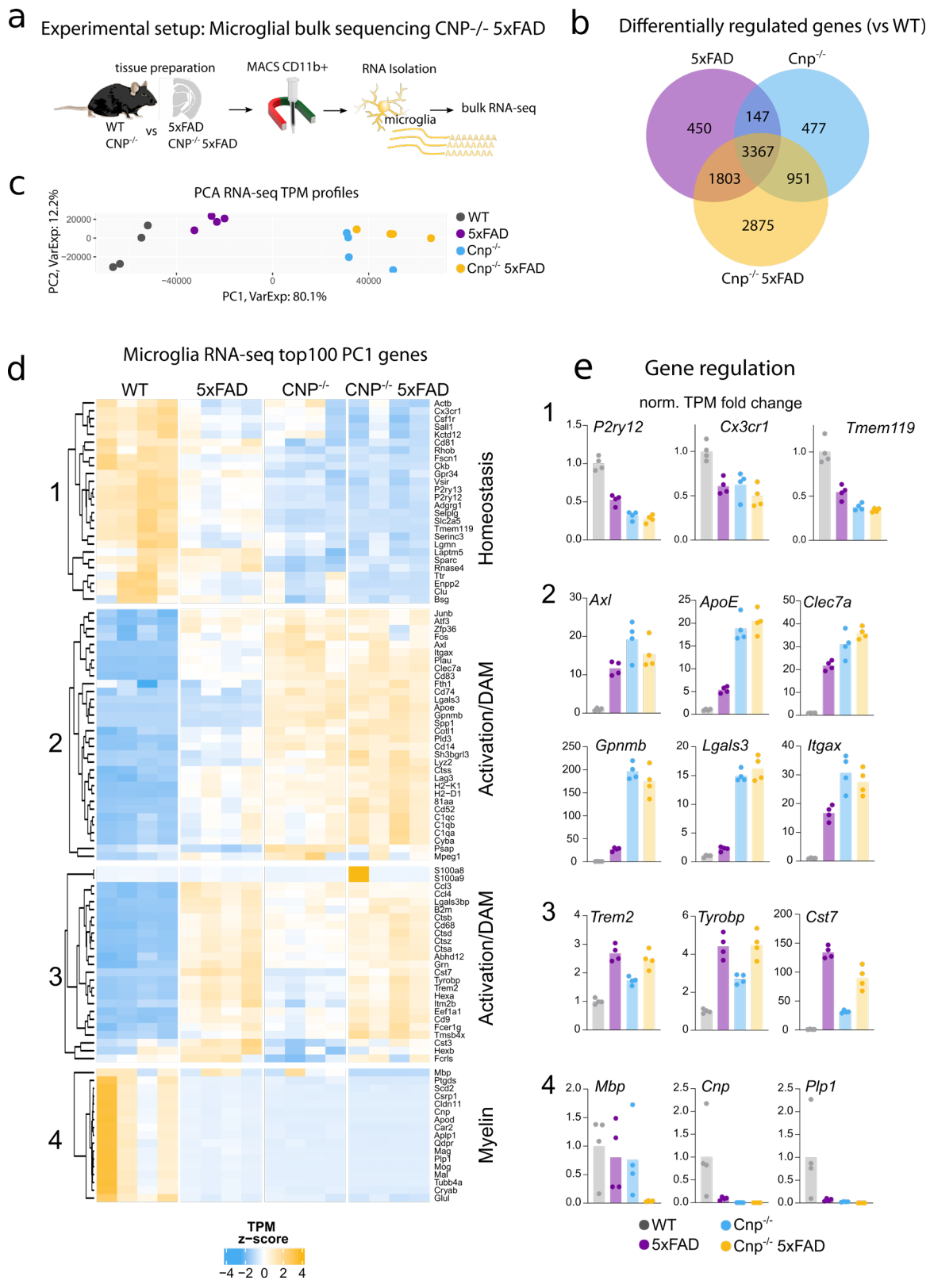

Figure 3.25 RNA-seq analysis of microglia in CNP$^{-/-}$ 5xFAD. **(a)** Experimental setup for microglia bulk RNA-seq. Microglia were isolated from hemispheres (without olfactory bulb and cerebellum) of 6-month-old wildtype (WT), CNP$^{-/-}$, 5xFAD and CNP$^{-/-}$ 5xFAD animals and subjected to RNA-seq (replicates n=4 for each genotype). **(b)** Venn-diagram showing the number of differentially regulated genes throughout the experimental group according to DESeq2 analysis pipeline (adj. p-value=0.05) **(c)** Principal component analysis (PCA) of normalised RNA TPM profiles. Dots represent replicates. Numbers mark four major clusters detected. **(d)** Heatmap of top100 genes contributing to PC1 variability. **(e)** Bar plots of selected from the different clusters. Analysis performed together with Ting Sun. Figure adapted from Depp et al. 2021.

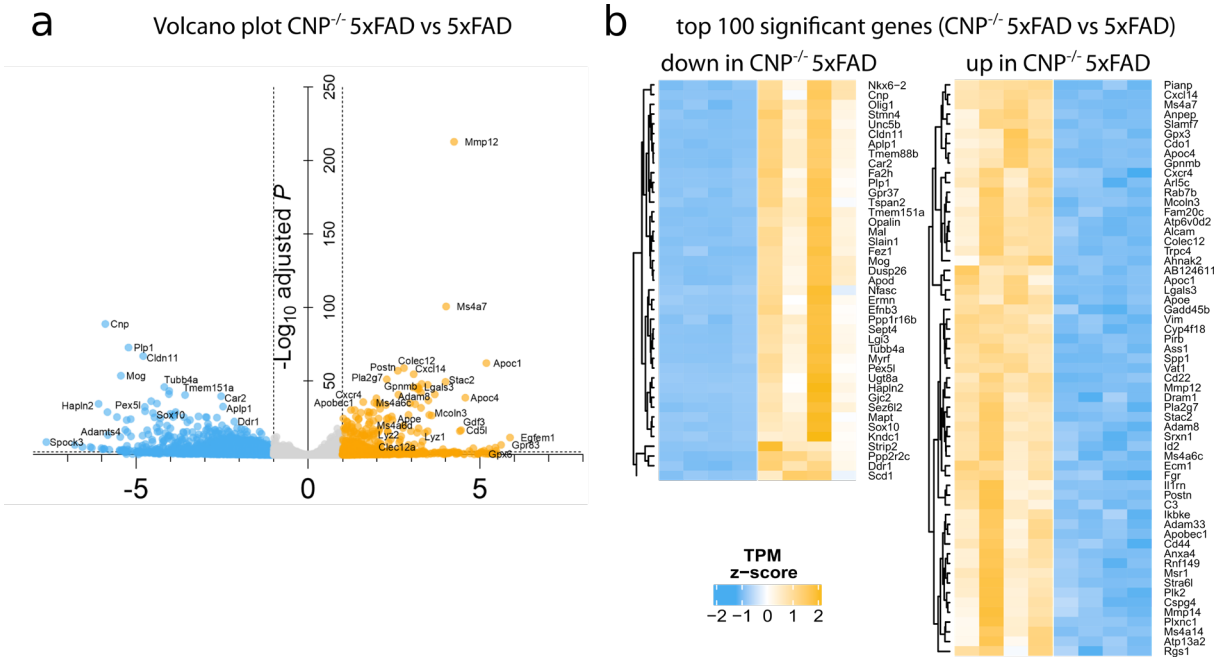

Figure 3.26 Direct comparison of the transcriptome signature of CNP$^{-/-}$ 5xFAD and 5xFAD microglia.
(a) Volcano plot visualisation of differentially expressed genes between CNP$^{-/-}$ and CNP$^{-/-}$ 5xFAD microglia (significant cutoff adjP < 0.01, log2FC > 1.0) **(b)** Heatmap represents normalised expression levels of top 100 significantly regulated genes between Cnp$^{-/-}$ 5xFAD vs 5xFAD microglia profiles as analysed by RNA-seq of isolated microglia. Figure adapted from Depp et al. 2021.

Cluster 1 consisted of genes associated with homeostatic microglia function such as *P2ry12*, *Tmem119* and *Cx3cr1*. These gene were downregulated in all three mutants with CNP$^{-/-}$ and CNP$^{-/-}$ 5xFAD microglia showing the strongest and similar degree of downregulation (Fig3.25d,e). This presumably reflects the amount of inflammatory microglia present in the sample. It is interesting that the amount of homeostatic microglia apparently did not further decrease in CNP$^{-/-}$ 5xFAD mice when compared to CNP$^{-/-}$ mice. This indeed might be an indication that there is no additive effect of the two genotypes. Cluster 2 was enriched in genes implicated previously in the DAM signature (*Itgax, Axl, Clec7a, Lgals3, Spp1, Apoe*). Intriguingly, this gene cluster showed induction in 5xFAD microglia validating previous findings but showed even higher induction in CNP$^{-/-}$ and CNP$^{-/-}$ 5xFAD microglia. Contrary to the imaging data that demonstrated that plaque-corralling DAM were lost in CNP$^{-/-}$ 5xFAD mice, on a transcriptional level the DAM signature induction was maintained or even hyper-induced in these animals. Cluster 3 that showed a more pronounced induction in both 5xFAD containing genotypes and modest induction in CNP$^{-/-}$ single mutants also contained DAM genes such as *Tyrobp* and *Trem2*. Importantly, *Trem2* and *Tyrobp* showed equal induction in 5xFAD and CNP$^{-/-}$ 5xFAD ruling out a *Trem2* loss of function as possible mechanism for diminished plaque-coralling in CNP$^{-/-}$ 5xFAD mice. Direct comparison of the signature of CNP$^{-/-}$ 5xFAD to 5xFAD mice (Fig3.26a,b) completed this picture: most DAM signature genes were not differentially regulated. The exception to this was *Apoe* and multiple other apolipoprotein such as *Apoc1* and *Apoc4* and other genes involved in lipid metabolism (*Msr1, Pla2g7*). Multiple genes upregulated in CNP$^{-/-}$ 5xFAD were proteins with functions related to the extracellular matrix such as *Spp1, Postn, Fam20c, Ecm1* and several matrix metalloproteases (*Mmp12, Mmp14*). Likewise, multiple family members of the *Ms4a* cluster were induced in CNP$^{-/-}$ 5xFAD microglia (*Ms4a7, Ms4a6c, Ms4a14*). Intriguingly, with *Apoe, Apoc1* and genes of the *Ms4a* cluster previously identified as AD risk loci were among the top differentially regulated genes between CNP$^{-/-}$ 5xFAD microglia and 5xFAD microglia.

3.11 APOE content in amyloid plaques is increased by myelin injury

Upregulation of lipoproteins, especially *Apoe* is of particular interest due to its strong allele specific effect on AD risk and due to its tight association with amyloid plaques. APOE enhances fibrillisation of amyloid (Ma et al. 1994) and APOE levels dictate the amount of fibrillar plaques with reductions in APOE levels exerting a protective effect against amyloid deposition (DeMattos et al. 2004; Bales et al. 1997; Kim et al. 2011). Likewise, interfering with amyloid/APOE interaction by immunotherapy or administration of blocking peptides, ameliorates Aβ deposition (Sadowski et al. 2006; Kim et al. 2012). Therefore, it is likely that the massive amount of secreted lipoproteins such as APOE in CNP$^{-/-}$ 5xFAD drives accumulation of Aβ in the brain. I tested this by directly assessing APOE accumulation in plaques of CNP$^{-/-}$ 5xFAD mice by immunohistochemistry. APOE immunostaining revealed abundant APOE accumulation in amyloid plaques in both 5xFAD and CNP$^{-/-}$ 5xFAD mice. In brains with myelin dysfunction, however, additional speckled, cellular staining throughout the white matter could be observed indicative of elevated APOE levels (Fig3.27a). It is likely that these cells represent microglia or astrocytes although double immunostainings have to be conducted to confirm this. Analysis of cortical plaque content revealed heightened APOE content in plaques in CNP$^{-/-}$ 5xFAD brain (Fig3.27b).

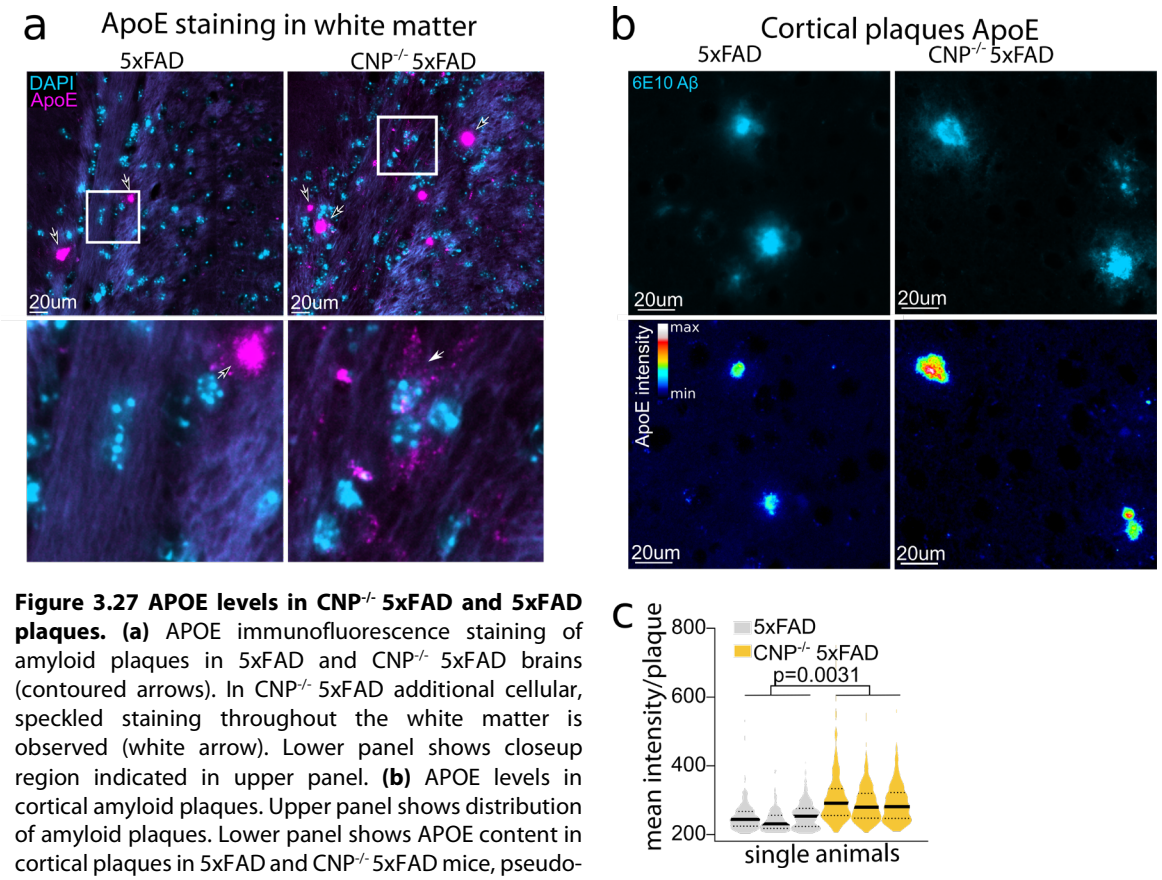

Figure 3.27 APOE levels in CNP$^{-/-}$ 5xFAD and 5xFAD plaques. (a) APOE immunofluorescence staining of amyloid plaques in 5xFAD and CNP$^{-/-}$ 5xFAD brains (contoured arrows). In CNP$^{-/-}$ 5xFAD additional cellular, speckled staining throughout the white matter is observed (white arrow). Lower panel shows closeup region indicated in upper panel. **(b)** APOE levels in cortical amyloid plaques. Upper panel shows distribution of amyloid plaques. Lower panel shows APOE content in cortical plaques in 5xFAD and CNP$^{-/-}$ 5xFAD mice, pseudo-coloured according to rainbow lookup table. **(c)** Quantification of APOE plaque content. Violin plots of mean APOE plaque content per plaque. Each violin plots represents a single animal (n=3 per genotype, 703 plaques for 5xFAD, 846 plaques for CNP$^{-/-}$5xFAD). For statistical analysis, unpaired, two-tailed Student's t-test was performed. Figure adapted from Depp et al. 2021.

3.12 Trem2 cleavage is not altered in CNP$^{-/-}$ 5xFAD microglia

Ms4a cluster genes were similar to *ApoE* upregulated in CNP$^{-/-}$ 5xFAD mice. Polymorphisms in the *Ms4a* cluster have been previously linked to AD risk (Ma, Yu, and Tan 2015) though the exact function of MS4A proteins is still poorly understood. A very interesting study reported that the *Ms4a* cluster regulated levels of soluble TREM2: MS4A4A and TREM2 are colocalised in lipid rafts and overexpression of MS4A4A increases TREM2 cleavage (Deming et al. 2019). Increases in the *Ms4a* cluster in CNP$^{-/-}$ 5xFAD microglia, could therefore increase TREM2 shedding removing ample amounts of functional, signalling competent full length Trem2 form. In the end, this could potentially phenocopy a transcriptional loss of function of Trem2. Likewise, lipids contained in myelin (phosphatidylserine, sulfatides, sphingomyelin) and myelin itself activate TREM2 signalling in a dose-dependent manner (Nugent et al. 2020; Poliani et al. 2015; Cignarella et al. 2020). Because TREM2 signalling seems to be terminated by shedding, overt myelin-dependent TREM2 activation could also lead to increases in the CTF leaving less full length TREM2 at the cell surface to interact with Aβ. I therefore investigated TREM2 protein levels and shedding of TREM2 using immunoblot analysis. I first validated this technique in regard to successful detection of TREM2 and the C-terminal fragment generated after shedding by comparing whole brain 5xFAD membrane-bound tissue lysates to wildtype brains. Expectedly, full length TREM2 gave a broad range of bands on the blot due to glycosylation and its C-terminal fragment was clearly upregulated in 5xFAD mice (Fig3.28a). In CNP$^{-/-}$ 5xFAD cortical lysates, however, no obvious differences in full length TREM2 or C-terminal fragments were observed (Fig3.28). These findings validate the RNA-seq findings regarding proper induction of *Trem2* in CNP$^{-/-}$ 5xFAD mice and rule-out the possibility of posttranslational mechanism altering TREM2 protein levels or MS4A-dependent increases in TREM2 cleavage.

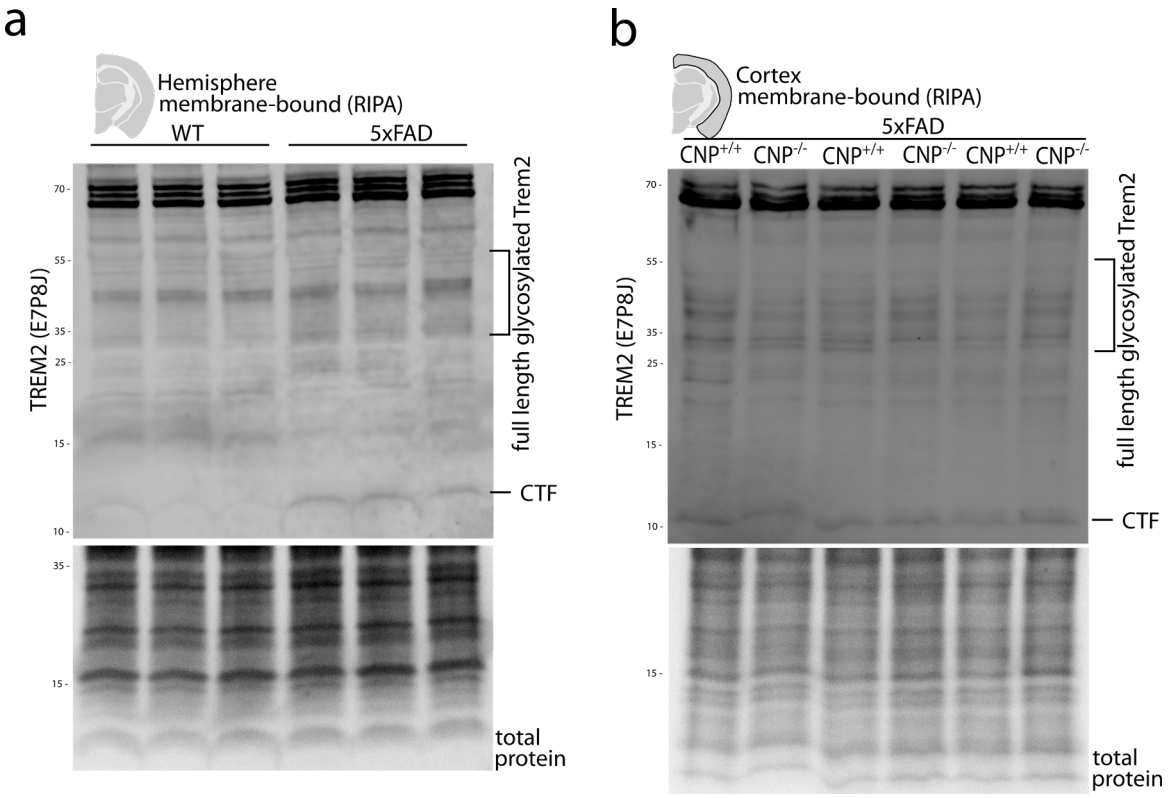

Figure 3.28 TREM2 levels and cleavage in CNP$^{-/-}$ 5xFAD and 5xFAD brains. (a) Validation of technique by comparison of wildtype and 5xFAD brain lysates in which TREM2 is upregulated. High molecular weight bands at 70kDa represent unspecific bands. **(b)** Levels of full length TREM2 and C-terminal fragment (CTF) generated after cleavage in CNP$^{-/-}$5xFAD and 5xFAD control mice. Lanes represent single animals. n=3 per group. Figure adapted from Depp et al. 2021.

3.13 Analysis of microglia response to myelin dysfunction at the single cell level

The transcriptional analysis of the CNP$^{-/-}$ single mutant alongside CNP$^{-/-}$ 5xFAD makes clear that myelin dysfunction *per se* is sufficient to incite a response that is very similar to the DAM response observed in AD. This is in agreement with the study by Krasemann and colleagues that detected the DAM signature in EAE as a model of demyelination (Krasemann et al. 2017). Together with the study by Keren-Shaul et al. that described the emergence of the DAM signature in an ALS model and ageing, this illustrates that the DAM signature is not confined to AD. The interpretation of the bulk-sequencing dataset is limited by the fact that the number of activated microglia is increased in CNP$^{-/-}$ mice so that a higher percentage of activated microglia will contribute to the bulk signature.

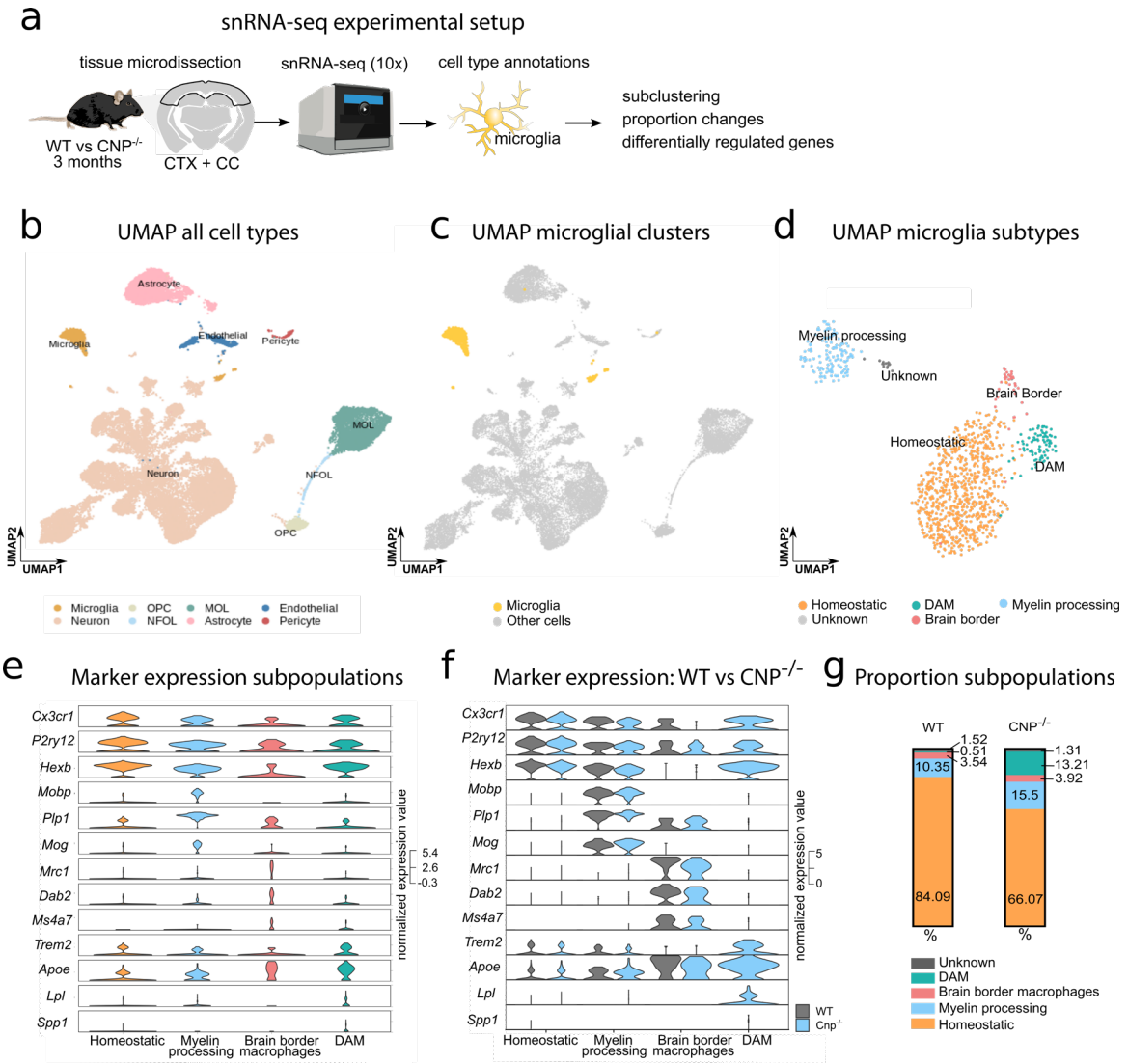

Figure 3.29 Myelin dysfunction induces DAM-like state as determined by snRNA-seq (a) Experimental setup for studying myelin-dysfunction induced microglia profiles at the single cell level. Cortex and adjacent callosal white matter were micro-dissected from 3-month-old wildtype and Cnp$^{-/-}$ mice and subjected to snRNA-seq (10x). **(b)** Identified cell types in the UMAP space **(c)** Microglia subset visualised in the UMAP space. **(d)** UMAP visualisation of annotated microglia subtypes. **(e)** Violin plots showing marker gene expressions in each microglia subpopulation. **(f)** Violin plots showing marker gene expressions in each microglia subpopulation separated by genotype. **(g)** Bar plot shows distribution of microglia subpopulations in wildtype and CNP$^{-/-}$. Right panel showing genotype distribution among microglia subpopulations visualised in the UMAP space. Analysis performed together with Ting Sun. Figure adapted from Depp et al. 2021.

In an attempt to fully understand the apparent DAM-like microglial signature in CNP$^{-/-}$ microglia, we performed snRNA-seq on cortical and callosal tissue prepared from younger (3-month-old) CNP deficient animals and annotated microglia population to perform subclustering and differential gene expression analysis (analysis was performed together with Ting Sun) (Fig3.29a,b,c). We identified 4 major clusters (Fig3.29d): A large homeostatic cluster and smaller clusters consisting of brain border macrophages, microglia with ample amounts of myelin transcript and a cluster with high expression of classical DAM genes such as *Trem2, Lpl* and *Spp1* which was therefore identified as DAM. Virtually all DAM-like microglia were derived from CNP deficient brain tissue and this pool of microglia expanded greatly in CNP$^{-/-}$ mice from 0.51% to 13.21% (Fig3.29g). We next assessed the similarities between DAM induced by myelin defects and DAMs induced by the presence of amyloid plaques. For this, integration was performed between our dataset and the study by Zhou and colleagues (Zhou et al. 2020) that performed snRNA-seq of cortical tissue of 7-month-old 5xFAD mice. DAMs were readily identified in the merged object by unbiased clustering (Fig3.30a) that showed high expression of *ApoE* and *Trem2*. This cluster was mainly occupied by 5xFAD microglia but also contained CNP$^{-/-}$ derived DAM (Fig3.30d) confirming their identity *as bona fide* DAM. Around 40% of 5xFAD microglia converted to DAM and around 20% of CNP$^{-/-}$ microglia (as identified in the merged object) (Fig3.30d). Expression analysis showed that on a single cell level a group of classical DAM marker genes including *Apoe, Lyz2* and *Axl* were expressed at a similar level in both CNP$^{-/-}$ DAM and 5xFAD DAM (Fig3.30e). This finding also helps further interpreting the bulk sequencing dataset (with the caveat that different ages were analysed): increased bulk levels of *Apoe* rather originate from increased proportion of inflammatory microglia than upregulation of *Apoe* on a single cell level. Intriguingly, *Ms4a7*, *Gpnmb* and *Lpl* were highly induced in myelin-dysfunction induced DAM but only moderately in 5xFAD DAM.

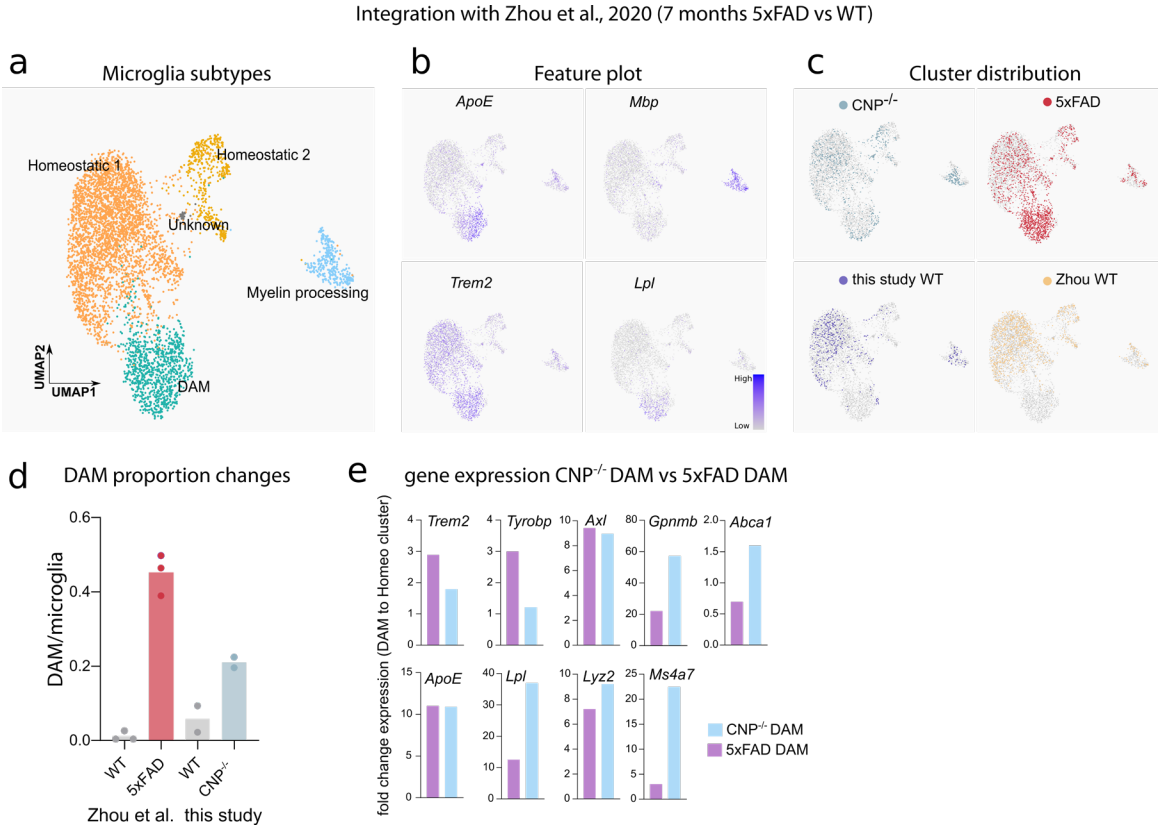

Figure 3.30 Comparison of microglia states induced by amyloidosis and myelin dysfunction. (a) Integrative analysis of this study and 7-month-old 5xFAD and wildtype microglia snRNA-seq profiles from Zhou et al. 2020. Visualisation of microglia in the UMAP space. Different microglia populations are colour-coded. **(b)** Feature plot showing normalised expression levels of *ApoE, Mbp,Trem2* and *Lpl* for identification of microglia subclusters. **(c)** Genotype distribution among microglia subpopulations visualised in the UMAP space. **(d)** Proportion of DAMs on microglial cells in different genotypes in the merged objects. **(e)** Bar plots representing average regulation levels of single genes in CNP$^{-/-}$ DAM and 5xFAD DAM. Regulation values are calculated by comparing gene average expression of DAM to the respective homeostatic microglia population. Analysis performed together with Ting Sun.

Elevation of *Ms4a7*, *Gpnmb* and *Lpl* in the bulk sequencing dataset are, therefore, also partially derived from increased induction on the single cell level. *Trem2* and especially *Tyrobp* were robustly upregulated in 5xFAD DAM but only to a lesser extent in CNP$^{-/-}$DAM suggesting that Aβ pathology is a stronger inducer of *Trem2/Tyrobp* than myelin dysfunction.

Our transcriptomic data in summary suggest that the DAM signature is adequately induced in microglia of CNP$^{-/-}$ mice and that these microglia in theory are adequately equipped to react to amyloid plaques. Why do these microglia fail to do so *in vivo* then? I propose a simple and comprehensible reason for this: the distraction and primary engagement of microglia with myelin. Indeed, in the snRNA-seq dataset of CNP$^{-/-}$ a subset of microglia was identified that surprisingly contained ample amounts of oligodendrocyte transcripts such as *Mbp, Mog, Plp1* and *Mag* (Fig3.29b). It was excluded that these cells were doublets (ergo sequencing reads derived from two cells being captured in the same droplet during sequencing). Due to the very similar transcriptional profile to oligodendrocytes in the presence of expression of microglial markers it is likely that these cells represent microglia that have recently phagocytosed large amounts of myelin. Indeed, such a population of microglia has been recently described in a snRNA-seq study of MS tissue (Schirmer et al. 2019) – though the exact mechanism of how phagocytosed mRNA ends up in the nucleus remains elusive. These cells entered a slightly activated state as suggested by downregulation of homeostatic markers *Tmem119*, *P2ry12* and *Cx3cr1* and increased expression of apolipoproteins and the fatty-acid breakdown enzyme *Acsl1* (Fig.2.31). This cluster of myelin processing microglia was increased in CNP$^{-/-}$ from 10% to around 15% indicative of enhanced myelin phagocytosis. Interestingly, CNP$^{-/-}$ DAM still displayed slightly elevated levels of *Mbp* mRNA while other myelin mRNAs were not present. Long-term survival of phagocytosed *Mbp* mRNA seems reasonable as one of the most abundant mRNAs in myelin sheets. It is tempting to speculate that those cells convert to DAM that phagocytose large amount myelin debris and might not efficiently degrade it.

Though profound microglia activation has been identified early in CNP$^{-/-}$ mice (Lappe-Siefke et al. 2003) the exact reason for this has remained elusive given no "acute demyelination" and the original description of "normal myelin". With my work showing structural alterations of myelin in CNP$^{-/-}$ mice that were even recognisable by immune fluorescence together with the transcriptomic analysis of microglia that show a lipid

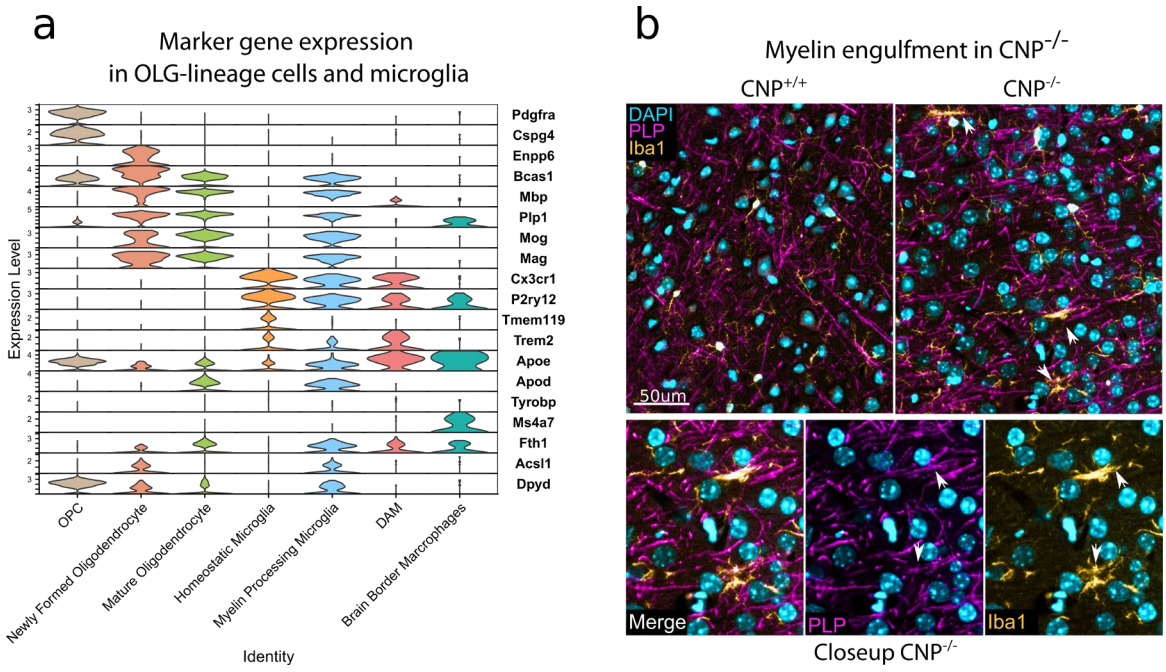

Figure 3.31 Myelin phagocytosis/engulfment in CNP$^{-/-}$ mice. (a) Violin plots shows expression levels of indicated genes in the oligodendroglial lineage cells and microglia marker genes throughout cell identities. Myelin processing microglia show robust presence of oligodendrocyte marker genes as well as microglial markers. **(b)** Immunofluorescence analysis of myelin engulfment (PLP^{+}) by microglia (Iba1^{+}) in the cortex microglia of CNP$^{-/-}$ mice.

digesting profile (upregulation of lipid handling genes *ApoE, Lpl, Abca1* and phagocytosis-related genes), it seems comprehensible that microglia actively phagocytose dysfunctional myelin. I validated this by immunofluorescence analysis of myelin engulfment in $CNP^{-/-}$ mice. Since specific association of microglia and myelin in the white matter is difficult to study due to full overlap of microglia with myelin, I focused on the cortex where myelination is sparser. In wildtype animals, thin and elongated microglia processes were seen throughout the cortex that occasionally contacted myelin sheaths (Fig3.31b). In $CNP^{-/-}$, I identified multiple scenarios in which myelin processes became thickened and seemingly engulfed entire myelin sheaths (arrows, Fig3.31b). Myelin, thus, clearly attracts microglia in $CNP^{-/-}$ mice. I envision the following: in the $CNP^{-/-}$ brain environment microglia become increasingly engaged with dysfunctional myelin which they attempt to phagocytose inducing activation and a DAM signature profile. When plaques are deposited by the additional 5xFAD genotype later in life, a large number of microglia is pre-occupied with the clearance of myelin throughout grey and white matter. As the attraction of microglia to plaques essentially uses the same signalling cascades (upregulated in the DAM signature) as recognition of myelin damage, microglia become unresponsive to amyloid.

3.14 Myelin damage in Alzheimer's disease patients

I finally assessed if my findings in myelin dysfunction and AD mouse models have clinical relevance to human AD. Supporting our findings, accelerated white matter decline has been demonstrated in neuroimaging studies in a more global manner in AD patients (Dean et al. 2017; Ringman et al. 2007; Stricker et al. 2009; Wang et al. 2019; Araque Caballero et al. 2018). Microscopic evidence of myelin alterations in AD, however, is scarce. I therefore studied intracortical myelin integrity in a small cohort of AD patients. Since myelination status varies significantly between gyri and cortical areas, I performed overview imaging of the entire medial temporal lobe biopsy material (paraffin-sections) stained for myelin, microglia and amyloid plaques. This gave me a good impression of local differences in amyloid pathology and allowed me to confidently identify the transentorhinal area for analysis (Fig3.32a). The transentorhinal area represents an area of high pathologic burden in AD in regards to both amyloid deposition and neurofibrillary tangle formation (Braak and Braak 1991). I observed a striking difference in the appearance of myelinated fibres as well as an overall decline in myelin density. This was not limited to the immediate vicinity of plaques in the sense of a focal demyelination but was observable in a general fashion in the upper cortical layers. Moreover, myelin sheaths were seemingly more "disrupted". Intracortical myelin loss, therefore, represents another cellular pathology associated with AD. Sites of myelin loss were also associated with increased microglia numbers as identified by Iba1 staining and coverage of amyloid plaques by microglia was not extensive. Intriguingly, both of these phenotypes are reminiscent of the phenotypes observed in $CNP^{-/-}$ 5xFAD mice. Of course, analysis of human autopsy material offers only a snapshot of rather late pathological stage (prior to death) and as such the question remains if myelin decline is secondary to AD pathology or could represent a primary driver of the disease (in more detail discussed later). The preliminary observation of myelin decline in human AD patients, however, is encouraging regarding the translation of our findings in mouse models and points towards clinical relevance of our findings (discussed later).

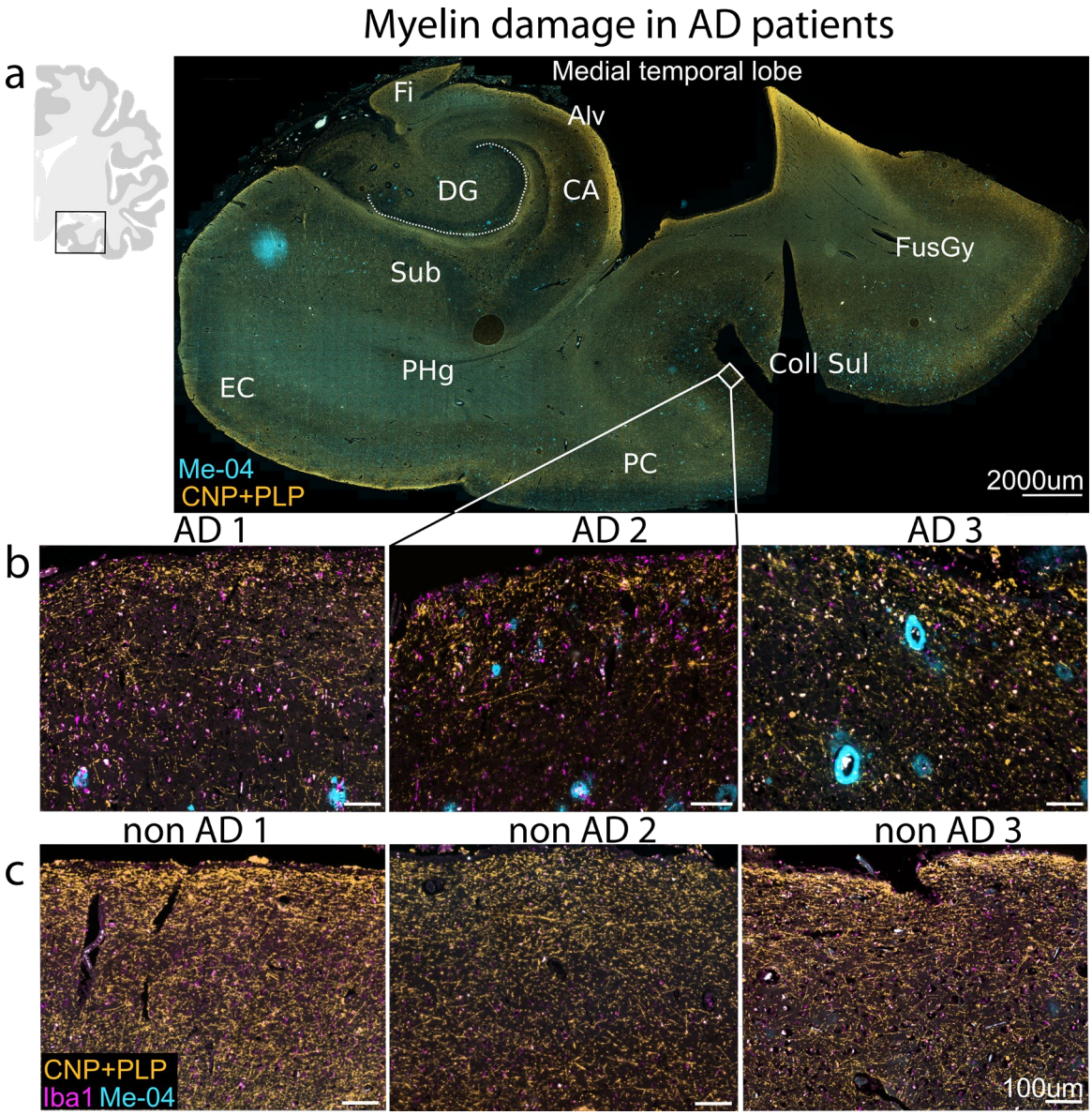

Figure 3.32 Intracortical myelin damage AD patients. (a) Autopsy samples from the medial temporal lobe of AD affected individuals and non-AD patients. Immunostaining against CNP and PLP1 to visualize myelinated fibres, Iba1 to stain microglia and Methoxy-X04 (Me-04) to stain amyloid-ß plaques. Annotated overview image of the medial temporal lobe of one AD patient indicates the location of the closeups which show upper cortical layers in the transentorhinal cortex in plaque^{+} individual AD patients and non-demented controls. DG: Dentate Gyrus, Fi:Fimbria, CA: Cornu Ammonis, Sub:subiculum, EC: Entorhinal cortex. PHg: Parahippocampal gyrus. FusGy: Fusiform gyrus. Coll Sul: Collateral Sulcus. **(b)** Closeup images of the indicated region in the transentorhinal cortex in three individuals with ample amounts of amyloid plaques (Me-04 positive). Note the instances of cerebral amyloid angiopathy in AD3. **(c)** Closeup images of indicated region in plaque-negative non-demented controls.

4 Discussion and Conclusion

4.1 A refined model of Alzheimer's disease

Combining quantitative light sheet microscopy, behavioural testing, biochemical analyses and both bulk and single-cell resolution RNA sequencing, the work presented in this thesis identifies myelin perturbations (genetic, inflammatory or toxin-induced) as an upstream driver of amyloid deposition in AD mouse models. In contrast, the absence of cortical myelin in a novel forebrain-specific shiverer mouse delayed Aβ deposition, demonstrating that myelin itself can act as a risk factor for AD pathology. Downstream of myelin dysfunction, axonal distress that is linked to enhance amyloid production and altered microglia responses to amyloid plaques are likely mediating the advancement in plaque pathology.

Based on these findings, I propose a new or refined model of AD development that puts oligodendrocytes centre-stage (Fig4.1): in the ageing brain, microglia become increasingly engaged with deteriorating myelin which exhausts their phagocytic activity and renders them unresponsive to amyloid plaques. Simultaneously, axonal problems arise due to lack of supportive functions from stressed oligodendrocytes that alter APP metabolism towards enhanced Aβ production. Importantly, such a model does not contradict the prevailing amyloid hypothesis of AD, but rather modifies it to include the role of oligodendrocytes in disease progression. A similar adaptation of the amyloid hypothesis has taken place to pay tribute to the large body of studies demonstrating the important role of microglia responses. Such a myelin-centred model of AD has been previously envisioned by the late Georg Bartzokis who was the first to carefully put together evidence linking myelin and more so myelin repair processes to ageing and AD (Bartzokis 2004). He attributed a unique vulnerability to oligodendrocytes and myelin due to slow biochemical turnover rates, high cholesterol and iron levels and the continuous burden of myelin maintenance (Bartzokis 2011). At the time Bartzokis formulated his hypothesis the role of oligodendrocyte metabolic support functions had not been unravelled yet. It offers a novel spin to his myelin hypothesis linking axonal/neuronal bioenergetics to oligodendroglial dysfunction. Future work should specifically address the question to what extent ageing effects metabolic support functions over structural myelin defects. It seems likely that decline in metabolic support function

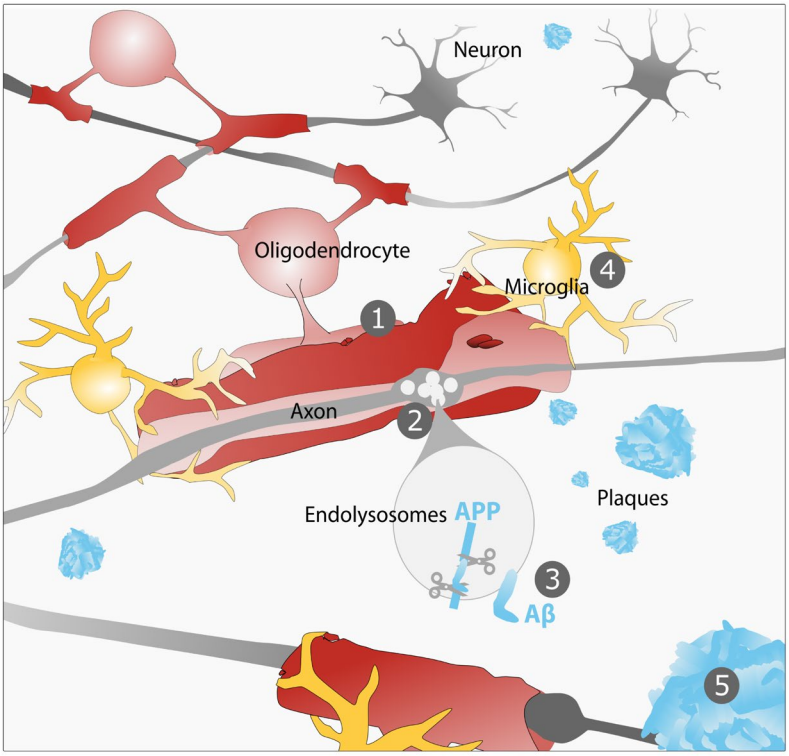

Figure 4.1 Model: Myelin defects as driver and risk factor for AD. Scheme illustrating a model of AD in which myelin dysfunction (1) induces axonal spheroids (2) in which endosomes/lysosomes accumulate and Aβ production is enhanced (3). Simultaneously, microglia become increasingly engaged with defective myelin and are distracted from amyloid plaques (4). Both contribute to enhanced formation of amyloid plaques (5).

precede the vanishing of myelin internodes, especially as non-compacted myelin regions appear to accumulate dense cytoplasm upon ageing (Peters 2009).

Bartzokis' hypothesis was based on the crucial, but not widely known observations by Heiko and Eva Braak that myelination and AD pathology show an inverse relationship: sparsely and in development lately myelinating tracts such as the frontal cortex are susceptible to AD neuropathology while heavily and early myelinating tracts such as the spinal cord remain unaffected until the late stages of the disease (Braak and Braak 1996). While it might seem counterintuitive to attribute a role to myelin in AD considering this description at first, it is important to understand that the late myelinating tracts are the ones that also show the most myelin degeneration upon ageing. Intracortical myelin in the frontal association areas is especially affected. A reason why Bartzokis' hypothesis and Braaks' observation has not become particularly popular among AD researchers, is the apparent spatial paradox of myelin in the white matter and amyloid deposition in cortex/hippocampus i.e. grey matter. In my judgement, this is to trace back to a general misconception about the extent of intracortical myelination and myelin being considered limited to white matter. In this regard, the work presented in this thesis helps reconcile this alleged spatial paradox clearly showing that myelin defects can drive amyloid deposition in the cortex.

4.2 Vulnerability of cortical oligodendrocytes

Why exactly heterogeneity exists in regards to vulnerability of myelin during ageing remains incompletely understood. A conceivable reason for this may lie directly in the heterogeneity of oligodendrocytes themselves. Recent single cell sequencing studies have shed light on the heterogeneity of oligodendrocytes (Marques et al. 2016) identifying 6 different mature oligodendrocyte clusters. Intriguingly, different oligodendrocyte subpopulation become enriched in different brain regions equipping them with a unique composition of myelinating oligodendrocytes (Marques et al. 2016). Of note, even inside the cortex there seems to be regional heterogeneity in terms of age-related myelin decline as motor and sensor areas are more resistant to myelin decline than frontal association areas. This indicates the existence of intracortical variability in oligodendrocyte that is yet to be determined. In humans, this heterogeneity in cortical oligodendrocytes is likely to be further increased due to cortical expansion. Transcriptional heterogeneity is possibly linked to a different molecular makeup of myelin structure or differences in other functions of oligodendrocytes such as trophic support. A well-known difference in CNS-region specific oligodendrocyte population is the length of myelin internodes. An elegant study using *in vitro* microfibres demonstrated that myelin sheet length is an intrinsic region-dependent property of oligodendrocytes with cortical oligodendrocytes producing smaller, but more sheaths than spinal oligodendrocytes (Bechler and Byrne 2015). With this cytoarchitecture, even when producing the same amount of total myelin, cortical oligodendrocytes display a larger fraction of non-compacted myelin areas (especially paranodal loops) than their spinal cord counterparts. It is tempting to speculate that the increased amount of myelinic channels and paranodal structures to maintain would put cortical oligodendrocytes at risk during ageing.

Another unique feature of cortical oligodendrocytes might be their dynamic nature. In the white matter myelination might be considered nearly "saturated" with axons receiving complete myelination. In the cortex, however, only stretches of axons become myelinated (Tomassy et al. 2014; Micheva et al. 2016) leaving room for adaptive myelination (Xin and Chan 2020). Experiences and learning have been shown to drive adaptive myelination on several levels including new differentiation of oligodendrocytes, the generation of new sheets from pre-existing oligodendrocytes and the remodelling of the sheet structure (Bacmeister et al. 2020). Axonal targets of myelination also differ: In the cortex a surprisingly large fraction of myelin sheets is found around local inhibitory axons (half of myelin sheets in layer2/3) (Micheva et al. 2016; Stedehouder et al. 2017). Local ensheathment of inhibitory axons presents an economical way to fine-tune the output of an entire local network. Moreover, energy demands of inhibitory neurons are exceptionally high due to their fast-spiking rate and rather than enabling faster conduction, oligodendrocytes could assist in energy supply. Inhibitory neuron myelin also shows structural specialisation such as larger amount of MBP and CNP (Micheva et al.

2018). While incompletely understood, all of these specialisations could render intracortical myelin especially vulnerable to ageing.

4.3 Oligodendrocyte dysfunction: upstream or downstream of amyloid?

The findings presented here position oligodendrocyte dysfunction upstream of amyloid deposition in AD. In principle, novel aspects can be integrated into the amyloid hypothesis upstream and downstream of amyloid pathology. I would argue, however, that such a linear cascade model is an oversimplification and underestimates the complex cellular interplay in the AD brain. For example, microglia responses have been shown to be regulated by amyloid deposition (e.g., induction of DAM response) and modulate amyloid plaque deposition. Originally studied from a neurocentric perspective, these glial responses are now well recognised players in AD etiology. It is interesting to note that in comparison to microglia and astrocytes oligodendrocytes have received considerably less attention in the AD research field. The role of oligodendrocytes in AD, however, might be just as multi-facetted - with upstream and downstream elements that in the end drive a vicious cycle of AD pathology.

While the study presented in this thesis is the first to show the effects of dysfunctional oligodendrocytes on amyloid deposition, a few studies have investigated oligodendrocyte responses downstream of amyloid deposition in both human AD and amyloid. The most obvious myelin phenotype around amyloid plaques is a focal demyelination that is well described in AD mouse models using myelin immunostaining and microscopy (C Schmued et al. 2013; Behrendt et al. 2013; Mitew et al. 2010). In myelin stainings, amyloid plaques are recognizable as apparent holes and myelin fibres usually do not pass through compacted plaques. In human AD, this phenotype is less well described. In my opinion, however, it remains to be determined if this is the consequence of real demyelination or if it is rather a consequence of myelin fibres being pushed aside by growing plaques. The very steep gradient in the density of myelin fibres from almost zero in the plaque core to normal density in the plaque periphery argues for the latter. *In vivo* live imaging tracing that could distinguish acute demyelination from displacement are unfortunately lacking to the best of my knowledge. However, there seems to be a proliferation of OPC throughout the cortex and white matter of AD mice indicative of remyelination (Schmued et al. 2013; Behrendt et al. 2013). Intriguingly, this does not occur in human AD patients (Behrendt et al. 2013). Using spatial transcriptomics, the DeStrooper lab recently identified the downregulation of an oligodendrocyte cluster in the vicinity of plaques which likely reflects the overall loss of oligodendrocyte lineage cells/myelin in the very late-stages of the APP^{NLGF} mouse model and human AD (Chen, Lu, et al. 2020). Another line of research suggests that OPCs become senescent around amyloid plaques in AD patients and mouse models which contributes to neuroinflammation (Zhang et al. 2019).

Importantly, myelin abnormalities in AD mouse models seem to be not restricted to amyloid plaques. Multiple labs using electron microscopy reported pathological alterations of myelin sheets in a more global manner and not limited to plaque proximity (Chen et al. 2021; Zhang et al. 2020; Desai et al. 2009; Behrendt et al. 2013). This was recently confirmed by usage of an elegant reporter line for newly generated myelin sheaths (NG2-CreERT2;stop-flox mtau-GFP) which showed induction of newly formed myelin sheath in APP/PS1 mice (Chen et al. 2021). This was insufficient, however, to rescue ongoing overall demyelination as evidenced by the decline in total myelinated profiles in the cortex (Chen et al. 2021). I would like to raise an important caveat regarding the reports of de/remyelination in AD mouse models: These effects were reported in mouse models overexpressing APP and PSEN1 (5xFAD, 3xTg, APP/PS1). It is important to exclude that demyelination is a consequence of massive overexpression of these genes and associated pathology. The lab of Peter Stys has recently reported the massive deposition of amyloid into threads underneath the myelin sheath, presumably in the periaxonal space, in 5xFAD mice (Chu et al. 2017). This kind of amyloid deposition even precedes deposition into plaques. Such myelinic amyloid aggregates are not found in APP^{NLGF} mice or AD patients (Depp, Sasmita and Nave, unpublished). It is likely that such amyloid aggregates disrupt myelin-axon-signalling and contribute to myelin degeneration in AD mouse. It is, thus, crucial in my opinion to investigate APP^{NLGF} in regards to myelin pathology to rule-out that myelin defects are only due to

overexpression artefacts. This is all the more important considering that three studies report that behavioural deficits in 5xFAD and APP/PS1 mice are fully abolished upon rescue of myelin pathology. In 5xFAD this was accomplished by reducing mitochondrial fission in oligodendrocytes by Drp1 heterozygosity (Zhang et al. 2020) or an anti-Lingo1 immunotherapy (Wu et al. 2018) and in APP/PS1 mice by targeting muscarinic receptors (Chen et al. 2021). This is very surprising considering that these studies do not report an effect on plaque deposition which indicates that myelin defects alone drive all the behavioural deficits in AD mouse models. This would have far-reaching consequences for the interpretation of the role of amyloid pathology in cognitive dysfunction in AD mouse models. Directly related to this, is the question what direct effect amyloid has on the oligodendrocyte lineage cells (independent of amyloid plaques). Consistent with demyelination around plaques, Aβ oligomers have been shown to inhibit myelin sheet formation *in vitro* (Horiuchi et al. 2012) and Aβ was cytotoxic to oligodendrocytes (Xu et al. 2001; Roth et al. 2005; Lee et al. 2004). In a later study, however, Aβ oligomers reportedly promoted oligodendrocyte differentiation and enhanced remyelination in *ex vivo* slice cultures (Quintela-López et al. 2019). Clearly, more careful work has to be carried out to determine the direct effect of amyloid on oligodendrocytes (controlling both for specific peptide forms and oligomerisation stages).

Recently, several single cell RNA-sequencing studies of the AD brain have sparked interest in the role of oligodendrocytes with myelination related genes being among the top altered clusters in AD patients (Mathys et al. 2019; Grubman et al. 2019; Lau et al. 2020; Zhou et al. 2020). Mathys et al. described upregulation of Lingo-1 in both neurons and oligodendrocytes which was consistently replicated in subsequent studies (Grubman et al. 2019; Lau et al. 2020). As Lingo-1 exerts a negative effect on myelination through homophilic *trans* interactions (Mi et al. 2005; Jepson et al. 2012) this would implicate blockage of myelination in AD patients. The study by Zhou et al. identified a mouse-specific disease-enriched oligodendrocyte cluster high in *Serpina3n* and *C4b* – a cluster that was also identified in snRNA-seq studies of EAE (Falcão et al. 2018). As they employ tissue of pronounced and definite AD pathology these studies are likely to report downstream effects of Aβ and tau pathology on oligodendrocytes at late disease stages. While they consistently describe marked changes to the oligodendrocytes signature, they so far offer very little mechanistic insight and reported gene expression changes have to be further corroborated in regards to their biological meaning in the upcoming years.

These microscopic and transcriptional evidences of myelin alterations in AD are supported by an ever-growing number of macroscopic imaging studies that report myelin dysfunction in AD patients. Most of these brain imaging studies investigated myelin structures by DTI and other MRI modi in cohorts of AD patients and therefore studied rather late disease stages (Bergamino, Walsh, and Stokes 2021; Palesi et al. 2018; Mayo et al. 2017; Benitez et al. 2014; Gao et al. 2011; Stricker et al. 2009a). These studies consistently show that the ageing-associated myelin deterioration is further exacerbated during AD. In mild cognitive impairment considered the prodromal phase of AD a multitude of studies describe deteriorated white matter as assessed by MRI (Wen et al. 2019; Cho et al. 2008; Fellgiebel et al. 2004; Kantarci et al. 2001; Maier-Hein et al. 2015; Benitez et al. 2014; Fischer et al. 2015). While considered an early stage in AD development, amyloid pathology is already found in a large fraction of cases of MCI as detected by biomarker changes or amyloid PET imaging (Fleisher et al. 2011; Hansson et al. 2007). A few very interesting studies focused on the analysis of white matter alterations in the definite preclinical phase in cohorts at risk for sporadic AD (Dean et al. 2017; Bendlin et al. 2012; Bendlin et al. 2010). In middle-aged, healthy individuals with an AD family history and/or ApoE4 genotype fractional anisotropy was decreased when compared to controls without increased risk for AD (Bendlin et al. 2010; Gold et al. 2010). Likewise, in such individuals AD-related changes in CSF biomarkers ($A\beta_{42}$, phospho-Tau/$A\beta_{42}$) were correlated with altered diffusion behaviour in predominantly late-myelinating tracts (Bendlin et al. 2012; Hoy et al. 2017; Gold et al. 2014; Dean et al. 2017). Such a correlation was also found in the fornix system in a cohort of cognitive healthy middle-agers without increased AD risk (Gold et al. 2014). Intriguingly, even in familial AD mutation carriers in which disease onset can be confidently predicted and with this the preclinical phase defined, myelin deterioration is detected prior to disease (Ringman et al. 2007). A later study confirmed this observation mapping white matter alteration to occur up to a decade before symptoms onset which was again correlated with changes in CSF

AD biomarkers (including sTrem2 for microglial activation) (Araque Caballero et al. 2018). While it is extremely challenging to (temporally) dissect cause and consequence of amyloid accumulation and myelin alterations in humans, the cited studies definitely argue that myelin damage does not only occur in advanced AD but that it is an early feature in disease progression.

To summarise, our study reporting that myelin defects can be a direct driver of amyloid pathology together with the multitude of evidences showing pathological alterations of myelin by amyloid establishes a vicious cycle in which the two pathologies would further enhance each other. Taken together, this makes the strong point of myelin dysfunction being an overall risk factor for amyloid deposition and a risk-altering comorbidity with both upstream (this study) and downstream elements (cited studies).

4.4 Mechanism: microglia distraction or APP metabolism changes?

In this study, I identified two possible mechanisms by which myelin dysfunction could drive enhanced amyloid deposition: First, changes in APP metabolism were observed that are consistent with elevated amyloid production and likely related to axonal swellings. Second, microglia became distracted by engagement with myelin and with this unresponsive to amyloid plaques. The work presented in this thesis does not allow to untie these mechanisms and determine to which extent they contribute to the observed effects on plaque load. In theory, this would require mouse mutants in which myelin dysfunction is fully uncoupled from microgliosis. In practice, such mouse models are hard to come by and myelin dysfunction is almost inevitably linked with gliotic reactions. Indeed, gliosis is present throughout the severity spectrum of myelin defects from fulminant demyelinating models to milder genetic myelin dysfunction models such as the PLP null mouse. This view is also supported by a previous collaborative study from the Ehrenreich and Nave labs demonstrating that microglia depletion by a CSF1 receptor antagonist alleviates CNP null associated catatonic signs as well as T-cell infiltration and most prominently APP spheroids (Janova et al. 2018). A 2-month period of microglia depletion at 6-month of age in CNP deficient animals reduced APP spheroids in the white matter by a striking 75%. This is remarkable as this indicates that APP swellings are not a direct consequence of deficits in trophic support function (which would remain untouched by microglia depletion) but involves a microglial element. This microglial element could be oxidative damage to oligodendrocytes from activated microglia. Indeed, it was shown that axonal swellings can be induced by hydrogen peroxide treatment and EAE-associated axonal swellings are resolved by antioxidant therapy (Nikić et al. 2011). This highlights that microglia could be also causally involved in APP metabolism changes observed in $CNP^{-/-}$ 5xFAD mice. It further complicates dissociation of microglia mediated effects from APP metabolism effects and potentially speaks for a prevailing role of microglia responses in mediated effects on plaque load.

To understand the downstream effects of microglia activation, it would be informative to perform anti-inflammatory treatment (e.g. minocycline (Kobayashi et al. 2013)) in $CNP^{-/-}$ 5xFAD to convert activated microglia back to a non-activated state and probe the effect on amyloid deposition. In a similar manner, microglia depletion experiments could be performed. Both of these experiments would probe if a plaque-promoting effect is independent of a microglial response. A caveat is that modification of the microglial behaviour in 5xFAD control mice could alter plaque deposition per se making interpretation of the experimental outcome difficult. For example, microglia depletion by PLX5622 in young pre-plaque 6-week-old - but not older - 5xFAD mice was shown to fully prevent plaque formation (Spangenberg et al. 2019). Therefore, such experiments have to be carefully designed in regards to the timing and duration of microglia depletion to not massively impair plaque seeding in control animals. Considering the development of the plaque-promoting phenotype between 3 and 6-months in $CNP^{-/-}$ 5xFAD mice, starting PLX5622 or minocycline treatment at 4-months for 2-months could represent an adequate paradigm without full inhibition of plaque formation in control animals. To specifically probe if the microglia distraction phenotype is the prevailing mechanism in $CNP^{-/-}$ 5xFAD, Aβ immunotherapy which increases microglia plaque engagement could be performed. This would represent a way to re-entice myelin-preoccupied microglia to interacts with amyloid plaques.

At this point I would like to revisit the initial hypothesis that it is rather the breakdown of trophic support than of compact myelin that drives enhanced amyloid processing. The test of this hypothesis requires analysis of mouse mutants that solely show decreased metabolic support functions. The oligodendroglial specific NMDA receptor knockout mouse was shown to present with deficits in adaptation of support functions (Saab et al. 2016). These animals, however, do not show signs of elevated gliosis or APP swellings until late age (18 months) (Saab et al. 2016). Crossbreedings of this mutant with 5xFAD mice did not lead to elevated amyloid plaque deposition (Depp, Sasmita, Nave; unpublished). This illustrates that milder forms of metabolic support defects (i.e. adaptation) are not sufficient to trigger changes in plaque load and hints at microglial reactions and/or APP swellings being crucially involved in exacerbation of plaque load. It remains to be determined if harsher metabolic support disruptions in the absence of microgliosis could trigger differences in amyloid load. Examining the effect of genetic inactivation of transporters directly shuttling metabolites from oligodendrocytes to axons could be a promising strategy. Recently, the Rothstein lab studied the effects of oligodendroglial specific MCT1 deletion in $MCT1^{fl/fl}$ mice (Philips et al. 2021). Surprisingly, optic nerves showed no deficits during high frequency stimulation and - very similar to NR1 mutant animals - only ageing-associated myelin alterations and axonal phenotypes that were again linked to gliosis (Philips et al. 2021). It would be interesting to compare the effects of this genetic modification with the negative findings in cNR1-KO/5xFAD mutant animals. Alternatively, interference with oligodendroglial lactate metabolism, exosome secretion or antioxidants defense (given such mutants do not display gross gliosis) could shed light on the specific role of metabolic support decline in governing promotion of amyloidosis during myelin dysfunction.

4.5 Does extensive myelination render humans vulnerable to AD?

It is not well understood why humans become vulnerable to developing AD upon ageing. Unique structural features of the human (or mammal) brain could be crucially involved here. In mammal evolution, the cerebral cortex has expanded massively over other brain areas. To accommodate an even larger number and volume of layered neurons in a confined space like the skull, cortical folding occurs in gyrencephalic species. Degree of folding is especially high for larger animals such as whales and elephants (Mota and Herculano-Houzel 2015) and white matter volume expands to a greater extent than grey matter volume with brain size (Zhang and Sejnowski 2000). As mentioned earlier, humans have acquired a large amount of subcortical white matter (and with that myelin) even when compared to other primates. This might be true for intracortical myelin as well though quantitative primary data on this controlling for axonal density is lacking – to the best of my knowledge. Might these features render the brains of certain mammalian species and especially us humans vulnerable to AD?

Such questions are inherently difficult to study. In a proof of principle experiment, I asked if the amount of intra- and subcortical myelin would modify amyloid deposition in mice. The results using forebrain-specific *shiverer* crossed to 5xFAD mice showed a promising initial amelioration of plaque deposition. This is intriguing given that the 5xFAD model is a very aggressive model of plaque deposition. However, further work is needed for fully understanding this phenomenon, especially in regards to oligodendroglial metabolic support, APP metabolism and glial responses to plaques. As oligodendrocytes still associate with axons in forebrain *shiverer* mice, metabolic support processes are generally believed to remain intact and no axonal degeneration can be observed. To a certain extent, access of axons to metabolites could be enhanced in *shiverer* since large proportions of the axon remain unmyelinated. Likewise, flow of metabolites from oligodendrocyte to axons could be improved as virtually all myelin that is formed is non-compacted. On the other side, metabolic needs of axons are likely heightened due to the lack of saltatory conduction. It remains to be determined which effect prevails in *shiverer* axons. In this context, it would be interesting to evaluate if enhanced metabolic support from oligodendrocytes to axons renders them more resistant to amyloid production (for example by faster axonal transport and efficient lysosomal degradation). To distinguish the role of better access to extracellular metabolites from the role of direct support by oligodendrocytes in reducing amyloid deposition, evaluation of amyloid pathology in a mouse model that fully lacks oligodendrocytes would be beneficial. Such an animal model that is long-lived due to restriction of

oligodendrocyte absence to certain brain regions has become recently available in our lab (Subramanian, Nave, unpublished). In an orthogonal approach, one could study the effect of heightened amount of healthy myelin in mouse models of hypermyelination in which the number of myelinated axons is increased.

An alternative explanation of decreased amyloid deposition in forebrain *shiverer* AD mice concerns effects on microglial cells. I have shown here that myelin dysfunction distracts microglia from engaging with amyloid plaques. In a *shiverer* scenario, though myelin does not assemble and only non-compacted *shiverer* membranes are found, microglia do not become activated. We recently confirmed this using snRNA-seq of forebrain *shiverer* mice (Sun, Depp, Nave, unpublished): Here we saw that although microglia were actively engulfing more myelin (as reported by heightened amount of myelin processing microglia) these microglia never converted to DAM. Indeed, even the small proportion of DAM occasionally found in wildtype animals, was lost. Of note, the myelin-associated microglia fraction makes up a significant amount of microglia (10% in normal wildtype animals) illustrating that indeed a larger pool of microglia is constantly surveilling myelin. These observations give rise to an interesting possible mechanism of action for decreased plaque deposition in myelin-deficient 5xFAD: With the loss of myelin the burden of clearance of "hard-to-digest" compact myelin is alleviated from microglia rendering them more capable of associating with plaques and phagocytosing amyloid. This hypothesis can be tested by investigating microglia/plaque corralling phenotypes in *shiverer*/5xFAD mice.

4.6 AD: a human-specific disease?

Clearly, young adults (<40 years old) with the most amount of myelin throughout the age-trajectory in humans, are not susceptible to AD - which is even true for the most aggressive familial forms. This illustrates that myelin *per se* is not a risk factor for AD. Rather the age-associated perturbations would render myelin a risk factor. In this scenario, two circumstances would predispose humans to AD: Having large amounts of myelin/white matter in conjunction with the unusual long lifespan of humans in which myelin massively deteriorates. If this holds true, AD should actually not be confined to humans but could be present in every species that is equipped with myelin and over-ages. In nature, animals rarely reach their organismal maximum lifespan and the "natural" akin observed lifespan in the wild is largely dependent on external factors (resources, hunting success, fighting, predation). We humans, however, live more than twice as long as our estimated "natural" lifespan (at around 40 years) in large part due to massive lifestyle changes during human history and development of current medical practices. To a certain degree, this is also true for our pets and other animals held in captivity that receive sufficient veterinarian care and feeding. Especially, dogs and cats as our closest companion animals exceed their natural lifespans to a similar extent to humans (6-8 average years for a wolfs versus 12-13 years for an average-sized dog; 10-12 years for wild forest cats versus up to 20+ years in domestic cats). Indeed, age-dependent amyloid deposition frequently occurs in the brains of dogs and cats where they elicit behavioural deficits very similar to AD symptomatology (canine/feline cognitive dysfunction syndrome) (Prpar Mihevc and Majdič 2019; Sordo and Gunn-Moore 2021). Though tau tangles are missing in dogs but have been reported in cats, this disease could be considered the pet equivalent to AD. It is interesting that in dogs where apparently no neurofibrillary tangles are found behavioural deficits akin to AD are described which hints towards amyloid pathology being sufficient to elicit AD-like symptoms.

Amyloid pathology has not only been described in cats and dogs, but in an astonishingly large number of old captive mammals including apes, monkeys, bears and see lions (Youssef et al. 2016; Gołaszewska et al. 2019; Takaichi et al. 2021). An intriguing study reported amyloid deposition in Gorillas even in the wild (Perez et al. 2016) and amyloid deposition in stranded dolphins (Davis et al. 2019). Less convincing - in my opinion - are reports on amyloid plaques in horses and cows as the reported amyloid to not resemble classical amyloid plaques (Vallino Costassa et al. 2016; Capucchio et al. 2010). A species' likelihood of developing amyloid plaques upon ageing is also likely related to the primary sequence of APP and amyloid. While rodents like mice and rats have not been found to develop amyloid plaques, they have been identified in the degu, a long-lived rodent species from Chile whose Aβ sequence is more similar to humans (Cisternas et al. 2018) though another study could not replicate these findings (Steffen et al. 2016). To what extent, the three amino acids

substitutions in mouse/rat Aβ renders rodents more resistant to age dependent brain amyloidosis is still a matter of debate: Overexpression of the wildtype mouse form (Jankowsky et al. 2007) as well as overexpression of the human form (Simón et al. 2009; Kreis et al. 2021; Mucke et al. 2000) or endogenous expression of the human form (Baglietto-Vargas et al. 2021) does not lead to amyloid plaque formation in 2-year-old mice. *In vitro* mouse Aβ aggregates into fibrils to a similar extent as human Aβ but shows resistance to zinc mediated aggregation (Bush et al. 1994; Fung et al. 2004).

This body of literature makes clear that the species vulnerability to amyloid deposition is dependent on several factors: It may include differences in the primary sequence, but the most important factor is lifespan. More specifically it is the exceeding of the natural occurring lifespan rather than absolute age that predisposes to AD as illustrated by the presence of amyloid plaques in dogs at only 10 years of age. Brain amyloidosis is, therefore, tightly linked to the species-specific aging-rate – and its molecular underpinnings from different metabolism rates to cellular clocks and DNA repair. Studying these ageing mechanisms and how different species evolved to escape them (like the bowhead whale (Keane et al. 2015)), could be crucial in also understanding how ageing renders the brain susceptible to amyloid deposition. As the extension of lifespan in late life is, however, largely an extension of post-reproductive periods, in general evolutionary pressure on "healthy ageing" and AD prevention might be low. This might only be different in animal societal structures that are highly matriarchal with the lead animal typically being a (great) grandmother. In such society structures, survival of the entire herd is critically dependent on intact memory in the lead animal that directs the herd to important food/water sources. Elephant herds and killer whale pods are examples for such societies, and it would be interesting to study these species in regards to amyloid deposition.

To summarise, considering the well described AD-like syndrome of dogs and cats manifesting with amyloid plaques and even tangles, AD in my eyes can hardly be considered a human-specific disease. I would argue that AD to a large extent is a natural bystander of ageing: in humans we see the full-blown/burned-out late stage of this to a quality and quantity not observed in other species due to our extremely pushed lifespan and its consequences on brain physiology – and maybe myelin. Nevertheless, comparative analyses of brain amyloid deposition in aged animals throughout the vertebrate kingdom could shed light on further mechanisms governing amyloid deposition.

4.7 Translational relevance and therapeutic implications

The findings and conclusions presented in this thesis are mainly based on work with mouse models of AD and myelin dysfunction. Though the finding of advanced myelin deterioration in a small cohort of AD patients is encouraging, translational relevance has to be further corroborated. First, it would be beneficial to replicate this finding in a much larger and more stratified cohort of AD patients (sex, age, ApoE genotype, educational level). It is also important to rule out that demyelination occurs as a consequence of axonal decay observed in AD by simultaneous assessment of axonal and myelin integrity. Here, it would be additionally beneficial to investigate early disease timepoints (amyloid Thal staging 1) in which only marginal amyloid plaque deposition is seen in the neocortex. In such a patient cohort, it would be interesting to determine if local hotspots of intracortical myelin degeneration correlate with the amount of deposited amyloid. To strengthen the role of myelin deterioration as an initiating factor, it could represent a superior approach to not limit analysis to diagnosed AD patients but to assess a larger cohort of elderly without AD or even MCI diagnosis and screen for the presence of amyloid plaques. With this approach, it would be possible to catch earlier timepoints of age-related amyloid deposition. While this requires without doubt enormous efforts in the recruitment of criteria-matching donors and in the tissue evaluation post-mortem, feasibility of this is demonstrated by studies showing that in a larger proportion of cognitively normal ageing cohorts amyloid plaques can be found (Davis et al. 1999; Bennett et al. 2006).

Microscopic post-mortem analysis is the most sensitive way to probe for the presence of amyloid plaques and its relation to myelin status. It, however, lacks longitudinal information regarding disease progression and is usually confined to smaller sampling areas. Additionally, availability of tissue samples of "completely healthy"

middle-aged donors is limited given their early death and hospitalisation. The simultaneous use of DTI measurements to assess myelin structure and amyloid PET tracing to probe amyloid/myelin correlations as performed for example by Racine and colleagues (Racine et al. 2014) offers a longitudinal momentum and the possibility of brain-wide analysis. In my opinion such analyses, however, come with the following caveats: first, the nature of DTI changes is not fully understood and not exclusively driven by deterioration of myelin. Second, amyloid PET tracers though solid predictors of post-mortem amyloid load for moderate and severe pathology do not have the same predictive power at initial stages of amyloidosis (Ikonomovic et al. 2016). This is tightly linked to the limited resolution of PET imaging. Third, usually analysis is restricted to proper white matter and does not assess intracortical myelin health. Reliable mapping of intracortical myeloarchitecture has been, however, recently demonstrated by application of magnetisation transfer as MRI imaging contrast (Paquola et al. 2019; Munsch et al. 2021). In combination with amyloid PET, this modality would offer the opportunity to assess correlations between intra- rather than subcortical myelin integrity and amyloid deposition.

In this work microglia distraction was identified as a possible mechanism of action enhancing plaque deposition in AD mouse models. While not specifically investigated in the human AD cohort, intracortical myelin decline in AD patients seemed to be linked to enhanced microglia coverage. It would be interesting to determine if similar to the mouse data microglia recruitment to degenerating myelin removes microglia from amyloid plaques. Here, local analysis of microglia/myelin interaction and microglia plaque coverage in its proximity could be conducted. Hinting towards a possible role of microglia distraction in human AD, human microglia corral to a far lesser extent around amyloid plaques than mouse microglia (own observation). While this is certainly partially governed by species differences (Hasselmann et al. 2019), this could also stem from the fact that in mouse models of AD relatively young and "unburdened" microglia are confronted with plaques while in humans old microglia react to amyloid plaques. Indeed, cell-type specific sequencing of microglia in human AD has revealed fundamental difference between the DAM response characterised in AD mice and the response of human Alzheimer microglia (HAM) (Srinivasan et al. 2020). In this regard, amyloid models on a myelin-dysfunction background could represent a mouse model that is more closely mimicking the human condition. Along this line, work in the Simons lab has shown that even in the relatively short lifespan of the mouse (when compared to humans) microglia are significantly burdened by the clearance of microglia which leads to microglial lipofuscin accumulations (Safaiyan et al. 2016). Very recently, it was shown – reproducing the findings obtained in $CNP^{-/-}$ mice - that microglia specifically in the ageing white matter acquire an activated status very similar to DAM (Safaiyan et al. 2021). Despite a large overlap in the transcriptional profiles, this study was able to differentiate this myelin-driven phenotype named white matter-associated microglia (WAM) from the microglial response elicited by amyloid (DAM). Since determination of subclusters of cell population is variable, this certainly has to be validated by other labs. A potential transcriptionally detectable difference between WAM and DAM could be used to determine if there is an enrichment of myelin-overloaded microglia in human AD. We aimed at determining if heightened myelin-phagocytosis occurs in human AD by analysis of the amount of myelin-processing microglia in human AD snRNA-seq datasets (Mathys et al. 2019; Zhou et al. 2020) but failed to detect differences between AD patients and controls (Depp, Sun, Nave unpublished). However, the relatively small number of microglia recovered from each patient was a potential confounder in the analysis.

A possible translational implication of our findings concerns the correlation/co-existence of Multiple Sclerosis as primary demyelinating disease and Alzheimer's Disease: do our findings implicate that MS patients would inevitably progress into AD and that amyloid pathology should be present in MS patients? The experiments showing enhanced plaque deposition in the perilesion environment in EAE could hint towards this. An excellent review by Luczynski and colleagues highlights the need for an epidemiological study concerning comorbidity of MS and AD given the increased lifespan of MS patients today (Luczynski et al. 2019). The authors identified a couple of case reports describing the co-existence of AD in MS but plaque deposition seemed not to be increased in the lesion environment. Further studies are needed to shed light on the relationship between MS and AD pathology. Of note, MS related myelin breakdown is much more

fulminant in nature than age-related "chronic" myelin breakdown with a much greater involvement of the immune system which could explain differences in the amyloid-promoting effect.

It is tempting to speculate that other comorbidities or other identified risk factors for AD exert their effect via damaging myelin or at least by the same underlying mechanism i.e. microglia distraction. Risk factors for AD include genetic variants such as the ApoE4 allele or the presence of other diseases/medical conditions such as diabetes, heart problems, traumatic brain injury, stroke, infection, high blood pressure, high cholesterol levels and psychologic illnesses. Additionally, "life-style factors" such as dietary choices, exercise, smoking, excessive alcohol consumption and educational level alter AD risk and what can be intuitively categorised as healthy life-style choices, not surprisingly, lowers AD risk collectively by up to 60% (Dhana et al. 2020). Many of these risk factors have also been shown to negatively influence white matter integrity and oligodendrocyte health. High fat diet was shown to detrimentally effect myelin health (Huang et al. 2019) and obesity is linked to decreased fractional anisotropy in DTI (Kullmann et al. 2015). Stroke/ischemia is well known to affect the white matter and oligodendrocytes are specifically vulnerable to ischemic insult (Dewar, Underhill, and Goldberg 2003; McIver et al. 2010). Schizophrenia is associated with altered white matter and myelin gene expression (Hagemeyer et al. 2012; Gouvêa-Junqueira et al. 2020) and a recent study reported an enormous increase in the rate of receiving a dementia diagnosis in old patients with schizophrenia (Stroup et al. 2021). Infection has likewise been linked to AD with herpes simplex virus infected patients displaying a hazard ratio of around 2.5 of developing AD (Tzeng et al. 2018) and herpes viruses being detected more frequently in the brains of AD patients (Readhead et al. 2018). Intriguingly, oligodendrocyte transcripts were also found to be downregulated during influenza-virus infection (Louie et al. 2021). Finally, the ApoE4 allele also significantly impacts white matter health (Heise et al. 2011) with ApoE4 carriers showing a greater rate of myelin decline upon ageing (Bartzokis et al. 2006). Intriguingly, this is even the case for ApoE4 carrying infants that show delayed myelin acquisition (Dean et al. 2014).

Conversely, risk lowering factors such as a healthy diet and sufficient exercise are linked to better white matter health. For example, high adherence to a Mediterranean diet rich in olive oil, legumes, fruits and vegetables and low in animal products and meat is associated with higher white matter integrity during ageing (Rodrigues et al. 2020). Likewise, omega-3 intake is associated with better normal appearing white matter integrity in early MS (Sand et al. 2021). While this has to be further investigated, there might be a positive effect of Mediterranean diet in MS (Langley, Triplet, and Scarisbrick 2020). Running exercise on the other side was shown to prevent white matter decline in aged rats (Chen, Chao, et al. 2020). These observations hint towards preventive measures to slow down myelin ageing and maintenance of myelin health during ageing could be boosted pharmacologically. Work in Jonah Chans lab has identified a class of muscarinic receptor inhibitors that promoted myelin differentiation in different settings with Clemastine being the most effective and biosafe (Mei et al. 2014; Mei et al. 2016; Cree et al. 2018). Recently, it was shown that Clemastine treatment boosted myelin renewal in aged mice and alleviated age-related behavioural deficits in the Morris water maze (Wang, Ren, et al. 2020). In a similar manner, other remyelinating drugs in clinical use or trials for the treatment of MS could be evaluated for their efficiency in reducing age-related myelin decline. Safety profile and efficiency of lower dosing would need to be evaluated here since such a drug would potentially be taken throughout long periods in late life. Recently, it was shown that food supplementation with squalene – an abundant compound in olive oil - was effective in the treatment of demyelination in mice by a mechanism involving both altered microglia reactions and direct promotion of remyelination (Berghoff et al. 2021).

In brain diseases in particular occurred damage cannot be reverted due to the limited regenerative capacities of neurons. It highlights the need for preventive measures over reactionary treatment of a fully developed disease according to the "prevention is better than a cure" principle. Though AD might be the inevitable disease of the hyper-aged human brain, cognitively healthy centenarians make the case for the existence of healthy brain ageing. I envision that a combination of protective life-style adaptations and early drug interventions will pave the way for healthier brain ageing – with a prospective focus on healthier myelin – and with that the prevention of AD.

5 Bibliography

Ahmed, Mahiuddin, Judianne Davis, Darryl Aucoin, Takeshi Sato, Shivani Ahuja, Saburo Aimoto, James I Elliott, William E Van Nostrand, and Steven O Smith. 2010. 'Structural conversion of neurotoxic amyloid-β 1–42 oligomers to fibrils', *Nature structural & molecular biology*, 17: 561-67.

Ainger, Kevin, Daniela Avossa, Frank Morgan, Sandra J Hill, Christopher Barry, Elisa Barbarese, and John H Carson. 1993. 'Transport and localization of exogenous myelin basic protein mRNA microinjected into oligodendrocytes', *The Journal of cell biology*, 123: 431-41.

Akay, Leyla Anne, Audrey H Effenberger, and Li-Huei Tsai. 2021. 'Cell of all trades: oligodendrocyte precursor cells in synaptic, vascular, and immune function', *Genes & Development*, 35: 180-98.

Al-Abdi, Lama, Fathiya Al Murshedi, Alaa Elmanzalawy, Asila Al Habsi, Rana Helaby, Anuradha Ganesh, Niema Ibrahim, Nisha Patel, and Fowzan S Alkuraya. 2020. 'CNP deficiency causes severe hypomyelinating leukodystrophy in humans', *Human genetics*, 139: 615-22.

Alzheimer, Alois. 1907. 'Uber eine eigenartige Erkrankung der Hirnrinde', *Zentralbl. Nervenh. Psych.*, 18: 177-79.

Alzheimer, Alois. 1911. 'Über eigenartige Krankheitsfälle des späteren Alters', *Zeitschrift für die gesamte Neurologie und Psychiatrie*, 4: 356.

Ando, Susumu, Yasukazu Tanaka, Yuriko Toyoda, and Kazuo Kon. 2003. 'Turnover of myelin lipids in aging brain', *Neurochemical research*, 28: 5-13.

Andrew, Robert J, Celia G Fernandez, Molly Stanley, Hong Jiang, Phuong Nguyen, Richard C Rice, Virginie Buggia-Prévot, Pierre De Rossi, Kulandaivelu S Vetrivel, Raza Lamb et al. 2017. 'Lack of BACE1 S-palmitoylation reduces amyloid burden and mitigates memory deficits in transgenic mouse models of Alzheimer's disease', *Proceedings of the National Academy of Sciences*, 114: E9665-E74.

Annaert, Wim, and Bart De Strooper. 1999. 'Presenilins: molecular switches between proteolysis and signal transduction', *Trends in neurosciences*, 22: 439-43.

Araque Caballero, Miguel Ángel, Marc Suárez-Calvet, Marco Duering, Nicolai Franzmeier, Tammie Benzinger, Anne M Fagan, Randall J Bateman, Clifford R Jack, Johannes Levin, Martin Dichgans et al. 2018. 'White matter diffusion alterations precede symptom onset in autosomal dominant Alzheimer's disease', *Brain*, 141: 3065-80.

Averbeck, Bruno B, Peter E Latham, and Alexandre Pouget. 2006. 'Neural correlations, population coding and computation', *Nature Reviews Neuroscience*, 7: 358-66.

Bacmeister, Clara M, Helena J Barr, Crystal R McClain, Michael A Thornton, Dailey Nettles, Cristin G Welle, and Ethan G Hughes. 2020. 'Motor learning promotes remyelination via new and surviving oligodendrocytes', *Nature neuroscience*, 23: 819-31.

Baglietto-Vargas, David, Stefania Forner, Lena Cai, Alessandra C Martini, Laura Trujillo-Estrada, Vivek Swarup, Marie Minh Thu Nguyen, Kelly Do Huynh, Dominic I Javonillo, Kristine Minh Tran et al. 2021. 'Generation of a humanized Aβ expressing mouse demonstrating aspects of Alzheimer's disease-like pathology', *Nature communications* , 12: 1-16.

Bales, Kelly R, Feng Liu, Su Wu, Suizhen Lin, Deanna Koger, Cynthia DeLong, Jeffrey C Hansen, Patrick M Sullivan, and Steven M Paul. 2009. 'Human APOE isoform-dependent effects on brain β-amyloid levels in PDAPP transgenic mice', *Journal of Neuroscience*, 29: 6771-79.

Bales, Kelly R, Tatyana Verina, Richard C Dodel, Yansheng Du, Larry Altstiel, Mark Bender, Paul Hyslop, Edward M Johnstone, Sheila P Little, David J Cummins et al. 1997. 'Lack of apolipoprotein E dramatically reduces amyloid β-peptide deposition', *Nature genetics*, 17: 263-64.

Barres, Ben A. 2008. 'The mystery and magic of glia: a perspective on their roles in health and disease', *Neuron*, 60: 430-40.

Bartzokis, George. 2011. 'Alzheimer's disease as homeostatic responses to age-related myelin breakdown', *Neurobiology of aging*, 32: 1341-71.

Bartzokis, George. 2004. 'Age-related myelin breakdown: a developmental model of cognitive decline and Alzheimer's disease', *J Neurobiology of aging*, 25: 5-18.

Bartzokis, George, Po H Lu, Daniel H Geschwind, Nancy Edwards, Jim Mintz, and Jeffrey L Cummings. 2006. 'Apolipoprotein E genotype and age-related myelin breakdown in healthy individuals: implications for cognitive decline and dementia', *Archives of General Psychiatry*, 63: 63-72.

Bartzokis, George, Po H Lu, Kathleen Tingus, Mario F Mendez, Aurore Richard, Douglas G Peters, Bolanle Oluwadara, Katherine A Barrall, J Paul Finn, Pablo Villablanca et al. 2010. 'Lifespan trajectory of myelin integrity and maximum motor speed', *Neurobiology of aging*, 31: 1554-62.

Bartzokis, George, David Sultzer, Po H Lu, Keith H Nuechterlein, Jim Mintz, and Jeffrey L Cummings. 2004. 'Heterogeneous age-related breakdown of white matter structural integrity: implications for cortical "disconnection" in aging and Alzheimer's disease', *Neurobiology of aging*, 25: 843-51.

Bean, Bruce P. 2007. 'The action potential in mammalian central neurons', *Nature Reviews Neuroscience*, 8: 451-65.

Bechler, Marie E, and Lauren Byrne. 2015. 'CNS myelin sheath lengths are an intrinsic property of oligodendrocytes', *Current Biology*, 25: 2411-16.

Behrendt, Gwendolyn, Kristin Baer, Annalisa Buffo, Maurice A Curtis, Richard L Faull, Mark I Rees, Magdalena Götz, and Leda Dimou. 2013. 'Dynamic changes in myelin aberrations and oligodendrocyte generation in chronic amyloidosis in mice and men', *Glia*, 61: 273-86.

Bendlin, Barbara B, Cynthia M Carlsson, Sterling C Johnson, Henrik Zetterberg, Kaj Blennow, Auriel A Willette, Ozioma C Okonkwo, Aparna Sodhi, Michele L Ries, Alex C Birdsill et al. 2012. 'CSF T-Tau/Aβ42 predicts white matter microstructure in healthy adults at risk for Alzheimer's disease', *PloS one* , 7: e37720.

Bendlin, Barbara B, Michele L Ries, Elisa Canu, Aparna Sodhi, Mariana Lazar, Andrew L Alexander, Cynthia M Carlsson, Mark A Sager, Sanjay Asthana, and Sterling C Johnson. 2010. 'White matter is altered with parental family history of Alzheimer's disease', *Alzheimer's & Dementia*, 6: 394-403.

Benilova, Iryna, Eric Karran, and Bart De Strooper. 2012. 'The toxic Aβ oligomer and Alzheimer's disease: an emperor in need of clothes', *Nature neuroscience*, 15: 349-57.

Benitez, Andreana, Els Fieremans, Jens H Jensen, Maria F Falangola, Ali Tabesh, Steven H Ferris, and Joseph A Helpern. 2014. 'White matter tract integrity metrics reflect the vulnerability of late-myelinating tracts in Alzheimer's disease', *NeuroImage: Clinical*, 4: 64-71.

Bennett, DA, JA Schneider, Z Arvanitakis, JF Kelly, NT Aggarwal, RC Shah, and RS Wilson. 2006. 'Neuropathology of older persons without cognitive impairment from two community-based studies', *Neurology*, 66: 1837-44.

Bera, Sujoy, Santiago Camblor-Perujo, Elena Calleja Barca, Albert Negrete-Hurtado, Julia Racho, Elodie De Bruyckere, Christoph Wittich, Nina Ellrich, Soraia Martins, James Adjaye et al. 2020. 'AP-2 reduces amyloidogenesis by promoting BACE 1 trafficking and degradation in neurons', *EMBO reports*, 21: e47954.

Bergamino, Maurizio, Ryan R Walsh, and Ashley M Stokes. 2021. 'Free-water diffusion tensor imaging improves the accuracy and sensitivity of white matter analysis in Alzheimer's disease', *Scientific reports*, 11: 1-12.

Berghoff, Stefan A, Nina Gerndt, Jan Winchenbach, Sina K Stumpf, Leon Hosang, Francesca Odoardi, Torben Ruhwedel, Carolin Böhler, Benoit Barrette, Ruth Stassart et al. 2017. 'Dietary cholesterol promotes repair of demyelinated lesions in the adult brain', *Nature communications*, 8: 1-15.

Berghoff, Stefan A, Lena Spieth, Ting Sun, Leon Hosang, Lennart Schlaphoff, Constanze Depp, Tim Düking, Jan Winchenbach, Jonathan Neuber, David Ewers et al. 2021. 'Microglia facilitate repair of demyelinated lesions via post-squalene sterol synthesis', *Nature neuroscience*, 24: 47-60.

Bergles, Dwight E, and William D Richardson. 2016. 'Oligodendrocyte development and plasticity', *Cold Spring Harbor perspectives in biology*, 8: a020453.

Bergles, Dwight E, J David B Roberts, Peter Somogyi, and Craig E Jahr. 2000. 'Glutamatergic synapses on oligodendrocyte precursor cells in the hippocampus', *Nature*, 405: 187-91.

Berto, Stefano, Isabel Mendizabal, Noriyoshi Usui, Kazuya Toriumi, Paramita Chatterjee, Connor Douglas, Carol A Tamminga, Todd M Preuss, V Yi Soojin, and Genevieve Konopka. 2019. 'Accelerated evolution of oligodendrocytes in the human brain', *Proceedings of the National Academy of Sciences*, 116: 24334-42.

Bertram, Lars, Matthew B McQueen, Kristina Mullin, Deborah Blacker, and Rudolph E Tanzi. 2007. 'Systematic meta-analyses of Alzheimer disease genetic association studies: the AlzGene database', *Nature genetics*, 39: 17-23.

Bhalla, Akhil, Christopher P Vetanovetz, Etienne Morel, Zeina Chamoun, Gilbert Di Paolo, and Scott A Small. 2012. 'The location and trafficking routes of the neuronal retromer and its role in amyloid precursor protein transport', *Neurobiology of disease*, 47: 126-34.

Blasko, I, R Veerhuis, M Stampfer-Kountchev, M Saurwein-Teissl, P Eikelenboom, and B Grubeck-Loebenstein. 2000. 'Costimulatory effects of interferon-γ and interleukin-1β or tumor necrosis factor α on the synthesis of Aβ1-40 and Aβ1-42 by human astrocytes', *Neurobiology of Disease*, 7: 682-89.

Blocq, Paul, and Gheorghe Marinescu. 1892. *Sur les lésions et la pathogénie de l'épilepsie dite essentielle*.

Boggs, JM. 2006. 'Myelin basic protein: a multifunctional protein', *Cellular and Molecular Life Sciences CMLS*, 63: 1945-61.

Boison, Detlev, and Wilhelm Stoffel. 1989. 'Myelin-deficient rat: a point mutation in exon III (A----C, Thr75----Pro) of the myelin proteolipid protein causes dysmyelination and oligodendrocyte death', *The EMBO journal*, 8: 3295-302.

Bolduc, David M, Daniel R Montagna, Yongli Gu, Dennis J Selkoe, and Michael S Wolfe. 2016. 'Nicastrin functions to sterically hinder γ-secretase–substrate interactions driven by substrate transmembrane domain', *Proceedings of the National Academy of Sciences*, 113: E509-E18.

Bolmont, Tristan, Florent Haiss, Daniel Eicke, Rebecca Radde, Chester A Mathis, William E Klunk, Shinichi Kohsaka, Mathias Jucker, and Michael E Calhoun. 2008. 'Dynamics of the microglial/amyloid interaction indicate a role in plaque maintenance', *Journal of Neuroscience*, 28: 4283-92.

Boullerne, Anne Isabelle. 2016. 'The history of myelin', *Experimental neurology*, 283: 431-45.

Braak, Heiko, and Eva Braak. 1991. 'Neuropathological stageing of Alzheimer-related changes', *Acta neuropathologica*, 82: 239-59.

Braak, Heiko, and Eva Braak. 1996. 'Development of Alzheimer-related neurofibrillary changes in the neocortex inversely recapitulates cortical myelogenesis', *Acta neuropathologica*, 92: 197-201.

Braun, PE, DWWS De Angelis, WW Shtybel, and L Bernier. 1991. 'Isoprenoid modification permits 2′, 3′-cyclic nucleotide 3′-phosphodiesterase to bind to membranes', *Journal of neuroscience research*, 30: 540-44.

Brickman, Adam M, Irene B Meier, Mayuresh S Korgaonkar, Frank A Provenzano, Stuart M Grieve, Karen L Siedlecki, Ben T Wasserman, Leanne M Williams, and Molly E Zimmerman. 2012. 'Testing the white matter retrogenesis hypothesis of cognitive aging', *Neurobiology of aging*, 33: 1699-715.

Buggia-Prévot, Virginie, Celia G Fernandez, Vinod Udayar, Kulandaivelu S Vetrivel, Aureliane Elie, Jelita Roseman, Verena A Sasse, Margaret Lefkow, Xavier Meckler, Sohinee Bhattacharyya et al. 2013. 'A function for EHD family proteins in unidirectional retrograde dendritic transport of BACE1 and Alzheimer's disease Aβ production', *Cell reports*, 5: 1552-63.

Bunge, Mary Bartlett, Richard P Bunge, and Hans Ris. 1961. 'Ultrastructural study of remyelination in an experimental lesion in adult cat spinal cord', *The Journal of cell biology*, 10: 67-94.

Burgold, Steffen, Tobias Bittner, Mario M Dorostkar, Daniel Kieser, Martin Fuhrmann, Gerda Mitteregger, Hans Kretzschmar, Boris Schmidt, and Jochen Herms. 2011. 'In vivo multiphoton imaging reveals gradual growth of newborn amyloid plaques over weeks', *Acta neuropathologica*, 121: 327-35.

Burgold, Steffen, Severin Filser, Mario M Dorostkar, Boris Schmidt, and Jochen Herms. 2014. 'In vivo imaging reveals sigmoidal growth kinetic of β-amyloid plaques', *Acta neuropathologica communications*, 2: 1-11.

Bush, Ashley I, Warren H Pettingell, GDPM Multhaup, Marc d Paradis, Jean-Paul Vonsattel, James F Gusella, Konrad Beyreuther, Colin L Masters, and Rudolph E Tanzi. 1994. 'Rapid induction of Alzheimer A beta amyloid formation by zinc', *Science*, 265: 1464-67.

Butovsky, Oleg, and Howard L Weiner. 2018. 'Microglial signatures and their role in health and disease', *Nature Reviews Neuroscience*, 19: 622-35.

Buxbaum, Joseph D, Kang-Nian Liu, Yuxia Luo, Jennifer L Slack, Kim L Stocking, Jacques J Peschon, Richard S Johnson, Beverly J Castner, Douglas Pat Cerretti, and Roy A Black. 1998. 'Evidence that tumor necrosis factor α converting enzyme is involved in regulated α-secretase cleavage of the Alzheimer amyloid protein precursor', *Journal of Biological Chemistry*, 273: 27765-67.

C Schmued, Larry, James Raymick, Merle G Paule, Melanie Dumas, and Sumit Sarkar. 2013. 'Characterization of myelin pathology in the hippocampal complex of a transgenic mouse model of Alzheimer's disease', *Current Alzheimer Research*, 10: 30-37.

Cai, Huaibin, Yanshu Wang, Diane McCarthy, Hongjin Wen, David R Borchelt, Donald L Price, and Philip C Wong. 2001. 'BACE1 is the major β-secretase for generation of Aβ peptides by neurons', *Nature neuroscience*, 4: 233-34.

Capucchio, Maria Teresa, M Márquez, Paola Pregel, L Foradada, M Bravo, Grazia Mattutino, Carlo Torre, Davide Schiffer, Deborah Catalano, Federico Valenza et al. 2010. 'Parenchymal and vascular lesions in ageing equine brains: histological and immunohistochemical studies', *Journal of comparative pathology*, 142: 61-73.

Casali, Brad T, Kathryn P MacPherson, Erin G Reed-Geaghan, and Gary E Landreth. 2020. 'Microglia depletion rapidly and reversibly alters amyloid pathology by modification of plaque compaction and morphologies', *Neurobiology of Disease*, 142: 104956.

Castellano, Joseph M, Jungsu Kim, Floy R Stewart, Hong Jiang, Ronald B DeMattos, Bruce W Patterson, Anne M Fagan, John C Morris, Kwasi G Mawuenyega, Carlos Cruchaga et al. 2011. 'Human apoE isoforms differentially regulate brain amyloid-β peptide clearance', *Science translational medicine*, 3: 89ra57-89ra57.

Catani, Marco, and Stefano Sandrone. 2015. *Brain renaissance: from Vesalius to modern neuroscience* (Oxford University Press).

Charles, Perrine, Steven Tait, Catherine Faivre-Sarrailh, Gilles Barbin, Frank Gunn-Moore, Natalia Denisenko-Nehrbass, Anne-Marie Guennoc, Jean-Antoine Girault, Peter J Brophy, and Catherine

Lubetzki. 2002. 'Neurofascin is a glial receptor for the paranodin/Caspr-contactin axonal complex at the axoglial junction', *Current Biology*, 12: 217-20.

Chartier-Harlin, Marie-Christine, Fiona Crawford, Henry Houlden, Andrew Warren, David Hughes, Liana Fidani, Alison Goate, Martin Rossor, Penelope Roques, John Hardy et al. 1991. 'Early-onset Alzheimer's disease caused by mutations at codon 717 of the β-amyloid precursor protein gene', *Nature* , 353: 844-46.

Chen, Guo-fang, Ting-hai Xu, Yan Yan, Yu-ren Zhou, Yi Jiang, Karsten Melcher, and H Eric Xu. 2017. 'Amyloid beta: structure, biology and structure-based therapeutic development', *Acta Pharmacologica Sinica*, 38: 1205-35.

Chen, Jing-Fei, Kun Liu, Bo Hu, Rong-Rong Li, Wendy Xin, Hao Chen, Fei Wang, Lin Chen, Rui-Xue Li, Shu-Yu Ren et al. 2021. 'Enhancing myelin renewal reverses cognitive dysfunction in a murine model of Alzheimer's disease', *Neuron*.

Chen, Lin, Feng-lei Chao, Wei Lu, Lei Zhang, Chun-xia Huang, Shu Yang, Xuan Qiu, Hao Yang, Yuan-yu Zhao, San-rong Wang et al. 2020. 'Long-term running exercise delays age-related changes in white matter in rats', *Frontiers in aging neuroscience*, 12: 359.

Chen, Wei-Ting, Ashley Lu, Katleen Craessaerts, Benjamin Pavie, Carlo Sala Frigerio, Nikky Corthout, Xiaoyan Qian, Jana Laláková, Malte Kühnemund, Iryna Voytyuk et al. 2020. 'Spatial transcriptomics and in situ sequencing to study Alzheimer's disease', *Cell*, 182: 976-91. e19.

Cherny, Robert A, Craig S Atwood, Michel E Xilinas, Danielle N Gray, Walton D Jones, Catriona A McLean, Kevin J Barnham, Irene Volitakis, Fiona W Fraser, Young-Seon Kim et al. 2001. 'Treatment with a copper-zinc chelator markedly and rapidly inhibits β-amyloid accumulation in Alzheimer's disease transgenic mice', *Neuron*, 30: 665-76.

Chia, LS, JE Thompson, and MA Moscarello. 1983. 'Changes in lipid phase behaviour in human myelin during maturation and aging: involvement of lipid peroxidation', *FEBS letters*, 157: 155-58.

Cho, Hyun, Dong Won Yang, Young Min Shon, Beum Saeng Kim, Yeong In Kim, Young Bin Choi, Kwang Soo Lee, Yong Soo Shim, Bora Yoon, Woojin Kim et al. 2008. 'Abnormal integrity of corticocortical tracts in mild cognitive impairment: a diffusion tensor imaging study', *Journal of Korean medical science*, 23: 477-83.

Chu, Tak-Ho, Karen Cummins, Joseph S Sparling, Shigeki Tsutsui, Craig Brideau, K Peter R Nilsson, Jeffrey T Joseph, and Peter K Stys. 2017. 'Axonal and myelinic pathology in 5xFAD Alzheimer's mouse spinal cord', *PloS one*, 12: e0188218.

Chung, Julia A, and Jeffrey L Cummings. 2000. 'Neurobehavioral and neuropsychiatric symptoms in Alzheimer's disease: characteristics and treatment', *Neurologic clinics*, 18: 829-46.

Cignarella, Francesca, Fabia Filipello, Bryan Bollman, Claudia Cantoni, Alberto Locca, Robert Mikesell, Melissa Manis, Adiljan Ibrahim, Li Deng, Bruno A Benitez et al. 2020. 'TREM2 activation on microglia promotes myelin debris clearance and remyelination in a model of multiple sclerosis', *Acta neuropathologica*, 140: 513-34.

Cirrito, John R, Kelvin A Yamada, Mary Beth Finn, Robert S Sloviter, Kelly R Bales, Patrick C May, Darryle D Schoepp, Steven M Paul, Steven Mennerick, and David M Holtzman. 2005. 'Synaptic activity regulates interstitial fluid amyloid-β levels in vivo', *Neuron*, 48: 913-22.

Cisternas, Pedro, Juan M Zolezzi, Carolina Lindsay, Daniela S Rivera, Alexis Martinez, Francisco Bozinovic, and Nibaldo C Inestrosa. 2018. 'New Insights into the spontaneous human Alzheimer's disease-like model Octodon degus: unraveling amyloid-β peptide aggregation and age-related amyloid pathology', *Journal of Alzheimer's Disease*, 66: 1145-63.

Citron, Martin, David Westaway, Weiming Xia, George Carlson, Thekla Diehl, Georges Levesque, Kelly Johnson-Wood, Michael Lee, Peter Seubert, Angela Davis et al. 1997. 'Mutant presenilins of

Alzheimer's disease increase production of 42-residue amyloid β-protein in both transfected cells and transgenic mice', *Nature medicine*, 3: 67-72.

Cohen, Charles CH, Marko A Popovic, Jan Klooster, Marie-Theres Weil, Wiebke Möbius, Klaus-Armin Nave, and Maarten HP Kole. 2020. 'Saltatory conduction along myelinated axons involves a periaxonal nanocircuit', *Cell*, 180: 311-22. e15.

Cole, Sarah L, and Roger Vassar. 2008. 'BACE1 structure and function in health and Alzheimer's disease', *Current Alzheimer Research*, 5: 100-20.

Condello, Carlo, Peng Yuan, Aaron Schain, and Jaime Grutzendler. 2015. 'Microglia constitute a barrier that prevents neurotoxic protofibrillar Aβ42 hotspots around plaques', *Nature communications*, 6: 1-14.

Corces, M Ryan, Alexandro E Trevino, Emily G Hamilton, Peyton G Greenside, Nicholas A Sinnott-Armstrong, Sam Vesuna, Ansuman T Satpathy, Adam J Rubin, Kathleen S Montine, Beijing Wu et al. 2017. 'An improved ATAC-seq protocol reduces background and enables interrogation of frozen tissues', *Nature methods*, 14: 959-62.

Cordy, Joanna M, Ishrut Hussain, Colin Dingwall, Nigel M Hooper, and Anthony J Turner. 2003. 'Exclusively targeting β-secretase to lipid rafts by GPI-anchor addition up-regulates β-site processing of the amyloid precursor protein', *Proceedings of the National Academy of Sciences*, 100: 11735-40.

Cox, Simon R, Stuart J Ritchie, Elliot M Tucker-Drob, David C Liewald, Saskia P Hagenaars, Gail Davies, Joanna M Wardlaw, Catharine R Gale, Mark E Bastin, and Ian J Deary. 2016. 'Ageing and brain white matter structure in 3,513 UK Biobank participants', *Nature communications*, 7: 1-13.

Cree, Bruce AC, Jianqin Niu, Kimberly K Hoi, Chao Zhao, Scott D Caganap, Roland G Henry, Dang Q Dao, Daniel R Zollinger, Feng Mei, Yun-An A Shen et al. 2018. 'Clemastine rescues myelination defects and promotes functional recovery in hypoxic brain injury', *Brain*, 141: 85-98.

Das, Utpal, David A Scott, Archan Ganguly, Edward H Koo, Yong Tang, and Subhojit Roy. 2013. 'Activity-induced convergence of APP and BACE-1 in acidic microdomains via an endocytosis-dependent pathway', *Neuron*, 79: 447-60.

Das, Utpal, Lina Wang, Archan Ganguly, Junmi M Saikia, Steven L Wagner, Edward H Koo, and Subhojit Roy. 2016. 'Visualizing APP and BACE-1 approximation in neurons yields insight into the amyloidogenic pathway', *Nature neuroscience*, 19: 55-64.

Davis, David A, Kiyo Mondo, Erica Stern, Ama K Annor, Susan J Murch, Thomas M Coyne, Larry E Brand, Misty E Niemeyer, Sarah Sharp, Walter G Bradley et al. 2019. 'Cyanobacterial neurotoxin BMAA and brain pathology in stranded dolphins', *PloS one*, 14: e0213346.

Davis, DG, FA Schmitt, DR Wekstein, and WR Markesbery. 1999. 'Alzheimer neuropathologic alterations in aged cognitively normal subjects', *Journal of neuropathology and experimental neurology*, 58: 376-88.

De Angelis, Dino A, and Peter E Braun. 1996. '2′, 3′-Cyclic nucleotide 3′-phosphodiesterase binds to actin-based cytoskeletal elements in an isoprenylation-independent manner', *Journal of neurochemistry*, 67: 943-51.

De Strooper, Bart. 2003. 'Aph-1, Pen-2, and nicastrin with presenilin generate an active γ-secretase complex', *Neuron*, 38: 9-12.

De Strooper, Bart, Takeshi Iwatsubo, and Michael S Wolfe. 2012. 'Presenilins and γ-secretase: structure, function, and role in Alzheimer disease', *Cold Spring Harbor perspectives in medicine*, 2: a006304.

De Strooper, Bart, Paul Saftig, Katleen Craessaerts, Hugo Vanderstichele, Gundula Guhde, Wim Annaert, Kurt Von Figura, and Fred Van Leuven. 1998. 'Deficiency of presenilin-1 inhibits the normal cleavage of amyloid precursor protein', *Nature*, 391: 387-90.

Dean, Douglas C, Samuel A Hurley, Steven R Kecskemeti, J Patrick O'Grady, Cristybelle Canda, Nancy J Davenport-Sis, Cynthia M Carlsson, Henrik Zetterberg, Kaj Blennow, Sanjay Asthana et al. 2017. 'Association of amyloid pathology with myelin alteration in preclinical Alzheimer disease', *JAMA neurology*, 74: 41-49.

Dean, Douglas C, Samuel A Hurley, Steven R Kecskemeti, J Patrick O'Grady, Cristybelle Canda, Nancy J Davenport-Sis, Cynthia M Carlsson, Henrik Zetterberg, Kaj Blennow, Sanjay Asthana et al. 2017. 'Association of amyloid pathology with myelin alteration in preclinical Alzheimer disease', JAMA neurology 74: 41-49.

Dean, Douglas C, Beth A Jerskey, Kewei Chen, Hillary Protas, Pradeep Thiyyagura, Auttawat Roontiva, Jonathan O'Muircheartaigh, Holly Dirks, Nicole Waskiewicz, Katie Lehman et al. 2014. 'Brain differences in infants at differential genetic risk for late-onset Alzheimer disease: a cross-sectional imaging study', *JAMA neurology*, 71: 11-22.

Deane, Rashid, Abhay Sagare, Katie Hamm, Margaret Parisi, Steven Lane, Mary Beth Finn, David M Holtzman, and Berislav V Zlokovic. 2008. 'apoE isoform–specific disruption of amyloid β peptide clearance from mouse brain', *The Journal of clinical investigation*, 118: 4002-13.

Del Rio-Hortega, Pío. 1921. 'Estudios Sobre la neurogia. La glia de escasas rediaciones (Oligodendroglia)', *Bol Real Soc Esp Hist Nat*, 21: 63-92.

DeMattos, Ronald B, John R Cirrito, Maia Parsadanian, Patrick C May, Mark A O'Dell, Jennie W Taylor, Judith AK Harmony, Bruce J Aronow, Kelly R Bales, Steven M Paul et al. 2004. 'ApoE and clusterin cooperatively suppress Aβ levels and deposition: evidence that ApoE regulates extracellular Aβ metabolism in vivo', *Neuron*, 41: 193-202.

Deming, Yuetiva, Fabia Filipello, Francesca Cignarella, Claudia Cantoni, Simon Hsu, Robert Mikesell, Zeran Li, Jorge L Del-Aguila, Umber Dube, Fabiana Geraldo Farias et al. 2019. 'The MS4A gene cluster is a key modulator of soluble TREM2 and Alzheimer's disease risk', *Science translational medicine*, 11.

Depp, Constanze, Ting Sun, Andrew Octavian Sasmita, Lena Spieth, Stefan A Berghoff, Agnes A Steixner-Kumar, Swati Subramanian, Wiebke Möbius, Sandra Göbbels, Gesine Saher et al. 2021. 'Ageing-associated myelin dysfunction drives amyloid deposition in mouse models of Alzheimer's disease', *bioRxiv*.

Desai, Maya K, Kelly L Sudol, Michelle C Janelsins, Michael A Mastrangelo, Maria E Frazer, and William J Bowers. 2009. 'Triple-transgenic Alzheimer's disease mice exhibit region-specific abnormalities in brain myelination patterns prior to appearance of amyloid and tau pathology', *Glia*, 57: 54-65.

Dewar, Deborah, Suzanne M Underhill, and Mark P Goldberg. 2003. 'Oligodendrocytes and ischemic brain injury', *Journal of Cerebral Blood Flow & Metabolism*, 23: 263-74.

Dhana, Klodian, Denis A Evans, Kumar B Rajan, David A Bennett, and Martha C Morris. 2020. 'Healthy lifestyle and the risk of Alzheimer dementia: Findings from 2 longitudinal studies', *Neurology*, 95: e374-e83.

Dhaunchak, Ajit-Singh, and Klaus-Armin Nave. 2007. 'A common mechanism of PLP/DM20 misfolding causes cysteine-mediated endoplasmic reticulum retention in oligodendrocytes and Pelizaeus–Merzbacher disease', *Proceedings of the National Academy of Sciences*, 104: 17813-18.

Dickson, TC, and JC Vickers. 2001. 'The morphological phenotype of β-amyloid plaques and associated neuritic changes in Alzheimer's disease', *Neuroscience*, 105: 99-107.

Dobin, Alexander, Carrie A Davis, Felix Schlesinger, Jorg Drenkow, Chris Zaleski, Sonali Jha, Philippe Batut, Mark Chaisson, and Thomas R Gingeras. 2013. 'STAR: ultrafast universal RNA-seq aligner', *Bioinformatics*, 29: 15-21.

Dodt, Hans-Ulrich, Saiedeh Saghafi, Klaus Becker, Nina Jährling, Axel Niendorf, Christian Hahn, Marko Pende, and Martina Wanis. 2015. 'Ultramicroscopy: development and outlook', *Neurophotonics*, 2: 041407.

Doucette, J Ronald, Rubin Jiao, and Adil J Nazarali. 2010. 'Age-related and cuprizone-induced changes in myelin and transcription factor gene expression and in oligodendrocyte cell densities in the rostral corpus callosum of mice', *Cellular and molecular neurobiology*, 30: 607-29.

Douglas, AJ, MF Fox, CM Abbott, LJ Hinks, G Sharpe, S Povey, and RJ Thompson. 1992. 'Structure and chromosomal localization of the human 2 ‘, 3’-cyclic nucleotide 3 ‘-phosphodiesterase gene', *Annals of human genetics*, 56: 243-54.

Dries, Daniel R, and Gang Yu. 2008. 'Assembly, maturation, and trafficking of the γ-secretase complex in Alzheimer's disease', *Current Alzheimer Research*, 5: 132-46.

Drummond, Eleanor, Shruti Nayak, Arline Faustin, Geoffrey Pires, Richard A Hickman, Manor Askenazi, Mark Cohen, Tracy Haldiman, Chae Kim, Xiaoxia Han et al. 2017. 'Proteomic differences in amyloid plaques in rapidly progressive and sporadic Alzheimer’s disease', *Acta neuropathologica*, 133: 933-54.

Drummond, George I, NT Iyer, and Jacqueline Keith. 1962. 'Hydrolysis of ribonucleoside 2 ‘, 3 ‘-cyclic phosphates by a diesterase from brain', *Journal of Biological Chemistry*, 237: 3535-39.

Duncan, ID, JP Hammang, and BD Trapp. 1987. 'Abnormal compact myelin in the myelin-deficient rat: absence of proteolipid protein correlates with a defect in the intraperiod line', *Proceedings of the National Academy of Sciences*, 84: 6287-91.

Eckman, Christopher B, Nitin D Mehta, Richard Crook, Jordi Perez-tur, Guy Prihar, Eric Pfeiffer, Neill Graff-Radford, Paul Hinder, Debra Yager, Brenda Zenk et al. 1997. 'A new pathogenic mutation in the APP gene (I716V) increases the relative proportion of Aβ42 (43)', *Human molecular genetics* , 6: 2087-89.

Edgar, JM, M McLaughlin, JA Barrie, MC McCulloch, J Garbern, and IR Griffiths. 2004. 'Age-related axonal and myelin changes in the rumpshaker mutation of the Plp gene', *Acta neuropathologica*, 107: 331-35.

Edgar, Julia M, Mark McLaughlin, Hauke B Werner, Mailis C McCulloch, Jennifer A Barrie, Angus Brown, Andrew Blyth Faichney, Nicolas Snaidero, Klaus-Armin Nave, and Ian R Griffiths. 2009. 'Early ultrastructural defects of axons and axon–glia junctions in mice lacking expression of Cnp1', *Glia*, 57: 1815-24.

Edgar, Julia M, Mark McLaughlin, Donald Yool, Su-Chun Zhang, Jill H Fowler, Paul Montague, Jennifer A Barrie, Mailis C McCulloch, Ian D Duncan, James Garbern et al. 2004. 'Oligodendroglial modulation of fast axonal transport in a mouse model of hereditary spastic paraplegia', *The Journal of cell biology*, 166: 121-31.

Efthymiou, Anastasia G, and Alison M Goate. 2017. 'Late onset Alzheimer’s disease genetics implicates microglial pathways in disease risk', *Molecular neurodegeneration*, 12: 1-12.

El Khoury, Joseph B, Kathryn J Moore, Terry K Means, Josephine Leung, Kinya Terada, Michelle Toft, Mason W Freeman, and Andrew D Luster. 2003. 'CD36 mediates the innate host response to β-amyloid', *The Journal of experimental medicine*, 197: 1657-66.

Ellis, David, and Sue Malcolm. 1994. 'Proteolipid protein gene dosage effect in Pelizaeus–Merzbacher disease', *Nature genetics*, 6: 333-34.

Elmore, Monica RP, Allison R Najafi, Maya A Koike, Nabil N Dagher, Elizabeth E Spangenberg, Rachel A Rice, Masashi Kitazawa, Bernice Matusow, Hoa Nguyen, Brian L West et al. 2014. 'Colony-stimulating factor 1 receptor signaling is necessary for microglia viability, unmasking a microglia progenitor cell in the adult brain', *Neuron*, 82: 380-97.

Emery, Ben. 2010. 'Regulation of oligodendrocyte differentiation and myelination', *Science*, 330: 779-82.

Emery, Ben, Dritan Agalliu, John D Cahoy, Trent A Watkins, Jason C Dugas, Sara B Mulinyawe, Adilijan Ibrahim, Keith L Ligon, David H Rowitch, and Ben A Barres. 2009. 'Myelin gene regulatory factor is a critical transcriptional regulator required for CNS myelination', *Cell*, 138: 172-85.

Emery, Ben, and Q Richard Lu. 2015. 'Transcriptional and epigenetic regulation of oligodendrocyte development and myelination in the central nervous system', *Cold Spring Harbor perspectives in biology*, 7: a020461.

Endres, Kristina, and Thomas Deller. 2017. 'Regulation of alpha-secretase ADAM10 in vitro and in vivo: genetic, epigenetic, and protein-based mechanisms', *Frontiers in molecular neuroscience*, 10: 56.

Engelhardt, Eliasz, Denise Madeira Moreira, and Jerson Laks. 2009. 'The brain subcortical white matter and aging: A quantitative fractional anisotropy analysis', *Dementia & neuropsychologia*, 3: 228-33.

Ertürk, Ali, and Frank Bradke. 2013. 'High-resolution imaging of entire organs by 3-dimensional imaging of solvent cleared organs (3DISCO)', *Experimental neurology*, 242: 57-64.

Esch, Fred S, Pamela S Keim, Eric C Beattie, Russell W Blacher, Alan R Culwell, Tilman Oltersdorf, Donald McClure, and Pamela J Ward. 1990. 'Cleavage of amyloid beta peptide during constitutive processing of its precursor', *Science*, 248: 1122-24.

Esler, William P, and Michael S Wolfe. 2001. 'A portrait of Alzheimer secretases--new features and familiar faces', *Science*, 293: 1449-54.

Eylar, EH, Steven Brostoff, George Hashim, Juanita Caccam, and Paul Burnett. 1971. 'Basic A1 protein of the myelin membrane: the complete amino acid sequence', *Journal of Biological Chemistry*, 246: 5770-84.

Falcão, Ana Mendanha, David van Bruggen, Sueli Marques, Mandy Meijer, Sarah Jäkel, Eneritz Agirre, Elisa M Floriddia, Darya P Vanichkina, Anna Williams, André Ortlieb Guerreiro-Cacais et al. 2018. 'Disease-specific oligodendrocyte lineage cells arise in multiple sclerosis', *Nature medicine*, 24: 1837-44.

Farrer, Lindsay A, L Adrienne Cupples, Jonathan L Haines, Bradley Hyman, Walter A Kukull, Richard Mayeux, Richard H Myers, Margaret A Pericak-Vance, Neil Risch, and Cornelia M Van Duijn. 1997. 'Effects of age, sex, and ethnicity on the association between apolipoprotein E genotype and Alzheimer disease: a meta-analysis', *Jama*, 278: 1349-56.

Fellgiebel, Andreas, Paulo Wille, Matthias J Müller, Georg Winterer, Armin Scheurich, Goran Vucurevic, Lutz G Schmidt, and Peter Stoeter. 2004. 'Ultrastructural hippocampal and white matter alterations in mild cognitive impairment: a diffusion tensor imaging study', *Dementia and geriatric cognitive disorders*, 18: 101-08.

Ferguson, Shawn M. 2018. 'Axonal transport and maturation of lysosomes', *Current opinion in neurobiology*, 51: 45-51.

Fernandez-Castaneda, Anthony, and Alban Gaultier. 2016. 'Adult oligodendrocyte progenitor cells–multifaceted regulators of the CNS in health and disease', *Brain, behavior, and immunity*, 57: 1-7.

Fernandez, Celia G, Mary E Hamby, Morgan L McReynolds, and William J Ray. 2019. 'The role of APOE4 in disrupting the homeostatic functions of astrocytes and microglia in aging and Alzheimer's disease', *Frontiers in aging neuroscience*, 11: 14.

Finak, Greg, Andrew McDavid, Masanao Yajima, Jingyuan Deng, Vivian Gersuk, Alex K Shalek, Chloe K Slichter, Hannah W Miller, M Juliana McElrath, Martin Prlic et al. 2015. 'MAST: a flexible statistical framework for assessing transcriptional changes and characterizing heterogeneity in single-cell RNA sequencing data', *Genome biology*, 16: 1-13.

Fischer, Florian Udo, Dominik Wolf, Armin Scheurich, Andreas Fellgiebel, and Alzheimer's Disease Neuroimaging Initiative. 2015. 'Altered whole-brain white matter networks in preclinical Alzheimer's disease', *NeuroImage: Clinical*, 8: 660-66.

Fischer, Priv-Doz Dr Oskar. 1907. 'Miliare Nekrosen mit drusigen Wucherungen der Neuro', *Monatsschrift für Psychiatrie und Neurologie*, 22: 361.

Fleisher, Adam S, Kewei Chen, Xiaofen Liu, Auttawut Roontiva, Pradeep Thiyyagura, Napatkamon Ayutyanont, Abhinay D Joshi, Christopher M Clark, Mark A Mintun, Michael J Pontecorvo et al. 2011. 'Using positron emission tomography and florbetapir F 18 to image cortical amyloid in patients with mild cognitive impairment or dementia due to Alzheimer disease', *Archives of neurology*, 68: 1404-11.

Francis, Ross, Garth McGrath, Jianhuan Zhang, David A Ruddy, Mary Sym, Javier Apfeld, Monique Nicoll, Mark Maxwell, Bing Hai, Michael C Ellis et al. 2002. 'aph-1 and pen-2 are required for Notch pathway signaling, γ-secretase cleavage of βAPP, and presenilin protein accumulation', *Developmental cell*, 3: 85-97.

Freeman, Marc R, and David H Rowitch. 2013. 'Evolving concepts of gliogenesis: a look way back and ahead to the next 25 years', *Neuron*, 80: 613-23.

Freeman, Sean A, Anne Desmazières, Jean Simonnet, Marie Gatta, Friederike Pfeiffer, Marie Stéphane Aigrot, Quentin Rappeneau, Serge Guerreiro, Patrick Pierre Michel, Yuchio Yanagawa et al. 2015. 'Acceleration of conduction velocity linked to clustering of nodal components precedes myelination', *Proceedings of the National Academy of Sciences*, 112: E321-E28.

Frenkel, Dan, Ruth Maron, David S Burt, and Howard L Weiner. 2005. 'Nasal vaccination with a proteosome-based adjuvant and glatiramer acetate clears β-amyloid in a mouse model of Alzheimer disease', *The Journal of clinical investigation*, 115: 2423-33.

Friedrich, Ralf P, Katharina Tepper, Raik Rönicke, Malle Soom, Martin Westermann, Klaus Reymann, Christoph Kaether, and Marcus Fändrich. 2010. 'Mechanism of amyloid plaque formation suggests an intracellular basis of Aβ pathogenicity', *Proceedings of the National Academy of Sciences*, 107: 1942-47.

Fröhlich, Dominik, Wen Ping Kuo, Carsten Frühbeis, Jyh-Jang Sun, Christoph M Zehendner, Heiko J Luhmann, Sheena Pinto, Joern Toedling, Jacqueline Trotter, and Eva-Maria Krämer-Albers. 2014. 'Multifaceted effects of oligodendroglial exosomes on neurons: impact on neuronal firing rate, signal transduction and gene regulation', *Philosophical Transactions of the Royal Society B: Biological Sciences*, 369: 20130510.

Frühbeis, Carsten, Dominik Fröhlich, Wen Ping Kuo, Jesa Amphornrat, Sebastian Thilemann, Aiman S Saab, Frank Kirchhoff, Wiebke Möbius, Sandra Goebbels, Klaus-Armin Nave et al. 2013. 'Neurotransmitter-triggered transfer of exosomes mediates oligodendrocyte–neuron communication', *PLoS biology*, 11: e1001604.

Frühbeis, Carsten, Wen Ping Kuo-Elsner, Christina Müller, Kerstin Barth, Leticia Peris, Stefan Tenzer, Wiebke Möbius, Hauke B Werner, Klaus-Armin Nave, Dominik Fröhlich et al. 2020. 'Oligodendrocytes support axonal transport and maintenance via exosome secretion', *PLoS biology*, 18: e3000621.

Füger, Petra, Jasmin K Hefendehl, Karthik Veeraraghavalu, Ann-Christin Wendeln, Christine Schlosser, Ulrike Obermüller, Bettina M Wegenast-Braun, Jonas J Neher, Peter Martus, Shinichi Kohsaka et al. 2017. 'Microglia turnover with aging and in an Alzheimer's model via long-term in vivo single-cell imaging', *Nature neuroscience*, 20: 1371-76.

Fukumoto, Hiroaki, Bonnie S Cheung, Bradley T Hyman, and Michael C Irizarry. 2002. 'β-Secretase protein and activity are increased in the neocortex in Alzheimer disease', *Archives of neurology*, 59: 1381-89.

Fünfschilling, Ursula, Lotti M Supplie, Don Mahad, Susann Boretius, Aiman S Saab, Julia Edgar, Bastian G Brinkmann, Celia M Kassmann, Iva D Tzvetanova, Wiebke Möbius et al. 2012. 'Glycolytic oligodendrocytes maintain myelin and long-term axonal integrity', *Nature*, 485: 517-21.

Fung, Justin, David Frost, Avijit Chakrabartty, and JoAnne McLaurin. 2004. 'Interaction of human and mouse Aβ peptides', *Journal of neurochemistry*, 91: 1398-403.

Games, Dora, David Adams, Ree Alessandrini, Robin Barbour, Patricia Borthelette, Catherine Blackwell, Tony Carr, James Clemens, Thomas Donaldson, Frances Gillespie et al. 1995. 'Alzheimer-type neuropathology in transgenic mice overexpressing V717F β-amyloid precursor protein', *Nature*, 373: 523-27.

Gao, Junling, Raymond Tak-Fai Cheung, Tatia Lee, Leung-Wing Chu, Ying-Shing Chan, Henry Ka-Fung Mak, John X Zhang, Deqiang Qiu, Germaine Fung, and Charlton Cheung. 2011. 'Possible retrogenesis observed with fiber tracking: an anteroposterior pattern of white matter disintegrity in normal aging and Alzheimer's disease', *Journal of Alzheimer's Disease*, 26: 47-58.

Gao, Yuan, Cong Guo, Jens O Watzlawik, Peter S Randolph, Elizabeth J Lee, Danting Huang, Scott M Stagg, Huan-Xiang Zhou, Terrone L Rosenberry, and Anant K Paravastu. 2020. 'Out-of-register parallel β-sheets and antiparallel β-sheets coexist in 150-kDa oligomers formed by amyloid-β (1–42)', *Journal of Molecular Biology*, 432: 4388-407.

Gefen, Tamar, Garam Kim, Kabriya Bolbolan, Andrew Geoly, Daniel Ohm, Carly Oboudiyat, Ryan Shahidehpour, Alfred Rademaker, Sandra Weintraub, Eileen H Bigio et al. 2019. 'Activated microglia in cortical white matter across cognitive aging trajectories', *Frontiers in aging neuroscience*, 11: 94.

Gellermann, Gerald P, Kathrin Ullrich, Astrid Tannert, Christiane Unger, Gernot Habicht, Simon RN Sauter, Peter Hortschansky, Uwe Horn, Ute Möllmann, Michael Decker et al. 2006. 'Alzheimer-like plaque formation by human macrophages is reduced by fibrillation inhibitors and lovastatin', *Journal of Molecular Biology*, 360: 251-57.

Geren, Betty Ben. 1954. 'The formation from the schwann cell surfaceof myelin in the peripheral nerves of chick embryos', *Experimental cell research*, 7: 558-62.

Giorgio, Antonio, Luca Santelli, Valentina Tomassini, Rose Bosnell, Steve Smith, Nicola De Stefano, and Heidi Johansen-Berg. 2010. 'Age-related changes in grey and white matter structure throughout adulthood', *Neuroimage*, 51: 943-51.

Glasser, Matthew F, and David C Van Essen. 2011. 'Mapping human cortical areas in vivo based on myelin content as revealed by T1-and T2-weighted MRI', *Journal of Neuroscience*, 31: 11597-616.

Glenner, George G, and Caine W Wong. 1984. 'Alzheimer's disease: initial report of the purification and characterization of a novel cerebrovascular amyloid protein', *Biochemical and biophysical research communications*, 120: 885-90.

Goate, Alison, Marie-Christine Chartier-Harlin, Mike Mullan, Jeremy Brown, Fiona Crawford, Liana Fidani, Luis Giuffra, Andrew Haynes, Nick Irving, Louise James et al. 1991. 'Segregation of a missense mutation in the amyloid precursor protein gene with familial Alzheimer's disease', *Nature*, 349: 704-06.

Goebbels, Sandra, Georg L Wieser, Alexander Pieper, Sonia Spitzer, Bettina Weege, Kuo Yan, Julia M Edgar, Oleksandr Yagensky, Sven P Wichert, Amit Agarwal et al. 2017. 'A neuronal PI (3, 4, 5) P 3-dependent program of oligodendrocyte precursor recruitment and myelination', *Nature neuroscience*, 20: 10-15.

Gołaszewska, Anita, Wojciech Bik, Tomasz Motyl, and Arkadiusz Orzechowski. 2019. 'Bridging the Gap between Alzheimer's Disease and Alzheimer's-like Diseases in Animals', *International journal of molecular sciences*, 20: 1664.

Gold, Brian T, David K Powell, Anders H Andersen, and Charles D Smith. 2010. 'Alterations in multiple measures of white matter integrity in normal women at high risk for Alzheimer's disease', *Neuroimage*, 52: 1487-94.

Gold, Brian T, Zude Zhu, Christopher A Brown, Anders H Andersen, Mary Jo LaDu, Leon Tai, Greg A Jicha, Richard J Kryscio, Steven Estus, Peter T Nelson et al. 2014. 'White matter integrity is associated with cerebrospinal fluid markers of Alzheimer's disease in normal adults', *Neurobiology of aging*, 35: 2263-71.

Goldgaber, Dmitry, Michael I Lerman, O Westley McBride, Umberto Saffiotti, and D Carleton Gajdusek. 1987. 'Characterization and chromosomal localization of a cDNA encoding brain amyloid of Alzheimer's disease', *Science*, 235: 877-80.

Goldsbury, Claire, Maria-Magdalena Mocanu, Edda Thies, Christoph Kaether, Christian Haass, Patrick Keller, Jacek Biernat, Eckhard Mandelkow, and Eva-Maria Mandelkow. 2006. 'Inhibition of APP trafficking by tau protein does not increase the generation of amyloid-β peptides', *Traffic*, 7: 873-88.

Gorski, Jessica A, Tiffany Talley, Mengsheng Qiu, Luis Puelles, John LR Rubenstein, and Kevin R Jones. 2002. 'Cortical excitatory neurons and glia, but not GABAergic neurons, are produced in the Emx1-expressing lineage', *Journal of Neuroscience*, 22: 6309-14.

Gould, Elizabeth A, Nicolas Busquet, Douglas Shepherd, Robert M Dietz, Paco S Herson, Fabio M Simoes De Souza, Anan Li, Nicholas M George, Diego Restrepo, and Wendy B Macklin. 2018. 'Mild myelin disruption elicits early alteration in behavior and proliferation in the subventricular zone', *Elife*, 7: e34783.

Goutte, Caroline, Makoto Tsunozaki, Valerie A Hale, and James R Priess. 2002. 'APH-1 is a multipass membrane protein essential for the Notch signaling pathway in Caenorhabditis elegans embryos', *Proceedings of the National Academy of Sciences*, 99: 775-79.

Gouvêa-Junqueira, Danielle, Ana Caroline Brambilla Falvella, André Saraiva Leão Marcelo Antunes, Gabriela Seabra, Caroline Brandão-Teles, Daniel Martins-de-Souza, and Fernanda Crunfli. 2020. 'Novel treatment strategies targeting myelin and oligodendrocyte dysfunction in schizophrenia', *Frontiers in Psychiatry*, 11: 379.

Gowrishankar, Swetha, Yumei Wu, and Shawn M Ferguson. 2017. 'Impaired JIP3-dependent axonal lysosome transport promotes amyloid plaque pathology', *Journal of Cell Biology*, 216: 3291-305.

Gowrishankar, Swetha, Peng Yuan, Yumei Wu, Matthew Schrag, Summer Paradise, Jaime Grutzendler, Pietro De Camilli, and Shawn M Ferguson. 2015. 'Massive accumulation of luminal protease-deficient axonal lysosomes at Alzheimer's disease amyloid plaques', *Proceedings of the National Academy of Sciences*, 112: E3699-E708.

Grathwohl, Stefan A, Roland E Kälin, Tristan Bolmont, Stefan Prokop, Georg Winkelmann, Stephan A Kaeser, Jörg Odenthal, Rebecca Radde, Therese Eldh, Sam Gandy et al. 2009. 'Formation and maintenance of Alzheimer's disease β-amyloid plaques in the absence of microglia', *Nature neuroscience*, 12: 1361-63.

Griffiths, Ian, Matthias Klugmann, Thomas Anderson, Donald Yool, Christine Thomson, Markus H Schwab, Armin Schneider, Frank Zimmermann, Mailise McCulloch, Nancy Nadon et al. 1998. 'Axonal swellings and degeneration in mice lacking the major proteolipid of myelin', *Science*, 280: 1610-13.

Griffiths, Ian R, I Scott, Mailis C McCulloch, Jennifer A Barrie, K McPhilemy, and Bruce M Cattanach. 1990. 'Rumpshaker mouse: a new X-linked mutation affecting myelination: evidence for a defect in PLP expression', *Journal of neurocytology*, 19: 273-83.

Groemer, Teja W, Cora S Thiel, Matthew Holt, Dietmar Riedel, Yunfeng Hua, Jana Hüve, Benjamin G Wilhelm, and Jürgen Klingauf. 2011. 'Amyloid precursor protein is trafficked and secreted via synaptic vesicles', *PloS one*, 6: e18754.

Grubman, Alexandra, Gabriel Chew, John F Ouyang, Guizhi Sun, Xin Yi Choo, Catriona McLean, Rebecca K Simmons, Sam Buckberry, Dulce B Vargas-Landin, Daniel Poppe et al. 2019. 'A single-cell atlas of

entorhinal cortex from individuals with Alzheimer's disease reveals cell-type-specific gene expression regulation', *Nature neuroscience*, 22: 2087-97.

Grydeland, Håkon, Kristine B Walhovd, Christian K Tamnes, Lars T Westlye, and Anders M Fjell. 2013. 'Intracortical myelin links with performance variability across the human lifespan: results from T1- and T2-weighted MRI myelin mapping and diffusion tensor imaging', *Journal of Neuroscience*, 33: 18618-30.

Gudi, Viktoria, Stefan Gingele, Thomas Skripuletz, and Martin Stangel. 2014. 'Glial response during cuprizone-induced de-and remyelination in the CNS: lessons learned', *Frontiers in cellular neuroscience*, 8: 73.

Guerreiro, Rita Joao, Miquel Baquero, Rafael Blesa, Mercè Boada, Jose Miguel Brás, Maria J Bullido, Ana Calado, Richard Crook, Carla Ferreira, Ana Frank et al. 2010. 'Genetic screening of Alzheimer's disease genes in Iberian and African samples yields novel mutations in presenilins and APP', *Neurobiology of aging*, 31: 725-31.

Guerreiro, Rita, Aleksandra Wojtas, Jose Bras, Minerva Carrasquillo, Ekaterina Rogaeva, Elisa Majounie, Carlos Cruchaga, Celeste Sassi, John SK Kauwe, Steven Younkin et al. 2013. 'TREM2 variants in Alzheimer's disease', *New England Journal of Medicine*, 368: 117-27.

Güner, Gökhan, and Stefan F Lichtenthaler. 2020. "The substrate repertoire of γ-secretase/presenilin." In *Seminars in Cell & Developmental Biology*. Elsevier.

Gunning-Dixon, Faith M, Adam M Brickman, Janice C Cheng, and George S Alexopoulos. 2009. 'Aging of cerebral white matter: a review of MRI findings', *International Journal of Geriatric Psychiatry: A journal of the psychiatry of late life and allied sciences*, 24: 109-17.

Guttmann, Charles RG, Ferenc A Jolesz, Ron Kikinis, Ron J Killiany, Mark B Moss, Tamas Sandor, and Marilyn S Albert. 1998. 'White matter changes with normal aging', *Neurology*, 50: 972-78.

Haass, Christian, Christoph Kaether, Gopal Thinakaran, and Sangram Sisodia. 2012. 'Trafficking and proteolytic processing of APP', *Cold Spring Harbor perspectives in medicine*, 2: a006270.

Haass, Christian, Michael G Schlossmacher, Albert Y Hung, Carmen Vigo-Pelfrey, Angela Mellon, Beth L Ostaszewski, Ivan Lieberburg, Edward H Koo, Dale Schenk, David B Teplow et al. 1992. 'Amyloid β-peptide is produced by cultured cells during normal metabolism', *Nature* , 359: 322-25.

Haass, Christian, and Dennis J Selkoe. 1993. 'Cellular processing of β-amyloid precursor protein and the genesis of amyloid β-peptide', *Cell*, 75: 1039-42.

Hagemeyer, Nora, Sandra Goebbels, Sergi Papiol, Anne Kästner, Sabine Hofer, Martin Begemann, Ulrike C Gerwig, Susann Boretius, Georg L Wieser, Anja Ronnenberg et al. 2012. 'A myelin gene causative of a catatonia-depression syndrome upon aging', *EMBO molecular medicine*, 4: 528-39.

Haim, Lucile Ben, and David H Rowitch. 2017. 'Functional diversity of astrocytes in neural circuit regulation', *Nature Reviews Neuroscience*, 18: 31-41.

Hamilton, Ryan, Michael Walsh, Rashmi Singh, Karl Rodriguez, Xiaoli Gao, Md Mizanur Rahman, Asish Chaudhuri, and Arunabh Bhattacharya. 2016. 'Oxidative damage to myelin proteins accompanies peripheral nerve motor dysfunction in aging C57BL/6 male mice', *Journal of the neurological sciences*, 370: 47-52.

Han, Huijong, Matti Myllykoski, Salla Ruskamo, Chaozhan Wang, and Petri Kursula. 2013. 'Myelin-specific proteins: A structurally diverse group of membrane-interacting molecules', *Biofactors*, 39: 233-41.

Hansson, Oskar, Henrik Zetterberg, Peder Buchhave, Ulf Andreasson, Elisabet Londos, Lennart Minthon, and Kaj Blennow. 2007. 'Prediction of Alzheimer's disease using the CSF Aβ42/Aβ40 ratio in patients with mild cognitive impairment', *Dementia and geriatric cognitive disorders*, 23: 316-20.

Hardy, John A, and Gerald A Higgins. 1992. 'Alzheimer's disease: the amyloid cascade hypothesis', *Science*, 256: 184-86.

Hartline, DK, and DR Colman. 2007. 'Rapid conduction and the evolution of giant axons and myelinated fibers', *Current Biology*, 17: R29-R35.

Hasselmann, Jonathan, Morgan A Coburn, Whitney England, Dario X Figueroa Velez, Sepideh Kiani Shabestari, Christina H Tu, Amanda McQuade, Mahshad Kolahdouzan, Karla Echeverria, Christel Claes et al. 2019. 'Development of a chimeric model to study and manipulate human microglia in vivo', *Neuron*, 103: 1016-33. e10.

Heise, V, N Filippini, KP Ebmeier, and CE Mackay. 2011. 'The APOE ε4 allele modulates brain white matter integrity in healthy adults', *Molecular psychiatry*, 16: 908-16.

Hendriks, Lydia, Cornelia M van Duijn, Patrick Cras, Marc Cruts, Wim Van Hul, Frans van Harskamp, Andrew Warren, Melvin G McInnis, Stylianos E Antonarakis, Jean-Jacques Martin et al. 1992. 'Presenile dementia and cerebral haemorrhage linked to a mutation at codon 692 of the β–amyloid precursor protein gene', *Nature genetics* , 1: 218-21.

Heneka, Michael T, Monica J Carson, Joseph El Khoury, Gary E Landreth, Frederic Brosseron, Douglas L Feinstein, Andreas H Jacobs, Tony Wyss-Coray, Javier Vitorica, Richard M Ransohoff et al. 2015. 'Neuroinflammation in Alzheimer's disease', *The Lancet Neurology*, 14: 388-405.

Hickman, Suzanne E, Elizabeth K Allison, and Joseph El Khoury. 2008. 'Microglial dysfunction and defective β-amyloid clearance pathways in aging Alzheimer's disease mice', *Journal of Neuroscience*, 28: 8354-60.

Hildebrand, C, S Remahl, H Persson, and C Bjartmar. 1993. 'Myelinated nerve fibres in the CNS', *Progress in neurobiology*, 40: 319-84.

Hill, Robert A, Alice M Li, and Jaime Grutzendler. 2018. 'Lifelong cortical myelin plasticity and age-related degeneration in the live mammalian brain', *Nature neuroscience*, 21: 683-95.

Hipp, Mark S, Prasad Kasturi, and F Ulrich Hartl. 2019. 'The proteostasis network and its decline in ageing', *Nature reviews Molecular cell biology*, 20: 421-35.

Hinman, Jason D, and Carmela R Abraham. 2007. 'What's behind the decline? The role of white matter in brain aging', *Neurochemical research*, 32: 2023-31.

Hinman, Jason D, Ci-Di Chen, Sun-Young Oh, William Hollander, and Carmela R Abraham. 2008. 'Age-dependent accumulation of ubiquitinated 2′, 3′-cyclic nucleotide 3′-phosphodiesterase in myelin lipid rafts', *Glia*, 56: 118-33.

Hodgkin, Alan L, and Andrew F Huxley. 1952. 'A quantitative description of membrane current and its application to conduction and excitation in nerve', *The Journal of physiology*, 117: 500-44.

Horiuchi, Makoto, Izumi Maezawa, Aki Itoh, Kouji Wakayama, Lee-Way Jin, Takayuki Itoh, and Charles DeCarli. 2012. 'Amyloid β1–42 oligomer inhibits myelin sheet formation in vitro', *Neurobiology of aging*, 33: 499-509.

Hou, Yujun, Xiuli Dan, Mansi Babbar, Yong Wei, Steen G Hasselbalch, Deborah L Croteau, and Vilhelm A Bohr. 2019. 'Ageing as a risk factor for neurodegenerative disease', *Nature Reviews Neurology*, 15: 565-81.

Hoy, Andrew R, Martina Ly, Cynthia M Carlsson, Ozioma C Okonkwo, Henrik Zetterberg, Kaj Blennow, Mark A Sager, Sanjay Asthana, Sterling C Johnson, Andrew L Alexander et al. 2017. 'Microstructural white matter alterations in preclinical Alzheimer's disease detected using free water elimination diffusion tensor imaging', *PloS one*, 12: e0173982.

Hsiao, Karen, Paul Chapman, Steven Nilsen, Chris Eckman, Yasuo Harigaya, Steven Younkin, Fusheng Yang, and Greg Cole. 1996. 'Correlative memory deficits, Aβ elevation, and amyloid plaques in transgenic mice', *Science*, 274: 99-103.

Huang, Hui-Ting, Sheng-Feng Tsai, Hung-Tsung Wu, Hsin-Ying Huang, Han-Hsueh Hsieh, Yu-Ming Kuo, Po-See Chen, Chung-Shi Yang, and Shun-Fen Tzeng. 2019. 'Chronic exposure to high fat diet triggers myelin disruption and interleukin-33 upregulation in hypothalamus', *BMC neuroscience*, 20: 1-11.

Huang, Youtong, Kaisa E Happonen, Patrick G Burrola, Carolyn O'Connor, Nasun Hah, Ling Huang, Axel Nimmerjahn, and Greg Lemke. 2021. 'Microglia use TAM receptors to detect and engulf amyloid β plaques', *Nature Immunology*, 22: 586-94.

Huse, Jason T, Donald S Pijak, George J Leslie, Virginia M-Y Lee, and Robert W Doms. 2000. 'Maturation and endosomal targeting of β-site amyloid precursor protein-cleaving enzyme: the Alzheimer's disease β-secretase', *Journal of Biological Chemistry*, 275: 33729-37.

Hussain, Ishrut, David Powell, David R Howlett, David G Tew, Thomas D Meek, Conrad Chapman, Israel S Gloger, Kay E Murphy, Christopher D Southan, Dominic M Ryan et al. 1999. 'Identification of a novel aspartic protease (Asp 2) as β-secretase', *Molecular and Cellular Neuroscience* , 14: 419-27.

Hyman, Bradley T, Creighton H Phelps, Thomas G Beach, Eileen H Bigio, Nigel J Cairns, Maria C Carrillo, Dennis W Dickson, Charles Duyckaerts, Matthew P Frosch, Eliezer Masliah et al. 2012. 'National Institute on Aging–Alzheimer's Association guidelines for the neuropathologic assessment of Alzheimer's disease', *Alzheimer's & Dementia*, 8: 1-13.

Ikonomovic, Milos D, Chris J Buckley, Kerstin Heurling, Paul Sherwin, Paul A Jones, Michelle Zanette, Chester A Mathis, William E Klunk, Aruna Chakrabarty, James Ironside et al. 2016. 'Post-mortem histopathology underlying β-amyloid PET imaging following flutemetamol F 18 injection', *Acta neuropathologica communications*, 4: 1-24.

Inoue, Ken. 2017. 'Cellular pathology of Pelizaeus-Merzbacher disease involving chaperones associated with endoplasmic reticulum stress', *Frontiers in molecular biosciences*, 4: 7.

Jackson, Edwin K. 2011. 'The 2′, 3′-cAMP-adenosine pathway', *American Journal of Physiology-Renal Physiology*, 301: F1160-F67.

Jahn, Olaf, Sophie B Siems, Kathrin Kusch, Dörte Hesse, Ramona B Jung, Thomas Liepold, Marina Uecker, Ting Sun, and Hauke B Werner. 2020. 'The CNS myelin proteome: deep profile and persistence after post-mortem delay', *Frontiers in Cellular Neuroscience*, 14: 239.

Jankowsky, Joanna L, Daniel J Fadale, Jeffrey Anderson, Guilian M Xu, Victoria Gonzales, Nancy A Jenkins, Neal G Copeland, Michael K Lee, Linda H Younkin, Steven L Wagner et al. 2004. 'Mutant presenilins specifically elevate the levels of the 42 residue β-amyloid peptide in vivo: evidence for augmentation of a 42-specific γ secretase', *Human molecular genetics* , 13: 159-70.

Jankowsky, Joanna L, Linda H Younkin, Victoria Gonzales, Daniel J Fadale, Hilda H Slunt, Henry A Lester, Steven G Younkin, and David R Borchelt. 2007. 'Rodent Aβ modulates the solubility and distribution of amyloid deposits in transgenic mice', *Journal of Biological Chemistry*, 282: 22707-20.

Janova, Hana, Sahab Arinrad, Evan Balmuth, Marina Mitjans, Johannes Hertel, Mohamad Habes, Robert A Bittner, Hong Pan, Sandra Goebbels, Martin Begemann et al. 2018. 'Microglia ablation alleviates myelin-associated catatonic signs in mice', *The Journal of clinical investigation*, 128: 734-45.

Jansen, Willemijn J, Rik Ossenkoppele, Dirk L Knol, Betty M Tijms, Philip Scheltens, Frans RJ Verhey, Pieter Jelle Visser, Pauline Aalten, Dag Aarsland, Daniel Alcolea et al. 2015. 'Prevalence of cerebral amyloid pathology in persons without dementia: a meta-analysis', *Jama*, 313: 1924-38.

Jawhar, Sadim, Anna Trawicka, Carolin Jenneckens, Thomas A Bayer, and Oliver Wirths. 2012. 'Motor deficits, neuron loss, and reduced anxiety coinciding with axonal degeneration and intraneuronal

Aβ aggregation in the 5XFAD mouse model of Alzheimer's disease', *Neurobiology of aging*, 33: 196. e29-96. e40.

Jay, Taylor R, Anna M Hirsch, Margaret L Broihier, Crystal M Miller, Lee E Neilson, Richard M Ransohoff, Bruce T Lamb, and Gary E Landreth. 2017. 'Disease progression-dependent effects of TREM2 deficiency in a mouse model of Alzheimer's disease', *Journal of Neuroscience*, 37: 637-47.

Jay, Taylor R, Crystal M Miller, Paul J Cheng, Leah C Graham, Shane Bemiller, Margaret L Broihier, Guixiang Xu, Daniel Margevicius, J Colleen Karlo, Gregory L Sousa et al. 2015. 'TREM2 deficiency eliminates TREM2 + inflammatory macrophages and ameliorates pathology in Alzheimer's disease mouse modelsTREM2 expression and function in AD', *The Journal of experimental medicine*, 212: 287-95.

Jepson, Scott, Bryan Vought, Christian H Gross, Lu Gan, Douglas Austen, J Daniel Frantz, Jacque Zwahlen, Derek Lowe, William Markland, and Raul Krauss. 2012. 'LINGO-1, a transmembrane signaling protein, inhibits oligodendrocyte differentiation and myelination through intercellular self-interactions', *Journal of Biological Chemistry*, 287: 22184-95.

Jollès, Jacqueline, Jean-Louis Nussbaum, and Pierre Jollès. 1983. 'Enzymic and chemical fragmentation of the apoprotein of the major rat brain myelin proteolipid: sequence data', *Biochimica et Biophysica Acta (BBA)-Protein Structure and Molecular Enzymology*, 742: 33-38.

Jonsson, Thorlakur, Jasvinder K Atwal, Stacy Steinberg, Jon Snaedal, Palmi V Jonsson, Sigurbjorn Bjornsson, Hreinn Stefansson, Patrick Sulem, Daniel Gudbjartsson, Janice Maloney et al. 2012. 'A mutation in APP protects against Alzheimer's disease and age-related cognitive decline', *Nature*, 488: 96-99.

Jonsson, Thorlakur, Hreinn Stefansson, Stacy Steinberg, Ingileif Jonsdottir, Palmi V Jonsson, Jon Snaedal, Sigurbjorn Bjornsson, Johanna Huttenlocher, Allan I Levey, James J Lah et al. 2013. 'Variant of TREM2 associated with the risk of Alzheimer's disease', *New England Journal of Medicine*, 368: 107-16.

Jorissen, Ellen, Johannes Prox, Christian Bernreuther, Silvio Weber, Ralf Schwanbeck, Lutgarde Serneels, An Snellinx, Katleen Craessaerts, Amantha Thathiah, Ina Tesseur et al. 2010. 'The disintegrin/metalloproteinase ADAM10 is essential for the establishment of the brain cortex', *Journal of Neuroscience*, 30: 4833-44.

Kamal, Adeela, Angels Almenar-Queralt, James F LeBlanc, Elizabeth A Roberts, and Lawrence SB Goldstein. 2001. 'Kinesin-mediated axonal transport of a membrane compartment containing β-secretase and presenilin-1 requires APP', *Nature*, 414: 643-48.

Kamenetz, Flavio, Taisuke Tomita, Helen Hsieh, Guy Seabrook, David Borchelt, Takeshi Iwatsubo, Sangram Sisodia, and Roberto Malinow. 2003. 'APP processing and synaptic function', *Neuron*, 37: 925-37.

Kanekiyo, Takahisa, Huaxi Xu, and Guojun Bu. 2014. 'ApoE and Aβ in Alzheimer's disease: accidental encounters or partners?', *Neuron*, 81: 740-54.

Kanekiyo, Takahisa, Juan Zhang, Qiang Liu, Chia-Chen Liu, Lijuan Zhang, and Guojun Bu. 2011. 'Heparan sulphate proteoglycan and the low-density lipoprotein receptor-related protein 1 constitute major pathways for neuronal amyloid-β uptake', *Journal of Neuroscience*, 31: 1644-51.

Kang, Jie, Hans-Georg Lemaire, Axel Unterbeck, J Michael Salbaum, Colin L Masters, Karl-Heinz Grzeschik, Gerd Multhaup, Konrad Beyreuther, and Benno Müller-Hill. 1987. 'The precursor of Alzheimer's disease amyloid A4 protein resembles a cell-surface receptor', *Nature*, 325: 733-36.

Kantarci, Kejal, Clifford R Jack Jr, Yue Cheng Xu, Norberg G Campeau, Peter C O'Brien, Glenn E Smith, Robert J Ivnik, Bradley F Boeve, Emre Kokmen, Eric G Tangalos et al. 2001. 'Mild cognitive impairment and Alzheimer disease: regional diffusivity of water', *Radiology*, 219: 101-07.

Karim, Saadia A, Jennifer A Barrie, Mailis C McCulloch, Paul Montague, Julia M Edgar, Douglas Kirkham, Thomas J Anderson, Klaus A Nave, Ian R Griffiths, and Mark Mclaughlin. 2007. 'PLP overexpression

perturbs myelin protein composition and myelination in a mouse model of Pelizaeus-Merzbacher disease', *Glia*, 55: 341-51.

Karlawish, Jason, and Joshua D Grill. 2021. 'The approval of Aduhelm risks eroding public trust in Alzheimer research and the FDA', *Nature Reviews Neurology*: 1-2.

Karran, Eric, Marc Mercken, and Bart De Strooper. 2011. 'The amyloid cascade hypothesis for Alzheimer's disease: an appraisal for the development of therapeutics', *Nature reviews Drug discovery*, 10: 698-712.

Keane, Michael, Jeremy Semeiks, Andrew E Webb, Yang I Li, Víctor Quesada, Thomas Craig, Lone Bruhn Madsen, Sipko van Dam, David Brawand, Patrícia I Marques et al. 2015. 'Insights into the evolution of longevity from the bowhead whale genome', *Cell reports*, 10: 112-22.

Keren-Shaul, Hadas, Amit Spinrad, Assaf Weiner, Orit Matcovitch-Natan, Raz Dvir-Szternfeld, Tyler K Ulland, Eyal David, Kuti Baruch, David Lara-Astaiso, Beata Toth et al. 2017. 'A unique microglia type associated with restricting development of Alzheimer's disease', *Cell*, 169: 1276-90. e17.

Kessaris, Nicoletta, Matthew Fogarty, Palma Iannarelli, Matthew Grist, Michael Wegner, and William D Richardson. 2006. 'Competing waves of oligodendrocytes in the forebrain and postnatal elimination of an embryonic lineage', *Nature neuroscience*, 9: 173-79.

Keszycki, Rachel M, Daniel W Fisher, and Hongxin Dong. 2019. 'The hyperactivity–impulsivity–irritiability–disinhibition–aggression–agitation domain in Alzheimer's disease: current management and future directions', *Frontiers in pharmacology*, 10: 1109.

Khrameeva, Ekaterina, Ilia Kurochkin, Dingding Han, Patricia Guijarro, Sabina Kanton, Malgorzata Santel, Zhengzong Qian, Shen Rong, Pavel Mazin, Marat Sabirov. et al 2020. 'Single-cell-resolution transcriptome map of human, chimpanzee, bonobo, and macaque brains', *Genome research*, 30: 776-89.

Kim, Jungsu, Joseph M Castellano, Hong Jiang, Jacob M Basak, Maia Parsadanian, Vi Pham, Stephanie M Mason, Steven M Paul, and David M Holtzman. 2009. 'Overexpression of low-density lipoprotein receptor in the brain markedly inhibits amyloid deposition and increases extracellular Aβ clearance', *Neuron*, 64: 632-44.

Kim, Jungsu, Adam EM Eltorai, Hong Jiang, Fan Liao, Philip B Verghese, Jaekwang Kim, Floy R Stewart, Jacob M Basak, and David M Holtzman. 2012. 'Anti-apoE immunotherapy inhibits amyloid accumulation in a transgenic mouse model of Aβ amyloidosis', *Journal of Experimental Medicine*, 209: 2149-56.

Kim, Jungsu, Hong Jiang, Seonha Park, Adam EM Eltorai, Floy R Stewart, Hyejin Yoon, Jacob M Basak, Mary Beth Finn, and David M Holtzman. 2011. 'Haploinsufficiency of human APOE reduces amyloid deposition in a mouse model of amyloid-β amyloidosis', *Journal of Neuroscience*, 31: 18007-12.

Kimura, Ayano, Saori Hata, and Toshiharu Suzuki. 2016. 'Alternative selection of β-site APP-cleaving enzyme 1 (BACE1) cleavage sites in amyloid β-protein precursor (APP) harboring protective and pathogenic mutations within the Aβ sequence', *Journal of Biological Chemistry*, 291: 24041-53.

Kirby, Leslie, Jing Jin, Jaime Gonzalez Cardona, Matthew D Smith, Kyle A Martin, Jingya Wang, Hayley Strasburger, Leyla Herbst, Maya Alexis, Jodi Karnell et al. 2019. 'Oligodendrocyte precursor cells present antigen and are cytotoxic targets in inflammatory demyelination', *Nature communications*, 10: 1-20.

Kirschner, DA, and AL Ganser. 1980. 'Compact myelin exists in the absence of basic protein in the shiverer mutant mouse', *Nature*, 283: 207-10.

Klein, Stefan, Marius Staring, Keelin Murphy, Max A Viergever, and Josien PW Pluim. 2009. 'Elastix: a toolbox for intensity-based medical image registration', *IEEE transactions on medical imaging*, 29: 196-205.

Kleinberger, Gernot, Yoshinori Yamanishi, Marc Suárez-Calvet, Eva Czirr, Ebba Lohmann, Elise Cuyvers, Hanne Struyfs, Nadine Pettkus, Andrea Wenninger-Weinzierl, Fargol Mazaheri et al. 2014. 'TREM2 mutations implicated in neurodegeneration impair cell surface transport and phagocytosis', *Science translational medicine*, 6: 243ra86-43ra86.

Klimov, Dmitri K, and D Thirumalai. 2003. 'Dissecting the assembly of Aβ16–22 amyloid peptides into antiparallel β sheets', *Structure*, 11: 295-307.

Klingberg, Anika, Anja Hasenberg, Isis Ludwig-Portugall, Anna Medyukhina, Linda Männ, Alexandra Brenzel, Daniel R Engel, Marc Thilo Figge, Christian Kurts, and Matthias Gunzer. 2017. 'Fully automated evaluation of total glomerular number and capillary tuft size in nephritic kidneys using lightsheet microscopy', *Journal of the American Society of Nephrology*, 28: 452-59.

Klugmann, Matthias, Markus H Schwab, Anja Pühlhofer, Armin Schneider, Frank Zimmermann, Ian R Griffiths, and Klaus-Armin Nave. 1997. 'Assembly of CNS myelin in the absence of proteolipid protein', *Neuron*, 18: 59-70.

Kobayashi, K, S Imagama, T Ohgomori, K Hirano, K Uchimura, K Sakamoto, A Hirakawa, H Takeuchi, A Suzumura, and N Ishiguro. 2013. 'Minocycline selectively inhibits M1 polarization of microglia', *Cell death & disease*, 4: e525-e25.

Koenigsknecht-Talboo, Jessica, Melanie Meyer-Luehmann, Maia Parsadanian, Monica Garcia-Alloza, Mary Beth Finn, Bradley T Hyman, Brian J Bacskai, and David M Holtzman. 2008. 'Rapid microglial response around amyloid pathology after systemic anti-Aβ antibody administration in PDAPP mice', *Journal of Neuroscience*, 28: 14156-64.

Koenigsknecht, Jessica, and Gary Landreth. 2004. 'Microglial phagocytosis of fibrillar β-amyloid through a β1 integrin-dependent mechanism', *Journal of Neuroscience*, 24: 9838-46.

Koike, Hisashi, Shigeo Tomioka, Hiroyuki Sorimachi, Takaomi C Saido, Kei Maruyama, Akira Okuyama, Atsuko Fujisawa-sehara, Shigeo Ohno, Koichi Suzuki, and Shoichi Ishiura. 1999. 'Membrane-anchored metalloprotease MDC9 has an α-secretase activity responsible for processing the amyloid precursor protein', *Biochemical Journal*, 343: 371-75.

Koo, Edward H, Sangram S Sisodia, David R Archer, Lee J Martin, Andreas Weidemann, Konrad Beyreuther, Peter Fischer, Colin L Masters, and Donald L Price. 1990. 'Precursor of amyloid protein in Alzheimer disease undergoes fast anterograde axonal transport', *Proceedings of the National Academy of Sciences*, 87: 1561-65.

Koo, Edward H, and Sharon L Squazzo. 1994. 'Evidence that production and release of amyloid beta-protein involves the endocytic pathway', *Journal of Biological Chemistry*, 269: 17386-89.

Kosel, Filip, Jessica MS Pelley, and Tamara B Franklin. 2020. 'Behavioural and psychological symptoms of dementia in mouse models of Alzheimer's disease-related pathology', *Neuroscience & Biobehavioral Reviews*, 112: 634-47.

Krabbe, Grietje, Annett Halle, Vitali Matyash, Jan L Rinnenthal, Gina D Eom, Ulrike Bernhardt, Kelly R Miller, Stefan Prokop, Helmut Kettenmann, and Frank L Heppner. 2013. 'Functional impairment of microglia coincides with Beta-amyloid deposition in mice with Alzheimer-like pathology', *PloS one*, 8: e60921.

Krämer-Albers, EM, N Bretz, S Tenzer, C Winterstein, W Möbius, and H Berger. 2007. 'Nave, KA; Schild, H.; Trotter J. Oligodendrocytes secrete exosomes containing 35 major myelin and stress-protective proteins: Trophic support for axons', *Proteomics 36 Clinical Applications*, 1: 1446-61.

Krämer-Albers, Eva-Maria, Katja Gehrig-Burger, Christoph Thiele, Jacqueline Trotter, and Klaus-Armin Nave. 2006. 'Perturbed interactions of mutant proteolipid protein/DM20 with cholesterol and lipid rafts in oligodendroglia: implications for dysmyelination in spastic paraplegia', *Journal of Neuroscience*, 26: 11743-52.

Krasemann, Susanne, Charlotte Madore, Ron Cialic, Caroline Baufeld, Narghes Calcagno, Rachid El Fatimy, Lien Beckers, Elaine O'Loughlin, Yang Xu, Zain Fanek et al. 2017. 'The TREM2-APOE pathway drives the transcriptional phenotype of dysfunctional microglia in neurodegenerative diseases', *Immunity*, 47: 566-81. e9.

Kreis, Anna, Jana Desloovere, Nuria Suelves, Nathalie Pierrot, Xavier Yerna, Farah Issa, Olivier Schakman, Roberta Gualdani, Marie de Clippele, and Nicolas Tajeddine. 2021. 'Overexpression of wild-type human amyloid precursor protein alters GABAergic transmission', *Scientific reports*, 11: 1-18.

Kuerten, Stefanie, Dilyana A Kostova-Bales, Lukas P Frenzel, Justine T Tigno, Magdalena Tary-Lehmann, Doychin N Angelov, and Paul V Lehmann. 2007. 'MP4-and MOG: 35–55-induced EAE in C57BL/6 mice differentially targets brain, spinal cord and cerebellum', *Journal of neuroimmunology*, 189: 31-40.

Kuhn, Peer-Hendrik, Huanhuan Wang, Bastian Dislich, Alessio Colombo, Ulrike Zeitschel, Joachim W Ellwart, Elisabeth Kremmer, Steffen Roßner, and Stefan F Lichtenthaler. 2010. 'ADAM10 is the physiologically relevant, constitutive α-secretase of the amyloid precursor protein in primary neurons', *The EMBO journal*, 29: 3020-32.

Kullmann, S, F Schweizer, R Veit, A Fritsche, and H Preissl. 2015. 'Compromised white matter integrity in obesity', *Obesity reviews*, 16: 273-81.

Kumar, Arvind, Stefan Rotter, and Ad Aertsen. 2010. 'Spiking activity propagation in neuronal networks: reconciling different perspectives on neural coding', *Nature Reviews Neuroscience*, 11: 615-27.

LaDu, Mary Jo, Michael T Falduto, Arlene M Manelli, Catherine A Reardon, Godfrey S Getz, and Donald E Frail. 1994. 'Isoform-specific binding of apolipoprotein E to beta-amyloid', *Journal of Biological Chemistry*, 269: 23403-06.

Lambert, Mary P, AK Barlow, Brett A Chromy, C Edwards, R Freed, M Liosatos, TE Morgan, I Rozovsky, B Trommer, and Kirsten L Viola. 1998. 'Diffusible, nonfibrillar ligands derived from Aβ1–42 are potent central nervous system neurotoxins', *Proceedings of the National Academy of Sciences*, 95: 6448-53.

Lammich, Sven, Elzbieta Kojro, Rolf Postina, Sandra Gilbert, Roland Pfeiffer, Marek Jasionowski, Christian Haass, and Falk Fahrenholz. 1999. 'Constitutive and regulated α-secretase cleavage of Alzheimer's amyloid precursor protein by a disintegrin metalloprotease', *Proceedings of the National Academy of Sciences*, 96: 3922-27.

Lanctôt, Krista L, Joan Amatniek, Sonia Ancoli-Israel, Steven E Arnold, Clive Ballard, Jiska Cohen-Mansfield, Zahinoor Ismail, Constantine Lyketsos, David S Miller, Erik Musiek et al. 2017. 'Neuropsychiatric signs and symptoms of Alzheimer's disease: New treatment paradigms', *Alzheimer's & Dementia: Translational Research & Clinical Interventions*, 3: 440-49.

Langley, Monica R, Erin M Triplet, and Isobel A Scarisbrick. 2020. 'Dietary influence on central nervous system myelin production, injury, and regeneration', *Biochimica et Biophysica Acta (BBA)-Molecular Basis of Disease*, 1866: 165779.

Lappe-Siefke, Corinna, Sandra Goebbels, Michel Gravel, Eva Nicksch, John Lee, Peter E Braun, Ian R Griffiths, and Klaus-Armin Nave. 2003. 'Disruption of Cnp1 uncouples oligodendroglial functions in axonal support and myelination', *Nature genetics*, 33: 366-74.

Lau, Shun-Fat, Han Cao, Amy KY Fu, and Nancy Y Ip. 2020. 'Single-nucleus transcriptome analysis reveals dysregulation of angiogenic endothelial cells and neuroprotective glia in Alzheimer's disease', *Proceedings of the National Academy of Sciences*, 117: 25800-09.

Laurén, Juha, David A Gimbel, Haakon B Nygaard, John W Gilbert, and Stephen M Strittmatter. 2009. 'Cellular prion protein mediates impairment of synaptic plasticity by amyloid-β oligomers', *Nature*, 457: 1128-32.

Lazarov, Orly, Gerardo A Morfini, Edward B Lee, Mohamed H Farah, Anita Szodorai, Scott R DeBoer, Vassilis E Koliatsos, Stefan Kins, Virginia M-Y Lee, Philip C Wong et al. 2005. 'Axonal transport, amyloid precursor protein, kinesin-1, and the processing apparatus: revisited', *Journal of Neuroscience*, 25: 2386-95.

Lee, Edward B, Bin Zhang, Kangning Liu, Eric A Greenbaum, Robert W Doms, John Q Trojanowski, and Virginia M-Y Lee. 2005. 'BACE overexpression alters the subcellular processing of APP and inhibits Aβ deposition in vivo', *The Journal of cell biology*, 168: 291-302.

Lee, Jiunn-Tay, Jan Xu, Jin-Moo Lee, Grace Ku, Xianlin Han, Ding-I Yang, Shawei Chen, and Chung Y Hsu. 2004. 'Amyloid-β peptide induces oligodendrocyte death by activating the neutral sphingomyelinase–ceramide pathway', *The Journal of cell biology*, 164: 123-31.

Lee, Youngjin, Brett M Morrison, Yun Li, Sylvain Lengacher, Mohamed H Farah, Paul N Hoffman, Yiting Liu, Akivaga Tsingalia, Lin Jin, Ping-Wu Zhang et al. 2012. 'Oligodendroglia metabolically support axons and contribute to neurodegeneration', *Nature*, 487: 443-48.

Lemke, Greg. 1988. 'Unwrapping the genes of myelin', *Neuron*, 1: 535-43.

Lessard, Christian B, Steven L Wagner, and Edward H Koo. 2010. 'And four equals one: Presenilin takes the γ-secretase role by itself', *Proceedings of the National Academy of Sciences*, 107: 21236-37.

Levy, Efrat, Mark D Carman, Ivan J Fernandez-Madrid, Michael D Power, Ivan Lieberburg, Sjoerd G van Duinen, G Th Bots, Willem Luyendijk, and Blas Frangione. 1990. 'Mutation of the Alzheimer's disease amyloid gene in hereditary cerebral hemorrhage, Dutch type', *Science*, 248: 1124-26.

Li, Rena, Kristina Lindholm, Li-Bang Yang, Xu Yue, Martin Citron, Riqiang Yan, Thomas Beach, Lucia Sue, Marwan Sabbagh, and Huaibin Cai. 2004. 'Amyloid β peptide load is correlated with increased β-secretase activity in sporadic Alzheimer's disease patients', *Proceedings of the National Academy of Sciences*, 101: 3632-37.

Li, Yue-Ming, Ming-Tain Lai, Min Xu, Qian Huang, Jillian DiMuzio-Mower, Mohinder K Sardana, Xiao-Ping Shi, Kuo-Chang Yin, Jules A Shafer, and Stephen J Gardell. 2000. 'Presenilin 1 is linked with γ-secretase activity in the detergent solubilized state', *Proceedings of the National Academy of Sciences*, 97: 6138-43.

Li, Yue-Ming, Min Xu, Ming-Tain Lai, Qian Huang, José L Castro, Jillian DiMuzio-Mower, Timothy Harrison, Colin Lellis, Alan Nadin, Joseph G Neduvelil et al. 2000. 'Photoactivated γ-secretase inhibitors directed to the active site covalently label presenilin 1', *Nature* , 405: 689-94.

Li, Zhenzhong, Youyi Zhang, Daqing Li, and Yue Feng. 2000. 'Destabilization and mislocalization of myelin basic protein mRNAs in quaking dysmyelination lacking the QKI RNA-binding proteins', *Journal of Neuroscience*, 20: 4944-53.

Liao, Yang, Gordon K Smyth, and Wei Shi. 2014. 'featureCounts: an efficient general purpose program for assigning sequence reads to genomic features', *Bioinformatics*, 30: 923-30.

Liebmann, Thomas, Nicolas Renier, Karima Bettayeb, Paul Greengard, Marc Tessier-Lavigne, and Marc Flajolet. 2016. 'Three-dimensional study of Alzheimer's disease hallmarks using the iDISCO clearing method', *Cell reports*, 16: 1138-52.

Lingwood, Daniel, and Kai Simons. 2010. 'Lipid rafts as a membrane-organizing principle', *Science*, 327: 46-50.

Lintl, P, and H Braak. 1983. 'Loss of intracortical myelinated fibers: a distinctive age-related alteration in the human striate area', *Acta neuropathologica*, 61: 178-82.

Liu, Chia-Chen, Takahisa Kanekiyo, Huaxi Xu, and Guojun Bu. 2013. 'Apolipoprotein E and Alzheimer disease: risk, mechanisms and therapy', *Nature Reviews Neurology*, 9: 106-18.

Liu, Chia-Chen, Na Zhao, Yuan Fu, Na Wang, Cynthia Linares, Chih-Wei Tsai, and Guojun Bu. 2017. 'ApoE4 accelerates early seeding of amyloid pathology', *Neuron*, 96: 1024-32. e3.

Liu, Pei-Pei, Yi Xie, Xiao-Yan Meng, and Jian-Sheng Kang. 2019. 'History and progress of hypotheses and clinical trials for Alzheimer's disease', *Signal transduction and targeted therapy*, 4: 1-22.

Liu, Zhiqiang, Carlo Condello, Aaron Schain, Roa Harb, and Jaime Grutzendler. 2010. 'CX3CR1 in microglia regulates brain amyloid deposition through selective protofibrillar amyloid-β phagocytosis', *Journal of Neuroscience*, 30: 17091-101.

Louie, Allison, Justin Kim, Katiria Soto-Diaz, Payam Dibaeinia, Hisami Koito, Saurabh Sinha, Romana Nowak, Aditi Das, and Andrew Steelman. 2021. 'Influenza causes alterations to oligodendrocyte-specific transcripts and the myelin lipidome in the adult mouse central nervous system'.

Love, Michael I, Wolfgang Huber, and Simon Anders. 2014. 'Moderated estimation of fold change and dispersion for RNA-seq data with DESeq2', *Genome biology*, 15: 1-21.

Lu, Jun-Xia, Wei Qiang, Wai-Ming Yau, Charles D Schwieters, Stephen C Meredith, and Robert Tycko. 2013. 'Molecular structure of β-amyloid fibrils in Alzheimer's disease brain tissue', *Cell*, 154: 1257-68.

Lu, Q Richard, Tao Sun, Zhimin Zhu, Nan Ma, Meritxell Garcia, Charles D Stiles, and David H Rowitch. 2002. 'Common developmental requirement for Olig function indicates a motor neuron/oligodendrocyte connection', *Cell*, 109: 75-86.

Luczynski, Pauline, Cornelia Laule, Ging-Yuek Robin Hsiung, GR Wayne Moore, and Helen Tremlett. 2019. 'Coexistence of Multiple Sclerosis and Alzheimer's disease: A review', *Multiple sclerosis and related disorders*, 27: 232-38.

Lüders, Katja A, Stefan Nessler, Kathrin Kusch, Julia Patzig, Ramona B Jung, Wiebke Möbius, Klaus-Armin Nave, and Hauke B Werner. 2019. 'Maintenance of high proteolipid protein level in adult central nervous system myelin is required to preserve the integrity of myelin and axons', *Glia*, 67: 634-49.

Lüders, Katja A, Julia Patzig, Mikael Simons, Klaus-Armin Nave, and Hauke B Werner. 2017. 'Genetic dissection of oligodendroglial and neuronal Plp1 function in a novel mouse model of spastic paraplegia type 2', *Glia*, 65: 1762-76.

Luengo-Fernandez, R, J Leal, and AM Gray. 'UK Research Expenditure on Dementia', *Heart Disease, Stroke and Cancer: Are Levels of Spending Related to Disease Burden*: 149-54.

Lührs, Thorsten, Christiane Ritter, Marc Adrian, Dominique Riek-Loher, Bernd Bohrmann, Heinz Döbeli, David Schubert, and Roland Riek. 2005. '3D structure of Alzheimer's amyloid-β (1–42) fibrils', *Proceedings of the National Academy of Sciences*, 102: 17342-47.

Luo, Yi, Brad Bolon, Steve Kahn, Brian D Bennett, Safura Babu-Khan, Paul Denis, Wei Fan, Hue Kha, Jianhua Zhang, Yunhua Gong et al. 2001. 'Mice deficient in BACE1, the Alzheimer's β-secretase, have normal phenotype and abolished β-amyloid generation', *Nature neuroscience* , 4: 231-32.

Ma, Jianyi, Ann Yee, H Bryan Brewer, Saumya Das, and Huntington Potter. 1994. 'Amyloid-associated proteins α 1-antichymotrypsin and apolipoprotein E promote assembly of Alzheimer β-protein into filaments', *Nature*, 372: 92-94.

Ma, Jing, Jin-Tai Yu, and Lan Tan. 2015. 'MS4A cluster in Alzheimer's disease', *Molecular neurobiology*, 51: 1240-48.

Maier-Hein, Klaus H, Carl-Fredrik Westin, Martha E Shenton, Michael W Weiner, Ashish Raj, Philipp Thomann, Ron Kikinis, Bram Stieltjes, and Ofer Pasternak. 2015. 'Widespread white matter degeneration preceding the onset of dementia', *Alzheimer's & Dementia*, 11: 485-93. e2.

Makin, Simon. 2018. 'The amyloid hypothesis on trial', *Nature*, 559: S4-S4.

March, M, F Biddle, and JR Miller. 1973. 'Research news: an apparently new mutation', *Mouse Newslett*, 48: 24.

Marner, Lisbeth, Jens R Nyengaard, Yong Tang, and Bente Pakkenberg. 2003. 'Marked loss of myelinated nerve fibers in the human brain with age', *Journal of comparative neurology*, 462: 144-52.

Marques, Sueli, Amit Zeisel, Simone Codeluppi, David van Bruggen, Ana Mendanha Falcão, Lin Xiao, Huiliang Li, Martin Häring, Hannah Hochgerner, Roman A Romanov et al. 2016. 'Oligodendrocyte heterogeneity in the mouse juvenile and adult central nervous system', *Science*, 352: 1326-29.

Maruyama, Kei, Fuyuki Kametani, Mihoko Usami, Wakako Yamao-Harigaya, and Kikuko Tanaka. 1991. '"Secretase," Alzheimer amyloid protein precursor secreting enzyme is not sequence-specific', *Biochemical and biophysical research communications*, 179: 1670-76.

Masters, Colin L, Gail Simms, Nicola A Weinman, Gerd Multhaup, Brian L McDonald, and Konrad Beyreuther. 1985. 'Amyloid plaque core protein in Alzheimer disease and Down syndrome', *Proceedings of the National Academy of Sciences*, 82: 4245-49.

Mathys, Hansruedi, Jose Davila-Velderrain, Zhuyu Peng, Fan Gao, Shahin Mohammadi, Jennie Z Young, Madhvi Menon, Liang He, Fatema Abdurrob, Xueqiao Jiang et al. 2019. 'Single-cell transcriptomic analysis of Alzheimer's disease', *Nature*, 570: 332-37.

Maurer, Konrad, Stephan Volk, and Hector Gerbaldo. 1997. 'Auguste D and Alzheimer's disease', *The lancet*, 349: 1546-49.

Mayo, Chantel D, Erin L Mazerolle, Lesley Ritchie, John D Fisk, Jodie R Gawryluk, and Alzheimer's Disease Neuroimaging Initiative. 2017. 'Longitudinal changes in microstructural white matter metrics in Alzheimer's disease', *NeuroImage: Clinical*, 13: 330-38.

McGowan, Eileen, Fiona Pickford, Jungsu Kim, Luisa Onstead, Jason Eriksen, Cindy Yu, Lisa Skipper, M Paul Murphy, Jenny Beard, Pritam Das et al. 2005. 'Aβ42 is essential for parenchymal and vascular amyloid deposition in mice', *Neuron* , 47: 191-99.

McInnes, Leland, John Healy, and James Melville. 2018. 'Umap: Uniform manifold approximation and projection for dimension reduction', *arXiv preprint arXiv:1802.03426*.

McIver, Sally R, Megan Muccigrosso, Ernesto R Gonzales, Jin-Moo Lee, Marie S Roberts, Mark S Sands, and Mark P Goldberg. 2010. 'Oligodendrocyte degeneration and recovery after focal cerebral ischemia', *Neuroscience*, 169: 1364-75.

Mei, Feng, Stephen PJ Fancy, Yun-An A Shen, Jianqin Niu, Chao Zhao, Bryan Presley, Edna Miao, Seonok Lee, Sonia R Mayoral, Stephanie A Redmond et al. 2014. 'Micropillar arrays as a high-throughput screening platform for therapeutics in multiple sclerosis', *Nature medicine*, 20: 954-60.

Mei, Feng, Klaus Lehmann-Horn, Yun-An A Shen, Kelsey A Rankin, Karin J Stebbins, Daniel S Lorrain, Kara Pekarek, Sharon A Sagan, Lan Xiao, Cory Teuscher et al. 2016. 'Accelerated remyelination during inflammatory demyelination prevents axonal loss and improves functional recovery', *Elife*, 5: e18246.

Merkler, Doron, Tristan Ernsting, Martin Kerschensteiner, Wolfgang Brück, and Christine Stadelmann. 2006. 'A new focal EAE model of cortical demyelination: multiple sclerosis-like lesions with rapid resolution of inflammation and extensive remyelination', *Brain*, 129: 1972-83.

Meschkat, Martin, Anna Maria Steyer, Marie-Theres Weil, Kathrin Kusch, Olaf Jahn, Lars Piepkorn, Paola Agüi-Gonzalez, Nhu TN Phan, Torben Ruhwedel, Boguslawa Sadowski et al. 2020. 'White matter integrity requires continuous myelin synthesis at the inner tongue', *bioRxiv*.

Meyer-Luehmann, Melanie, Tara L Spires-Jones, Claudia Prada, Monica Garcia-Alloza, Alix De Calignon, Anete Rozkalne, Jessica Koenigsknecht-Talboo, David M Holtzman, Brian J Bacskai, and Bradley T Hyman. 2008. 'Rapid appearance and local toxicity of amyloid-β plaques in a mouse model of Alzheimer's disease', *Nature*, 451: 720-24.

Meyer, Niklas, Nadine Richter, Zoya Fan, Gabrielle Siemonsmeier, Tatyana Pivneva, Philipp Jordan, Christian Steinhäuser, Marcus Semtner, Christiane Nolte, and Helmut Kettenmann. 2018.

'Oligodendrocytes in the mouse corpus callosum maintain axonal function by delivery of glucose', *Cell reports*, 22: 2383-94.

Mi, Sha, Robert H Miller, Xinhua Lee, Martin L Scott, Svetlane Shulag-Morskaya, Zhaohui Shao, Jufang Chang, Greg Thill, Melissa Levesque, Mingdi Zhang et al. 2005. 'LINGO-1 negatively regulates myelination by oligodendrocytes', *Nature neuroscience*, 8: 745-51.

Micheva, Kristina D, Edward F Chang, Alissa L Nana, William W Seeley, Jonathan T Ting, and Charles Cobbs. 2018. 'Distinctive structural and molecular features of myelinated inhibitory axons in human neocortex', *Eneuro*, 5.

Micheva, Kristina D, Dylan Wolman, Brett D Mensh, Elizabeth Pax, JoAnn Buchanan, Stephen J Smith, and Davi D Bock. 2016. 'A large fraction of neocortical myelin ensheathes axons of local inhibitory neurons', *Elife*, 5: e15784.

Milner, Robert J, Cary Lai, Klaus-Armin Nave, Dominique Lenoir, Judy Ogata, and J Gregor Sutcliffe. 1985. 'Nucleotide sequences of two mRNAs for rat brain myelin proteolipid protein', *Cell*, 42: 931-39.

Milner, Robert J, and J Gregor Sutcliffe. 1983. 'Gene expression in rat brain', *Nucleic acids research*, 11: 5497-520.

Mitew, Stanislaw, Matthew TK Kirkcaldie, Glenda M Halliday, Claire E Shepherd, James C Vickers, and Tracey C Dickson. 2010. 'Focal demyelination in Alzheimer's disease and transgenic mouse models', *Acta neuropathologica*, 119: 567-77.

Molbay, Muge, Zeynep Ilgin Kolabas, Mihail Ivilinov Todorov, Tzu-Lun Ohn, and Ali Ertürk. 2021. 'A guidebook for DISCO tissue clearing', *Molecular Systems Biology*, 17: e9807.

Monoh, Katsumi, Tadashi Kurihara, Yasuo Takahashi, Tomio Ichikawa, Toshiro Kumanishi, Shigenobu Hayashi, Shinsei Minoshima, and Nobuyoshi Shimizu. 1993. 'Structure, expression and chromosomal localization of the gene encoding human 2', S'-cyclic-nucleotide S'-phosphodiesterase', *Gene*, 129: 297-301.

Mota, Bruno, and Suzana Herculano-Houzel. 2015. 'Cortical folding scales universally with surface area and thickness, not number of neurons', *Science*, 349: 74-77.

Mucke, Lennart, Eliezer Masliah, Gui-Qiu Yu, Margaret Mallory, Edward M Rockenstein, Gwen Tatsuno, Kang Hu, Dora Kholodenko, Kelly Johnson-Wood, and Lisa McConlogue. 2000. 'High-level neuronal expression of Aβ1–42 in wild-type human amyloid protein precursor transgenic mice: synaptotoxicity without plaque formation', *Journal of Neuroscience*, 20: 4050-58.

Mukherjee, Chaitali, Tina Kling, Belisa Russo, Kerstin Miebach, Eva Kess, Martina Schifferer, Liliana D Pedro, Ulrich Weikert, Maryam K Fard, Nirmal Kannaiyan et al. 2020. 'Oligodendrocytes provide antioxidant defense function for neurons by secreting ferritin heavy chain', *Cell metabolism*, 32: 259-72. e10.

Mullan, Mike, Fiona Crawford, Karin Axelman, Henry Houlden, Lena Lilius, Bengt Winblad, and Lars Lannfelt. 1992. 'A pathogenic mutation for probable Alzheimer's disease in the APP gene at the N–terminus of β–amyloid', *Nature genetics*, 1: 345-47.

Munsch, Fanny, Gopal Varma, Manuel Taso, Olivier Girard, Arnaud Guidon, Guillaume Duhamel, and David C Alsop. 2021. 'Characterization of the cortical myeloarchitecture with inhomogeneous magnetization transfer imaging (ihMT)', *Neuroimage*, 225: 117442.

Murrell, Jill, Martin Farlow, Bernardino Ghetti, and Merrill D Benson. 1991. 'A mutation in the amyloid precursor protein associated with hereditary Alzheimer's disease', *Science*, 254: 97-99.

Myllykoski, Matti, Arne Raasakka, Huijong Han, and Petri Kursula. 2012. 'Myelin 2′, 3′-cyclic nucleotide 3′-phosphodiesterase: active-site ligand binding and molecular conformation', *PloS one*, 7: e32336.

Nag, TC, and Shashi Wadhwa. 2012. 'Accumulation of lipid inclusions in astrocytes of aging human optic nerve', *Acta Biologica Hungarica*, 63: 54-64.

Nave, Klaus-Armin. 2010. 'Myelination and support of axonal integrity by glia', *Nature*, 468: 244-52.

Nave, Klaus-Armin, Cary Lai, Floyd E Bloom, and Robert J Milner. 1986. 'Jimpy mutant mouse: a 74-base deletion in the mRNA for myelin proteolipid protein and evidence for a primary defect in RNA splicing', *Proceedings of the National Academy of Sciences*, 83: 9264-68.

Nave, Klaus-Armin, Cary Lai, Floyd E Bloom, and Robert J Milner. 1987. 'Splice site selection in the proteolipid protein (PLP) gene transcript and primary structure of the DM-20 protein of central nervous system myelin', *Proceedings of the National Academy of Sciences*, 84: 5665-69.

Niederst, Emily D, Sol M Reyna, and Lawrence SB Goldstein. 2015. 'Axonal amyloid precursor protein and its fragments undergo somatodendritic endocytosis and processing', *Molecular biology of the cell*, 26: 205-17.

Nikić, Ivana, Doron Merkler, Catherine Sorbara, Mary Brinkoetter, Mario Kreutzfeldt, Florence M Bareyre, Wolfgang Brück, Derron Bishop, Thomas Misgeld, and Martin Kerschensteiner. 2011. 'A reversible form of axon damage in experimental autoimmune encephalomyelitis and multiple sclerosis', *Nature medicine*, 17: 495-99.

Nilsberth, Camilla, Anita Westlind-Danielsson, Christopher B Eckman, Margaret M Condron, Karin Axelman, Charlotte Forsell, Charlotte Stenh, Johan Luthman, David B Teplow, Steven G Younkin et al. 2001. 'The'Arctic'APP mutation (E693G) causes Alzheimer's disease by enhanced Aβ protofibril formation', *Nature neuroscience* , 4: 887-93.

Nugent, Alicia A, Karin Lin, Bettina Van Lengerich, Steve Lianoglou, Laralynne Przybyla, Sonnet S Davis, Ceyda Llapashtica, Junhua Wang, Dan Xia, and Anthony Lucas. 2020. 'TREM2 regulates microglial cholesterol metabolism upon chronic phagocytic challenge', *Neuron*, 105: 837-54. e9.

O'Connor, Tracy, Katherine R Sadleir, Erika Maus, Rodney A Velliquette, Jie Zhao, Sarah L Cole, William A Eimer, Brian Hitt, Leslie A Bembinster, Sven Lammich et al. 2008. 'Phosphorylation of the translation initiation factor eIF2α increases BACE1 levels and promotes amyloidogenesis', *Neuron* , 60: 988-1009.

O'Neill, Ryan C, Jeffrey Minuk, Martha E Cox, Peter E Braun, and Michel Gravel. 1997. 'CNP2 mRNA directs synthesis of both CNP1 and CNP2 polypeptides', *Journal of neuroscience research*, 50: 248-57.

O'Donnell, Lauren J, and Carl-Fredrik Westin. 2011. 'An introduction to diffusion tensor image analysis', *Neurosurgery Clinics*, 22: 185-96.

O'Sullivan, MRCP, Derek K Jones, PE Summers, RG Morris, SCR Williams, and HS Markus. 2001. 'Evidence for cortical "disconnection" as a mechanism of age-related cognitive decline', *Neurology*, 57: 632-38.

Oakley, Holly, Sarah L Cole, Sreemathi Logan, Erika Maus, Pei Shao, Jeffery Craft, Angela Guillozet-Bongaarts, Masuo Ohno, John Disterhoft, Linda Van Eldik et al. 2006. 'Intraneuronal β-amyloid aggregates, neurodegeneration, and neuron loss in transgenic mice with five familial Alzheimer's disease mutations: potential factors in amyloid plaque formation', *Journal of Neuroscience*, 26: 10129-40.

Oddo, Salvatore, Antonella Caccamo, Jason D Shepherd, M Paul Murphy, Todd E Golde, Rakez Kayed, Raju Metherate, Mark P Mattson, Yama Akbari, and Frank M LaFerla. 2003. 'Triple-transgenic model of Alzheimer's disease with plaques and tangles: intracellular Aβ and synaptic dysfunction', *Neuron*, 39: 409-21.

Oltersdorf, T, PJ Ward, T Henriksson, EC Beattie, R Neve, I Lieberburg, and LC Fritz. 1990. 'The Alzheimer amyloid precursor protein. Identification of a stable intermediate in the biosynthetic/degradative pathway', *Journal of Biological Chemistry*, 265: 4492-97.

Ou-Yang, Ming-Hsuan, and William E Van Nostrand. 2013. 'The absence of myelin basic protein promotes neuroinflammation and reduces amyloid β-protein accumulation in Tg-5xFAD mice', *Journal of neuroinflammation*, 10: 1-12.

Palesi, Fulvia, Andrea De Rinaldis, Paolo Vitali, Gloria Castellazzi, Letizia Casiraghi, Giancarlo Germani, Sara Bernini, Nicoletta Anzalone, Matteo Cotta Ramusino, Federica M Denaro et al. 2018. 'Specific patterns of white matter alterations help distinguishing Alzheimer's and vascular dementia', *Frontiers in neuroscience*, 12: 274.

Paquola, Casey, Richard AI Bethlehem, Jakob Seidlitz, Konrad Wagstyl, Rafael Romero-Garcia, Kirstie J Whitaker, Reinder Vos De Wael, Guy B Williams, Petra E Vértes, Daniel S Margulies et al. 2019. 'Shifts in myeloarchitecture characterise adolescent development of cortical gradients', *Elife*, 8: e50482.

Paravastu, Anant K, Richard D Leapman, Wai-Ming Yau, and Robert Tycko. 2008. 'Molecular structural basis for polymorphism in Alzheimer's β-amyloid fibrils', *Proceedings of the National Academy of Sciences*, 105: 18349-54.

Paresce, Donata M, Haeyong Chung, and Frederick R Maxfield. 1997. 'Slow degradation of aggregates of the Alzheimer's disease amyloid β-protein by microglial cells', *Journal of Biological Chemistry*, 272: 29390-97.

Paresce, Donata M, Richik N Ghosh, and Frederick R Maxfield. 1996. 'Microglial cells internalize aggregates of the Alzheimer's disease amyloid β-protein via a scavenger receptor', *Neuron*, 17: 553-65.

Parhizkar, Samira, Thomas Arzberger, Matthias Brendel, Gernot Kleinberger, Maximilian Deussing, Carola Focke, Brigitte Nuscher, Monica Xiong, Alireza Ghasemigharagoz, Natalie Katzmarski et al. 2019. 'Loss of TREM2 function increases amyloid seeding but reduces plaque-associated ApoE', *Nature neuroscience*, 22: 191-204.

Perez, Sylvia E, Chet C Sherwood, Michael R Cranfield, Joseph M Erwin, Antoine Mudakikwa, Patrick R Hof, and Elliott J Mufson. 2016. 'Early Alzheimer's disease–type pathology in the frontal cortex of wild mountain gorillas (Gorilla beringei beringei)', *Neurobiology of aging*, 39: 195-201.

Peters, Alan. 2002. 'The effects of normal aging on myelin and nerve fibers: a review', *Journal of neurocytology*, 31: 581-93.

Peters, Alan. 2009. 'The effects of normal aging on myelinated nerve fibers in monkey central nervous system', *Frontiers in neuroanatomy*, 3: 11.

Peters, Alan, and Claire Sethares. 2002. 'Aging and the myelinated fibers in prefrontal cortex and corpus callosum of the monkey', *Journal of comparative neurology*, 442: 277-91.

Peters, Alan, and Claire Sethares. 2003. 'Is there remyelination during aging of the primate central nervous system?', *Journal of comparative neurology*, 460: 238-54.

Peters, Alan, and Claire Sethares. 2004. 'Oligodendrocytes, their progenitors and other neuroglial cells in the aging primate cerebral cortex', *Cerebral cortex*, 14: 995-1007.

Petkova, Aneta T, Yoshitaka Ishii, John J Balbach, Oleg N Antzutkin, Richard D Leapman, Frank Delaglio, and Robert Tycko. 2002. 'A structural model for Alzheimer's β-amyloid fibrils based on experimental constraints from solid state NMR', *Proceedings of the National Academy of Sciences*, 99: 16742-47.

Petkova, Aneta T, Wai-Ming Yau, and Robert Tycko. 2006. 'Experimental constraints on quaternary structure in Alzheimer's β-amyloid fibrils', *Biochemistry*, 45: 498-512.

Philips, Thomas, Yevgeniya A Mironova, Yan Jouroukhin, Jeannie Chew, Svetlana Vidensky, Mohamed H Farah, Mikhail V Pletnikov, Dwight E Bergles, Brett M Morrison, and Jeffrey D Rothstein. 2021. 'MCT1 deletion in oligodendrocyte lineage cells causes late-onset hypomyelination and axonal degeneration', *Cell reports*, 34: 108610.

Poitelon, Yannick, Ashley M Kopec, and Sophie Belin. 2020. 'Myelin fat facts: an overview of lipids and fatty acid metabolism', *Cells*, 9: 812.

Poliani, Pietro Luigi, Yaming Wang, Elena Fontana, Michelle L Robinette, Yoshinori Yamanishi, Susan Gilfillan, and Marco Colonna. 2015. 'TREM2 sustains microglial expansion during aging and response to demyelination', *The Journal of clinical investigation*, 125: 2161-70.

Ponte, P, P Gonzalez DeWhitt, J Schilling, J Miller, D Hsu, B Greenberg, K Davis, W Wallace, I Lieberburg, and F Fuller. 1988. 'A new A4 amyloid mRNA contains a domain homologous to serine proteinase inhibitors', *Nature*, 331: 525-27.

Portelius, Erik, Nenad Bogdanovic, Mikael K Gustavsson, Inga Volkmann, Gunnar Brinkmalm, Henrik Zetterberg, Bengt Winblad, and Kaj Blennow. 2010. 'Mass spectrometric characterization of brain amyloid beta isoform signatures in familial and sporadic Alzheimer's disease', *Acta neuropathologica*, 120: 185-93.

Prince, Martin James, Anders Wimo, Maelenn Mari Guerchet, Gemma Claire Ali, Yu-Tzu Wu, and Matthew Prina. 2015. 'World Alzheimer Report 2015-The Global Impact of Dementia: An analysis of prevalence, incidence, cost and trends'.

Prins, Niels D, and Philip Scheltens. 2015. 'White matter hyperintensities, cognitive impairment and dementia: an update', *Nature Reviews Neurology*, 11: 157-65.

Prpar Mihevc, Sonja, and Gregor Majdič. 2019. 'Canine Cognitive Dysfunction and Alzheimer's Disease–Two Facets of the Same Disease?', *Frontiers in neuroscience*, 13: 604.

Qiang, Wei, Wai-Ming Yau, Yongquan Luo, Mark P Mattson, and Robert Tycko. 2012. 'Antiparallel β-sheet architecture in Iowa-mutant β-amyloid fibrils', *Proceedings of the National Academy of Sciences*, 109: 4443-48.

Qiu, Chengxuan, Miia Kivipelto, and Eva von Strauss. 2009. 'Epidemiology of Alzheimer's disease: occurrence, determinants, and strategies toward intervention', *Dialogues in clinical neuroscience*, 11: 111.

Quintela-López, Tania, Carolina Ortiz-Sanz, Mari Paz Serrano-Regal, Adhara Gaminde-Blasco, Jorge Valero, Jimena Baleriola, Maria Victoria Sánchez-Gómez, Carlos Matute, and Elena Alberdi. 2019. 'Aβ oligomers promote oligodendrocyte differentiation and maturation via integrin β1 and Fyn kinase signaling', *Cell death & disease*, 10: 1-16.

Raasakka, Arne, and Petri Kursula. 2014. 'The myelin membrane-associated enzyme 2′, 3′-cyclic nucleotide 3′-phosphodiesterase: on a highway to structure and function', *Neuroscience bulletin*, 30: 956-66.

Raasakka, Arne, Salla Ruskamo, Julia Kowal, Robert Barker, Anne Baumann, Anne Martel, Jussi Tuusa, Matti Myllykoski, Jochen Bürck, Anne S Ulrich et al. 2017. 'Membrane association landscape of myelin basic protein portrays formation of the myelin major dense line', *Scientific reports*, 7: 1-18.

Racine, Annie M, Nagesh Adluru, Andrew L Alexander, Bradley T Christian, Ozioma C Okonkwo, Jennifer Oh, Caitlin A Cleary, Alex Birdsill, Ansel T Hillmer, Dhanabalan Murali. et al 2014. 'Associations between white matter microstructure and amyloid burden in preclinical Alzheimer's disease: a multimodal imaging investigation', *NeuroImage: Clinical*, 4: 604-14.

Radde, Rebecca, Tristan Bolmont, Stephan A Kaeser, Janaky Coomaraswamy, Dennis Lindau, Lars Stoltze, Michael E Calhoun, Fabienne Jäggi, Hartwig Wolburg, Simon Gengler et al. 2006. 'Aβ42-driven cerebral amyloidosis in transgenic mice reveals early and robust pathology', *EMBO reports* , 7: 940-46.

Raj, Divya, Zhuoran Yin, Marjolein Breur, Janine Doorduin, Inge R Holtman, Marta Olah, Ietje J Mantingh-Otter, Debby Van Dam, Peter P De Deyn, Wilfred den Dunnen. et al 2017. 'Increased white matter inflammation in aging-and Alzheimer's disease brain', *Frontiers in molecular neuroscience*, 10: 206.

Rajendran, Lawrence, Masanori Honsho, Tobias R Zahn, Patrick Keller, Kathrin D Geiger, Paul Verkade, and Kai Simons. 2006. 'Alzheimer's disease β-amyloid peptides are released in association with exosomes', *Proceedings of the National Academy of Sciences*, 103: 11172-77.

Rasband, Matthew N, and Elior Peles. 2016. 'The nodes of Ranvier: molecular assembly and maintenance', *Cold Spring Harbor Perspectives in Biology*, 8: a020495.

Readhead, Ben, Jean-Vianney Haure-Mirande, Cory C Funk, Matthew A Richards, Paul Shannon, Vahram Haroutunian, Mary Sano, Winnie S Liang, Noam D Beckmann, Nathan D Price et al. 2018. 'Multiscale analysis of independent Alzheimer's cohorts finds disruption of molecular, genetic, and clinical networks by human herpesvirus', *Neuron*, 99: 64-82. e7.

Redlich, E. 1898. 'Uber miliare Sklerose der Hirnrinde bei seniler Atrophie', *Jahrb Psychiatry Neurol*, 17: 208-16.

Reisberg, Barry, Emile H Franssen, Syed Mahmood Hasan, Isabel Monteiro, Istvan Boksay, Liduin EM Souren, Sunnie Kenowsky, Stefanie R Auer, Shahid Elahi, and Alan Kluger. 1999. 'Retrogenesis: clinical, physiologic, and pathologic mechanisms in brain aging, Alzheimer's and other dementing processes', *European Archives of Psychiatry and Clinical Neuroscience*, 249: S28-S36.

Renier, Nicolas, Zhuhao Wu, David J Simon, Jing Yang, Pablo Ariel, and Marc Tessier-Lavigne. 2014. 'iDISCO: a simple, rapid method to immunolabel large tissue samples for volume imaging', *Cell*, 159: 896-910.

Réu, Pedro, Azadeh Khosravi, Samuel Bernard, Jeff E Mold, Mehran Salehpour, Kanar Alkass, Shira Perl, John Tisdale, Göran Possnert, Henrik Druid et al. 2017. 'The lifespan and turnover of microglia in the human brain', *Cell reports*, 20: 779-84.

Reutskiy, Sergiy, Enrico Rossoni, and Brunello Tirozzi. 2003. 'Conduction in bundles of demyelinated nerve fibers: computer simulation', *Biological cybernetics*, 89: 439-48.

Rice, Heather C, Gabriele Marcassa, Iordana Chrysidou, Katrien Horré, Tracy L Young-Pearse, Ulrike C Müller, Takashi Saito, Takaomi C Saido, Robert Vassar, Joris De Wit et al. 2020. 'Contribution of GABAergic interneurons to amyloid-β plaque pathology in an APP knock-in mouse model', *Molecular neurodegeneration*, 15: 1-8.

Ringman, John M, Joseph O'Neill, Daniel Geschwind, Luis Medina, Liana G Apostolova, Yaneth Rodriguez, Barbara Schaffer, Arousiak Varpetian, Benjamin Tseng, Freddy Ortiz et al. 2007. 'Diffusion tensor imaging in preclinical and presymptomatic carriers of familial Alzheimer's disease mutations', *Brain*, 130: 1767-76.

Roach, Arthur, Kevin Boylan, Suzanna Horvath, Stanley B Prusiner, and Leroy E Hood. 1983. 'Characterization of cloned cDNA representing rat myelin basic protein: absence of expression in brain of shiverer mutant mice', *Cell*, 34: 799-806.

Rodrigues, Belina, Ana Coelho, Carlos Portugal-Nunes, Ricardo Magalhães, Pedro Silva Moreira, Teresa Costa Castanho, Liliana Amorim, Paulo Marques, José Miguel Soares, Nuno Sousa et al. 2020. 'Higher adherence to the Mediterranean diet is associated with preserved white matter integrity and altered structural connectivity', *Frontiers in neuroscience*, 14: 786.

Rogaev, EI, R Sherrington, EA Rogaeva, G Levesque, M Ikeda, Y Liang, H Chi, C Lin, K Holman, and T Tsuda. 1995. 'Familial Alzheimer's disease in kindreds with missense mutations in a gene on chromosome 1 related to the Alzheimer's disease type 3 gene', *Nature*, 376: 775-78.

Rosenbluth, Jack. 1999. 'A brief history of myelinated nerve fibers: one hundred and fifty years of controversy', *Journal of neurocytology*, 28: 251-62.

Rosenbluth, Jack, Klaus-Armin Nave, Amanda Mierzwa, and Rolf Schiff. 2006. 'Subtle myelin defects in PLP-null mice', *Glia*, 54: 172-82.

Roth, Alejandro D, Gigliola Ramírez, Rodrigo Alarcón, and Rommy Von Bernhardi. 2005. 'Oligodendrocytes damage in Alzheimer's disease: beta amyloid toxicity and inflammation', *Biological research*, 38: 381-87.

Saab, Aiman S, Iva D Tzvetavona, Andrea Trevisiol, Selva Baltan, Payam Dibaj, Kathrin Kusch, Wiebke Möbius, Bianka Goetze, Hannah M Jahn, Wenhui Huang et al. 2016. 'Oligodendroglial NMDA receptors regulate glucose import and axonal energy metabolism', *Neuron*, 91: 119-32.

Sadleir, Katherine R, Patty C Kandalepas, Virginie Buggia-Prévot, Daniel A Nicholson, Gopal Thinakaran, and Robert Vassar. 2016. 'Presynaptic dystrophic neurites surrounding amyloid plaques are sites of microtubule disruption, BACE1 elevation, and increased Aβ generation in Alzheimer's disease', Acta neuropathologica, *Acta neuropathologica*, 132: 235-56.

Sadowski, Martin J, Joanna Pankiewicz, Henrieta Scholtzova, Pankaj D Mehta, Frances Prelli, David Quartermain, and Thomas Wisniewski. 2006. 'Blocking the apolipoprotein E/amyloid-β interaction as a potential therapeutic approach for Alzheimer's disease', *Proceedings of the National Academy of Sciences*, 103: 18787-92.

Safaiyan, Shima, Simon Besson-Girard, Tuğberk Kaya, Ludovico Cantuti-Castelvetri, Lu Liu, Hao Ji, Martina Schifferer, Garyfallia Gouna, Fumere Usifo, Nirmal Kannaiyan et al. 2021. 'White matter aging drives microglial diversity', *Neuron*, 109: 1100-17. e10.

Safaiyan, Shima, Nirmal Kannaiyan, Nicolas Snaidero, Simone Brioschi, Knut Biber, Simon Yona, Aimee L Edinger, Steffen Jung, Moritz J Rossner, and Mikael Simons. 2016. 'Age-related myelin degradation burdens the clearance function of microglia during aging', *Nature neuroscience*, 19: 995-98.

Saher, Gesine, Fabian Rudolphi, Kristina Corthals, Torben Ruhwedel, Karl-Friedrich Schmidt, Siegrid Löwel, Payam Dibaj, Benoit Barrette, Wiebke Möbius, and Klaus-Armin Nave. 2012. 'Therapy of Pelizaeus-Merzbacher disease in mice by feeding a cholesterol-enriched diet', *Nature medicine*, 18: 1130-35.

Saito, Takashi, Yukio Matsuba, Naomi Mihira, Jiro Takano, Per Nilsson, Shigeyoshi Itohara, Nobuhisa Iwata, and Takaomi C Saido. 2014. 'Single App knock-in mouse models of Alzheimer's disease', *Nature neuroscience*, 17: 661-63.

Salat, David H, Jeffrey A Kaye, and Jeri S Janowsky. 1999. 'Prefrontal gray and white matter volumes in healthy aging and Alzheimer disease', *Archives of neurology*, 56: 338-44.

Sanchez-Varo, Raquel, Laura Trujillo-Estrada, Elisabeth Sanchez-Mejias, Manuel Torres, David Baglietto-Vargas, Ines Moreno-Gonzalez, Vanessa De Castro, Sebastian Jimenez, Diego Ruano, Marisa Vizuete et al. 2012. 'Abnormal accumulation of autophagic vesicles correlates with axonal and synaptic pathology in young Alzheimer's mice hippocampus', *Acta neuropathologica*, 123: 53-70.

Sand, IB Katz, Kathryn C Fitzgerald, Yian Gu, Rachel Brandstadter, Claire S Riley, Korhan Buyukturkoglu, Victoria M Leavitt, Stephen Krieger, Aaron Miller, Fred Lublin et al. 2021. 'Dietary factors and MRI metrics in early Multiple Sclerosis', *Multiple sclerosis and related disorders*, 53: 103031.

Sannerud, Ragna, Cary Esselens, Paulina Ejsmont, Rafael Mattera, Leila Rochin, Arun Kumar Tharkeshwar, Greet De Baets, Veerle De Wever, Roger Habets, Veerle Baert et al. 2016. 'Restricted location of PSEN2/γ-secretase determines substrate specificity and generates an intracellular Aβ pool', *Cell*, 166: 193-208.

Satizabal, Claudia L, Alexa S Beiser, Vincent Chouraki, Geneviève Chêne, Carole Dufouil, and Sudha Seshadri. 2016. 'Incidence of dementia over three decades in the Framingham Heart Study', *New England Journal of Medicine*, 374: 523-32.

Schindelin, Johannes, Ignacio Arganda-Carreras, Erwin Frise, Verena Kaynig, Mark Longair, Tobias Pietzsch, Stephan Preibisch, Curtis Rueden, Stephan Saalfeld, Benjamin Schmid et al. 2012. 'Fiji: an open-source platform for biological-image analysis', *Nature methods*, 9: 676-82.

Schirmer, Lucas, Dmitry Velmeshev, Staffan Holmqvist, Max Kaufmann, Sebastian Werneburg, Diane Jung, Stephanie Vistnes, John H Stockley, Adam Young, Maike Steindel et al. 2019. 'Neuronal vulnerability and multilineage diversity in multiple sclerosis', *Nature*, 573: 75-82.

Schneider, Armin, Paul Montague, Ian Griffiths, Monica Fanarraga, Peter Kennedy, Peter Brophy, and Klaus-Armin Nave. 1992. 'Uncoupling of hypomyelination and glial cell death by a mutation in the proteolipid protein gene', *Nature*, 358: 758-61.

Schoenemann, P Thomas, Michael J Sheehan, and L Daniel Glotzer. 2005. 'Prefrontal white matter volume is disproportionately larger in humans than in other primates', *Nature neuroscience*, 8: 242-52.

Semple, Bridgette D, Klas Blomgren, Kayleen Gimlin, Donna M Ferriero, and Linda J Noble-Haeusslein. 2013. 'Brain development in rodents and humans: Identifying benchmarks of maturation and vulnerability to injury across species', *Progress in neurobiology*, 106: 1-16.

Senova, Suhan, Anton Fomenko, Elise Gondard, and Andres M Lozano. 2020. 'Anatomy and function of the fornix in the context of its potential as a therapeutic target', *Journal of Neurology, Neurosurgery & Psychiatry*, 91: 547-59.

Seubert, Peter, Tilman Oltersdorf, Michael G Lee, Robin Barbour, Cheryl Blomquist, David L Davis, Karin Bryant, Lawrence C Fritz, Douglas Galasko, Leon J Thal et al. 1993. 'Secretion of β-amyloid precursor protein cleaved at the amino terminus of the β-amyloid peptide', *Nature* , 361: 260-63.

Seubert, Peter, Carmen Vigo-Pelfrey, Fred Esch, Michael Lee, Harry Dovey, Dave Davis, Sukanto Sinha, Michael Schiossmacher, Justine Whaley, Cathy Swindlehurst et al. 1992. 'Isolation and quantification of soluble Alzheimer's β-peptide from biological fluids', *Nature* , 359: 325-27.

Shen, Siming, Aixiao Liu, Jiadong Li, Candy Wolubah, and Patrizia Casaccia-Bonnefil. 2008. 'Epigenetic memory loss in aging oligodendrocytes in the corpus callosum', *Neurobiology of aging*, 29: 452-63.

Sherrington, R, EI Rogaev, Y al Liang, EA Rogaeva, G Levesque, M Ikeda, H Chi, C Lin, G Li, and K Holman. 1995. 'Cloning of a gene bearing missense mutations in early-onset familial Alzheimer's disease', *Nature*, 375: 754-60.

Sidman, Richard L, Margaret M Dickie, and Stanley H Appel. 1964. 'Mutant mice (quaking and jimpy) with deficient myelination in the central nervous system', *Science*, 144: 309-11.

Siems, Sophie B, Olaf Jahn, Maria A Eichel, Nirmal Kannaiyan, Lai Man N Wu, Diane L Sherman, Kathrin Kusch, Dörte Hesse, Ramona B Jung, Robert Fledrich et al. 2020. 'Proteome profile of peripheral myelin in healthy mice and in a neuropathy model', *Elife*, 9: e51406.

Simón, Ana-María, Lucio Schiapparelli, Pablo Salazar-Colocho, Mar Cuadrado-Tejedor, Luis Escribano, Rakel López de Maturana, Joaquín Del Río, Alberto Pérez-Mediavilla, and Diana Frechilla. 2009. 'Overexpression of wild-type human APP in mice causes cognitive deficits and pathological features unrelated to Aβ levels', *Neurobiology of Disease*, 33: 369-78.

Simons, M, E Ikonen, PJ Tienari, A Cid-Arregui, U Mönning, K Beyreuther, and CG Dotti. 1995. 'Intracellular routing of human amyloid protein precursor: axonal delivery followed by transport to the dendrites', *Journal of neuroscience research*, 41: 121-28.

Simons, Mikael, Patrick Keller, Bart De Strooper, Konrad Beyreuther, Carlos G Dotti, and Kai Simons. 1998. 'Cholesterol depletion inhibits the generation of β-amyloid in hippocampal neurons', *Proceedings of the National Academy of Sciences*, 95: 6460-64.

Singmann, Henrik, Ben Bolker, Jake Westfall, Frederik Aust, S Højsgaard, J Fox, MA Lawrence, U Mertens, and J Love. 2016. 'afex: analysis of factorial experiments. R package version 0.16-1', *R Package Version 0.16*, 1.

Sinha, Sukanto, John P Anderson, Robin Barbour, Guriqbal S Basi, Russell Caccavello, David Davis, Minhtam Doan, Harry F Dovey, Normand Frigon, Jin Hong et al. 1999. 'Purification and cloning of amyloid precursor protein β-secretase from human brain', *Nature*, 402: 537-40.

Sisodia, Sangram S. 1992. 'Beta-amyloid precursor protein cleavage by a membrane-bound protease', *Proceedings of the National Academy of Sciences*, 89: 6075-79.

Sisodia, SS, EH Koo, K Beyreuther, A Unterbeck, and DL Price. 1990. 'Evidence that beta-amyloid protein in Alzheimer's disease is not derived by normal processing', *Science*, 248: 492-95.

Skaper, Stephen D, Nicholas A Evans, Peter E Soden, Claudia Rosin, Laura Facci, and Jill C Richardson. 2009. 'Oligodendrocytes are a novel source of amyloid peptide generation', *Neurochemical research*, 34: 2243-50.

Snaidero, Nicolas, Wiebke Möbius, Tim Czopka, Liesbeth HP Hekking, Cliff Mathisen, Dick Verkleij, Sandra Goebbels, Julia Edgar, Doron Merkler, David A Lyons et al. 2014. 'Myelin membrane wrapping of CNS axons by PI (3, 4, 5) P3-dependent polarized growth at the inner tongue', *Cell*, 156: 277-90.

Snaidero, Nicolas, Caroline Velte, Matti Myllykoski, Arne Raasakka, Alexander Ignatev, Hauke B Werner, Michelle S Erwig, Wiebke Möbius, Petri Kursula, Klaus-Armin Nave et al. 2017. 'Antagonistic functions of MBP and CNP establish cytosolic channels in CNS myelin', *Cell reports*, 18: 314-23.

Sobottka, Bettina, Urs Ziegler, Andres Kaech, Burkhard Becher, and Norbert Goebels. 2011. 'CNS live imaging reveals a new mechanism of myelination: the liquid croissant model', *Glia*, 59: 1841-49.

Söldner, Christian A, Heinrich Sticht, and Anselm HC Horn. 2017. 'Role of the N-terminus for the stability of an amyloid-β fibril with three-fold symmetry', *PloS one*, 12: e0186347.

Sorbara, Catherine Diamante, Naomi Elizabeth Wagner, Anne Ladwig, Ivana Nikić, Doron Merkler, Tatjana Kleele, Petar Marinković, Ronald Naumann, Leanne Godinho, Florence Martine Bareyre et al. 2014. 'Pervasive axonal transport deficits in multiple sclerosis models', *Neuron*, 84: 1183-90.

Sordo, Lorena, and Danièlle A Gunn-Moore. 2021. 'Cognitive dysfunction in cats: Update on neuropathological and behavioural changes plus clinical management', *Veterinary Record*, 188: e3.

Soreq, Lilach, Jamie Rose, Eyal Soreq, John Hardy, Daniah Trabzuni, Mark R Cookson, Colin Smith, Mina Ryten, Rickie Patani, Jernej Ule et al. 2017. 'Major shifts in glial regional identity are a transcriptional hallmark of human brain aging', *Cell reports*, 18: 557-70.

Sosna, Justyna, Stephan Philipp, Ricardo Albay, Jorge Mauricio Reyes-Ruiz, David Baglietto-Vargas, Frank M LaFerla, and Charles G Glabe. 2018. 'Early long-term administration of the CSF1R inhibitor PLX3397 ablates microglia and reduces accumulation of intraneuronal amyloid, neuritic plaque deposition and pre-fibrillar oligomers in 5XFAD mouse model of Alzheimer's disease', *Molecular neurodegeneration*, 13: 1-11.

Spangenberg, Elizabeth E, Rafael J Lee, Allison R Najafi, Rachel A Rice, Monica RP Elmore, Mathew Blurton-Jones, Brian L West, and Kim N Green. 2016. 'Eliminating microglia in Alzheimer's mice prevents neuronal loss without modulating amyloid-β pathology', *Brain*, 139: 1265-81.

Spangenberg, Elizabeth, Paul L Severson, Lindsay A Hohsfield, Joshua Crapser, Jiazhong Zhang, Elizabeth A Burton, Ying Zhang, Wayne Spevak, Jack Lin, Nicole Y Phan et al. 2019. 'Sustained microglial depletion with CSF1R inhibitor impairs parenchymal plaque development in an Alzheimer's disease model', *Nature communications*, 10: 1-21.

Srinivasan, Karpagam, Brad A Friedman, Ainhoa Etxeberria, Melanie A Huntley, Marcel P van Der Brug, Oded Foreman, Jonathan S Paw, Zora Modrusan, Thomas G Beach, Geidy E Serrano et al. 2020. 'Alzheimer's patient microglia exhibit enhanced aging and unique transcriptional activation', *Cell reports*, 31: 107843.

St George-Hyslop, Peter H, Rudolph E Tanzi, Ronald J Polinsky, Jonathan L Haines, Linda Nee, Paul C Watkins, Richard H Myers, Robert G Feldman, Daniel Pollen, David Drachman et al. 1987. 'The genetic defect causing familial Alzheimer's disease maps on chromosome 21', *Science*, 235: 885-90.

Stalder, M, T Deller, M Staufenbiel, and M Jucker. 2001. '3D-Reconstruction of microglia and amyloid in APP23 transgenic mice: no evidence of intracellular amyloid', *Neurobiology of aging*, 22: 427-34.

Stassart, Ruth M, Wiebke Möbius, Klaus-Armin Nave, and Julia M Edgar. 2018. 'The axon-myelin unit in development and degenerative disease', *Frontiers in neuroscience*, 12: 467.

Stedehouder, Jeffrey, Jonathan J Couey, D Brizee, B Hosseini, Johan A Slotman, CMF Dirven, Guy Shpak, AB Houtsmuller, and SA Kushner. 2017. 'Fast-spiking parvalbumin interneurons are frequently myelinated in the cerebral cortex of mice and humans', *Cerebral cortex*, 27: 5001-13.

Steffen, Johannes, Markus Krohn, Kristin Paarmann, Christina Schwitlick, Thomas Brüning, Rita Marreiros, Andreas Müller-Schiffmann, Carsten Korth, Katharina Braun, and Jens Pahnke. 2016. 'Revisiting rodent models: Octodon degus as Alzheimer's disease model?', *Acta neuropathologica communications*, 4: 1-11.

Steyer, Anna M, Torben Ruhwedel, Christos Nardis, Hauke B Werner, Klaus-Armin Nave, and Wiebke Möbius. 2020. 'Pathology of myelinated axons in the PLP-deficient mouse model of spastic paraplegia type 2 revealed by volume imaging using focused ion beam-scanning electron microscopy', *Journal of structural biology*, 210: 107492.

Stoffel, Wilhelm, Heinz Hillen, Werner Schröder, and Rainer Deutzmann. 1983. 'The primary structure of bovine brain myelin lipophilin (proteolipid apoprotein)'.

Stokin, Gorazd B, Concepción Lillo, Tomás L Falzone, Richard G Brusch, Edward Rockenstein, Stephanie L Mount, Rema Raman, Peter Davies, Eliezer Masliah, David S Williams et al. 2005. 'Axonopathy and transport deficits early in the pathogenesis of Alzheimer's disease', *Science*, 307: 1282-88.

Stricker, Nikki H, BC Schweinsburg, Lisa Delano-Wood, Christina E Wierenga, Katherine J Bangen, KY Haaland, Lawrence R Frank, David P Salmon, and Mark W Bondi. 2009. 'Decreased white matter integrity in late-myelinating fiber pathways in Alzheimer's disease supports retrogenesis', *Neuroimage*, 45: 10-16.

Stricker, Nikki H, BC Schweinsburg, Lisa Delano-Wood, Christina E Wierenga, Katherine J Bangen, KY Haaland, Lawrence R Frank, David P Salmon, and Mark W Bondi. 2009. 'Decreased white matter integrity in late-myelinating fiber pathways in Alzheimer's disease supports retrogenesis', *Neuroimage*, 45: 10-16.

Stroup, T Scott, Mark Olfson, Cecilia Huang, Melanie M Wall, Terry Goldberg, Davangere P Devanand, and Tobias Gerhard. 2021. 'Age-Specific Prevalence and Incidence of Dementia Diagnoses Among Older US Adults With Schizophrenia', *JAMA psychiatry*, 78: 632-41.

Stuart, Tim, Andrew Butler, Paul Hoffman, Christoph Hafemeister, Efthymia Papalexi, William M Mauck III, Yuhan Hao, Marlon Stoeckius, Peter Smibert, and Rahul Satija. 2019. 'Comprehensive integration of single-cell data', *Cell*, 177: 1888-902. e21.

Sullivan, EV, and A Pfefferbaum. 2011. 'Diffusion tensor imaging in aging and age-related neurodegenerative disorders', *Diffusion MRI: Theory, methods, and applications Oxford University Press, New York*: 624-43.

Sun, Jichao, and Subhojit Roy. 2018. 'The physical approximation of APP and BACE-1: a key event in Alzheimer's disease pathogenesis', *Developmental neurobiology*, 78: 340-47.

Suzuki, Nobuhiro, Tobun T Cheung, Xe Dm Cai, Asano Odaka, Laszlo Otvos, Christopher Eckman, Todd E Golde, and Steven G Younkin. 1994. 'An increased percentage of long amyloid beta protein secreted by familial amyloid beta protein precursor (beta APP717) mutants', *Science*, 264: 1336-40.

Szodorai, Anita, Yung-Hui Kuan, Silke Hunzelmann, Ulrike Engel, Ayuko Sakane, Takuya Sasaki, Yoshimi Takai, Joachim Kirsch, Ulrike Müller, Konrad Beyreuther et al. 2009. 'APP anterograde transport requires Rab3A GTPase activity for assembly of the transport vesicle', *Journal of Neuroscience*, 29: 14534-44.

Takaichi, Yuta, James K Chambers, Kei Takahashi, Yoshiyuki Soeda, Riki Koike, Etsuko Katsumata, Chiaki Kita, Fuko Matsuda, Makoto Haritani, Akihiko Takashima et al. 2021. 'Amyloid β and tau pathology

in brains of aged pinniped species (sea lion, seal, and walrus)', *Acta neuropathologica communications*, 9: 1-15.

Tanzi, Rudolph E, James F Gusella, Paul C Watkins, GA Bruns, Peter St George-Hyslop, Margaret L Van Keuren, David Patterson, Susan Pagan, David M Kurnit, and Rachael L Neve. 1987. 'Amyloid beta protein gene: cDNA, mRNA distribution, and genetic linkage near the Alzheimer locus', *Science*, 235: 880-84.

Tasaki, Ichiji. 1939. 'The electro-saltatory transmission of the nerve impulse and the effect of narcosis upon the nerve fiber', *American Journal of Physiology-Legacy Content*, 127: 211-27.

Thal, Dietmar R, Udo Rüb, Mario Orantes, and Heiko Braak. 2002. 'Phases of Aβ-deposition in the human brain and its relevance for the development of AD', *Neurology*, 58: 1791-800.

Thinakaran, Gopal, David R Borchelt, Michael K Lee, Hilda H Slunt, Lia Spitzer, Grace Kim, Tamara Ratovitsky, Frances Davenport, Christer Nordstedt, Mary Seeger et al. 1996. 'Endoproteolysis of presenilin 1 and accumulation of processed derivatives in vivo', *Neuron*, 17: 181-90.

Toh, Wei Hong, Jing Zhi A Tan, Khalisah L Zulkefli, Fiona J Houghton, and Paul A Gleeson. 2017. 'Amyloid precursor protein traffics from the Golgi directly to early endosomes in an Arl5b-and AP4-dependent pathway', *Traffic*, 18: 159-75.

Tomassy, Giulio Srubek, Daniel R Berger, Hsu-Hsin Chen, Narayanan Kasthuri, Kenneth J Hayworth, Alessandro Vercelli, H Sebastian Seung, Jeff W Lichtman, and Paola Arlotta. 2014. 'Distinct profiles of myelin distribution along single axons of pyramidal neurons in the neocortex', *Science*, 344: 319-24.

Tombaugh, Tom N, and Nancy J McIntyre. 1992. 'The mini-mental state examination: a comprehensive review', *Journal of the American Geriatrics Society*, 40: 922-35.

Torvund-Jensen, Julie, Jes Steengaard, Lasse Reimer, Linda B Fihl, and Lisbeth S Laursen. 2014. 'Transport and translation of MBP mRNA is regulated differently by distinct hnRNP proteins', *Journal of cell science*, 127: 1550-64.

Toyama, Brandon H, Jeffrey N Savas, Sung Kyu Park, Michael S Harris, Nicholas T Ingolia, John R Yates III, and Martin W Hetzer. 2013. 'Identification of long-lived proteins reveals exceptional stability of essential cellular structures', *Cell*, 154: 971-82.

Treiber, H, Nora Hagemeyer, Hannelore Ehrenreich, and Mika Simons. 2012. 'BACE1 in central nervous system myelination revisited', *Molecular psychiatry*, 17: 237-39.

Trevisiol, Andrea, Kathrin Kusch, Anna M Steyer, Ingo Gregor, Christos Nardis, Ulrike Winkler, Susanne Köhler, Alejandro Restrepo, Wiebke Möbius, Hauke B Werner et al. 2020. 'Structural myelin defects are associated with low axonal ATP levels but rapid recovery from energy deprivation in a mouse model of spastic paraplegia', *PLoS biology*, 18: e3000943.

Trevisiol, Andrea, Aiman S Saab, Ulrike Winkler, Grit Marx, Hiromi Imamura, Wiebke Möbius, Kathrin Kusch, Klaus-Armin Nave, and Johannes Hirrlinger. 2017. 'Monitoring ATP dynamics in electrically active white matter tracts', *Elife*, 6: e24241.

Tripathi, Richa B, Laura E Clarke, Valeria Burzomato, Nicoletta Kessaris, Patrick N Anderson, David Attwell, and William D Richardson. 2011. 'Dorsally and ventrally derived oligodendrocytes have similar electrical properties but myelinate preferred tracts', *Journal of Neuroscience*, 31: 6809-19.

Truscott, Roger JW, and Michael G Friedrich. 2018. 'Can the fact that myelin proteins are old and break down explain the origin of multiple sclerosis in some people?', *Journal of clinical medicine*, 7: 281.

Tyszka, J Michael, Carol Readhead, Elaine L Bearer, Robia G Pautler, and Russell E Jacobs. 2006. 'Statistical diffusion tensor histology reveals regional dysmyelination effects in the shiverer mouse mutant', *Neuroimage*, 29: 1058-65.

Tzeng, Nian-Sheng, Chi-Hsiang Chung, Fu-Huang Lin, Chien-Ping Chiang, Chin-Bin Yeh, San-Yuan Huang, Ru-Band Lu, Hsin-An Chang, Yu-Chen Kao, Hui-Wen Yeh et al. 2018. 'Anti-herpetic medications and reduced risk of dementia in patients with herpes simplex virus infections—a nationwide, population-based cohort study in Taiwan', *Neurotherapeutics*, 15: 417-29.

Ubelmann, Florent, Tatiana Burrinha, Laura Salavessa, Ricardo Gomes, Cláudio Ferreira, Nuno Moreno, and Cláudia Guimas Almeida. 2017. 'Bin1 and CD 2 AP polarise the endocytic generation of beta-amyloid', *EMBO reports*, 18: 102-22.

Udayar, Vinod, Virginie Buggia-Prévot, Rita L Guerreiro, Gabriele Siegel, Naresh Rambabu, Amanda L Soohoo, Moorthi Ponnusamy, Barbara Siegenthaler, Jitin Bali, Rita Guerreiro et al. 2013. 'A paired RNAi and RabGAP overexpression screen identifies Rab11 as a regulator of β-amyloid production', *Cell reports* , 5: 1536-51.

Ueda, Hiroki R, Ali Ertürk, Kwanghun Chung, Viviana Gradinaru, Alain Chédotal, Pavel Tomancak, and Philipp J Keller. 2020. 'Tissue clearing and its applications in neuroscience', *Nature Reviews Neuroscience*, 21: 61-79.

Ulrich, Jason D, Mary Beth Finn, Yaming Wang, Alice Shen, Thomas E Mahan, Hong Jiang, Floy R Stewart, Laura Piccio, Marco Colonna, and David M Holtzman. 2014. 'Altered microglial response to Aβ plaques in APPPS1-21 mice heterozygous for TREM2', *Molecular neurodegeneration*, 9: 1-9.

Vagnoni, Alessio, Michael S Perkinton, Emma H Gray, Paul T Francis, Wendy Noble, and Christopher CJ Miller. 2012. 'Calsyntenin-1 mediates axonal transport of the amyloid precursor protein and regulates Aβ production', *Human molecular genetics*, 21: 2845-54.

Vallino Costassa, Elena, Michele Fiorini, Gianluigi Zanusso, Simone Peletto, Pierluigi Acutis, Elisa Baioni, Cristiana Maurella, Fabrizio Tagliavini, Marcella Catania, Marina Gallo et al. 2016. 'Characterization of Amyloid-β Deposits in Bovine Brains', *Journal of Alzheimer's Disease* , 51: 875-87.

Van Broeckhoven, C, J Haan, E Bakker, JA Hardy, W Van Hul, A Wehnert, M Vegter-Van der Vlis, and RA Roos. 1990. 'Amyloid beta protein precursor gene and hereditary cerebral hemorrhage with amyloidosis (Dutch)', *Science*, 248: 1120-22.

Vassar, R, and SL Cole. 2007. 'The basic biology of BACE1: A key therapeutic target for Alzheimer's disease', *Current genomics*, 8: 509-30.

Vassar, Robert, Brian D Bennett, Safura Babu-Khan, Steve Kahn, Elizabeth A Mendiaz, Paul Denis, David B Teplow, Sandra Ross, Patricia Amarante, Richard Loeloff et al. 1999. 'β-Secretase cleavage of Alzheimer's amyloid precursor protein by the transmembrane aspartic protease BACE', *Science*, 286: 735-41.

Veeraraghavalu, Karthikeyan, Can Zhang, Xiaoqiong Zhang, Rudolph E Tanzi, and Sangram S Sisodia. 2014. 'Age-dependent, non-cell-autonomous deposition of amyloid from synthesis of β-amyloid by cells other than excitatory neurons', *Journal of Neuroscience*, 34: 3668-73.

Venegas, Carmen, Sathish Kumar, Bernardo S Franklin, Tobias Dierkes, Rebecca Brinkschulte, Dario Tejera, Ana Vieira-Saecker, Stephanie Schwartz, Francesco Santarelli, Markus P Kummer et al. 2017. 'Microglia-derived ASC specks cross-seed amyloid-β in Alzheimer's disease', *Nature* , 552: 355-61.

Verrier, Jonathan D, Travis C Jackson, Rashmi Bansal, Patrick M Kochanek, Ava M Puccio, David O Okonkwo, and Edwin K Jackson. 2012. 'The brain in vivo expresses the 2′, 3′-cAMP-adenosine pathway', *Journal of neurochemistry*, 122: 115-25.

Verrier, Jonathan D, Travis C Jackson, Delbert G Gillespie, Keri Janesko-Feldman, Rashmi Bansal, Sandra Goebbels, Klaus-Armin Nave, Patrick M Kochanek, and Edwin K Jackson. 2013. 'Role of CNPase in the oligodendrocytic extracellular 2′, 3′-cAMP-adenosine pathway', *Glia*, 61: 1595-606.

Walsh, Dominic M, Igor Klyubin, Julia V Fadeeva, William K Cullen, Roger Anwyl, Michael S Wolfe, Michael J Rowan, and Dennis J Selkoe. 2002. 'Naturally secreted oligomers of amyloid β protein potently inhibit hippocampal long-term potentiation in vivo', *Nature*, 416: 535-39.

Wälti, Marielle Aulikki, Francesco Ravotti, Hiromi Arai, Charles G Glabe, Joseph S Wall, Anja Böckmann, Peter Güntert, Beat H Meier, and Roland Riek. 2016. 'Atomic-resolution structure of a disease-relevant Aβ (1–42) amyloid fibril', *Proceedings of the National Academy of Sciences*, 113: E4976-E84.

Wang, Fei, Shu-Yu Ren, Jing-Fei Chen, Kun Liu, Rui-Xue Li, Zhi-Fang Li, Bo Hu, Jian-Qin Niu, Lan Xiao, Jonah R Chan et al. 2020. 'Myelin degeneration and diminished myelin renewal contribute to age-related deficits in memory', *Nature neuroscience*, 23: 481-86.

Wang, Qing, Yong Wang, Jingxia Liu, Courtney L Sutphen, Carlos Cruchaga, Tyler Blazey, Brian A Gordon, Yi Su, Charlie Chen, Joshua Shimony et al. 2019. 'Quantification of white matter cellularity and damage in preclinical and early symptomatic Alzheimer's disease', *NeuroImage: Clinical*, 22: 101767.

Wang, Quanxin, Song-Lin Ding, Yang Li, Josh Royall, David Feng, Phil Lesnar, Nile Graddis, Maitham Naeemi, Benjamin Facer, Anh Ho et al. 2020. 'The Allen mouse brain common coordinate framework: a 3D reference atlas', *Cell*, 181: 936-53. e20.

Wang, Yaming, Marina Cella, Kaitlin Mallinson, Jason D Ulrich, Katherine L Young, Michelle L Robinette, Susan Gilfillan, Gokul M Krishnan, Shwetha Sudhakar, Bernd H Zinselmeyer et al. 2015. 'TREM2 lipid sensing sustains the microglial response in an Alzheimer's disease model', *Cell*, 160: 1061-71.

Wang, Yaming, Tyler K Ulland, Jason D Ulrich, Wilbur Song, John A Tzaferis, Justin T Hole, Peng Yuan, Thomas E Mahan, Yang Shi, Susan Gilfillan et al. 2016. 'TREM2-mediated early microglial response limits diffusion and toxicity of amyloid plaques', *Journal of Experimental Medicine*, 213: 667-75.

Weidemann, Andreas, Gerhard König, Dirk Bunke, Peter Fischer, J Michael Salbaum, Colin L Masters, and Konrad Beyreuther. 1989. 'Identification, biogenesis, and localization of precursors of Alzheimer's disease A4 amyloid protein', *Cell*, 57: 115-26.

Weil, Marie-Theres, Saskia Heibeck, Mareike Töpperwien, Susanne tom Dieck, Torben Ruhwedel, Tim Salditt, María C Rodicio, Jennifer R Morgan, Klaus-Armin Nave, Wiebke Möbius et al. 2018. 'Axonal ensheathment in the nervous system of lamprey: implications for the evolution of myelinating glia', *Journal of Neuroscience*, 38: 6586-96.

Weil, Marie-Theres, Torben Ruhwedel, Martin Meschkat, Boguslawa Sadowski, and Wiebke Möbius. 2019. 'Transmission electron microscopy of oligodendrocytes and myelin.' in, *Oligodendrocytes: Methods and protocols*.

Wen, Qiuting, Sourajit M Mustafi, Junjie Li, Shannon L Risacher, Eileen Tallman, Steven A Brown, John D West, Jaroslaw Harezlak, Martin R Farlow, Frederick W Unverzagt et al. 2019. 'White matter alterations in early-stage Alzheimer's disease: A tract-specific study', *Alzheimer's & Dementia: Diagnosis, Assessment & Disease Monitoring*, 11: 576-87.

Werner, Hauke B, Eva-Maria Krämer-Albers, Nicola Strenzke, Gesine Saher, Stefan Tenzer, Yoshiko Ohno-Iwashita, Patricia De Monasterio-Schrader, Wiebke Möbius, Tobias Moser, Ian R Griffiths et al. 2013. 'A critical role for the cholesterol-associated proteolipids PLP and M6B in myelination of the central nervous system', *Glia*, 61: 567-86.

Westlye, Lars T, Kristine B Walhovd, Anders M Dale, Atle Bjørnerud, Paulina Due-Tønnessen, Andreas Engvig, Håkon Grydeland, Christian K Tamnes, Ylva Østby, and Anders M Fjell. 2010. 'Life-span changes of the human brain white matter: diffusion tensor imaging (DTI) and volumetry', *Cerebral cortex*, 20: 2055-68.

Wilder Penfield and Oxon. 1924. 'Oligodendroglia and its relation to classical neuroglia.'', *Brain: A Journal of Neurology*, 47: 430.

Willard, Huntington F. 1985. 'Assignment of the gene for myelin proteolipid protein to the X chromosome: implications for X-linked myelin disorders', *Science*, 230: 940-42.

Willem, Michael, Alistair N Garratt, Bozidar Novak, Martin Citron, Steve Kaufmann, Andrea Rittger, Bart DeStrooper, Paul Saftig, Carmen Birchmeier, and Christian Haass. 2006. 'Control of peripheral nerve myelination by the ß-secretase BACE1', *Science*, 314: 664-66.

Wirths, Oliver, Susanne Walter, Inga Kraus, Hans W Klafki, Martina Stazi, Timo J Oberstein, Jorge Ghiso, Jens Wiltfang, Thomas A Bayer, and Sascha Weggen. 2017. 'N-truncated Aβ 4–x peptides in sporadic Alzheimer's disease cases and transgenic Alzheimer mouse models', *Alzheimer's research & therapy*, 9: 1-12.

Wisco, Jonathan J, Ronald J Killiany, Charles RG Guttmann, Simon K Warfield, Mark B Moss, and Douglas L Rosene. 2008. 'An MRI study of age-related white and gray matter volume changes in the rhesus monkey', *Neurobiology of aging*, 29: 1563-75.

Wolfe, Michael S, Weiming Xia, Chad L Moore, Dartha D Leatherwood, Beth Ostaszewski, Talat Rahmati, Isaac O Donkor, and Dennis J Selkoe. 1999. 'Peptidomimetic probes and molecular modeling suggest that Alzheimer's γ-secretase is an intramembrane-cleaving aspartyl protease', *Biochemistry*, 38: 4720-27.

Wolfe, Michael S, Weiming Xia, Beth L Ostaszewski, Thekla S Diehl, W Taylor Kimberly, and Dennis J Selkoe. 1999. 'Two transmembrane aspartates in presenilin-1 required for presenilin endoproteolysis and γ-secretase activity', *Nature*, 398: 513-17.

Woodruff, Grace, Jessica E Young, Fernando J Martinez, Floyd Buen, Athurva Gore, Jennifer Kinaga, Zhe Li, Shauna H Yuan, Kun Zhang, and Lawrence SB Goldstein. 2013. 'The presenilin-1 ΔE9 mutation results in reduced γ-secretase activity, but not total loss of PS1 function, in isogenic human stem cells', *Cell reports*, 5: 974-85.

Wu, Chun, Justin Scott, and Joan-Emma Shea. 2012. 'Binding of Congo red to amyloid protofibrils of the Alzheimer Aβ9–40 peptide probed by molecular dynamics simulations', *Biophysical journal*, 103: 550-57.

Wu, Di, Xiang Tang, Li-Hua Gu, Xiao-Li Li, Xin-Yang Qi, Feng Bai, Xiao-Chun Chen, Jian-Zhi Wang, Qing-Guo Ren, and Zhi-Jun Zhang. 2018. 'LINGO-1 antibody ameliorates myelin impairment and spatial memory deficits in the early stage of 5 XFAD mice', *CNS neuroscience & therapeutics*, 24: 381-93.

Xiao, Lin, David Ohayon, Ian A McKenzie, Alexander Sinclair-Wilson, Jordan L Wright, Alexander D Fudge, Ben Emery, Huiliang Li, and William D Richardson. 2016. 'Rapid production of new oligodendrocytes is required in the earliest stages of motor-skill learning', *Nature neuroscience*, 19: 1210.

Xiao, Yiling, Buyong Ma, Dan McElheny, Sudhakar Parthasarathy, Fei Long, Minako Hoshi, Ruth Nussinov, and Yoshitaka Ishii. 2015. 'Aβ (1–42) fibril structure illuminates self-recognition and replication of amyloid in Alzheimer's disease', *Nature structural & molecular biology*, 22: 499-505.

Xie, Sheng, Zhe Zhang, Feiyan Chang, Yishi Wang, Zhenxia Zhang, Zhenyu Zhou, and Hua Guo. 2016. 'Subcortical white matter changes with normal aging detected by multi-shot high resolution diffusion tensor imaging', *PloS one*, 11: e0157533.

Ximerakis, Methodios, Scott L Lipnick, Brendan T Innes, Sean K Simmons, Xian Adiconis, Danielle Dionne, Brittany A Mayweather, Lan Nguyen, Zachary Niziolek, Ceren Ozek et al. 2019. 'Single-cell transcriptomic profiling of the aging mouse brain', *Nature neuroscience*, 22: 1696-708.

Xin, Wendy, and Jonah R Chan. 2020. 'Myelin plasticity: sculpting circuits in learning and memory', *Nature Reviews Neuroscience*, 21: 682-94.

Xiong, Feng, Wei Ge, and Chao Ma. 2019. 'Quantitative proteomics reveals distinct composition of amyloid plaques in Alzheimer's disease', *Alzheimer's & Dementia*, 15: 429-40.

Xiong, Monica, Hong Jiang, Javier Remolina Serrano, Ernesto R Gonzales, Chao Wang, Maud Gratuze, Rosa Hoyle, Nga Bien-Ly, Adam P Silverman, Patrick M Sullivan et al. 2021. 'APOE immunotherapy reduces cerebral amyloid angiopathy and amyloid plaques while improving cerebrovascular function', *Science translational medicine*, 13.

Xu, Jan, Shawei Chen, S Hinan Ahmed, Hong Chen, Grace Ku, Mark P Goldberg, and Chung Y Hsu. 2001. 'Amyloid-β peptides are cytotoxic to oligodendrocytes', *Journal of Neuroscience*, 21: RC118-RC18.

Xu, Ke, and Susumu Terakawa. 2013. 'Three Mechanisms or Strategies for Increasing Conduction Velocity of Nerve Fibers.' in, *Myelinated Fibers and Saltatory Conduction in the Shrimp* (Springer).

Yan, Riqiang, Michael J Bienkowski, Mary E Shuck, Huiyi Miao, Monica C Tory, Adele M Pauley, John R Brashler, Nancy C Stratman, W Rodney Mathews, Allen E Buhl et al. 1999. 'Membrane-anchored aspartyl protease with Alzheimer's disease β-secretase activity', *Nature*, 402: 533-37.

Ye, Xuan, and Qian Cai. 2014. 'Snapin-mediated BACE1 retrograde transport is essential for its degradation in lysosomes and regulation of APP processing in neurons', *Cell reports*, 6: 24-31.

Yeatman, Jason D, Brian A Wandell, and Aviv A Mezer. 2014. 'Lifespan maturation and degeneration of human brain white matter', *Nature communications*, 5: 1-12.

Yergert, Katie M, Caleb A Doll, Rebecca O'Rouke, Jacob H Hines, and Bruce Appel. 2021. 'Identification of 3′ UTR motifs required for mRNA localization to myelin sheaths in vivo', *PLoS biology*, 19: e3001053.

Yeung, Maggie SY, Sofia Zdunek, Olaf Bergmann, Samuel Bernard, Mehran Salehpour, Kanar Alkass, Shira Perl, John Tisdale, Göran Possnert, Lou Brundin et al. 2014. 'Dynamics of oligodendrocyte generation and myelination in the human brain', *Cell*, 159: 766-74.

Yin, Xinghua, Rena C Baek, Daniel A Kirschner, Alan Peterson, Yasuhisa Fujii, Klaus-Armin Nave, Wendy B Macklin, and Bruce D Trapp. 2006. 'Evolution of a neuroprotective function of central nervous system myelin', *Journal of Cell Biology*, 172: 469-78.

Yin, Xinghua, Grahame J Kidd, Nobuhiko Ohno, Guy A Perkins, Mark H Ellisman, Chinthasagar Bastian, Sylvain Brunet, Selva Baltan, and Bruce D Trapp. 2016. 'Proteolipid protein–deficient myelin promotes axonal mitochondrial dysfunction via altered metabolic coupling', *Journal of Cell Biology*, 215: 531-42.

Youmans, Katherine L, Leon M Tai, Takahisa Kanekiyo, W Blaine Stine Jr, Sara-Claude Michon, Evelyn Nwabuisi-Heath, Arlene M Manelli, Yifan Fu, Sean Riordan, William A Eimer et al. 2012. 'Intraneuronal Aβ detection in 5xFAD mice by a new Aβ-specific antibody', *Molecular neurodegeneration* , 7: 1-14.

Youssef, SA, Maria Teresa Capucchio, JE Rofina, JK Chambers, K Uchida, H Nakayama, and E Head. 2016. 'Pathology of the aging brain in domestic and laboratory animals, and animal models of human neurodegenerative diseases', *Veterinary pathology*, 53: 327-48.

Yu, Gang, Masaki Nishimura, Shigeki Arawaka, Diane Levitan, Lili Zhang, Anurag Tandon, You-Qiang Song, Ekaterina Rogaeva, Fusheng Chen, Toshitaka Kawarai et al. 2000. 'Nicastrin modulates presenilin-mediated notch/glp-1 signal transduction and βAPP processing', *Nature*, 407: 48-54.

Yuan, Peng, Carlo Condello, C Dirk Keene, Yaming Wang, Thomas D Bird, Steven M Paul, Wenjie Luo, Marco Colonna, David Baddeley, and Jaime Grutzendler. 2016. 'TREM2 haplodeficiency in mice and humans impairs the microglia barrier function leading to decreased amyloid compaction and severe axonal dystrophy', *Neuron*, 90: 724-39.

Zalc, Bernard, Daniel Goujet, and David Colman. 2008. 'The origin of the myelination program in vertebrates', *Current Biology*, 18: R511-R12.

Zeisel, Amit, Hannah Hochgerner, Peter Lönnerberg, Anna Johnsson, Fatima Memic, Job Van Der Zwan, Martin Häring, Emelie Braun, Lars E Borm, Gioele La Manno et al. 2018. 'Molecular architecture of the mouse nervous system', *Cell*, 174: 999-1014. e22.

Zhan, Jiangshan, Teresa Mann, Sarah Joost, Newshan Behrangi, Marcus Frank, and Markus Kipp. 2020. 'The cuprizone model: dos and do nots', *Cells*, 9: 843.

Zhang, Kechen, and Terrence J Sejnowski. 2000. 'A universal scaling law between gray matter and white matter of cerebral cortex', *Proceedings of the National Academy of Sciences*, 97: 5621-26.

Zhang, Peisu, Yuki Kishimoto, Ioannis Grammatikakis, Kamalvishnu Gottimukkala, Roy G Cutler, Shiliang Zhang, Kotb Abdelmohsen, Vilhelm A Bohr, Jyoti Misra Sen, Myriam Gorospe et al. 2019. 'Senolytic therapy alleviates Aβ-associated oligodendrocyte progenitor cell senescence and cognitive deficits in an Alzheimer's disease model', *Nature neuroscience*, 22: 719-28.

Zhang, Shuting, Zhe Wang, Fang Cai, Mingming Zhang, Yili Wu, Jing Zhang, and Weihong Song. 2017. 'BACE1 cleavage site selection critical for amyloidogenesis and Alzheimer's pathogenesis', *Journal of Neuroscience*, 37: 6915-25.

Zhang, Xinwen, Rihua Wang, Di Hu, Xiaoyan Sun, Hisashi Fujioka, Kathleen Lundberg, Ernest R Chan, Quanqiu Wang, Rong Xu, Margaret E Flanagan et al. 2020. 'Oligodendroglial glycolytic stress triggers inflammasome activation and neuropathology in Alzheimer's disease', *Science advances*, 6: eabb8680.

Zhang, Ye, Kenian Chen, Steven A Sloan, Mariko L Bennett, Anja R Scholze, Sean O'Keeffe, Hemali P Phatnani, Paolo Guarnieri, Christine Caneda, Nadine Ruderisch et al. 2014. 'An RNA-sequencing transcriptome and splicing database of glia, neurons, and vascular cells of the cerebral cortex', *Journal of Neuroscience*, 34: 11929-47.

Zhao, Jie, Tracy O'Connor, and Robert Vassar. 2011. 'The contribution of activated astrocytes to Aβ production: implications for Alzheimer's disease pathogenesis', *Journal of neuroinflammation*, 8: 1-17.

Zhao, Ruohe, Wanling Hu, Julia Tsai, Wei Li, and Wen-Biao Gan. 2017. 'Microglia limit the expansion of β-amyloid plaques in a mouse model of Alzheimer's disease', *Molecular neurodegeneration*, 12: 47.

Zhou, Yingyue, Wilbur M Song, Prabhakar S Andhey, Amanda Swain, Tyler Levy, Kelly R Miller, Pietro L Poliani, Manuela Cominelli, Shikha Grover, Susan Gilfillan et al. 2020. 'Human and mouse single-nucleus transcriptomics reveal TREM2-dependent and TREM2-independent cellular responses in Alzheimer's disease', *Nature medicine*, 26: 131-42.

6 Appendix

6.1 List of tables

6.2 List of figures

6.3 List of abbreviations

3D	3-dimensional
5xFAD	5x Familial Alzheimer's Disease; mouse model
Aa	Amino acids
ABCA7	ATP-Binding Cassette Subfamily A Member 7
AD	Alzheimer's Disease
ADAM10	A Disintegrin and Metalloproteinase Domain-containing Protein 10
ADDL	Amyloid-beta Derived Diffusible Ligands
Alv	Alveus
ANOVA	Analysis of Variance
AP2	Adaptor Protein Complex 2
Aph1	Anterior Pharynx-Defective 1
APP	Amyloid-beta Precursor Protein
ASC	Apoptosis-associated speck-like protein containing a CARD
Aß	Amyloid-beta
BACE1	Beta-site Amyloid precursor protein cleavage enzyme 1
BBB	Blood brain barrier
BIN1	Myc box-dependent-interacting protein 1
CA	Cornu Ammonis
CAA	Cerebral Amyloid Angiopathy
cAMP	Cyclic Adenosin Monophosphate
CC	Corpus Callosum
CD2AP	CD2-associated protein
CD33	Cluster of Differentiation 33
CD36	Cluster of Differentiation 33
cDNA	Complementary Desoxyribonucleic Acid
CNP	2'-3' Cyclic Nucleotide Phosphodiesterase

CNS	Central nervous system
CR1	Complement Receptor 1
CSF	Cerebrospinal fluid
CSF1R	Colony Stimulating Factor 1 Receptor
CSPG4	Chrondoitin sulfate proteoglycan 4
CT	Computer Tomography
Ctx	Cortex
DAM	Disease-Associated microglia
DEA	Diethylamine
DNA	Desoxyribonucleic Acid
DTI	Diffusion Tensor Imaging
DTT	Dithiothreitol
E	embryonic day
e.g.	Exempli Gratia
EAE	Experimental Autoimmune Encephalomyelitis
EC	Entorhinal Cortex
EHD1	Eps15 homology domain-containing protein 1
EHD3	Eps15 homology domain-containing protein 3
ELISA	Enzyme-linked Immunosorbent Assay
EM	Electron Microscopy
EMX	Empty Spiracles Homeobox 1
ENPP6	Ectonucleotide pyrophosphatase/phosphodiesterase 6
EPM	Elevated Plus Maze
ER	Endoplasmic Reticulum
FAD	Familial Alzheimer's Disease
FG-W	Fastgreen-Wash
FIB-SEM	Focused ion beam serial electron microscopy

fl	flanked by LoxP sites; “floxed”
GWAS	Genome wide association studies
HPF-EM	High Pressure Freezing Electron Microscopy
i.e.	id est
IHC	Immunohistochemistry
IPL	Intraperiod line
JIP3	C-Jun-amino-terminal kinase interacting protein 2
KNN	K-nearest neighbour
LAMP1	Lysosomal-Associated Membrane Protein 1
LC3	Light chain 3B
LSM	Light Sheet Microscopy
MAP2	Microtubule associated protein 2
MAP2	Microtubule associated protein 2
MBP	Myelin Basic Protein
MCI	Mild Cognitive Impairment
MDL	Major Dense Line
Me-04	Methoxy-X04
MMSE	Mini mental state examination
MOG	Myelin Oligodendrocyte Glycoprotein
MRI	Magnetic Resonance Imaging
mRNA	Messenger Ribonucleic Acid
MS	Multiple Sclerosis
MS4A	Membrane-spanning 4A
mV	milliVolt
MYRF	Myelin regulatory factor
NaV	Voltage-gated Sodiumchannels
NG2	Neural/glial antigen 2

NIA-AA	National Institute on Aging and Alzheimer's Association
OLIG1	Oligodendrocyte transcription factor 1
OLIG2	Oligodendrocyte transcription factor 2
OPC	Oligodendrocyte Precursor Cells
PBS	Phopshate-buffered Saline
PCA	Principal Component Analysis
PEN2	Presenilin Enhancer 2
PET	Positron Emission Tomography
PHG	Parahippocampal Gyrus
PIP3	Phosphatidylinositol (3,4,5)-trisphosphate
PLP	Proteolipid Protein
PNS	Peripheral nervous system
Prp	Cellular Prion Protein
PSEN 2	Presenilin 2
PSEN1	Presenilin 1
PTwH	PBS-Tween with Heparin
RAB	Ras-associated binding protein
RIPA	Radioimmunoprecipiation assay
ROI	Region of Interest
sAPPalpha	Soluble Amyloid Precursor Protein alpha
sAPPbeta	Soluble Amyloid Precursor Protein beta
Sub	Subiculum
TGN	Trans-Golgi Network
Thy1	Thymocyte antigen 1
Trem2	Triggering Receptor Expressed on Myloid Cells 2
tRNA	Transfer Ribonucleic Acid
UMAP	Uniform Manifold Approximation and Projection

UMI	Unique Molecular Identifier
VGLUT	Vesicular Glutamate Transporter
WAM	White matter associated microglia
WB	Western Blot
YM	Y-maze

7 Acknowledgements

I would like to express by sincerest and greatest gratitude towards my supervisor and mentor Prof. Klaus-Armin Nave. I couldn't have imagined the amazing journey we embarked on when he recruited me to his lab. I would like to thank him for entrusting me with this project while at the same time giving me the freedom to follow my own ideas. I would like to thank him for his continuous support and especially for challenging my ideas and thinking by frequently playing the devil's advocate. The time working with him had a truly formative influence on me as a scientist: I will be always reminded to not forget the bigger picture and to be brave enough to ask big questions.

My gratitude expands to other lab members of the Nave Department. Ting Sun has been crucially involved in taking this project to the next level and I truly loved joining forces with her on this. I would like to thank her for our discussions, for teaching me about sequencing techniques and especially for always radiating positivity and joy while doing science. During my doctorate, I had the pleasure of supervising Andrew Octavian Sasmita as a Master's thesis student. His continuous support throughout the project significantly contributed to its success. I hope he knows how much I appreciate his work – as well as his entertainer qualities. Lena Spieth and Dr. Stefan Berghoff critically supported me in this work with their expertise. I would like to thank both of them for their continuous help, understandings ears and the endless discussions. Further, I would like to thank the members of our KAGS subgroup for critical scientific input and comments on my work. For my time in Göttingen, the Neurogenetics Department has truly become my home and many lab members were not only colleagues but became dear friends. I would like to thank them for making my doctorate not only scientifically fulfilling but also simply a great time. Thanks for coffee breaks, food, drinks, chats – and for sharing the highs and lows of doing a PhD. Thanks also goes to the Neurogenetics postdocs/group leaders from whose often decade-long experience I benefited greatly. Thank you for supporting me whenever I approached you. Special thank goes to Dr. Wiebke Möbius and Dr. Sandra Goebbels who were directly involved in this project. Special thanks go to the animalcare takers at the MPI-EM, Conny Casper, Tanja Pawelz and Denise Kuchenbuch. Their work was absolutely essential. I would like to thank Annette Fahrenholz and Katharina Overhoff for their outstanding technical assistance. Further, I want to thank Michaela Schmalstieg for the great administrative support from the very beginning.

I would like to thank Prof. Nils Brose and Prof. Thomas Bayer for their valuable input during my TAC meetings. Thanks to Prof. Hannelore Ehrenreich for her advice on this project and further for bringing me in on exciting projects in her group. My thank expands to other scientific collaborators for their critical scientific input and help during my doctorate, especially Prof. Christian Haass, Dr. Michael Willem and Prof. Oliver Wirths. I would further like to thank Dr. Ruth Stassart for generously providing us with human tissue samples. Thank goes to Dr. Takashi Saito and Prof. Takaomi Saido for providing us with APP^{NLGF} mice. Further, I would like to thank Dr. Ewa Smajek (LaVision BioTec) for the excellent technical support I received from her regarding the UltramicroscopeII. I would like to express my deepest gratitude towards the Boehringer Ingelheim Fonds I received a PhD fellowship for this work. Being part of this young and vibrant scientific community has filled me with pride and joy.

Finally, I would like to thank my family, friends and especially my partner from the bottom of my heart. Thanks for supporting me throughout this journey in so many ways.